PROCEEDINGS

OF THE

AMERICAN SOCIETY OF CIVIL ENGINEERS

VOL. 61 SEPTEMBER, 1935 NO. 7

TECHNICAL PAPERS

AND

DISCUSSIONS

Published monthly, except June and July, at 99–129 North Broadway, Albany, N. Y., by the American Society of Civil Engineers, Editorial and General Offices at 33 West Thirty-ninth Street, New York, N. Y. Reprints from this publication may be made on condition that the full title of Paper, name of Author, page reference, and date of publication by the Society, are given.

Entered as Second-Class Matter, December 28, 1931, at the Post Office at Albany, N. Y., under the Act of March 3, 1879. Acceptance for mailing at special rate of postage provided for in Section 1103, Act of October 3, 1917, authorized on July 5, 1918.

Subscription (if entered before January 1) $8.00 per annum. Price $1.00 per copy.

CURRENT PAPERS AND DISCUSSIONS

		Discussion closes
An Asymmetric Probability Function. *J. J. Slade, Jr.*	Oct., 1934	
Discussion (Author's closure)	Dec., 1934, Jan., Feb., Mar., Apr., May, Sept., 1935	Closed
Analysis of Continuous Structures by Traversing the Elastic Curves. *Ralph W. Stewart*	Oct., 1934	
Discussion (Author's closure)	Dec., 1934, Feb., Mar., May, Sept., 1935	Closed
Relation Between Rainfall and Run-Off from Small Urban Areas. *W. W. Horner and F. L. Flynt*	Oct., 1934	
Discussion	May 1935	Sept., 1935
The Silt Problem. *J. C. Stevens*	Oct., 1934	
Discussion	Feb., Mar., May, Sept., 1935	Uncertain
Effect of Secondary Stresses Upon Ultimate Strength. *John I. Parcel and Eldred B. Murer*	Nov., 1934	
Discussion	Jan., Mar., Aug., 1935	Sept., 1935
The Springwells Filtration Plant, Detroit, Michigan. *Eugene A. Hardin*	Nov., 1934	
Discussion (Author's closure)	Jan., Sept., 1935	Closed
Analysis of Multiple Arches. *Alexander Hrennikoff*	Dec., 1934	
Discussion	May, Sept., 1935	Sept., 1935
Rational Design of Steel Columns. *D. H. Young*	Dec., 1934	
Discussion	Mar., May, Aug., 1935	Sept., 1935
A Direct Method of Moment Distribution. *T. Y. Lin*	Dec., 1934	
Discussion	Mar., May, Aug., 1935	Sept., 1935
Elastic Properties of Riveted Connections. *J. Charles Rathbun*	Jan., 1935	
Discussion	Feb., May, Aug., 1935	Oct., 1935
Analysis of Thick Arch Dams, Including Abutment Yield. *Philip Cravitz*	Jan., 1935	
Discussion	Sept., 1935	Oct., 1935
Hydraulic Laboratory Results and Their Verification in Nature. *Herbert D. Vogel*	Jan., 1935	
Discussion	May, Aug., 1935	Oct., 1935
The Hydraulic Jump in Terms of Dynamic Similarity. *Boris A. Bakhmeteff and Arthur E. Matzke*	Feb., 1935	
Discussion	Mar., May, Aug., Sept., 1935	Oct., 1935
Frictional Resistance in Artificially Roughened Pipes. *Victor L. Streeter*	Feb., 1935	
Discussion	Aug., 1935	Oct., 1935
Stabilizing Constructed Masonry Dams by Means of Cement Injections. *D. W. Cole*	Feb., 1935	
Discussion	Aug., Sept., 1935	Uncertain
Weights of Metal in Steel Trusses. *J. A. L. Waddell*	Feb., 1935	
Discussion	May, 1935	Oct., 1935
Line Load Action on Thin Cylindrical Shells. *Herman Schorer*	Mar., 1935	
Discussion	Sept., 1935	Nov., 1935
Underground Corrosion. *K. H. Logan*	Mar., 1935	
Discussion	Apr., Aug., 1935	Nov., 1935
The Adjustment of a Level Net. *George H. Dell*	Apr., 1935	
Discussion	Aug., 1935	Nov., 1935
Structural Beams in Torsion. *Inge Lyse and Bruce G. Johnston*	Apr., 1935	
Discussion	Aug., 1935	Nov., 1935
Photo-Elastic Determination of Shrinkage Stresses. *Howard G. Smits*	May, 1935	
Discussion	Sept., 1935	Nov., 1935
The Shear-Area Method. *Horace B. Compton and Clayton O. Dohrenwend*	May, 1935	
Discussion	Aug., 1935	Nov., 1935
Flood-Stage Records of the River Nile. *C. S. Jarvis*	Aug., 1935	Nov., 1935
Distribution of Stresses under a Foundation. *A. E. Cummings*	Aug., 1935	Nov., 1935
Some Low-Temperature Characteristics of Bituminous Paving Compositions. *Hugh W. Skidmore*	Aug., 1935	Nov., 1935
Failure Theories of Materials Subjected to Combined Stresses. *Joseph Marin*	Aug., 1935	Nov., 1935

NOTE.—The closing dates herein published, are final except when names of prospective discussers are registered for special extension of time.

CONTENTS FOR SEPTEMBER, 1935

PAPERS

DISCUSSIONS

CONTENTS FOR SEPTEMBER, 1935 (*Continued*)

For Index to all Papers, the discussion of which is current in PROCEEDINGS, *see page 2*

AMERICAN SOCIETY OF CIVIL ENGINEERS

Founded November 5, 1852

PAPERS

ADAPTATION OF VENTURI FLUMES TO FLOW MEASUREMENTS IN CONDUITS

By Harold K. Palmer[1], M. Am. Soc. C. E., and Fred D. Bowlus[2], Assoc. M. Am. Soc. C. E.

Synopsis

A weir can be considered as a control section through which water flows at critical depth. The sharp angle at the face and the fact that the flow is convex where it passes the critical section introduce energy losses between the point of measurement and the control section, the amount of these losses depending upon the setting of the weir in the channel. The ordinary weir formula is an empirical equation that is accurate only as long as the fundamental conditions upon which it was developed can be duplicated. These conditions can rarely be complied with in a confined channel, such as a sewer or an irrigation canal.

This paper presents the theoretical hydraulic principles involved, and the results of special tests made, in the adaptation and construction of various Venturi flumes for measuring flow in conduits of uniform cross-section, where weirs have proved unsatisfactory.

Since the uncertainties or variations in weir coefficients are due to indeterminable energy losses, it is reasonable to suppose that if these losses can be eliminated or reduced to a negligible amount by the use of some other device, the uncertainties in the rating curve will be eliminated. Such conditions are found in the so-called Venturi flume which, in this paper, includes any streamlined device placed in an open channel, or a closed channel partly full, having a sufficient constriction to cause water to flow at critical depth with parallel filaments.

Any shape of throat may be used, and the flow can be determined from a single depth measurement, using a rating curve drawn from rational formulas. Several of these Venturi flumes have been constructed, including one that

Note.—Discussion on this paper will be closed in December, 1935, *Proceedings*.

[1] Chf. Draftsman, Los Angeles County Sanitation Dists., Los Angeles, Calif.

[2] Res. Engr., Los Angeles County Sanitation Dist. No. 2, Whittier, Calif.

was simply a flat slab on the bottom, and had no side contractions; one that was rectangular in cross-section; and several with trapezodial-shaped throats, all of which have given good results.

The writers show how the rating curve may be drawn, and give graphs for use with circular conduits.

Introduction

Weirs have long been considered the standard devices for measuring running water, but their use involves empirical formulas, and they must be built under restricted conditions, unattainable in many classes of conduits. The ponding effect of the water up stream from the weir causes deposits of suspended matter which often alter the hydraulic conditions so that the empirical formula fails to give the correct flow. In the case of sewers, sludge deposited in this manner will decompose in time and become an added source of trouble. Another objection to the use of weirs in a closed conduit is the relatively large loss of head.

Many factors affect the proper installation of weirs as shown by Schoder and Turner[3] in an able discussion of precise weir measurements. The United States Bureau of Reclamation has found from experiments[4] that the ordinary sharp-crested Cipolletti or rectangular type of weir must have certain very definite requirements for a fair degree of accuracy; for instance, the distances from the bottom and sides of the channel to the edges of the weir must not be less than twice the depth of water over the weir, and the channel above the weir for a distance of 20 or 30 ft must have a cross-sectional area at least six times that of the over-flowing sheet of water at the weir crest. When the depth of the water passing over a weir exceeds three-tenths of its width, the engineers of the Reclamation Bureau have found that the standard formulas indicate quantities that are too small. The error ranges from zero at three-tenths to 30% when the depth equals its width. These restrictions limit the capacity of the weir to about 40% of the capacity of a closed conduit.

Occasionally, the true Venturi flume has been used to advantage because it gives a minimum of ponding and the frictional losses, being small, result in little loss of head. However, it has the disadvantage of requiring the measurement of the area of cross-section as well as the velocity of the water flowing in the throat. This has only been possible in the past by making two simultaneous depth measurements.

Use of the Parshall meter,[5] which is one form of a Venturi flume, obviates some of the difficulties previously mentioned, but it is not readily installed in conduits already constructed because of the required 3-in. drop in the invert grade at the throat. It could scarcely be adapted to an existing, standard sewer manhole, say, 4 ft in diameter. In the design of a new system of con-

[3] "Precise Weir Measurements," by E. W. Schoder, M. Am. Soc. C. E., and the late Kenneth B. Turner, Esq., *Transactions*, Am. Soc. C. E., Vol. 93 (1929), p. 999.

[4] "Measurement of Irrigation Water", U. S. Dept. of Interior, Bureau of Reclamation. Third Edition, 1925.

[5] "The Improved Venturi Flume", by R. L. Parshall, Assoc. M. Am. Soc. C. E., *Transactions*, Am. Soc. C. E., Vol. 89 (1926), p. 841.

duits for which the desired points of flow determinations might be predetermined and a few inches of grade sacrificed, Parshall meters could be (and have been) installed to advantage. They have certain disadvantages in the continuous measurement of sewage, requiring daily inspection when a week or more of record is required, because the orifice between the channel and the wet-well often becomes clogged and the formation of sludge after a day or two in the wet-well tends to raise the float, thereby causing an error in the stage recorder reading.

Ordinary Venturi tubes may also be used for liquid flow measurement, but larger structures are required for their installation. Such a tube must be entirely submerged and in sewers this is likely to prevent the proper handling of light floating material. Its efficiency is often impaired by clogging of the pressure recording pipes and, including the recorders, the initial installation is more costly than the weir and stage recorder units.

In 1920, Hinds[6] suggested placing a sufficient constriction in a channel to cause the water to flow at critical depth, on the assumption that in this case the energy head is fixed, whereas the depth is uncertain. He presented experiments made by the U. S. Bureau of Reclamation,[7] on a flume similar in many respects to one type considered by the writers and showed an error of less than 5% in measurement of flow, assuming no transition losses.

The following analysis of the adaptation of the Venturi flume to flow measurements in conduits of regular cross-section is applicable not only to clear water, but also to any liquid carrying suspended matter. Among the latter are included silt-laden irrigation water, storm water, and sewage. The investigations herein reported were made in connection with a sanitary sewerage system and as sewage presents most of the difficulties encountered in the other classes of water, the word, "sewage," will be used subsequently to denote water that carries settleable solids.

In passing, it may be stated that an accurate measurement of sewage flows in various parts of a sewerage system is quite important in order to be able to predict with reasonable accuracy the need of future works, relief sewers, additional pump capacity where pumping is required, etc. In joint sewerage works an accurate measurement of sewage is necessary to apportion costs to respective participants. Furthermore, as a check on pumping efficiency and power requirements, knowledge of the actual sewage flow is necessary. An accurate gauge of the flow is required for efficient and economical operation, where pre-chlorination[8] is practiced since the chlorine feed depends on both the strength and the quantity of the sewage. One difficulty encountered in an accurate measurement of sewage flow in new sewerage works is the fact that a sewer is usually constructed of a greater capacity than is required at the time it is first placed in operation. The flow in the line is then relatively shallow. Furthermore, in a new system of any large

[6] "Venturi Flume Data Throws Light Upon Control Weir", by Julian Hinds, M. Am. Soc. C. E., *Engineering News-Record* (1920), p. 1223.

[7] "The Improved Venturi Flume", by R. L. Parshall, Assoc. M. Am. Soc. C. E., discussion by Julian Hinds, M. Am. Soc. C. E., *Transactions*, Am. Soc. C. E., Vol. 89 (1926), p. 864.

[8] "Control of Sewage Condition by Chlorination", by F. D. Bowlus, and A. P. Banta, Assoc. Members, Am. Soc. C. E., *Water Works and Sewerage*, November, 1932, Vol. 79, p. 369.

extent, the increase in sewage from month to month or year to year is relatively large and many measuring devices which might be satisfactory at one time would prove totally inadequate at a later date. Sewage flows range from a minimum in the early morning to a maximum of as much as two or three times the minimum amount later in the day; it will also vary from day to day, and any meter used for the purpose must be adaptable to such variations.

Difficulties encountered with ordinary weirs and other similar devices in the measurement of sewage indicate that the most satisfactory meter would incorporate the use of a stream-lined flume, with minimum head loss, preventing deposits of sludge above it; without sharp edges to catch rags and other floating refuse; and with sufficient capacity to measure the entire designed flow and yet be sensitive enough to record low flows in the first years of its use. The flume must be adaptable to the use of a simple float mechanism for water-stage recording, and must be designed so as to be readily installed in an existing conduit with minimum interference to the sewage flow. This paper deals with a measuring flume designed so that the flow may pass without objectionable ponding up stream; which offers no obstruction to floating or suspended solids; and which affords an opportunity to measure the flow from a continuous record of the water-surface elevation at a single point in the channel up stream from the flume.

The formulas developed for the flume are not empirical but are based entirely on theory and can be applied to conduits of any regular size or shape. Irregular channels would require regulation for a short distance up stream by lining of some kind. Uniformity of shape rather than factors affecting friction are important. The method has been developed especially for sewers, but is equally applicable to other channels, irrigation canals, storm drains, etc.

Notation

The symbols introduced in this paper are defined as follows:

b = a bottom width.
c = a subscript denoting "a critical depth."
f = "function of."
g = acceleration due to gravity.
n = Kutter's coefficient of roughness.
v = a subscript denoting "velocity."
A = area.
B = surface width; width of water surface.
C = Chezy's coefficient.
D = diameter.
H = head; H_v = velocity head.
K = a constant in Kutter's formula $= A\,C\sqrt{R}$.
Q = rate of flow, or discharge.
R = hydraulic radius.
S = hydraulic slope; slope of a conduit, expressed as a percentage.
V = average velocity in a section.
Δ = "difference in;" ΔH_v = difference in velocity heads in throat and conduit.
ϵ = energy head; ϵ_c = energy head at critical depth.
ϕ = "function of."

Theory of Design

According to Bernoulli's theorem, the energy head of each pound of water in a conduit is the height of the water surface above a given datum plane, plus the velocity head. In passing from one section of a conduit to another, frictional and other losses are measured by the decrease in the total energy head regardless of changes in depths and velocities at the two places. Therefore, measurement of the total energy head is the logical basis for the development of any theory in the design of a Venturi flume of the general type illustrated in Fig. 1.

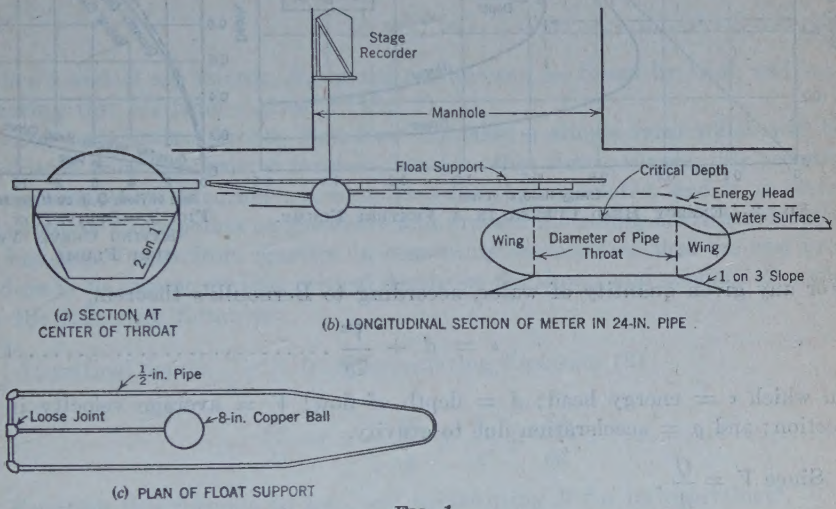

Fig. 1.

Under certain conditions a calculation of the flow may be made by simply measuring the depth of the water flowing in a conduit of regular cross-section at any convenient point immediately above the throat of the measuring flume. This is only possible when the throat is designed to cause the water to flow through it at critical depth. For any given quantity of water, and size and shape of conduit, Fig. 2 shows that the energy head has a minimum value when the water is flowing at critical depth in the throat. For a given channel this critical depth is a function of the quantity of water, and attempts have been made by Woodburn[9] to use a broad-crested weir as a measuring device recording the critical depth. However, in this case, it was found impossible to locate the section of critical depth accurately as it changed position with different quantities of flow. Near the section of critical depth in the throat of the Venturi flume, the depth is uncertain, but the energy head is fixed; therefore, if the throat is designed so as to cause the water to flow at critical depth the depth in the conduit of the regular cross-section above will be the average energy head less the velocity head at that point, except for frictional losses, which will be discussed subsequently.

[9] "Tests of Broad-Crested Weirs", by James G. Woodburn, Assoc. M. Am. Soc. C. E., *Transactions*, Am. Soc. C. E., Vol. 96 (1932), p. 387.

The proposed method of measurement is best illustrated by reference to Fig. 2. For simplicity, consider that a rectangular conduit is contracted on the sides only, forming a rectangular throat one-half the width of the conduit.

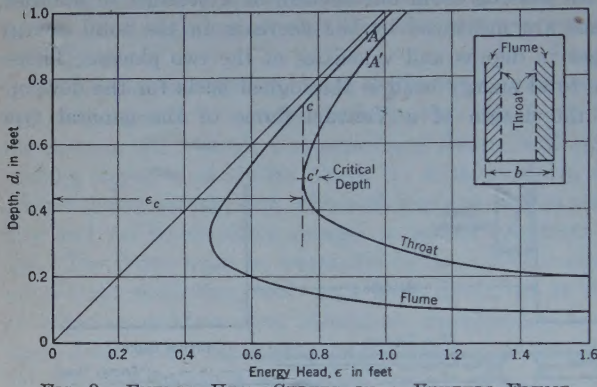

FIG. 2.—ENERGY HEAD CURVES IN A VENTURI FLUME.

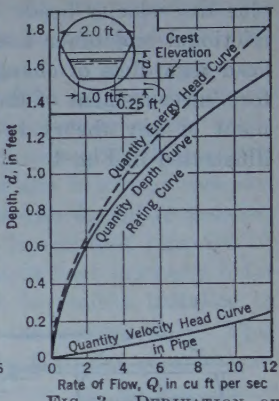

FIG. 3.—DERIVATION OF RATING CURVE, VENTURI FLUME.

For any given quantity of water, according to Bernoulli's theorem,

$$\epsilon = d + \frac{V^2}{2g} \quad \ldots\ldots\ldots\ldots\ldots\ldots\ldots\ldots\ldots\ldots (1)$$

in which ϵ = energy head; d = depth of flow; V = average velocity in a section; and g = acceleration due to gravity.

Since $V = \frac{Q}{A}$,

$$\epsilon = d + \left(\frac{Q}{A}\right)^2 \frac{1}{2g} \quad \ldots\ldots\ldots\ldots\ldots\ldots\ldots\ldots\ldots\ldots (2)$$

in which Q = rate of discharge; and A = area of cross-section. For a rectangular cross-section:

$$A = bd \quad \ldots\ldots\ldots\ldots\ldots\ldots\ldots\ldots\ldots\ldots (3a)$$

$$V = \frac{Q}{bd} \quad \ldots\ldots\ldots\ldots\ldots\ldots\ldots\ldots\ldots\ldots (3b)$$

and,

$$\epsilon = d + \left(\frac{Q}{bd}\right)^2 \frac{1}{2g} \quad \ldots\ldots\ldots\ldots\ldots\ldots\ldots\ldots\ldots\ldots (4)$$

in which b = the bottom width of a channel; and ϵ and d are the variables. In Fig. 2, Curves F and T represent Equation (4) for the conduit and throat, respectively, Q being the same in both cases. Neglecting frictional losses there would be no loss of energy in or through the Venturi flume, and if Q cu ft per sec flowed at a depth, A, in the conduit, it would flow at a depth, A', in the throat. Theoretically, Q could be determined by measuring these two depths, A and A'. The necessity in the past for the two measure-

ments has been an inconvenience in the use of the Venturi flume. If Q, in cubic feet per second, flowed at the critical depth in the throat (Point C'), its depth in the conduit would be represented by Point C which would be its minimum depth above the throat, because for shallower depths the energy is insufficient to force Q through the throat.

By drawing similar pairs of curves for other values of Q, a rating curve showing the relationship between Q and d could be drawn, but in practice this requires an unnecessary amount of labor.

For a given size and shape of throat, the value of ϵ_c is a definite function of Q, or to write the inverse case:

$$Q = f(\epsilon_c) \quad \ldots\ldots\ldots\ldots\ldots\ldots\ldots\ldots\ldots\ldots (5)$$

When ϵ and Q are known, H_v in the conduit can be found by trial, and subtracting this H_v from ϵ gives d (Fig. 3).

For rectangular throats, Equation (5) takes a simple form which will be evaluated from the general formula, but for other throat shapes, this becomes a transcendental function too complicated to be considered, and it is easier to compute a few points on the curve and prepare the rating curve graphically. It has been found from practice in computing these points that the best procedure is to assume various critical depths in the throat and compute Q and ϵ by the following formulas:

At critical depth, $\frac{d\epsilon}{dd} = 0$; differentiating Equation (2):

$$\frac{d\epsilon}{dd} = 1 - \frac{Q^2}{g} \times \frac{1}{A^3} + \frac{dA}{dd} \quad \ldots\ldots\ldots\ldots\ldots\ldots\ldots\ldots (6)$$

Equating this formula to zero, and substituting B for its equivalent[10], $\frac{dA}{dd}$, Equation (6) becomes:

$$1 - \frac{Q^2}{g} \times \frac{B}{A^3} = 0 \quad \ldots\ldots\ldots\ldots\ldots\ldots\ldots\ldots\ldots\ldots (7)$$

and, therefore,

$$Q = A\sqrt{\frac{A}{B}\,g} \quad \ldots\ldots\ldots\ldots\ldots\ldots\ldots\ldots\ldots\ldots (8)$$

Equation (8) is the accepted formula for the quantity flowing at a critical depth in a channel of any shape. Since $Q = A\,V$, by substituting the value of Q in Equation (8):

$$\frac{V^2}{2g} = \frac{A}{2B} \quad \ldots\ldots\ldots\ldots\ldots\ldots\ldots\ldots\ldots\ldots (9)$$

and Bernoulli's equation becomes,

$$\epsilon = d_c + \frac{A}{2B} \quad \ldots\ldots\ldots\ldots\ldots\ldots\ldots\ldots\ldots\ldots (10)$$

[10] "Hydraulics of Open Channels", by B. A. Bakhmeteff, M. Am. Soc. C. E., p. 31, Equation (19).

In a rectangular throat in which $A = B\,d_c$, Equation (8) becomes,

$$Q = B\sqrt{g}\,d_c^{\frac{3}{2}} \quad \ldots\ldots(11)$$

$$\frac{V^2}{2g} = \frac{d_c}{2} \quad \ldots\ldots(12)$$

and,

$$\epsilon = \frac{3}{2}\,d_c \quad \ldots\ldots(13)$$

Substituting the value of d_c obtained from Equation (13) in Equation (11):

$$Q = 3.09\,B\,\epsilon^{\frac{3}{2}} \quad \ldots\ldots(14)$$

which is the form taken by Equation (5) for a rectangular throat. For all other shapes it is necessary to use Equations (8) and (10).

Having drawn the quantity-energy head curve for a given throat (see Fig. 3), it is necessary to compute and draw the quantity-velocity head curve for the conduit section. If the conduit is circular this may be done by means of Fig. 4, which gives for various depths the velocity and velocity head for 1 cu ft per sec on a logarithmic scale, and, for other quantities, by merely adding log Q graphically. The intersection of the velocity abscissa with the "guide" line falls on the ordinate of the velocity head. The procedure is best

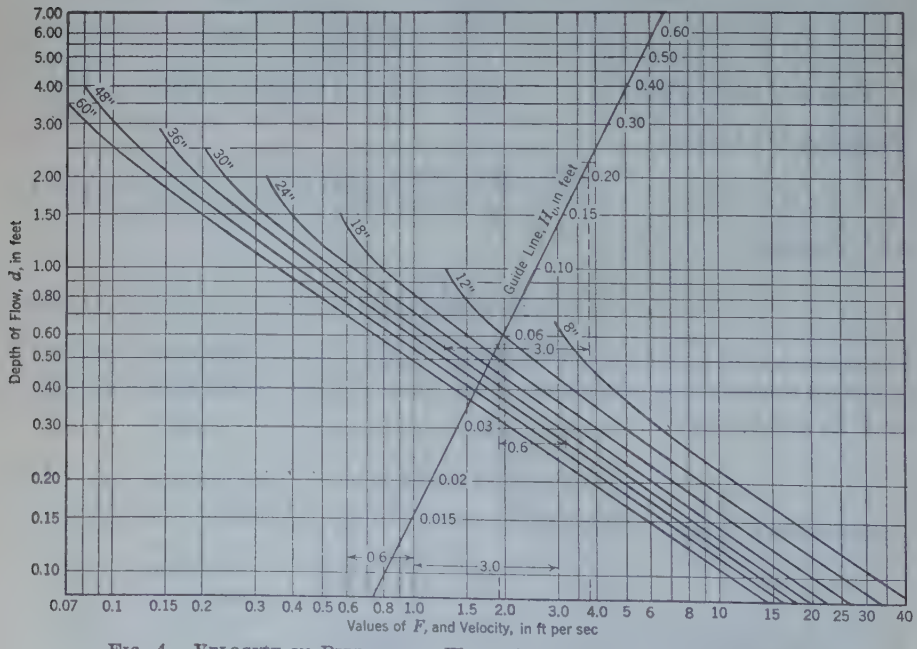

FIG. 4.—VELOCITY IN PIPES WITH WATER FLOWING AT VARIOUS DEPTHS.

explained by two examples: First, when $Q > 1$; and, second, when $Q < 1$. For example, let $Q = 3$ cu ft per sec with water flowing 0.55 ft deep in a 30-in. pipe. Set a pair of dividers to the distance from 1 to 3 and measure this distance to the right from the intersection of the 30-in. pipe with $d = 0.55$ ft, giving $v = 3.8$ ft per sec. The vertical line for $v = 3.8$ intersects the "guide line" at $H_v = 0.225$. In the second case let $Q = 0.6$ cu ft per sec, with water flowing 0.27 ft deep in a 36-in. pipe. Set the dividers for the distance 1.0 to the left to 0.6 and measure this distance to the left from the intersection of the 36-in. pipe with the $d = 0.27$ horizontal line, finding $v = 1.86$ ft per sec. The vertical line for $v = 1.86$ intersects the guide line at $H_v = 0.056$ ft.

To find the velocity head for any value of Q, first assume an approximate value of the velocity head, subtract it from the quantity-energy head, and note the assumed depth. Enter Fig. 4 with these values of Q and d and read the velocity head. If this differs materially from the assumed value, a second approximation should be made. To draw the velocity-head curve it is obviously better to begin with a small value of Q because the error in the assumed value of the velocity head is correspondingly small and one or two approximations are usually sufficient. It will be found that only a few points are required to draw in the quantity-velocity head curve. Ordinates on the quantity-depth curve are merely the differences between the ordinates of the quantity-energy head curve and the quantity-velocity head curve. This quantity-depth curve is the required rating curve.

As an illustration of the method of computing a rating curve, consider a Venturi flume with trapezodial throat cross-section as in Fig. 1(*a*), 12 in. wide at the base with side slopes of 2 on 1 and a flat slab base 3 in. above the invert of a 24-in. pipe. All measurements are in feet and quantities in cubic feet per second. As previously recommended, various critical depths will be assumed and Q and ϵ computed. In this case the formulas for the cross-sectional area and water-surface width in the throat are:

$$A = \left(1 + \frac{d_c}{2}\right) d_c \qquad (15)$$

and,

$$B = 1 + d_c \qquad (16)$$

The computations for energy heads are arranged in Table 1. In computing the velocity heads (see Table 2), it must be remembered that the crest of the throat is 0.25 ft above the invert; hence, the depth in the conduit must be increased by that amount. The velocity head in the conduit can be obtained only by trials preferably starting with the small values of Q. In Table 2 when $Q = 2$ cu ft per sec, the depth in the conduit will be somewhat less than $\epsilon + {}^{+}0.25 = 908$. For 2 cu ft per sec, at a depth of 0.9 ft in a 24-in. pipe, Fig. 4 gives $H_v > 0.03$. Assuming $H_v = 0.03$, the depth becomes 0.88 with a resultant value of $H_v = 0.035$. This is not a sufficient change to effect the result so 0.035 can be assumed as the final value. Since the crest of the

throat is taken as the datum, this 0.035 is to be subtracted from the value of ϵ. The velocity heads for other values of Q are found in the same way, except that after two or more have been computed an assumed value for the next one may be obtained by extending the curve drawn through the known points.

TABLE 1.—QUANTITY-ENERGY HEAD CURVE

d_c	0.2	0.4	0.6	0.8	1.0	1.2
0.5 d_c	0.1	0.2	0.3	0.4	0.5	.....
1 + 0.5 d_c	1.1	1.2	1.3	1.4	1.5	.....
A	0.22	0.48	0.78	1.12	1.50	1.88*
B	1.2	1.4	1.6	1.8	1.93*	1.79*
$\frac{A}{B}$	0.183	0.343	0.487	0.622	0.777	1.050
Q	0.53	1.60	3.09	5.02	7.50	11.00
H_v	0.092	0.172	0.244	0.311	0.389	0.525
ϵ	0.292	0.572	0.844	1.111	1.389	1.725

* By scale and planimeter (see Fig. 1).

Table 1 is extended to a value, $Q = 11.0$. The energy head was so regular that it was extended by eye to $Q = 12$, and Table 2 is computed to this limit although it is subject to some suspicion for $Q > 11.0$. These curves are all shown in Fig. 3.

TABLE 2.—QUANTITY-VELOCITY HEAD CURVE.

Q =	2	4	6	8	10	12
ϵ =	0.658	0.978	1.225	1.438	1.630	1.812
ϵ+0.25 =	0.908	1.23	1.48	1.69	1.88	2.06
Assumed H_v =	0.03	0.07	0.09	0.14	0.19	0.25
ϵ+0.25−H_v =	0.88	1.16	1.39	1.55	1.69	1.81
H_v (final) =	0.035	0.064	0.100	0.145	0.198	0.256
d=ϵ−H_v =	0.623	0.914	1.125	1.293	1.432	1.556

An exponential formula may be written for some small sections of the final rating curve, but it is not advisable. The inaccuracies of such a formula can be appreciated by equating the value of ϵ in Equation (2) for both the throat and conduit sections; thus,

$$d_c + \left(\frac{Q}{A_c}\right)^2 \frac{1}{2g} = d + \left(\frac{Q}{A}\right)^2 \frac{1}{2g} \quad \text{.....(17)}$$

which reduces to,

$$Q = \sqrt{2g \frac{(d - d_c)\, A\, A_c}{A - A_c}} \quad \text{.....(18)}$$

Writing $A = f(d)$ and $A_c = \phi\ (d_c)$:

$$Q = \sqrt{2g \frac{(d - d_c)\, f\,(d)\, \phi\ (d_c)}{f\,(d) - \phi\ (d_c)}} \quad \text{.....(19)}$$

Since $f(d)$ is not a simple function in a circular pipe, it is evident that the use of an exponential formula is generally inadvisable because of the many different combinations depending on the relative size of the pipe and throat, and the height of the crest of the throat above the invert.

Energy Losses

One of the chief disadvantages of water measurement with a weir is the relatively large and uncertain loss of energy. Schoder and Turner[a] show how the so-called constant of a weir is subject to wide changes depending on the size and setting. This change in the constant can be interpreted as a variation in the energy loss, and it follows that if such variations can be limited by the use of other devices, the change in so-called constants will likewise be restricted. In the case of the weir such control is difficult and at times impossible; with a Venturi flume it may be accomplished easily.

In the adaptation of the Venturi flume, to the writers' ideas, considerable attention was given to the design of the transitions to minimize loss of energy. In the hydraulic design of flume transitions Hinds[11] found, in making twenty-nine tests on ten flume inlets, that only three had losses amounting to more than $0.1\,\Delta H_v$. In a number of cases no measurable loss occurred and the average was about $0.04\,\Delta H_v$. The 4-ft diameter of a standard sewer manhole limits the length of the transition that can be built readily in an existing sewer. In the sewerage system of the Los Angeles County Sanitation Districts, a ratio of three longitudinally to one transversely has been adopted as a compromise. To determine the energy losses through Venturi flumes constructed by the Districts, a differential meter acting on the principle of a Pitot meter was devised. This is shown in Fig. 5.

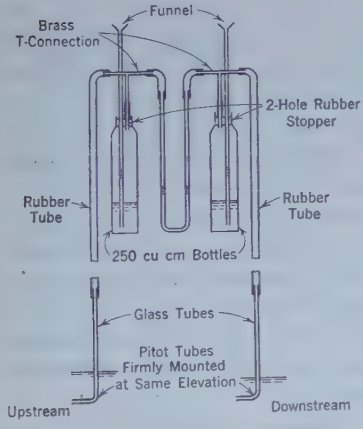

Fig. 5.—Differential Energy Meter.

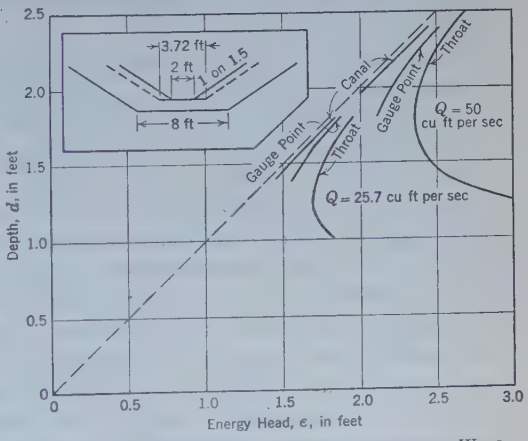

Fig. 6.—Energy Curves, Control Section Weir.

Two bent tubes are set at two points in the stream with orifices at the same elevation and pointing up stream, one in the throat and one above the inlet transition. These two tubes are connected by means of air tubes to a manometer filled with colored water; the displacement of the water column in the manometer after all water is blown out of the bent tubes measures the difference in energy head at the two points. To allow for any compression of the

[11] "The Hydraulic Design of Flume and Siphon Transitions", by Julian Hinds, M. Am. Soc. C. E., *Transactions*, Am. Soc. C. E., Vol. 92 (1928), p. 1423.

air which might occur in the tubes it was found advisable to blow air into each from time to time during the test. This was accomplished by pouring water into the two bottles, forcing air out through the orifice tubes. In sewage, one or the other of the orifice tubes may become clogged by floating matter, throwing the manometer out of balance. The manometer resumes its balance when the obstruction has been cleared away and a little more air forced into the tubes. Any type of meter in which water is drawn into the tubes will be clogged by sewage. This simple, head-differential apparatus has been found to be accurate and sensitive.

Several tests with the differential-energy meter (Fig. 5) integrated over the entire cross-section have shown that no energy losses greater than 0.005 ft occur in any of the meter throats thus far installed, and as many stage recorders are not sensitive to such small changes this energy loss is practically negligible. Should an appreciable loss be found in a given installation for high velocities it can be added to the quantity-energy head curve.

In sewage measurement, the mean daily flow is usually required. This may be calculated with sufficient accuracy by using a planimeter on a water-stage record to get the mean depth. If it is suspected that there are energy losses through the Venturi flume at higher flows the differential energy meter can be used at various stages, including the maximum, to correct the curve; and if the flow is increasing from year to year, the corrections may be determined beforehand, as the maximum flow of to-day will be the mean flow some months or some years hence.

Another possible source of error seems to be that in an open conduit the surface velocity is about 25% greater than the mean, which should cause the velocity head at the surface (where the float is installed for measurements), to vary as the ratio of 1.00^2 to 1.25^2, or 56% greater than the mean. If this condition existed, 1.56 H_v should be subtracted from the quantity-energy head instead of 1.0 H_v, in order to obtain the proper depth in making a rating curve. This condition was tested at one meter formed by placing a flat slab, 6 in. thick (at the invert), on the bottom of a 54-in. sewer pipe without side contractions. In the regular pipe channel, at the upper end of the transition section and at mid-stream, a Pitot tube was turned up stream and then at right angles to the current. The difference between these two measurements was the true velocity head, which, added to the measured depth, gave the total-energy head. Applying this energy head to the previously computed quantity-energy head curve gave the quantity. Readings taken at various depths between the center and sides of the stream showed substantially

TABLE 3.—Relation Between the Measured and the Theoretical Velocity Heads at Mid-Stream.

Quantity, Q, in cubic feet per second	Calculated velocity, V, in feet per second	Theoretical head, H_v, in feet	Measured head, H_v, in feet
8.2	2.18	0.074	0.076
10.25	2.50	0.097	0.096
17.5	3.15	0.153	0.142

the same velocity head at all points. Table 3 shows the relation between the measured and the theoretical velocity heads at mid-stream. These results indicate that within the accuracy of the measurements the velocity had in the conduit may be assumed to be the mean velocity head.

An investigation of the velocity-head correction for hydraulic flow by O'Brien and Johnson[12] indicates that, in this case, such a correction might amount to from 4 to 10% of the velocity head. As this is less than the limit of accuracy for a stage recorder with a float set in the main stream it may be neglected. For measurements in clear water, using a float-well for more accurate measurements, it should be determined experimentally.

When the velocity above the meter is less than 2 ft per sec the water surface is usually smooth, but above this velocity waves begin to form, probably caused by the difference in velocity heads in the region adjacent to the sides of the conduit. The waves are too small to affect the ball-float, but would affect very precise measurements made with a hook-gauge. Where they are usable float wet-wells would obviate this trouble, but in sewers the floats are affected by the accumulation of decomposing sludge.

One question that may be raised is the effect on the energy head of different velocities at various points in the cross-section of the throat. It was found that the energy head was the same at all points in a transverse plane. As another check, small floats were dropped simultaneously into the upper end of the throat in pairs, one being near the side and the other nearer the center. Every time, both floats reached the lower end together. As another test a string was dropped into the throat transversely to the flow line and reached the lower end straight. The explanation of this phenomenon is that at, and near, the critical velocity in a short flume the side friction is not an appreciable factor.

Efforts were made to find a coefficient to be applied to H_v in the conduit. The flow was determined by measuring the energy head in the throat with a Pitot tube. Using this value of Q, the measured depth was subtracted from the energy head to give $C\,H_v$. Within the accuracy of measurements, flows of 10.3 cu ft per sec, at a velocity of 2.4 ft per sec, and 17.5 cu ft per sec, at a velocity of 3 ft per sec, in the conduit both gave $C = 1$. These were the largest flows and velocities available.

Experimental Verification

In the experiments made by the U. S. Bureau of Reclamation,[7] a wooden throat with a bottom width of 2 ft and side slopes of 1 on $1\frac{1}{2}$ was installed in an earthen canal with a bottom width of 8 ft and similar side slopes. The bottom of the throat was 8 in. above the base of the canal and the downstream apron end of the throat sloped downward to a point 8 in. below the elevation of the canal base, similar to the Parshall meter. The gauge-point was placed in the upper transition where the bottom width was approximately

[12] "Velocity Head Correction for Hydraulic Flow", by M. P. O'Brien, Assoc. M. Am. Soc. C. E., and J. W. Johnson, Jun. Am. Soc. C. E., *Engineering News-Record*, Vol. 113, 1934, p. 214.

3.72 ft. It was placed only 0.4 ft down stream from the upper end of the wooden flume section where it was certain no silt deposit would occur. The writers have drawn energy curves for the flume (Fig. 6) at the control, or throat section, the gauge-point, and in the main canal for 50 and 25.7 cu ft per sec, respectively.

Had the gauge-point been moved back into the main canal, the measured depth would have been greater by about 0.1 ft in the case when $Q = 50$ cu ft per sec, but the main argument in favor of moving up stream is that the drop in the water surface indicates convexity, especially as it increases rapidly with the tapering of the channel, and it is in the convex water surfaces that the relation of the water surface to energy head is not correctly given by the Bernoulli theorem. Had the gauging-point been placed in the regular channel above as suggested, and the sides and bottom lined for a few feet to maintain a uniform cross-section, the stream filaments would have been parallel and the calculated flow would have followed more closely the volumetric measurements. Friction due to the longer distance between the point of measurement and the throat could have been measured by means of the differential energy-head meter (Fig. 5) and the energy head increased by this amount.

With this change in the point of measurement the recorded tests would have shown closer agreement with the calculated rating curve. Since the quantity of water flowing through this Venturi flume tested by the Bureau of Reclamation was carefully measured volumetrically the data are considered most reliable. From the known dimensions a quantity-depth or rating curve was readily constructed by the writers using the method previously outlined. As stated by Hinds the difference between the quantities taken from this curve for given depths and the actual measurements in no case exceeded 5 per cent. Since the writers have pointed out that greater accuracy could have been attained by the selection of a better place for measuring the depths, and by measurement of frictional losses, this test is sufficient proof that all forms of the Venturi flume will give accurate measurements when it is possible to measure the depth in the conduit of a regular cross-section immediately above the throat and where the throat is properly designed to insure that the water reaches critical depth.

In the absence of an experimental laboratory the writers have had to make use of active sanitary sewers in the development and adaptation of the Venturi flume designs. Standard weirs were set in adjacent manholes, but comparative results were poor except where the flow was small in comparison with the capacity of the sewer, since the weir coefficients were uncertain. Therefore, these measurements were not considered sufficiently accurate to verify those obtained from the Venturi flumes.

The experiments made by the U. S. Bureau of Reclamation, previously referred to, were considered a positive check on the accuracy of the method outlined herein. Furthermore, a field test, comparing measurements of a temporarily installed Venturi flume with a permanent Parshall meter (made through the co-operation of the Cities of Los Angeles and Beverly Hills), supplied added proof of the accuracy of the adapted Venturi flume.

At the point selected for the test an elaborate underground structure was constructed on a 21-in. sewer line which included a standard 12-in. Parshall meter and an indicating and recording register, showing the depth of flow through the flume and the rate of flow, in cubic feet per second. Water continuously running into the float-well prevented the accumulation of sludge which otherwise would affect the float results. The wooden throat of the temporary Venturi flume was installed in an ordinary standard manhole about 1 000 ft above the permanent gauging station, where the grade of the 21-in. sewer was 0.70 per cent. The bottom of the throat with a width of 10 in. was placed 2 in. above the invert. Although the boards forming the side slopes were intended to be set at a slope of 2 on 1, the irregularities of the pipe caused them actually to be placed on slopes of 2 on 1 to 12 on 1.

Tin transitions for stream-lining the upper end were attached to the boards, but could not be set in exact position due to the roughness of the channel through the manholes. Some caulking had to be done with oakum. The entire apparatus was quickly installed in the sewer during the low early morning flow and readily withdrawn a few hours later when the flow was at its peak of about 6 cu ft per sec. The elevation of the bottom of the throat was referred to a straight-edge placed across the manhole rim in the street pavement and measurements to the water surface above the flume were made with a steel tape.

Readings were taken simultaneously at the Venturi flume and the Parshall meter, a correction in time being made between the two stations as determined by passing floats occasionally from one to the other. A correction was also required for the small flow entering the sewer from a side branch at a point between the two testing stations. Occasional depth measurements over a V-notch gave this correction with sufficient accuracy.

Table 4 gives the results of tests when the flow was within the capacity of the Venturi flume. In Table 4(*a*) the average discrepancy between the two methods of measurement was 4.2%, with a probable error of $\pm$ 0.4 per cent.

During the period of high flow (8:28 to 8:58) it was found that the critical depth in the throat exceeded the depth of the Venturi flume. These results are shown in Table 4. In this second group the discrepancy was + 6% $\pm$ 0.7%, showing that even when poorly adapted it was still comparatively correct. The 4% error in the first group could be corrected by allowing a head loss of 0.25 H_v, or by subtracting 0.75 H_v instead of H_v from the energy head. Doubtless the discrepancy could be reduced materially by carefully installing a permanent concrete Venturi flume instead of the temporary wooden one which was used. Any obstruction placed in this sewer laid on a slope greater than the critical causes the water to jump immediately to the conjugate depth on the energy-head curve (Fig. 1) and unless allowance is made for this effect, the capacity of the sewer would be curtailed seriously. Therefore, it was necessary to use a large throat with a consequent rather high velocity of approach. It has been found that the slower the velocity of approach the greater the accuracy. This is limited by the capacity of the conduit and the possibility of forming deposits in the approach channel which would affect the rating curve.

TABLE 4.—COMPARATIVE MEASUREMENTS WITH A VENTURI FLUME AND PARSHALL METER.

(Flow Q, in cubic feet per second.)

Time	Venturi Flume		Parshall, Q'_p	Side inflow, Q''_p	Q_p = Column (4) minus Column (5)	$\triangle Q$ = Column (6) minus Column (3)	Ratio: Column (6) / Column (3)
	Depth, in feet	Q_v					
(1)	(2)	(3)	(4)	(5)	(6)	(7)	(8)
			(*a*) First Group				
5:57	0.545	1.45	1.57	0.14	1.43	−0.02	0.98
6:01	0.545	1.45	1.57	0.14	1.43	−0.02	0.98
6:03	.....	....	1.50	0.14	1.36	....	.....
6:05	.....	....	1.43	0.14	1.29	....	....
6:06	0.495	1.22	....	....	1.23	+0.01	1.01
6:07	.....	....	1.30	0.13	1.17	.....	.....
6:08	0.485	1.18	....	....	1.12	−0.06	0.95
6:09	.....	....	1.20	0.13	1.07	....	....
6:10	0.465	1.11	....	....	1.06	−0.05	0.95
6:13	0.443	1.04	....	....	1.02	−0.02	0.98
6:15	0.443	1.04	....	....	0.99	−0.05	0.95
6:17	.....	....	1.10	0.13	0.97	.....	.....
6:18	0.443	1.04	....	....	0.96	−0.08	0.92
6:19	.....	....	1.07	0.12	0.95	.....	....
6:22	0.433	0.98	1.07	0.12	0.95	−0.03	0.97
6:24	.....	....	1.07	0.12	0.95	.....	....
6:27	0.437	1.00	1.05	0.12	0.93	−0.07	0.93
6:31	0.433	0.98	....	....	0.92	−0.06	0.94
6:32	.....	....	1.04	0.12	0.92	.....	....
6:37	0.453	1.06	1.09	0.13	0.96	−0.10	0.91
6:42	0.516	1.31	1.39	0.13	1.26	−0.05	0.96
6:48	.....	....	1.48	0.14	1.34	.....	....
6:50	0.558	1.50	....	....	1.41	−0.09	0.94
6:52	.....	....	1.62	0.14	1.48	.....	....
7:23	0.730	2.43	2.47	0.16	2.31	−0.12	0.95
7:26	0.745	2.53	....	....	2.48	−0.05	0.98
7:28	0.790	2.78	....	....	2.58	−0.20	0.93
7:31	0.813	2.91	....	....	2.77	−0.14	0.95
7:33	.....	....	3.05	0.17	2.88	.....	....
7:34	0.830	3.00	....	....	2.95	−0.05	0.98
7:35	0.850	3.13	....	....	3.02	−0.11	0.97
7:37	0.870	3.28	....	....	3.17	−0.11	0.97
7:38	.....	....	3.42	0.18	3.24	.....	....
7:39	0.910	3.56	....	....	3.31	−0.25	0.93
7:41	0.953	3.86	....	....	3.54	−0.32	0.92
7:43	.....	....	3.80	0.19	3.61	.....	....
7:48	.....	....	3.89	0.19	3.70	.....	....
7:52	0.985	4.12	....	....	3.89	−0.23	0.94
7:53	.....	....	4.18	0.19	3.99	.....	....
7:55	0.975	4.02	....	....	4.08	+0.06	1.02
7:58	1.015	4.37	4.40	0.19	4.21	−0.16	0.96
8.01	.....	....	4.47	0.20	4.27	.....	....
8:03	1.015	4.37	....	....	4.31	−0.06	0.99
Mean...	.....	....	....	....	....	.....	0.958
			(*b*) Second Group				
8:28	1.057	4.75	5.33	0.20	5.13	+0.38	1.08
8:32	1.067	4.87	....	....	5.26	+0.39	1.08
8:33	1.077	4.97	5.50	0.21	5.29	+0.32	1.06
8:38	.....	....	5.65	0.21	5.44	.....	....
8.40	1.083	5.00	....	....	5.51	+0.51	1.10
8:43	.....	....	5.79	0.21	5.58	.....	....
8:44	1.120	5.35	....	....	5.59	+0.24	1.04
8:48	.....	....	5.83	0.21	5.62	.....	....
8:50	1.120	5.35	....	....	5.61	+0.26	1.05
8:53	.....	....	5.81	0.21	5.60	.....	....
8:56	1.135	5.50	....	....	5.65	+0.15	1.03
8:58	1.140	5.55	5.92	0.21	5.71	+0.16	1.03
Mean...	.....	....	....	.....	....	.....	1.06

Design of Venturi Flume

The proper design of a Venturi flume requires that parallel flow occur in the channel[13] above the flume and in the throat. The necessary critical velocity is obtained only when a drop in the energy head occurs just below the throat. A small jump in the water surface at this point (see Fig. 1) is positive evidence that critical velocity is occurring. In addition, the throat section must have sufficient length or the water will not be flowing in parallel filaments at the point of critical depth. The first meter stations installed by the Sanitation Districts of Los Angeles (Calif.) County had short throats which gave good results only on the small flows. Lengthening the throat to 3 ft insured parallel flow through more of the length, and tests with a Pitot tube showed no apparent change in energy head except at the ends. Data are lacking to formulate a rule as to the proper length, but experience indicates that the throat should be at least as long as the diameter of the pipe. A comparison of flow through two Venturi flumes in consecutive manholes, with 36-in. and 6-in. throat lengths, respectively, showed a ratio of 1.0 to 0.8, the longer throat indicating the larger flow.

The important features of the Venturi flume are its adaptation to stream-flow measurement in all shapes of conduits not flowing under pressure and its ready installation in lines to which access is much restricted. The device can always be installed in an existing line and often without serious interruption to the flow.

The size of the flume throat depends upon the size and grade of the conduit and the range of flow it is desired to measure. The ideal flume throat would have such a size and shape that the ratio of the cross-section of the water in the throat to that in the conduit would be the same for all quantities; but such a throat would be impossible to design and build because the ratio of the critical depth to the depth in the conduit is not a constant.

For a flow that is only a small percentage of the designed capacity of a conduit, a throat, V-shaped, or narrow at the bottom, with sloping sides, is satisfactory. However, such side walls are difficult to hold in place. A rectangular narrow throat may contract the flow so much as to give inadequate capacities for larger flows.

For circular pipes it has generally been found advisable to install a bottom slab in addition to the two sides, a feature which helps to support the side walls. The slab acts as a broad-crested weir when flows are only a small percentage of the designed capacity. Since a thin bottom slab properly stream-lined by approach transitions causes no deposition of solids except possibly at the very lowest velocities, such a slab is recommended, especially on the lighter grades, to offset any possible chance of back-water from an unforeseen obstruction below that might otherwise prevent critical velocity from being attained. In general, the flatter the slope, the more necessary is this precaution and the greater the slab thickness needed.

A throat of rectangular cross-section with proper transitions may be adaptable in some cases, as in the instance of a semi-elliptical section, or a rec-

[13] "Hydraulics of Open Channels", by B. A. Bakhmeteff, M. Am. Soc. C. E., 1932, p. 28.

tangular-shaped conduit, where its use is recommended. Lack of accuracy in very low flows and inability always to pass the full design capacity, however, are restricting limitations to its general use.

Where a large flow in either rectangular or circular-shaped conduits prevents the placing of forms for building the side walls, a simple device to create critical velocity consists of placing on the invert a pre-cast flat slab with transitions. Deposition can only occur above this type at extremely low velocities. In similar cases involving large flows critical velocity may be produced by simply inserting vertical side walls with the proper transitions.

The important factor in the construction and installation of any form of Venturi device is that a constriction of some sort be placed in the channel to produce critical velocity with the least loss of energy, and that the shape, size, and dimensions of the device are important only in so far as they meet the specific problem at hand in a practical manner.

The correct size and shape of throat for use in a given conduit is that one for which the energy head is greater than the normal energy head in the free flowing conduit at all values of Q, and with a bottom slab thin enough to prevent deposition of sludge at low flow. A practical method of making this selection is first to prepare quantity-energy head curves for several sizes of Venturi flume throats (Fig. 7) on tracing cloth. Table 5 can be used for

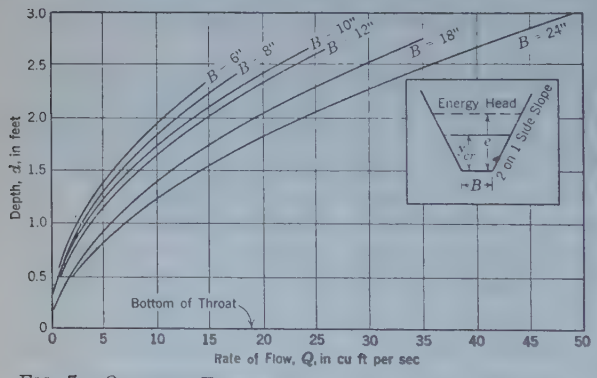

FIG. 7.—QUANTITY-ENERGY HEAD CURVE FOR VARIOUS THROAT SIZES WITH SIDE SLOPES OF 2 ON 1.

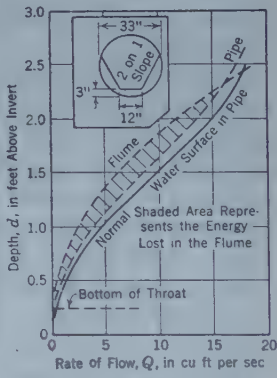

FIG. 8.—ENERGY HEAD CURVE, VARIOUS THROAT SIZES.

constructing these curves for trapezoidal throats having side slopes of 2 on 1. Next, on the same scale, a quantity-energy head curve is drawn for the conduit under consideration, assuming unobstructed flow. Any formula for flow in open channels may be used for first constructing a quantity-depth curve, but the following procedure is suggested. Bakhmeteff[14] expresses the Chezy formula, as follows,

$$Q = K \sqrt{S} \quad \ldots\ldots\ldots\ldots\ldots\ldots\ldots\ldots\ldots\ldots (20)$$

in which,

$$K = A C \sqrt{R} \quad \ldots\ldots\ldots\ldots\ldots\ldots\ldots\ldots\ldots\ldots (21)$$

[14] "Hydraulics of Open Channels", by B. A. Bakhmeteff, M. Am. Soc. C. E., 1932, p. 13.

Computing K as a function of the depth in a pipe is rather tedious. Values of K are shown for several pipe sizes in Fig. 9 which has been computed for $n = 0.013$ and $S = 0.01$ in Kutter's formula. Drawn to a logarithmic scale,

TABLE 5.—ENERGY-HEAD TABLES FOR THROATS WITH SLIDE SLOPES OF 2 ON 1

Rate of flow, Q, in cubic feet per second	Energy Head, in Feet, for Bottom Widths, in Inches					Rate of flow, Q, in cubic feet per second	Energy Head, in Feet, for Bottom Widths, in Inches				
	6	8	10	12	18		6	8	10	12	18
0.2	0.232	0.198	0.176	0.156	0.121	10.00	1.941	1.820	1.719	1.623	1.388
0.5	0.401	0.348	0.311	0.280	0.219	12.00	2.117	1.993	1.887	1.786	1.540
1.0	0.594	0.526	0.474	0.431	0.342	14.0	2.276	2.149	2.041	1.936	1.679
2.0	0.865	0.779	0.713	0.654	0.529	16.0	2.422	2.294	2.183	2.075	1.809
3.0	1.070	0.975	0.897	0.829	0.680	18.0	2.558	2.428	2.315	2.205	1.930
4.0	1.239	1.136	1.054	0.978	0.810	20.0	.....	.....	2.439	2.327	2.045
5.0	1.384	1.279	1.191	1.109	0.926	25.0	.....	.....	.....	2.604	2.308
6.0	1.515	1.406	1.314	1.228	1.032	30.0	.....	.....	.....	2.852	2.544
7.0	1.634	1.522	1.426	1.337	1.130	35.0	.....	.....	.....	3.078	2.759
8.0	1.743	1.628	1.530	1.438	1.221	40.0	.....	.....	.....	.....	2.958
9.0	1.845	1.727	1.627	1.532	1.306	....	.....	.....	.....	.....	.....

it is merely necessary to add one-half the logarithm of the slope (expressed as a percentage) to obtain the quantity for any depth in the pipe. Velocity heads are obtained from Fig. 4 in the manner previously described. Adding these velocity heads to the depths shown on the quantity-depth curve gives the quantity-energy head curve. Fig. 8 shows a typical diagram.

Referring to Fig. 9, the capacity, Q, of a pipe is given by Equation (20) when S = the slope, expressed as a percentage; $K = A \times \frac{C}{10} \sqrt{R}$ for any given depth; and C = Chezy's coefficient. The curves are drawn for a 1% slope. For values of S less than 1% the flow for any depth will be to the left of the curve and for more than 1% to the right. To find the value of $\sqrt{S}$ measure from the slope guide to the right 10-line for $S < 1\%$ and to the left for $S > 1$ per cent. For example: Let $S = 0.25\%$; D = 8-in. pipe; and, $Q = 0.1$ cu ft per sec. In this case $S < 1$ per cent. Set the dividers for the distance between the inclined slope line in percentage line and the right 1.0-line of the diagram at $S = 0.25$. Transfer this distance to the $Q = 0.1$-line, measuring to the right and intersect the 8-in. curve at $d = 0.20$ ft. If Q is given in million gallons daily, set the dividers for the distance between the inclined line and the million-gallon-daily guide line on the extreme right. For $S = 0.25\%$ and $Q = 0.1$ mgd, $d = 0.25$ ft in an 8-in. pipe.

On the other hand, let $S = 2.25$; D = 60-in. pipe; and $Q = 15$ cu ft per sec. In this case $S > 1$ per cent. Set the dividers for the distance from the inclined slope line to the 0.1-line to the left at $S = 2.25$. Transfer this distance to the $Q = 15$-line, measuring to the left and intersect the D = 60-in. line at $d = 0.66$ ft.

By superimposing the quantity-energy head curves for the throat upon that for the pipe and then moving the throat tracing up or down, it is possible to decide quickly which throat size should be used and how high it should be set above the invert. The difference in the two energy heads shows the

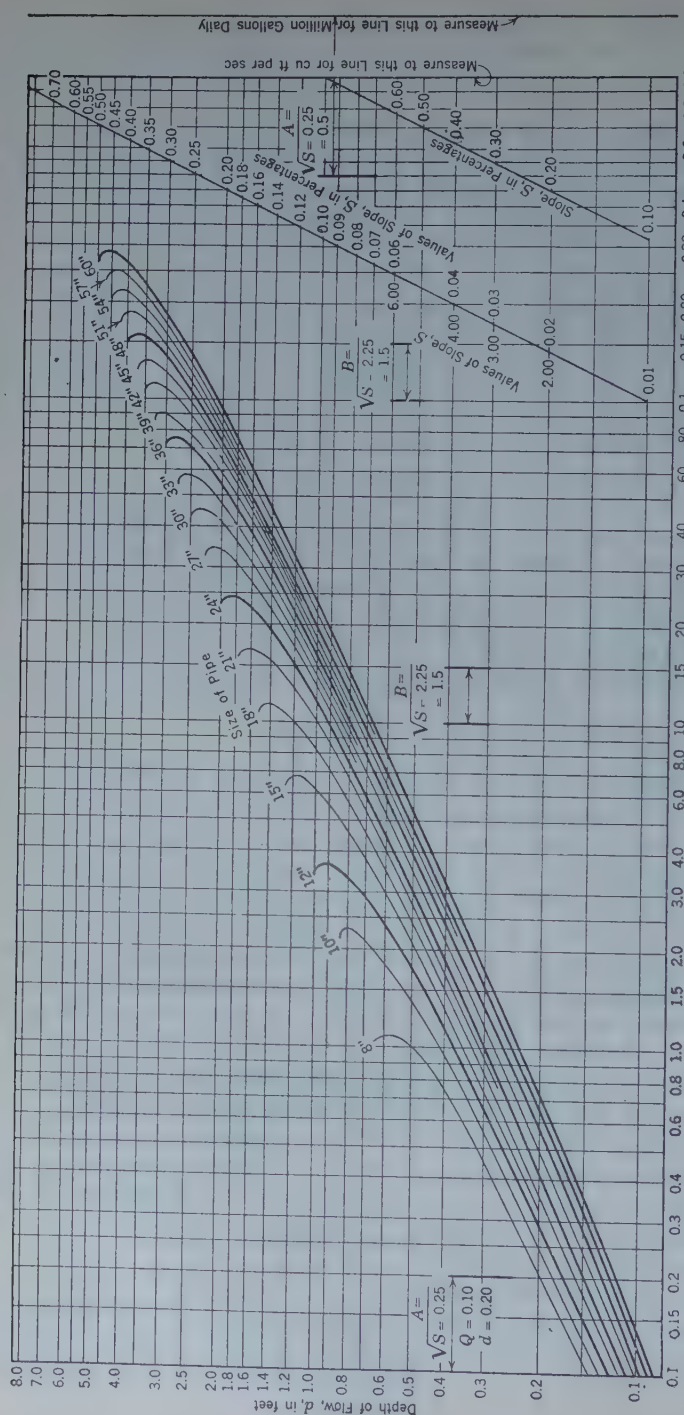

FIG. 9.—DISCHARGE OF PIPES WITH WATER FLOWING AT VARIOUS DEPTHS WHEN KUTTER'S $n = 0.013$.

loss caused by the Venturi flume for all quantities. Fig. 10 shows typical quantity-energy head curves for both a trapezoidal and a rectangular throat superimposed upon a quantity-energy head curve for a 33-in. circular pipe,

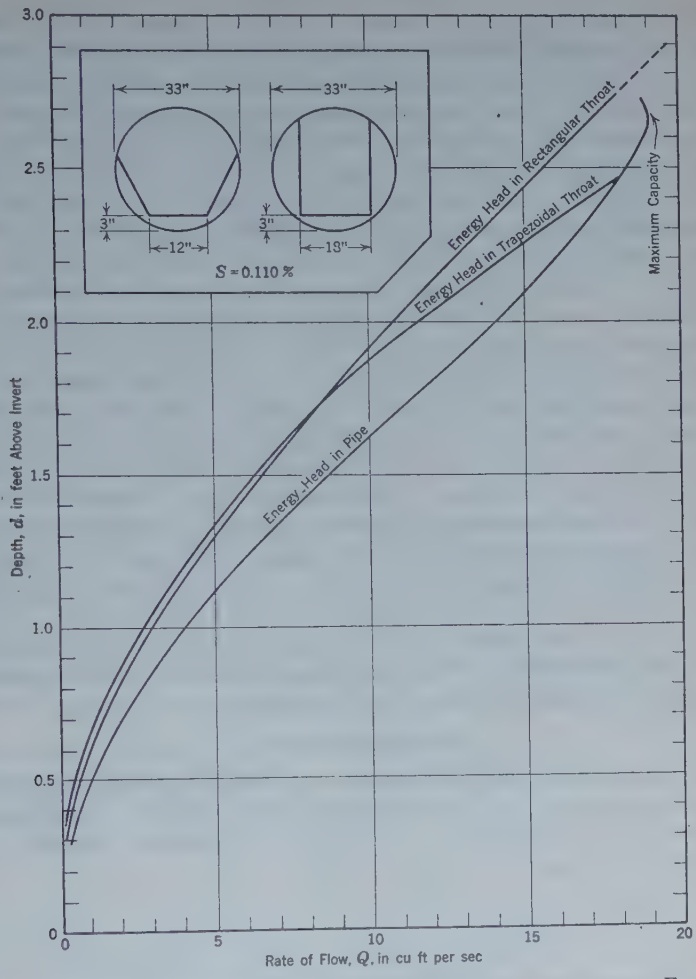

FIG. 10.—COMPARATIVE ENERGY HEAD IN TRAPEZOIDAL AND RECTANGULAR FLUMES.

and it is easily seen that the trapezoidal section can be used as a meter for flows as great as 18 cu ft per sec and that at 19 cu ft per sec, which is the maximum capacity of the pipe (there being no loss in energy through the flume), the carrying capacity of the pipe is not curtailed. The quantity-energy head curve of the rectangular flume (Fig. 10) being always above the energy head for the pipe, shows loss of energy through the flume at maximum designed capacity. This type of Venturi flume would interfere with the use of the sewer at full capacity. It is more accurate to compute the rat-

ing or quantity-depth curve from actual measurements of the flume as constructed than to base it upon the design curves. Figs 4 and 9 are for use with circular pipes, but similar curves may be computed for conduits of any shape.

For permanent installation in sewers of the Los Angeles County Sanitation Districts the Venturi flumes were readily constructed of concrete directly in the sewer manhole without interruption to sewage flow. A layout sketch of the meter was prepared for a single installation in a circular pipe and, using the plan as a pattern, forms for other sizes were obtained by proportion. When possible the entire form for the flume was assembled in the sewer manhole invert and concrete was poured into the forms from one side until the bottom slab was filled in order to assure complete displacement of the sewage. Use of a fast-setting cement had distinct advantages in such installations.

Placing the center of the throat at about the lower side of a manhole gave proper space for installing the stage-recorder float near the upper side at a point where the flow in the pipe was uniform. The float consists of an 8-in. copper ball fastened to a 2-ft length of $\frac{1}{2}$-in. pipe, hinged loosely up stream to a pipe framework (see Fig. 1). The latter is attached to the top of a plank placed cross-wise to the sewer and supported by the shelves of the manhole. Without some such apparatus to hold the ball, it tends to float down stream and disturb the record. The stage recorder is suspended on a specially built steel seat immediately under the manhole cover where it is readily accessible. Repeated checks of indicated stage records against actual measured depths show no appreciable error during the daily range of velocities. Braided, insulated, copper wire connects the float to the recorder. Considerable difficulty was experienced in keeping the stage recorder clocks running for a week at a time in the damp, gas-laden, sewer air, but the purchase of sealed clocks has practically solved this problem.

Acknowledgments

The writers are particularly indebted to A. K. Warren and to A. M. Rawn, Members, Am. Soc. C. E., for the opportunity to make the experiments and studies for this investigation, and for their constructive criticism in the preparation of the paper.

AMERICAN SOCIETY OF CIVIL ENGINEERS

Founded November 5, 1852

PAPERS

THE STRESS FUNCTION AND PHOTO-ELASTICITY APPLIED TO DAMS

By John H. A. Brahtz,[1] Esq.

Synopsis

The object of Part I of this paper is to familiarize engineers with the use of the Airy stress function for the solution of problems in plane stress and plane strain when ordinary engineering methods fail to give even approximate results.

The object of Part II is to familiarize the engineer with the photo-elastic phenomenon and its application to civil engineering structures and to compare results obtained in this way with the theoretical results obtained in Part I.

A brief popular outline of the theory is given accompanied by a description of the apparatus developed at the California Institute of Technology, at Pasadena, Calif. Methods of evaluating stresses are explained and applied to experiments on Morris Dam.

Introduction

Ordinarily, the theory of the Airy function found in textbooks[2] is based on the assumption that body forces (weight and inertia) can be neglected. This is entirely inadequate in civil engineering structures in which the stresses due to weight often are greater than those caused by boundary forces. Furthermore, in texts in which the body forces are included the definitions of stresses are generally such that the form of the function is not invariant to a change in co-ordinates. The stress definitions given herein, including both boundary and body forces, are such that the stress function will be of the same form in rectangular and polar co-ordinates.[3]

Note.—Discussion on this paper will be closed in December, 1935, *Proceedings*.

[1] With the U. S. Bureau of Reclamation, Denver, Colo.

[2] See, for example, "Applied Elasticity", by J. Prescott.

[3] "Notes on the Airy Stress Function", by John H. A. Brahtz, *Bulletin*, Am. Math. Soc., June, 1934.

The stress function is restricted to isotropic materials which follow Hooke's law in both compression and tension. It may also be applied, however, to concrete masonry structures if the resulting stresses are those of compression, or very slight tension, even if the elastic constants are not strictly constant for all stresses. It is generally conceded that a slight variation in the elastic modulus has little effect on the final stress distribution, except, of course, at singular points or at points of high stress concentration. With these assumptions the stress function may then be applied to a slice of a gravity dam. The question of uplift is not considered in this treatment, but it is assumed: (1) That there is sufficient resultant average compression at all points of the dam to overcome any internal pore pressures that may exist; and (2) that the pores are so small that the average stress distribution at a point may still be found as in isotropic material.

This paper, together with theoretical and experimental work done by others, shows that for purposes of analysis the triangular gravity dam on an elastic foundation may be divided conveniently into three regions: (1) The upper two-thirds of the dam proper; (2) the lower one-third, including the base region of the foundation; and (3) the foundation proper. Finally, special investigation must be made in the regions close to the heel and toe as to whether they are sharp corners or fillets, and near the crown. Consequently, in the present application, stress functions have been derived for four cases and a twofold purpose is served: (*a*) To show the methods of deriving stress functions; and (*b*) to obtain specific results applicable to the gravity dam on an elastic foundation. In most cases the derivations have been omitted, due to the limitation of space. The original manuscript is on file in Engineering Societies' Library, in New York, N. Y., and at the California Institute of Technology, at Pasadena, Calif.

Application I.—The stress functions, stresses, and deflections valid in the upper part of triangular dams are derived for hydrostatic, and are given for body, forces with computed results plotted in the case of Morris Dam. In addition, the stress functions are given for a number of special loadings.

Application II.—The stress functions applicable in the foundation are given with stresses and deflections for concentrated and distributed loads, the computed results being plotted for a study of Grand Coulee Dam.

Application III.—The "corner-function" applicable at sharp re-entrant corners is derived. Two methods of procedure are given for the determination of stresses in the lower part of gravity dams. The results are plotted for a study of Grand Coulee Dam.

Application IV.—An approximate method is derived for the determination of stresses at re-entrant sharp and rounded corners. Examples are computed for Morris Dam.

It should be emphasized that even if the gravity dam is used for illustrative examples of application, the aim is not to advance new design criteria. The writer hopes, however, that the methods described will help to obtain a closer estimate of the stresses that actually occur. It is worthy of note that a state of stress computed by the Airy stress function is in equilibrium and compatible with Hooke's generalized law.

ACKNOWLEDGMENT

Acknowledgment is freely given to Theodor von Kármán, Elwood Mead, S. B. Morris, J. L. Savage, and R. F. Walter, Members, Am. Soc. C. E., and to Professor H. Bateman, of the California Institute of Technology, Pasadena, Calif., for their valuable suggestions and co-operation in the preparation of this paper. The photo-elastic experiments on Morris Dam were made possible through the financial support of the Pasadena Water Department.

PART I.—THE THEORY OF THE AIRY STRESS FUNCTION

In this section the stress function is defined in rectangular and polar co-ordinates. Convenient forms of boundary conditions are treated.

A two-dimensional elastic system under plane stress or plane strain is in equilibrium if the stress components are defined as follows:

By rectangular co-ordinates:

$$\sigma_x = \frac{\partial^2 F}{\partial y^2} - g_x x - g_y y \quad \ldots\ldots (1a)$$

$$\sigma_y = \frac{\partial^2 F}{\partial x^2} - g_x x - g_y y \quad \ldots\ldots (1b)$$

and,

$$\tau_{x,y} = -\frac{\partial^2 F}{\partial x\, \partial y} \quad \ldots\ldots (1c)$$

in which σ_x and σ_y = components of normal stress parallel to the X-axis and the Y-axis, respectively; $\tau_{x,y}$ = shear stress in the direction of the X-axis or the Y-axis; F = a stress function; and g = the total body force per unit volume.

In the polar co-ordinates:

$$\sigma_r = \frac{\partial^2 F}{r^2\, \partial \theta^2} + \frac{\partial F}{r\, \partial r} - gr \cos(\theta - \beta) \quad \ldots\ldots (2a)$$

$$\sigma_\theta = \frac{\partial^2 F}{\partial r^2} - gr \cos(\theta - \beta) \quad \ldots\ldots (2b)$$

and,

$$\tau_{r,\theta} = -\frac{\partial}{\partial r}\left(\frac{\partial F}{r\, \partial \theta}\right) \quad \ldots\ldots (2c)$$

If, now, F is so restricted that it is a solution to the differential equation:

$$\nabla^4 F \equiv \frac{\partial^4 F}{\partial x^4} + 2\frac{\partial^4 F}{\partial x^2\, \partial y^2} + \frac{\partial^4 F}{\partial y^4} = 0 \quad \ldots\ldots (3a)$$

or,

$$\nabla^4 F \equiv \left(\frac{\partial^2}{\partial r^2} + \frac{\partial}{r\, \partial r} + \frac{\partial^2}{r^2\, \partial \theta^2}\right)^2 F = 0 \quad \ldots\ldots (3b)$$

the stress defined in Equations (1) and (2) will also be compatible with the generalized Hooke's law. Problems in plane stress or plane strain have thus

been reduced to the determination of the functions, F, that satisfy Equations (3) and such that the stresses determined by Equations (1) or Equations (2) agree with the given force distributions over the boundaries of the structure. The first part is very simple because it can be verified that both the real and imaginary parts of the expression:

$$F = A_1 f_1(z) + A_2 x f_2(z) + A_3 y f_3(z) + A_4 r^2 f_4(z) \ldots\ldots\ldots (4)$$

satisfy Equations (3). A_1, A_2, A_3, and A_4 are arbitrary constants; f_1, f_2, f_3, and f_4 are arbitrary analytic functions of the complex variable, $z = x + iy$; $r^2 = x^2 + y^2$; and $i = \sqrt{-1}$.

The second part of the problem (to satisfy the boundary conditions) is usually difficult, and must be solved for each individual case. It is important to realize that as soon as the stress function is known the stresses are also known at all points by Equations (1) or Equations (2).

Boundary Conditions

Referring to Fig. 1 the boundary conditions to be satisfied by $F(x, y)$ may be formulated in terms of well-known engineering concepts, as follows: Let

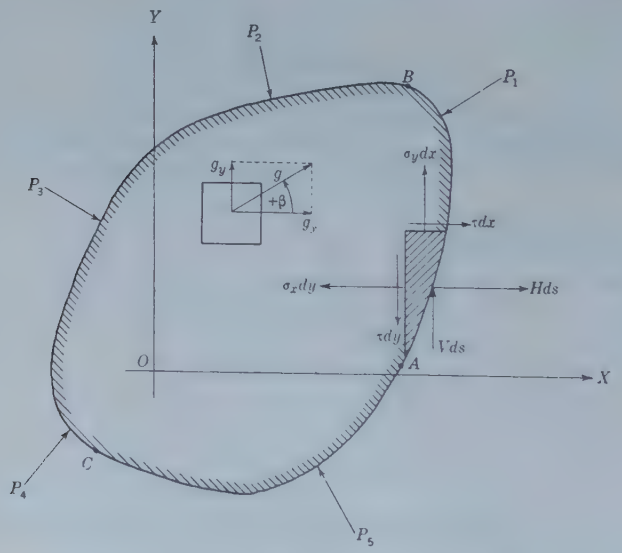

Fig. 1.

the area enclosed by the hatched boundary curve represent a plane elastic body of unit thickness, held in equilibrium by a system of forces, P_n (concentrated or continuously distributed), acting on the boundary, ABC, and body forces, g, per unit volume; g_x and g_y = components of g along the co-ordinate axes; and H and V = the forces along the X-axis and Y-axis per unit length of the boundary.

Consider an element, ds, at the boundary with co-ordinates (x, y). It is in equilibrium under the stresses and the boundary forces, $H\,ds$ and $V\,ds$, (Fig. 1). By projecting all forces on the co-ordinate axes and taking moments about a point, B, of the boundary with co-ordinates, $x_B\ y_B$, the conditions of equilibrium are:

$$\sigma_x\,dy - \tau\,dx = H\,ds \quad \ldots\ldots(5a)$$

$$\sigma_y\,dx - \tau\,dy = -V\,ds \quad \ldots\ldots(5b)$$

and,

$$(\sigma_x\,dy - \tau\,dx)\,(y_B - y) + (\sigma_y dx - \tau\,dy)\,(x_B - x) = dM \ldots.(5c)$$

in which dM indicates the moment of $H\,ds$ and $V\,ds$ about Point B, positive in direction (counter-clockwise about Point O, Fig. 1). The body forces of the element are of higher order of magnitude and need not be considered.

By substituting the stresses as defined by Equations (1) and integrating the equations from Point A, Fig. 1, along the boundary in the positive direction to Point B, the following equations are obtained:

$$\left(\frac{\partial F}{\partial y}\right)_B - \left(\frac{\partial F}{\partial y}\right)_A = X + g_x \int_A^B x\,dy + g_y \int_A^B y\,dy \ldots\ldots(6a)$$

$$\left(\frac{\partial F}{\partial x}\right)_B - \left(\frac{\partial F}{\partial x}\right)_A = -Y + g_x \int_A^B x\,dx + g_y \int_A^B y\,dx \ldots(6b)$$

and,

$$F_B - F_A - (x_B - x_A)\left(\frac{\partial F}{\partial x}\right)_A - (y_B - y_A)\left(\frac{\partial F}{\partial y}\right)_A = M$$

$$+ \int_A^B (xg_x + yg_y)\left[(x_B - x)\,dx + (y_B - y)\,dy\right] \ldots\ldots(6c)$$

in which X and Y are the projections along the X-axis and Y-axis; and M = the moment about B of all boundary forces between A and B. By a suitable choice of co-ordinate axes Equations (6) can be simplified somewhat. From the definition of the stresses in Equations (1), etc., it follows that a constant and terms that are linear in x and y, added to the stress function, contribute no stress. Therefore, by choosing the origin at Point A, Fig. 1, it is always possible to arrange matters so that $F_A = \left(\frac{\partial F}{\partial x}\right)_A = \left(\frac{\partial F}{\partial y}\right)_A = 0$.

The boundary equations then become:

$$\left(\frac{\partial F}{\partial y}\right)_B = X_B + g_x \int_0^B x\,dy + \frac{1}{2}\,g_y\,y^2{}_B \ldots\ldots(7a)$$

$$\left(\frac{\partial F}{\partial x}\right)_B = -Y_B + \frac{1}{2}\,g_x\,x^2{}_B + g_y \int_0^B y\,dx \ldots\ldots(7b)$$

and,

$$F_B = M_B + g_x \int_0^B (y_B - y)\, x\, dy + g_y \int_0^B (x_B - x)\, y\, dx + \frac{1}{6} x^3{}_B\, g_x + \frac{1}{6} y^3{}_B\, g_y \quad \ldots\ldots\ldots\ldots\ldots\ldots (7c)$$

In the definitions of X_B, Y_B, and M_B, it must be remembered that the integrations are to be carried out from the origin (Point O, Fig. 1) in the positive (X-Y) direction. Hence, if Point B is located in the negative direction from the origin, the signs of X_B, Y_B, and M_B, as defined in connection with Equations (6), must be reversed, exactly as in taking moments, thrust, and shear at a section of a beam in bending. This formulation of the boundary conditions will be found especially useful when approximate solutions are desired; that is, in case the boundary conditions are to be satisfied only at a few points.

In the cases of exact solutions (that is, if the boundary conditions can be satisfied at all point of the boundary), only two of the three sets of formulas Equations (5), (6), and (7) become especially simple and instructive. In be satisfied automatically. If no body forces exist (that is, if $g_x = g_y = 0$) Equations (5), (6), and (7) become especially simple and instructive. In this case the following simple interpretations of the stress function, F_P, and its partial derivatives, $\frac{\partial F}{\partial x}$ and $\frac{\partial F}{\partial y}$, are evident by Equations (7).

The value of F_P (the stress function for the given boundary forces) at any point, B, of the boundary is equal to the moment of all forces acting on the boundary between the origin and Point B. The value of $\frac{\partial F_P}{\partial y}$ at Point B is equal to the projection on the X-axis of the same forces and $\frac{\partial F_P}{\partial x}$ equals the negative projection on the Y-axis.

It is often convenient to determine two functions, F_P and F_g, the first representing the boundary forces and the second the body forces; then, $F = F_P + F_g$. If no mass forces exist the boundary conditions can be given a simple form on the portions of the boundary where no forces are acting, namely:

$$F = 0 \quad \ldots\ldots\ldots\ldots\ldots\ldots\ldots\ldots\ldots\ldots (8a)$$

and, the derivative normal to the boundary,

$$\frac{\partial F}{\partial n} = 0 \quad \ldots\ldots\ldots\ldots\ldots\ldots\ldots\ldots\ldots\ldots (8b)$$

When the stress function, F, is known, the displacements, u, parallel to the X-axis, and v, parallel to the Y-axis, can be determined in the case of plane stress by the expressions:

$$E\, u = -(1 + \mu) \frac{\partial F}{\partial x} - \frac{1 - \mu}{2} (g_x\, x^2 - g_x\, y^2 + 2\, g_y\, x\, y) + f_1 + A\, y + B \ldots (9a)$$

and,

$$E\,v = -(1+\mu)\,\frac{\partial F}{\partial y} - \frac{1-\mu}{2}\,(g_y\,y^2 - g_y\,x^2 + 2\,g_x\,x\,y) + f_2 - A\,x + C\,. \quad (9b)$$

in which, E is Young's modulus; μ is Poisson's ratio; f_1 = real part of $\int f(z)\,dz$; f_2 = imaginary part of $\int f(z)\,dz$; and, $f(z)$ is the analytic function of the complex variable:

$$z = x + iy = r\,e^{i\theta} \quad \ldots\ldots\ldots\ldots\ldots\ldots\ldots\ldots\ldots\ldots (10)$$

such that $\nabla^2 F$ = the real part of $f(z)$. The constants A, B, and C in Equations (9) determine the reference axis for u and v and only effect a solid-body rotation and translation.

In polar co-ordinates the radial and tangential displacements, u_r and v_θ, are given by:

$$E\,u_r = -(1+\mu)\,\frac{\partial F}{\partial r} - \frac{1-\mu}{2}\,g\,r^2\cos(\theta-\beta) + f'_1 + B\cos\theta + C\sin\theta\,. \quad (11)$$

and,

$$E\,v_\theta = -(1+\mu)\,\frac{\partial F}{r\,\partial\theta} - \frac{1-\mu}{2}\,g\,r^2\sin(\theta-\beta) + f'_2 + A\,r + C\cos\theta - B\sin\theta \quad \ldots\ldots\ldots\ldots\ldots\ldots\ldots\ldots\ldots\ldots (12)$$

in which f' = real part of $e^{-i\theta}\int f(z)\,dz$; f'_2 = imaginary part of $e^{-i\theta}\int f(z)\,dz$; and, $f(z)$ is defined as in connection with Equations (9). In Equations (11) and (12), the constants, A, B, and C, have the same meaning as in Equations (9). If no mass forces occur, $g = 0$. Displacements in the case of plane strain are found by Equations (9), (11), and (12), by replacing E with $\frac{E}{1-\mu^2}$ and μ with $\frac{\mu}{1-\mu}$.

Application I.—Stresses in the Upper Part of Triangular Gravity Dams

In order to indicate the general procedure for determining the stress function in the case of two-dimensional structures for a given loading the case of the infinite wedge with hydrostatic pressure on one side, and no body forces, will be developed in some detail. The solution was first offered by M. Levy.[4]

Assume the hydrostatic pressure on the up-stream face, $y = 0$, to be p at a unit distance from the top measured along the face; then, by Equation (11) with $y = 0$, the boundary conditions are (remembering that no mass forces occur so that $g_x = g_y = 0$):

$$\sigma_y \equiv \frac{\partial^2 F}{\partial x^2} = -\,px \quad \ldots\ldots\ldots\ldots\ldots\ldots\ldots\ldots\ldots\ldots (13)$$

[4] *Comptes Rendus*, Vol. 127, 1908, pp. 10–15.

and,

$$\tau \equiv -\frac{\partial^2 F}{\partial x\,\partial y} = 0 \ldots\ldots\ldots\ldots\ldots\ldots\ldots\ldots (14)$$

When $y = x \tan \gamma = x K$; and, therefore, $\frac{dy}{dx} = K$.

By Equations (5*a*) and (5*b*) (remembering that no boundary forces exist on the rear face):

$$\frac{\partial^2 F}{\partial y^2} K + \frac{\partial^2 F}{\partial x\,\partial y} = 0 \ldots\ldots\ldots\ldots\ldots\ldots (15a)$$

and,

$$\frac{\partial^2 F}{\partial x^2}\frac{1}{K} + \frac{\partial^2 F}{\partial x\,\partial y} = 0 \ldots\ldots\ldots\ldots\ldots\ldots (15b)$$

It is evident that the polynomial,

$$F_p = Ax^3 + By^3 + Cx^2 y + Dx y^2 \ldots\ldots\ldots\ldots\ldots\ldots (16)$$

satisfies Equations (3), and, therefore, F_p is an Airy stress function. If the arbitrary constants A, B, C, and D, can be determined such that the boundary conditions are satisfied, Equation (16) is the solution.

By substitution of F_p into Equations (13) and (14) and with $y = 0$: $6Ax = -px$. Consequently, $A = \frac{-p}{6}$; $-2Cx = 0$; and, $C = 0$. By substitution of F_p into Equations (15) and with $y = Kx$; $6BxK^2 + 4DxK = 0$; $-\frac{px}{k} + 2DxK = 0$; $B = -\frac{p}{3K^3}$; and $D = +\frac{p}{2K^2}$.

With these values of A, B, C, and D, introduced into Equation (16) the stress function for the hydrostatic forces becomes:

$$F_p = -\frac{p}{6K^3}(x^3K^3 + 2y^3 - 3xy^2K) \ldots\ldots\ldots\ldots\ldots\ldots (17)$$

By the definitions expressed as Equations (1), with $g_x = g_y = 0$, the stresses are:

$$\sigma_x = \frac{p}{K^3}(xK - 2y) \ldots\ldots\ldots\ldots\ldots\ldots (18a)$$

$$\sigma_y = -px \ldots\ldots\ldots\ldots\ldots\ldots (18b)$$

and,

$$\tau = -\frac{p}{K^2} y \ldots\ldots\ldots\ldots\ldots\ldots (18c)$$

The displacements corresponding to Equation (17) are derived in some detail in order to illustrate the use of the general equations (9); thus: $\frac{\sigma F_p}{\sigma x} = -\frac{p}{2K^3}(K^3x^2 - Ky^2)$; $\frac{\partial F_p}{\partial y} = -\frac{p}{K^3}(y^2 - Kxy)$; and,

$$\nabla^2 F \equiv \frac{\partial^2 F}{\partial x^2} + \frac{\partial^2 F}{\partial y^2} = \frac{p}{K^3}(xK - xK^3 - 2y) \equiv ax + by$$

in which $a = \frac{p}{K^3}(K - K^3)$; and, $b = -\frac{2p}{K^3}$. Referring to Equation (10), $\nabla^2 F$ = real part of $f(z) = f(x + iy)$. Hence, $f(z) = az - ibz = (a - ib)z$; and,

$$\int f(z)\,dz = \frac{1}{2}(a - ib)z^2 = \left[\frac{a}{2}(x^2 - y^2) + bxy\right] + i\left[axy - \frac{b}{2}(x^2 - y^2)\right] \quad \ldots\ldots(19)$$

Then, referring to Equations (9), $f_1 = \frac{a}{2}(x^2 = y^2) + bxy$ = real part of Equation (19); and, $f_2 = axy - \frac{b}{2}(x^2 - y^2)$ = imaginary part of Equation (19). Substituting these quantities into Equations (9):

$$u = \frac{p}{2E_1K^3}\left[(1 + \mu_1)(K^3x^2 - Ky^2) + (K - K^3)(x^2 - y^2) - 4xy + Ay + B\right] \quad \ldots\ldots(20a)$$

and,

$$v = \frac{p}{E_1K^3}\left[(1 + \mu_1)(y^2 - Kxy) + x^2 - y^2 + (K - K^3)xy - Ax + C\right]. \quad (20b)$$

In Equations (20) E_1 and μ_1 are Young's modulus and Poisson's ratio, respectively, for the dam in case of plane stress ($\sigma_z = 0$). In case of plane strain, E_1 and μ_1 are found, as explained in connection with Equations (11) and (12).

Mass Forces.—Let the components of the mass forces (weight and earthquake forces) be g_x and g_y along the X-axis and Y-axis, and assume that no forces are acting on the faces of the dam. It may be verified that the function:

$$F_g = \frac{1}{6K^2}\left[g_xK^2x^3 + (g_xK + g_yK^2 - 2g_y)y^3 + 3g_yKxy^2\right] \quad \ldots(21)$$

will satisfy the boundary conditions expressed by Equations (5) or Equations (7). By Equations (1) the stresses are:

$$\sigma_x = \frac{1}{K}\left[(g_y - g_xK)x + \left(g_x - \frac{2g_y}{K}\right)y\right] \quad \ldots\ldots(22a)$$

$$\sigma_y = -g_yy \quad \ldots\ldots(22b)$$

and,

$$\tau = -\frac{yg_y}{K} \quad \ldots\ldots(22c)$$

The displacements corresponding to Equation (21) are found by substituting,

$$\frac{\partial F_g}{\partial x} = \frac{1}{2K}\,(Kg_x\,x^2 + g_y\,y^2) \quad \ldots\ldots\ldots\ldots\ldots\ldots (23a)$$

$$\frac{\partial F_g}{\partial y} = \frac{1}{2K^2}\,[(g_x K + g_y K^2 - 2g_y)\,y^2 + 2K\,g_y\,x\,y] \ldots\ldots (23b)$$

$$f_1 = \frac{1}{2K}\,(Kg_x + g_y)\,(x^2 - y^2) + \frac{1}{K^2}\,(Kg_x + K^2 g_y - 2\,g_y)\,xy \ldots (23c)$$

and,

$$f_2 = \frac{1}{K}\,(Kg_x + g_y)\,xy - \frac{1}{2K^2}\,(Kg_x + K^2 g_y - 2g_y)\,(x^2 - y^2) \ldots (23d)$$

into Equations (9).

It will be seen by Equations (18) and (22) that all stresses are linear along any straight line in the triangular dam of infinite height. This agrees with the assumptions of engineering practice. It will be shown subsequently that this is not true near the base in a dam of finite height.

The boundary stresses computed by Equations (17) and (21) for Morris Dam, in California, are plotted in Fig. 2.

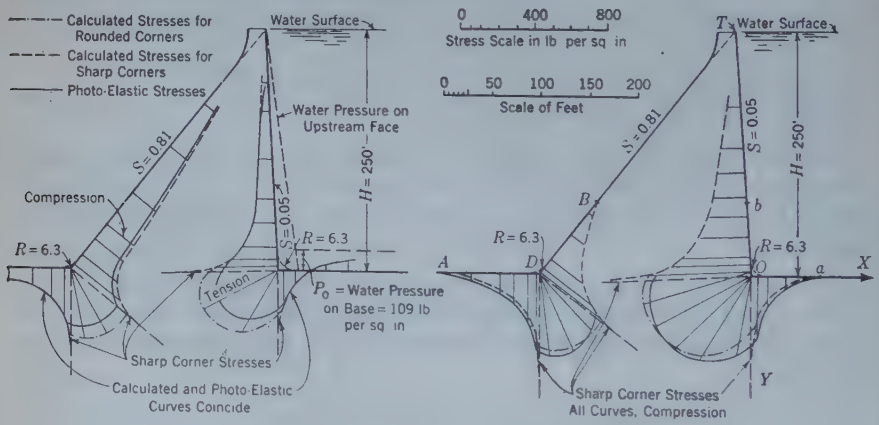

FIG. 2.—PRINCIPAL STRESSES ALONG BOUNDARY.

Additional Solutions in Polar Co-Ordinates[5] *for the Triangular Dam of Infinite Height.*—Simple expressions are obtained when the bisector of the top angle, $\gamma = 2\alpha$, is chosen as the X-axis, and the Y-axis is positive down stream; as, for example:

(1) When the full hydrostatic pressure, pr, is exerted on the up-stream face, and with no forces on the down-stream face:

$$F_p = \frac{pr^3}{24}\left[(3\sin^2\alpha - \sin^2\theta)\,\frac{\sin\theta}{\sin^3\alpha} - (3\cos^2\alpha - \cos^2\theta)\,\frac{\cos\theta}{\cos^3\alpha}\right]$$

[5] For greater detail refer to Carothers' "Plain Strains in a Wedge, with Applications for Masonry Dams", *Proceedings*, Royal Soc., Edinburgh, Vol. 53 (1913), pp. 292–303.

(2) When a uniform pressure, p, is exerted on both faces:

$$F = -\frac{1}{2} pr^2 \quad \ldots\ldots\ldots\ldots\ldots\ldots\ldots\ldots (24)$$

(3) When a uniform pressure, p, is exerted on the up-stream face and uniform tension, p, is exerted on the down-stream face:

$$F = \frac{pr^2 (\sin 2\theta - 2\theta \cos 2\alpha)}{2 (\sin 2\alpha - 2\alpha \cos 2\alpha)} \quad \ldots\ldots\ldots\ldots\ldots\ldots (25)$$

(4) When a uniform pressure is exerted on the up-stream face, with no force on the down-stream face:

$$F = \frac{1}{4} pr^2 \frac{\sin 2\theta - \sin 2\alpha - (2\theta - 2\alpha) \cos 2\alpha}{\sin 2\alpha - 2\alpha \cos 2\alpha} \quad \ldots\ldots\ldots\ldots (26)$$

(5) With a pressure, pr, on the up-stream face and tension, pr, on the down-stream face:

$$F = \frac{pr^3}{6} \frac{\cos \alpha \sin 3\theta - 3 \cos 3\alpha \sin \theta}{\cos \alpha \sin 3\alpha - 3 \cos 3\alpha \sin \alpha} \quad \ldots\ldots\ldots\ldots\ldots (27)$$

(6) With a pressure, pr, on both faces use Equation (27), substituting "sin" for "cos" and "cos" for "sin" throughout.

(7) With a moment, M, per unit of the Z-axis (positive in direction $+\theta$) acting at the vertex:

$$F = -\frac{M}{2} \frac{\sin 2\theta - 2\theta \cos 2\alpha}{\sin 2\alpha - 2\alpha \cos 2\alpha} \quad \ldots\ldots\ldots\ldots\ldots\ldots (28)$$

(8) With a force, P, per unit length of the Z-axis acting at the vertex and directed along the positive Y-axis:

$$F = P \frac{r\theta \cos \theta}{2\alpha - \sin 2\alpha} \quad \ldots\ldots\ldots\ldots\ldots\ldots\ldots (29)$$

(6) With a pressure, pr, on both faces use Equation (27) substituting directed along the positive X-axis, use Equation (29), substituting "sin θ" for "cos θ"; and

(10) With body forces, g, per unit volume, directed at an angle, β, with the X-axis:

$$F_g = \frac{gr^3}{12} \left[\frac{\cos \beta}{\cos^2} (3 \cos^2 \alpha \cos \theta - \cos^3 \theta) + \frac{\sin \beta}{\sin^2 \alpha} (3 \sin^2 \alpha \sin \theta - \sin^3 \theta) \right] \quad \ldots\ldots\ldots\ldots\ldots (30)$$

The stresses are obtained by Equations (2) with $g = 0$ if no mass forces exist.

Application II.—Stresses in Foundations.[6]

Let a tangential line load, Q, act per unit thickness of the infinite half plane (foundation). With the co-ordinate system in Fig. 3 it is easily verified

[6] For a more detailed solution, see "Applications Potentiels à l'Etude de Equilibre et du Mouvements des Solides Elastiques", by J. Bouissinesq, Paris, 1885.

that the function, $F = \frac{-Q}{\pi} r\,\theta \sin\theta = -\frac{Q}{\pi} y \tan^{-1}\frac{y}{x}$, is an Airy function because Equations (3) are satisfied. It satisfies the boundary conditions, $F = 0$, when $\theta = 0$, and $\theta = \pi$. Therefore, by Equations (8) no normal forces act on the X-axis. Furthermore, $\frac{\partial F}{\partial y} = 0$ when $\theta = 0$, and $-Q$ when

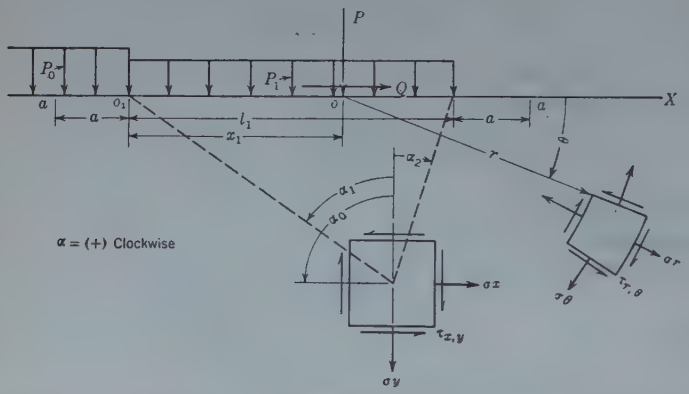

FIG. 3.

$\theta = \pi$. Therefore, by Equations (7) no tangential force distribution occurs when $r > 0$, or when $r < 0$, but a force, $+Q$, occurs at $r = 0$ because here $\frac{\partial F}{\partial y}$ makes a jump equal to $+Q$.

The stresses are found by Equations (2) with $g = 0$; thus:

$$\sigma_r = -\frac{2Q}{\pi}\frac{\cos\theta}{r} \qquad \text{.....(31}a\text{)}$$

and,

$$\sigma_\theta = \tau_{r\theta} = 0 \qquad \text{.....(31}b\text{)}$$

The rectangular stress components in the foundation may be found by the formulas:

$$\sigma_x = \sigma_r \cos^2\theta = -\frac{2Q}{\pi}\frac{\cos^3\theta}{r} \qquad \text{.....(32}a\text{)}$$

$$\sigma_y = \sigma_r \sin^2\theta = -\frac{2Q}{\pi}\frac{\cos\theta \sin^2\theta}{r} \qquad \text{.....(32}b\text{)}$$

and,

$$\tau_{x,y} = \frac{\sigma_r}{2}\sin 2\theta = -\frac{2Q}{\pi}\frac{\cos^2\theta \sin\theta}{r} \qquad \text{.....(32}c\text{)}$$

The influence function,

$$F = -\frac{1}{\pi} y \tan^{-1}\frac{y}{x - x_1} \qquad \text{.....(33)}$$

gives the stresses in the foundation due to a unit tangential force acting at a point, $(x_1, 0)$, and directed along the positive X-axis in a positive direction. For a uniform distribution, q_1, over a distance, l_1, it will be found by integration of Equation (33) that the stresses are:

$$\sigma_x = \frac{q_1}{\pi}\left[-(\log\cos^2\alpha_1 - \cos^2\alpha_1) + (\log\cos^2\alpha_2 - \cos^2\alpha_2)\right] \ldots (34a)$$

$$\sigma_y = \frac{q_1}{2\pi}\left[+\cos 2\alpha_1 - \cos 2\alpha_2\right] \ldots\ldots\ldots\ldots (34b)$$

and,

$$\tau_{x,y} = \frac{q_1}{2\pi}\left[+(2\alpha_1 - \sin 2\alpha_1) - (2\alpha_2 - \sin 2\alpha_2)\right] \ldots\ldots (34c)$$

in which the angles, α_1 and α_2, are as shown in Fig. 3. Equations (34) are easily extended to a number of uniform distributions, q_1, q_2, q_3, etc.

At Point a of the surface, $\sigma_y = \tau = 0$ (see Fig. 2(b)) and σ_x by Equations (34) becomes invalid; $\sigma_x = \sigma_r$ is then obtained by direct integration of Equations (31); thus:

$$\sigma_x = \mp\int_a^{a+l_1}\sigma_r\,dr = \mp\frac{2q_1}{\pi}\int_0^{a+l_1}\frac{dr}{r} = \mp\frac{2\,q_1}{\pi}\log\frac{a+l_1}{a} \ldots . (35)$$

in which minus is to be used if a is on the positive side of the distribution, q_1.

By Equations (9) (remembering that $g = 0$) the displacements due to Equation (33) are:

$$u = -\frac{1}{\pi E_2}\left\{(1+\mu_2)\frac{(x-x_1)^2}{(x-x_1)^2+y^2} + \log\left[(x-x_1)^2+y^2\right] - Ay + C\right\} . . (36a)$$

and,

$$v = \frac{1}{\pi E_2}\left\{(1+\mu_2)\left[y\frac{x-x_1}{(x-x_1)^2+y^2} + \tan^{-1}\frac{y}{x-x_1}\right] - 2\tan^{-1}\frac{y}{x-x_1} + Ax + B\right\} \ldots\ldots\ldots\ldots\ldots (36b)$$

Next, let a normal compression, P, act per unit thickness. The stress function for this load, $F = +\frac{P}{\pi}\,r\,\theta\cos\theta = +\frac{P}{\pi}\,x\tan^{-1}\left(\frac{y}{x}\right)$, will satisfy the boundary conditions. The stresses by Equations (2), with $g = 0$, are: $\sigma_r = -\frac{2\,P}{\pi}\frac{\sin\theta}{r}$; $\sigma_\theta = 0$; and $\tau = 0$.

The rectangular components of stress due to P are:

$$\sigma_x = -\frac{2P}{\pi}\frac{\sin\theta\cos^2\theta}{r}; \quad \sigma_y = -\frac{2P}{\pi}\frac{\sin^3\theta}{r}; \text{ and, } \sigma_{x,y} = -\frac{2P}{\pi}\frac{\sin^2\theta\cos\theta}{r}$$

The influence function,

$$F = \frac{1}{\pi}(x - x_1)\tan^{-1}\left(\frac{y}{x-x_1}\right) \ldots\ldots\ldots\ldots (37)$$

will give the stresses in the foundation due to a unit normal pressure at the point, $(x_1, 0)$.

For a uniform distribution, p_1, over the distance, l_1 (Fig. 3), the stresses are:

$$\sigma_x = \frac{p_1}{2\pi}\,[+\,(2\alpha_1 - \sin 2\alpha_1) - (2\alpha_2 - \sin 2\alpha_2)] \ldots\ldots (38a)$$

$$\sigma_y = \frac{p_1}{2\pi}\,[+\,(2\alpha_1 + \sin 2\alpha_1) - (2\alpha_2 + \sin 2\alpha_2)] \ldots\ldots (38b)$$

and,

$$\tau_{x,y} = \frac{p_1}{2\pi}\,[+\,\cos 2\alpha_1 - \cos 2\alpha_2] \ldots\ldots (38c)$$

Equations (38) can be extended to several uniform distributions, p_1, p_2, p_3, etc. The displacements due to Equation (37) are:

$$u = \frac{1}{\pi E_2}\left\{(1 + \mu_2)\left[y\,\frac{x - x_1}{(x - x_1)^2 + y^2} - \tan^{-1}\frac{y}{x - x_1}\right] + 2\tan^{-1}\frac{y}{x - x_1} + Ay + B\right\}$$

and,

$$v = -\frac{1}{\pi E_2}\left\{(1 + \mu_2)\,\frac{(x - x_1)^2}{(x - x_1)^2 + y^2} + \log\left[(x - x_1)^2 + y^2\right] - Ax + C\right\}$$

An interesting case occurs when p_0 is the uniform reservoir pressure on the foundation above a dam. If the X-axis is chosen positive down stream, the stresses are:

$$\sigma_x = \frac{-p_0}{2\pi}\,[\pi + 2\alpha_1 - \sin 2\alpha_1] \ldots\ldots (39a)$$

$$\sigma_y = \frac{-p_0}{2\pi}\,[\pi + 2\alpha_1 + \sin 2\alpha_1] \ldots\ldots (39b)$$

and,

$$\tau_{x,y} = \frac{-p_0}{2\pi}\,[1 + \cos 2\alpha_1] \ldots\ldots (39c)$$

The corresponding stress function is $F = +\,\frac{p_0 r^2}{4}\,(\sin 2\theta - 2\theta)$, with the origin at the heel. The corresponding displacements are:

$$u = \frac{p_0}{\pi E_2}\left\{(1 + \mu_2)\,x\tan^{-1}\frac{y}{x} + 2x\tan^{-1}\frac{y}{x} - y\log(x^2 + y^2) + Ay + B\right\} \ldots (40a)$$

and,

$$v = \frac{p_0}{\pi E_2}\left\{(1 + \mu_2)\,y\tan^{-1}\frac{y}{x} - 2y\tan^{-1}\frac{y}{x} + x\log(x^2 + y^2) - Ax + C\right\} \ldots (40b)$$

Finally, the stresses in the foundation due to the weight, g, per unit volume are: $\sigma_x = \sigma_y = -gy$; and $\tau_{x,y} = 0$.

APPLICATION III.—STRESSES IN THE REGION OF THE BASE OF THE GRAVITY DAM

In the third application of the theory, polar co-ordinates will be used to determine "corner-functions" for a wedge or a corner with an angle, γ. The "corner-function" is defined such as to give no forces on the straight boundaries of the wedge or the corner. For the present purpose it is convenient to choose the co-ordinate system shown in Fig. 4. These functions appear in connec-

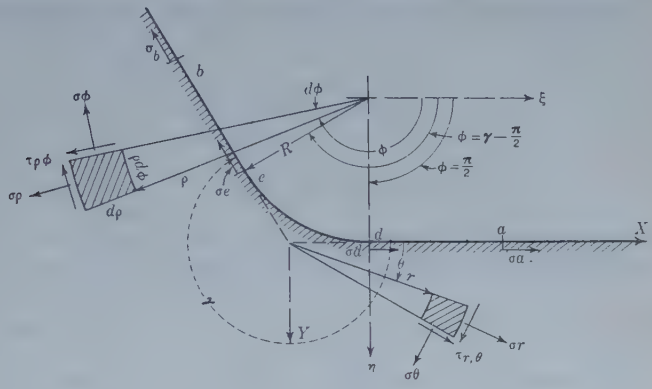

FIG. 4.

tion with the exact solutions by the writer[7] for stresses in two-dimensional corners. H. M. Westergaard, M. Am. Soc. C. E., in a communication to Professor von Kármán, has called attention to the existence of such functions, which he used for the investigation of stresses in the region of the toe and heel of dams, cracks in concrete, etc.

The definition of this function is expressed by Equations (8); hence, when $\theta = 0$ and $\theta = \gamma$:

$$F = 0 \ldots\ldots\ldots\ldots\ldots\ldots\ldots\ldots\ldots\ldots (41a)$$

and,

$$\frac{\partial F}{\partial n} = \frac{\partial F}{r\,\partial\theta} = 0 \ldots\ldots\ldots\ldots\ldots\ldots\ldots\ldots (41b)$$

Consider the real part of the following function which, by Equation (4), is known to be a solution of Equations (3):

$$F = [(B - iA)\,x + (C - iD)\,y]\,z^n \ldots\ldots\ldots\ldots\ldots (42)$$

in which $x = r\cos\theta$; $y = r\sin\theta$; $z = re^{i\theta} = r(\cos\theta + i\sin\theta)$; and, $z^n = re^{in\theta} = r^n(\cos n\theta + i\sin n\theta)$. By substitution of these expressions into Equation (42) and taking the real part only:

$$F = r^{n+1}[B\cos n\theta\cos\theta + A\sin n\theta\cos\theta + C\cos n\theta\sin\theta + D\sin n\theta\sin\theta] \ldots\ldots\ldots\ldots\ldots\ldots (43)$$

[7] Presented to the California Institute of Technology in 1932, in partial fulfillment of the requirement for the degree of Doctor of Philosophy; also contained in *Technical Memorandum No. 420*, U. S. Bureau of Reclamation, Denver, Colo.; excerpt published in *Applied Mechanics*, April–June, 1933, Vol. 1, No. 2; and in *Physics*, Vol. 4, No. 2, February, 1933.

It is to be noted that, by starting with a complex function of the type of Equation (4), Airy functions are easily produced and the task of verifying Equations (3) is avoided.

The constants, A, B, C, D, and n, must be determined by the boundary conditions expressed in Equations (41) and it will be found that the "corner-function" (Equation (43)) becomes:

$$F = A' r^{n+1} [n \cos n\theta \sin\theta + m \sin n\theta \sin\theta - \sin n\theta \cos\theta] \ldots (44)$$

in which,

$$n \sin\gamma = \pm \sin n\gamma \ldots (45)$$

and,

$$m = \cot\gamma - n \cot n\gamma \ldots (46)$$

The stresses produced by Equation (44) are found by Equations (3) with $g = 0$. The displacements corresponding to Equation (44) are:

$$u = \frac{r^n}{E_1}\Big\{(1+\mu_1)[n\cos\theta\sin(n-1)\theta + \sin n\theta - n^2\sin\theta\cos(n-1)\theta - m\,n\sin\theta\sin(n-1)\theta] - 2\sin n\theta - 2n\sin n\theta + 2m\cos n\theta + Cr\sin\theta + D\Big\}$$

and,

$$v = \frac{r^n}{E_1}\Big\{(1+\mu_1)[n\cos\theta\cos(n-1)\theta - n\cos n\theta - m\sin n\theta + n^2\sin\theta\sin(n-1)\theta - m\,n\sin\theta\cos(n-1)\theta] + 2\cos n\theta + 2n\cos n\theta + 2m\sin n\theta - Cr\cos\theta + E\Big\}$$

in which C, D, and E are arbitrary constants used to fix the reference system for u and v. The values of n that satisfy Equation (45) will be referred to as "corner-values." It will be found that when $\pi < \gamma < 2\pi$, there are two significant real roots, n_0 and n_1, the others are complex; when $\gamma = \pi$, all roots are real: 1, 2, 3, etc.; when $\gamma = 2\pi$, all roots are real: $\frac{1}{2}, 1, \frac{3}{2}$, 2, etc.; and, when $0 < \gamma < \pi$, all roots are complex. The real roots, n_0 and n_1, for various values of γ are given in Fig. 5, based on the formulas:

$$\sin n_0\gamma = -n_0 \sin\gamma \ldots (47a)$$

and,

$$\sin n_1\gamma = +n_1 \sin\gamma \ldots (47b)$$

The complex roots may be found as follows: Let $n = a + ib$, which, substituted in Equation (45) gives:

$$\pm(a+ib)\sin\gamma = \sin a\gamma \cosh b\gamma + i\cos a\gamma \sinh b\gamma$$

Equating real and imaginary parts, the following simultaneous equations are obtained:

$$\sin a\gamma \cosh \gamma b = \pm a \sin \gamma \quad \ldots\ldots\ldots\ldots\ldots\ldots (48a)$$

and,

$$\cos a\gamma \sinh b\gamma = \pm b \sin \gamma \quad \ldots\ldots\ldots\ldots\ldots\ldots (48b)$$

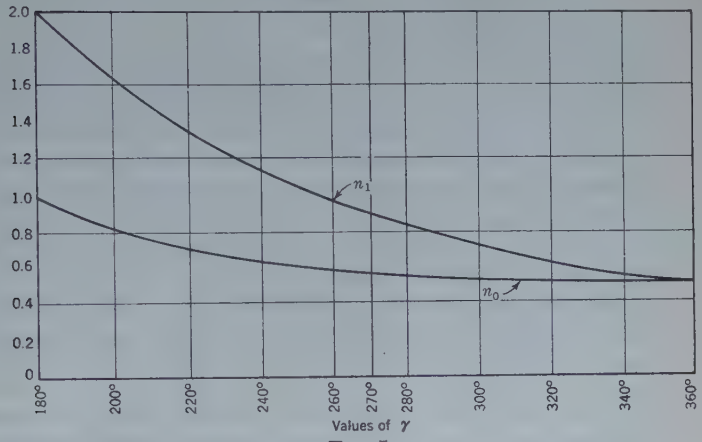

FIG. 5.

When γ is known, approximate values for a and b are found by:

$$a_k = \pm \frac{\pi (2k - 1) - \epsilon_k}{2\gamma} \quad \ldots\ldots\ldots\ldots\ldots\ldots (49a)$$

and,

$$b_k = \pm \frac{1}{\gamma} \log \left\{ \frac{\pi (2k - 1) - \epsilon_k}{\gamma} \sin \gamma \right\} \quad \ldots\ldots\ldots\ldots (49b)$$

in which,

$$\epsilon_k = \frac{4 \log \left(\frac{\pi (2k - 1) \sin \gamma}{\gamma} \right)}{\pi (2k - 1)} \quad \ldots\ldots\ldots\ldots\ldots (49c)$$

and, $k = 2, 3, 4, 5$, etc.

The values, a_k and b_k, obtained by Equations (49*a*) and (49*b*) will not satisfy Equations (48) exactly; therefore, they must be further adjusted.[8]

When n_k is known the corresponding value of m_k is found by Equation (46). Let $m = d + ie$ which, substituted into Equation (46), separating real and imaginary parts and making use of Equations (48), gives $e = b \tan a\gamma$; and $d = \cot \gamma - a \cot a\gamma$.

The various quantities in Equations (44) have now been expressed in terms of γ so that, when the angle, γ, is known, the "corner-function" is fully determined except for the arbitrary constant, A'. Each complex value of n will furnish a real and imaginary part of Equation (44). Both parts will satisfy the required boundary conditions; therefore, two functions are obtained

[8] Adjustment demonstrated in record manuscript, filed for reference in Engineering Societies Library, New York, N. Y.

for each value of n, each with an arbitrary constant, A and B, respectively. Furthermore, the sum of the functions obtained for all values of n will satisfy the boundary conditions. This function may be written:

$$F_\gamma = \text{real part of } \sum_{0,\,1,\,2,\,3,\,\text{etc.}}^{k=} (A_k - i\,B_k)\,F_k \quad \ldots\ldots\ldots\ldots (50)$$

in which F_k is given by Equation (44).

The function, F_γ, contains a double infinity of arbitrary constants, A_k and B_k, and is constituted so that it corresponds to the case in which there are no forces acting on the straight boundaries of the corner, γ, irrespective of the values of A_k and B_k. At points inside the corner the stresses will not be zero, but the stress distribution will be such that the resultant of the stresses acting on any line terminating at points of the boundaries will be zero. In other words the function, F_γ, will only affect the distribution of the stresses. It is important that the full significance of F is realized. It is extremely useful for the investigation of stresses at sharp corners and for the correction of stresses in structures if the boundary lines differ from those assumed in the original computations.

Application of F_γ for the Determination of Stresses Near the Base of a Straight Triangular Gravity Dam on an Infinite Elastic Foundation

Two cases will serve to demonstrate the foregoing theory. In Case 1, the elastic properties of the dam and foundation are assumed to be the same throughout; and, in Case 2, they are different in the dam and foundation, but constant throughout in each of the two.

Case 1.—Consider an infinite elastic homogeneous plate of unit thickness. On this plate imagine the boundary lines of the cross-section of the dam and its foundation. These lines will divide the plane into two separate regions one of which is a slice of the dam and its foundation. The problem is to determine a function, F, that will deliver stresses between the two regions equal to the loads on the dam and its foundation. This function then will deliver the correct stresses throughout. Incidentally, it is interesting to note that F will give the stresses in both regions of the infinite plate.

Select the height of the dam (see Fig. 2), measured along the up-stream face, as the unit of length. Assume a full hydrostatic load on the up-stream face and constant pressure, p, on the up-stream foundation. Let the uniform mass forces (weight and inertia) be g per unit volume acting at an angle, β, with the X-axis. It is assumed that the forces, if any, acting on the rear face and the down-stream foundation are known.

Then the boundary conditions which must be satisfied by the stress function, F, are: (1) When $\theta = 0$; $y = 0$; (up-stream face): $\sigma_\theta = -p\,(1 - r)$; and, $\tau = 0$; (2) when $\theta = \gamma$; $y = x \tan \gamma = x\,K$; (up-stream foundation): $\sigma_\theta = -p$; and $\tau = 0$; and, (3) the rear face and down-stream foundation will be considered later. Let,

$$F = -F_p + F_0 + F_g + F \quad \ldots\ldots\ldots\ldots (51)$$

in which F_p, F_g, F_o, and F_γ are given in Equations (17), (21), (24), and (50); γ is the re-entrant angle at the heel ($\gamma > \pi$); and, $K = \tan \gamma$.

By adding the stresses when $y = 0$ and $y = K x$, respectively, due to the various functions in Equation (51), it will be found that Conditions (1) and (2) are satisfied exactly. (It is to be noted that F_γ was determined so as to give no contribution on these lines.)

There remains the matter of satisfying the conditions along the line, *T B D A*, in Fig. 2(*b*). For this purpose the form of the boundary conditions derived in Equations (7) is utilized.

In Equation (51), F is determinate with the exception of the arbitrary constants, A_k and B_k, in the function, F_γ. This double infinity of constants is used to satisfy Equations (7*a*) and (7*b*), at all points of the line, *T B D A*. The right-hand sides of Equations (7*a*) and (7*b*) are completely known and can be computed at all points when the forces on the dam are known. A double infinity of simultaneous equations is obtained with a double infinity of unknowns, A_k and B_k. This problem is solved, mathematically, by expanding the right-hand sides of Equations (7*a*) and (7*b*) in terms of the "corner-functions," F_γ. In the practical solution of the problem it is only necessary to satisfy Equations (7) for a finite number of points. In this case it is better to include all three of Equations (7). It will be found that if they are satisfied at three points, *B*, *D*, and *A* (Fig. 2(*b*)), Equations (7) will be closely satisfied at intermediate points. This can be checked by plotting F, $\frac{\partial F}{\partial x}$, and $\frac{\partial F}{\partial y}$, along the line, *T B D A*, and comparing the results with the values computed by the right-hand sides of Equations (7).

Three equations of conditions are thus obtained at each point, *B*, *D*, and *A*, a total of nine equations. This means that nine constants, A_k and B_k, must be included in F_γ.

When only a finite number of points, *B*, *D*, *A*, etc., are used, it is necessary to compute the stress functions for both the heel and the toe; that is, for the two different angles, γ. As soon as the constants, A_k and B_k are determined, F_γ is known by Equation (50). Thus, the total stress function valid in the region of the corner is known by Equation (51) and the stresses can be determined by Equations (2).

The stresses computed in one of the preliminary studies of Grand Coulee Dam[9] are given in Figs. 6 and 7. The stresses in the foundation were found by Equations (34), (35), (38), and (39), after the normal stress and shear distributions along the base had been computed. The stresses in the upper two-thirds of the dam are not shown. They may be computed by Equations (18) and (22), or by the usual engineering methods.

It will be seen that all stresses are compressive and tend to become infinite at the heel and toe. Of course, this is not possible because the material will become plastic before such magnitudes are reached and redistributions will occur near the corners, which must be considered as singular points where

[9] The details are contained in *Technical Memorandum No. 403* by Chief Designing Engineer J. L. Savage, U. S. Bureau of Reclamation, Denver, Colo.

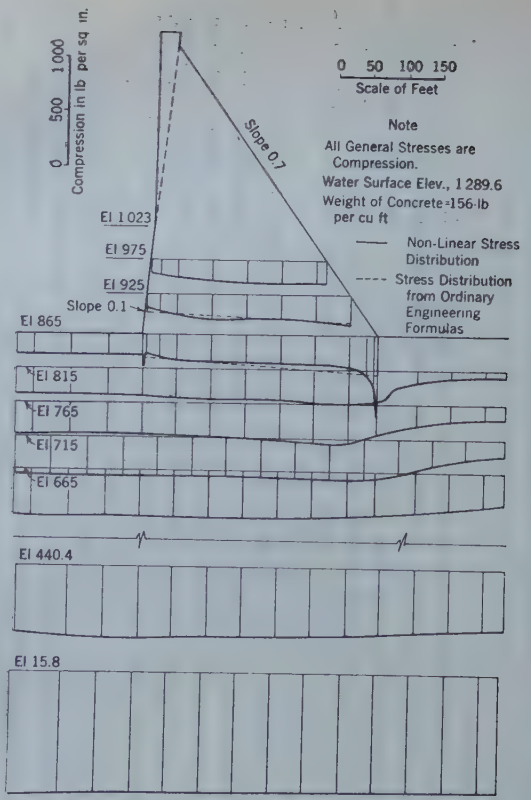

(*a*) VERTICAL STRESSES

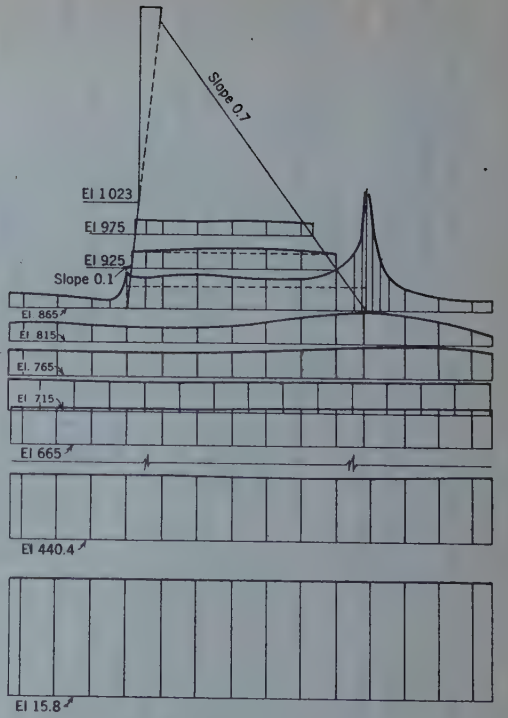

(*b*) HORIZONTAL STRESSES

FIG. 6.

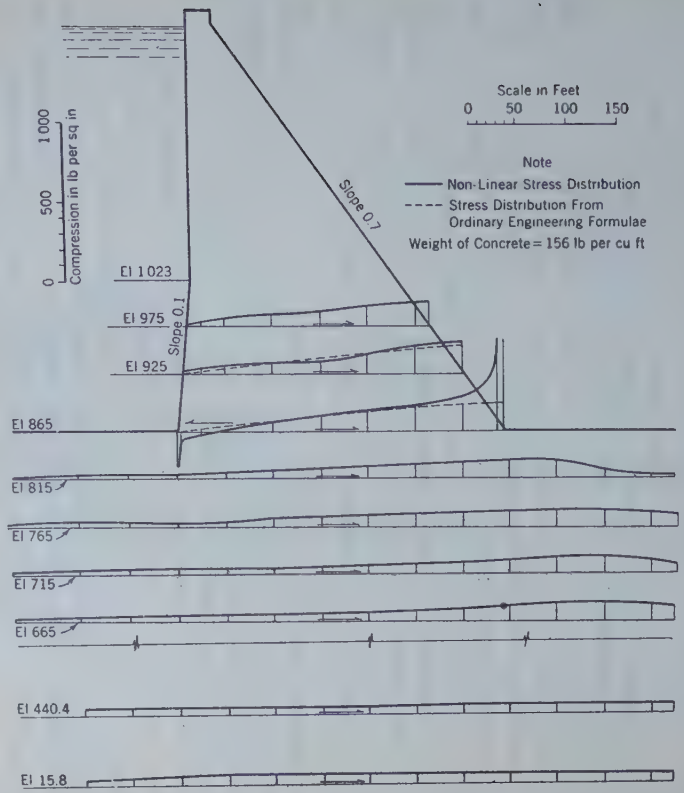

(a) SHEARING STRESSES

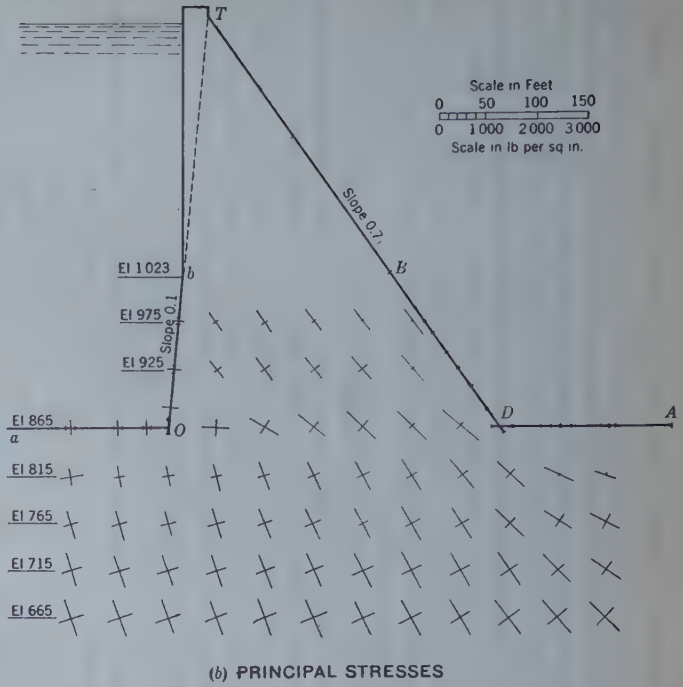

(b) PRINCIPAL STRESSES

FIG. 7.

the elastic assumptions do not hold. The redistribution cannot be computed by the elastic theory, but it is evident that, after the plastic flow takes place, the stresses will be decreased near the corner and slightly increased a short distance from the corner. It will be noticed that the theoretical stresses are extremely high over only a minute distance so that the actual forces involved are very small. The effect of a redistribution, therefore, can only be slight.

In order to be able to predict the elastic stresses at the heel and toe it would be necessary to fillet the corner with a large enough curvature to keep the theoretical stresses within the elastic limit at all times. This was done in other studies of this dam.

Case 2.—Referring to Fig. 2, consider the dam as a triangle with elastic modulus, E_1, and Poisson's ratio, μ_1, resting on an elastic foundation which is considered as an infinite half plane with modulus, E_2, and Poisson's ratio, μ_2. A slice, one unit wide, across the dam and into the foundation is considered. It will be assumed that no separation or slippage will occur between the base and the foundation. This implies that, when all effects are considered, the resulting normal stresses are compression, and that the shear stresses are within the permissible relation to the normal stresses.

All forces acting on the dam and on the foundations are known, except the reactions between the two. The problem is to determine these reactions such that the elastically deformed base and foundation make a perfect fit when equilibrium exists. This is expressed by demanding that the relative displacements of the dam and the foundation must be zero along the base.

With the co-ordinate system as in Fig. 4, let the stress function for the dam be $F = F_p + F_g + F_\gamma$, corresponding to full hydrostatic pressure on the up-stream face, and the mass forces, g, per unit volume. Functions F_p and F_g are given by Equations (17) and (21); and F_γ is the "corner-function" derived in Equation (50) with γ equal to the top angle of the dam ($\gamma < \pi$). In this case F_γ may be considered as a correction to the basic function, $F_p + F_g$, for the infinite wedge. It has already been indicated that F_γ does not alter the force system which acts on the faces of the dam. Its value is known except for the arbitrary constants, A_k and B_k, which must be determined by making the deformed base of the dam congruent with the deformed foundation line. By this method it is possible to determine: (1) The effect of a variation of the ratio, $\frac{E_1}{E_2}$, on the stresses, in which E_1 and E_2 are Young's modulus for the dam and foundation, respectively; (2) the effect of uniform shrinkage of the dam relative to the foundation; and (3) it includes Case 1 when $E_1 = E_2$ and $\mu_1 = \mu_2$.

Application IV.—Approximate Boundary Stresses at Sharp and Rounded Corners or Fillets

Formulas are developed herein for the boundary stresses at sharp and rounded corners of elastic structures, using only the real "corner-values," n_0 and n_1, given in Fig. 5. The method is applicable to any structure with any loading. Numerical examples are computed in the case of a triangular dam.

Theory Pertaining to Sharp Corners.—Assume that the body forces and the forces acting on the boundaries, $\theta = 0$ and $\theta = \gamma$, of the corner in Fig. 4 is represented by a function, F_2, and that the stresses, σ_a and σ_b, at the points, $r = a$ and $r = b$, of the boundaries are known, or have been computed by ordinary engineering methods. It is required to determine a function, F, to represent the state of stress at the corner such that, when $\theta = 0$:

$$F = F_2 \ldots\ldots\ldots\ldots\ldots\ldots\ldots\ldots\ldots\ldots (52a)$$

and,

$$\frac{\partial F}{\partial \theta} = \frac{\partial F_2}{\partial \theta} \ldots\ldots\ldots\ldots\ldots\ldots\ldots\ldots\ldots\ldots (52b)$$

Then by Equations (2),

$$\left[\frac{\partial^2 F}{r^2\,\partial\,\theta^2} + \frac{1}{r}\,\frac{\partial F}{\partial r} - r\,g\cos(\theta - \beta)\right]_{\binom{\theta=0}{r=a}} = \sigma_a \ldots\ldots\ldots (53)$$

On the boundary, $\theta = \gamma$, Equations (52) and (53) apply likewise except, of course, that here $\theta = \gamma$, $r = b$, and σ_a is replaced by σ_b. Let,

$$F = F_2 + F_\gamma \ldots\ldots\ldots\ldots\ldots\ldots\ldots\ldots\ldots\ldots (54)$$

Function F_γ is the "corner-function" for γ given by Equation (50), with $k = 0$ and 1; that is, only the real values, n_0 and n_1, found by Fig. 5 are involved. Hence, $F_\gamma = F_0 + F_1$, in which F_0 and F_1 are given by Equation (44) for $n = n_0$ and $n = n_1$.

It will be seen that F defined by Equation (54) satisfies Equation (52). It only remains to determine the constants, A_0 and A_1, such that Equation (53) will be satisfied.

By substituting F into this formula and re-arranging:

$$\left[\frac{\partial^2 F_\gamma}{r^2\,\partial\,\theta^2} + \frac{1}{r}\,\frac{\partial F_\gamma}{\partial r}\right]_{\binom{\theta=0}{r=a}} = \sigma_a - \left[\frac{\partial^2 F_2}{r^2\,\partial\,\theta^2} + \frac{1}{r}\,\frac{\partial F^2}{\partial r} - r\,g\cos(\theta - \beta)\right]_{\binom{\theta=0}{r=a}} \ldots\ldots\ldots\ldots\ldots (55)$$

and, the analogous equation for $\theta = \gamma$, $r = b$, in which every term is known except A_0 and A_1. The brackets on the right side of Equation (55) are the stresses σ_r, computed from the function F_2 by Equations (2). The derivation of F_2 will be given subsequently herein. Denote these terms by $Q_{0,a}$ and $Q_{\gamma,b}$. In general, let

$$Q_{r,\theta} = \frac{\partial^2 F_2}{r^2\,\partial\,\theta^2} + \frac{1}{r}\,\frac{\partial F_2}{\partial r} - r\,g\cos(\theta - \beta) \ldots\ldots\ldots\ldots (56)$$

and let subscripts denote the co-ordinates of the point at which the quantities are to be computed.

By partial differentiations of F_γ given by Equation (44):

$$\left[\frac{\partial^2 F_\gamma}{r^2\,\partial\theta^2} + \frac{1}{r}\frac{\partial F_\gamma}{\partial r}\right]_{\theta=0} = 2A_o n_o m_o r^{n_o-1} + 2A_1 n_1 m_1 r^{n_1-1} \quad \ldots\ldots(57a)$$

and,

$$\left[\frac{\partial^2 F_\gamma}{r^2\,\partial\theta^2} + \frac{1}{r}\frac{\partial F_\gamma}{\partial r}\right]_{\theta=\gamma} = 2A_o n_o m_o r^{n_o-1} - 2A_1 n_1 m_1 r^{n_1-1} \quad \ldots\ldots(57b)$$

Substituting back into Equation (55), the following equations are obtained:

$$2A_o n_o m_o a^{n_o-1} + 2A_1 n_1 m_1 a^{n_1-1} = \sigma_a - Q_{o,a} \quad \ldots\ldots(58a)$$

and,

$$2A_o n_o m_o b^{n_o-1} - 2A_1 n_1 m_1 b^{n_1-1} = \sigma_b - Q_{\gamma,b} \quad \ldots\ldots(58b)$$

In most cases it is possible to choose $a = b$, and, if so, further simplification is possible: Placing $a = b$ in Equations (58) and solving:

$$A_o = \frac{\sigma_a - Q_{o,a} + \sigma_b - Q_{\gamma,b}}{4\,n_o\,m_o\,a^{n_o-1}} \quad \ldots\ldots(59a)$$

and,

$$A_1 = \frac{\sigma_a - Q_{o,a} - \sigma_b + Q_{\gamma,b}}{4\,n_1\,m_1\,a^{n_1-1}} \quad \ldots\ldots(59b)$$

The stress function, $F = F_2 + F_\gamma = F_o + F_1 + F_2$, is now completely known and the stresses can be found by the definitions in Equations (2); thus:

$$(\sigma_r)_{\theta=0} = \frac{\sigma_a - Q_{o,a} + \sigma_b - Q_{\gamma,b}}{2}\left(\frac{r}{a}\right)^{n_o-1} + \frac{\sigma_a - Q_{o,a} - \sigma_b + Q_{\gamma,b}}{2}\left(\frac{r}{a}\right)^{n_1-1} + Q_{o,r} \quad \ldots\ldots(60a)$$

and,

$$(\sigma_r)_{\theta=\gamma} = \frac{\sigma_a - Q_{o,a} + \sigma_b - Q_{\gamma,b}}{2}\left(\frac{r}{a}\right)^{n_o-1} - \frac{\sigma_a - Q_{o,a} - \sigma_b + Q_{\gamma,b}}{2}\left(\frac{r}{a}\right)^{n_1-1} + Q_{\gamma,r} \quad \ldots\ldots(60b)$$

The function, F_2, will now be given for a dam. Let $F_2 = F_p + F_g$, in which F_p is the part of F_2 due to the external forces acting on the boundaries, $\theta = 0$ and $\theta = \gamma$ (Fig. 4); and, F_g is the part of F_2 entirely due to the body forces, g, per unit volume.

Case 1.—In this case there are no external forces acting on the boundaries, $\theta = 0$ and $\theta = \gamma$, on the stretch, a to b. Hence, $F_p = 0$, and by Equation (56), $Q_{r,\theta} = 0$.

Case 2.—There is a constant pressure, p, on the boundary $\theta = 0$, and a pressure $(1 - r)\ p$ on $\theta = \gamma$. By a co-ordinate transformation in Equation (17) and superposing $-\frac{1}{2}\ p\ r^2$, it will be found that,

$$F_p = \frac{pr^3 \sin^2 \theta}{12 \sin^3 \gamma} [3 \cos \theta \sin 2\gamma + 6 \sin \theta \sin^2 \gamma - 4 \sin \theta] - \tfrac{1}{2}\ pr^2 \ldots (61)$$

will satisfy the conditions of this case. Then by Equation (56):

$$Q_{o,r} = \frac{pr \cos \gamma}{\sin^2 \gamma} - p \ldots (62a)$$

and,

$$Q_{\gamma,r} = -\frac{pr \cos^2 \gamma}{\sin^2 \gamma} - p \ldots (62b)$$

Case 3.—Only mass forces are considered, and the function, F_g, must be such that σ_θ and $\tau_{r,\theta}$ are zero along the straight boundaries, $\theta = 0$, and $\theta = \gamma$. Substituting polar co-ordinates into Equation (21) and placing $g_x = g \cos \beta$ and $g_y = g \sin \beta$:

$$F_g = \frac{g r^3}{6} \left[\frac{\cos \beta}{\tan \gamma} \sin^3 \theta + \frac{3 \sin \beta}{\tan \gamma} \cos \theta \sin^2 \theta - \frac{2 \sin \beta}{\tan^2 \gamma} \sin^3 \theta \right.$$
$$\left. + \sin \beta \sin^3 \theta + \cos \beta \cos^3 \theta \right] \ldots (63)$$

By Equation (56):

$$Q_{o,r} = -\frac{rg \sin (\gamma - \beta)}{\sin \gamma} \ldots (64a)$$

and,

$$Q_{\gamma,r} = -\frac{rg \sin \beta}{\sin \gamma} \ldots (64b)$$

It will be seen in Fig. 5 that n_o is always less than unity for angles between 180 and 360 degrees. This means that the stresses found by Equations (60) will approach infinity as the radius vector, r, approaches zero. In other words, a mathematically sharp re-entrant corner cannot occur in a structure without having the stresses exceed the elastic limit, contrary to the assumptions of the mathematical theory of elasticity. The material becomes plastic and the stresses in the immediate neighborhood must be redistributed.

Theory Pertaining to Fillets.—In order to predict the elastic stresses it is necessary to abandon the sharp corner and assume a finite curvature. In this case the preceding formulas no longer are valid in the immediate neighborhood of the corner. Photo-elastic experimentation has shown, as might be expected, that a slight curvature only will effect the stresses in the immediate neighborhood (that is, at distances of the order of magnitude of the radius of curvature). The stresses, σ_r, at the tangent points, d and e, Fig. 4, may still be computed (on the side of safety) as if the corner was sharp.

With the foregoing assumption an approximate method is developed herein for the determination of the stresses on the boundary of the fillet. The origin

is chosen in the center of curvature and the axes, ξ and η, are parallel to Axes X and Y. The notations, ρ, ϕ, are used for the polar co-ordinates in the new system.

Assume that the stresses, σ_d and σ_e, have been computed by the methods shown (such as, by Equations (60)), and assume that a constant pressure is exerted on the curved boundary, $\rho = R$. If there is no pressure, $p = 0$. Now, consider the stress function:

$$F = (B_1 \cos \phi + B_2 \sin \phi) \left(\frac{1}{\rho} + \frac{2 \rho \log \rho}{R^2} \right) - \frac{1}{2} \rho^2 p + \frac{1}{2} gR^2 \rho \phi \sin (\phi - \beta) \quad \ldots\ldots\ldots\ldots\ldots\ldots (65)$$

With Equations (2) applied to Equation (65) it is easily verified that when $\rho = R$, $\sigma_\rho = -p$; and $\tau_{\rho, \phi} = 0$ for any value of ϕ.

The arbitrary constants, B_1 and B_2, are now to be determined such that when $\rho = R$, and $\phi = \frac{\pi}{2}$:

$$\sigma_\phi = \sigma_d \quad \ldots\ldots\ldots\ldots\ldots\ldots\ldots\ldots\ldots\ldots (66a)$$

and when $\rho = R$, and $\phi = \gamma - \frac{\pi}{2}$:

$$\sigma_\phi = \sigma_e \quad \ldots\ldots\ldots\ldots\ldots\ldots\ldots\ldots\ldots\ldots (66b)$$

By applying Equations (2) to Equation (65):

$$\sigma_\phi = (B_1 \cos \phi + B_2 \sin \phi) \left(\frac{2}{\rho^3} + \frac{2}{\rho R^2} \right) - p - \rho g \cos (\phi - \beta) \ldots (67)$$

Hence, by the conditions expressed in Equations (66):

$$B_1 = [\sigma_e + p + (\sigma_d + p) \cos \gamma + gR \cos \beta \sin \gamma] \frac{R^3}{4 \sin \gamma} \quad \ldots (68a)$$

and,

$$B_2 = [\sigma_d + p + gR \sin \beta] \frac{R^3}{4} \quad \ldots\ldots\ldots\ldots\ldots\ldots (68b)$$

Substituting back into Equation (67) with $\rho = R$:

$$(\sigma_\phi)_{\rho = R} = [\sigma_e + p + (\sigma_d + p) \cos \gamma] \frac{\cos \phi}{\sin \gamma} + (\sigma_d + p) \sin \phi - p \quad \ldots (69)$$

The method of procedure is best shown by a few typical examples.

Examples Computed by Approximate Theory

The underlying assumptions are based, to a large extent, on results of photo-elastic experiments conducted in connection with the Morris Dam (see Part II). It is natural, therefore, to base the example on computations for this dam, because verification is possible. A cross-section of the Morris Dam is shown in Fig. 2. Theory and experiments have shown that the stresses in the upper two-thirds of the dam can be computed accurately by Equations (17)

and (21). The height of the dam is taken as the unit of length. All stresses must be multiplied later by the actual height, H.

Up-Stream Corner, Hydrostatic Loading.—Consider first the up-stream corner with full hydrostatic pressure, $p\,(1 - r)$, on the up-stream face and constant pressure, p, on the foundation above the dam. The body forces will be considered subsequently; that is, $g = 0$.

For this loading the value of $F_2 = F_p$ is given in Equation (61). Points a and b (Figs. 2 and 4) are chosen as $r = a = b = 0.3$; the stress, σ_a, can be computed with reasonable accuracy by superposing Equations (35) and (39a); q_1 in Equation (35) is the total horizontal water pressure on the dam uniformly distributed over the base l_1; and p_o in Equation (39a) is the pressure, p, on the up-stream foundation.

In the present application, a is an up-stream point; $q_1 = \dfrac{p}{2\,l_1}$; and, $l_1 = 0.86$. The total stress, then, is $\sigma_a = + \dfrac{p}{0.86\,\pi} \log \dfrac{1.16}{0.3} - p = - 0.500\,p$.

Point b is sufficiently far from the base so that σ_b may be computed as σ_x by Equation (18a). In the present application, $K = \tan 41° 52' = 0.8963$; $x = 0.7$; $y = 0$; and $\sigma_b = + 0.871\,p$.

The up-stream corner angle, γ, $= 267° 08'$. By Fig. 5, $n_o = 0.55$; and $n_1 = 0.93$; and, by Equation (46), $m_o = 0.895$; and $m_1 = - 0.318$. The quantities, $Q_{o,a}$ and $Q_{\gamma,b}$, are now found by placing $a = b = 0.3$ in Equations (62); thus: $Q_{o,r} = - (1 + 0.05\,r)\,p$; $Q_{\gamma,r} = - (1 + 0.0025\,r)\,p$; $Q_{o,a} = - 1.015\,p$; and $Q_{\gamma,b} = - 1.001\,p$. By substitution in Equations (60);

$$(\sigma_r)_{\theta=o} = \left[0.6945\left(\frac{1}{r}\right)^{0.45} - 0.6078\left(\frac{1}{r}\right)^{0.07} - 0.05\,r - 1\right]p \quad \ldots(70a)$$

and,

$$(\sigma_r)_{\theta=\gamma} = \left[0.6945\left(\frac{1}{r}\right)^{0.45} + 0.6078\left(\frac{1}{r}\right)^{0.07} - 0.0025\,r - 1\right]p \quad \ldots(70b)$$

In Equations (70), it is to be noted that: r is measured in units of height of dam and p is the actual hydrostatic pressure at the base. By Equations (70), σ_r becomes infinite as $r \to 0$. To eliminate this condition assume a finite radius of curvature, $R = 0.025$, at the corner with tangent points at $d = e - R \cot 0.5\,\gamma = 0.0238$ (see Figs. 2 and 4).

Now, compute σ_d by Equation (70a) and σ_e by Equation (70b) for $r = e = d = 0.0238$; thus, $\sigma_d = + 1.943\,p$; and $\sigma_e = + 3.523\,p$. Substitute in Equation (69) with $g = 0$:

$$(\sigma_\phi)_{\rho=R} = [- 4.3813 \cos\phi + 2.943 \sin\phi - 1]\,p \quad \ldots\ldots\ldots(71)$$

The maximum occurs when $\phi = 146° 07'$; and σ_ϕ (max.) $= + 4.278\,p$. The stresses computed by Equations (70) and (71) are plotted in Fig. 2(a).

Up-Stream Corner, Mass Forces.—Now, consider mass forces only; that is, let $p = 0$. Only vertical forces are assumed to exist; hence, $\beta = 90°$; $g_x = 0$; and $g = g_y =$ weight per unit volume. The stress, σ_a, computed by

Equation (39*a*) is zero; σ_b is computed as σ_x by Equation (22*a*) (for $x = 0.7$; $y = 0$, and $K = 0.8963$); and, therefore, $\sigma_a = 0$, and $\sigma_b = -0.660\,g$.

Now, compute the quantities, Q, etc., by Equations (64), with $\beta = 90°$; $\gamma = 267° 08'$; and $a = b = 0.3$; thus: $Q_{o,r} = +0.0501\,r\,g$; $Q_{\gamma,r} = +1.001\,r\,g$; $Q_{o,a} = +0.015\,g$; and $Q_{\gamma,b} = +0.3003\,g$.

By substitution in Equations (60) with $p = 0$, and n_o and n_1 as before:

$$(\sigma_r)_{\theta=o} = \left[-0.2837\left(\frac{1}{r}\right)^{0.45} + 0.4345\left(\frac{1}{r}\right)^{0.07} + 0.0501\,r \right] g \quad \ldots(72a)$$

and,

$$(\sigma_r)_{\theta=\gamma} = \left[-0.2837\left(\frac{1}{r}\right)^{0.45} - 0.4345\left(\frac{1}{r}\right)^{0.07} + 1.001\,r \right] g \quad \ldots(72b)$$

in which r is measured in units of H. Again, the stresses become infinite for the sharp corner when $r \to 0$. The radius of curvature, $R = 0.025$, is assumed as before, and $d = e = 0.0238$. By Equations (72) with $r = d = e = 0.0238$: $\sigma_d = -0.9596\,g$; and $\sigma_e = -2.0657\,g$. Substitute in Equation (69) with $p = 0$, thus:

$$(\sigma_r)_{\rho=R} = [+2.0202\cos\phi - 0.9695\sin\phi]\,g \quad \ldots\ldots\ldots\ldots(73)$$

The maximum occurs when $\phi = 154° 36'$; and maximum $\sigma_\phi = -2.237\,g$. The stresses computed by Equations (72) and (73) are plotted in Fig. 2(*b*). For the section under consideration let $p = 108.5$ lb per sq in., and $g = 2.5\,p = 271$ lb per sq in., corresponding to 156-lb concrete.

In computing the stresses for the down-stream corner the procedure is exactly the same as for the up-stream corner. The origin is chosen at the toe with the X-axis along the down-stream foundation and the Y-axis positive into the foundation. If no pressures act on the down-stream face and foundation, $F_p = 0$; and F_g is again given by Equation (63), with γ equal to the re-entrant corner angle of the toe, and $\beta = 90°$, if the foundation is horizontal and if inertia forces do not exist. Point b (Fig. 2 (*b*)) is chosen on the down-stream face and Point a on the down-stream foundation, such that $r_a = r_b = -\dfrac{0.3}{\sin\gamma}$. The radial stress, $\sigma_b = \sigma_x + \sigma_y$, is computed by Equations (18) in the case of hydrostatic loading and by Equations (22) in the case of mass forces. The stress, σ_a, is computed by Equation (35) and becomes negative. The results are plotted in Fig. 2 for the Morris Dam, assuming a fillet radius of $0.025\,H$ as at the up-stream corner.

The Morris Dam is not designed with fillets, but it was necessary to manufacture the models used for the photo-elastic experiments (scale, 1:600) with a $\frac{1}{8}$-in. radius ($0.025 \times$ height) at the corners to prevent failure when hydrostatic load was applied in the absence of body forces. For this reason the same radius was used in the computations for stresses in the fillets.

The approximate method of analysis is recommended only for preliminary work, in order to fix suitable dimensions in the base region of the section. In the final analysis one of the methods explained in Application III should be used.

Based on the present computations and those for other radii of fillets it would seem that, for stable gravity dams, radii of $0.4\,H$ to $0.08\,H$ would be suitable at the heel and $0.10\,H$ to $0.20\,H$ at the toe, depending on the height of the dam and the quality of the masonry. The up-stream fillet is determined for the case of an empty reservoir, the down-stream one for the case of a full reservoir.

PART II.—PHOTO-ELASTIC EXPERIMENTS IN CONNECTION WITH THE MORRIS DAM, IN CALIFORNIA

Brief Outline of the Photo-Elastic Phenomenon

Although the principles involved in photo-elastic stress analysis may be found in treatises on photo-elasticity[10] a short description is given herewith, for the sake of completeness.

About 125 years ago the English physicist, Sir David Brewster, discovered that isotropic media become doubly refracting when placed under stress. They then behave optically as crystalline media. The planes of principal stress correspond to the crystal planes. If a plane-polarized monochromatic ray (see Fig. 8), is sent normally through a plate stressed in its own plane,

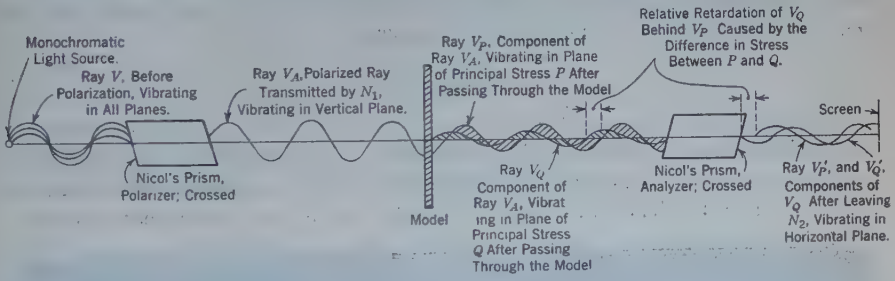

FIG. 8.

the ray will be resolved into two component rays each vibrating in a plane of principal stress. The two ray components will usually have different velocities in the plates; therefore, while passing through the plate, the wave front of one ray will get ahead of the wave front of the other ray a small distance, δ, which is called the relative optical displacement of the two ray components. If, after leaving the plate, the two components are combined so as to vibrate again in the same plane, interference will take place due to the relative displacement, δ. Complete interference will occur when $\delta = 0, 1, \ldots n$, wave lengths. This furnishes a means of measuring the displacements. It has been shown theoretically by Clerk Maxwell[11], and verified experimentally that the difference in magnitudes of the two principal stresses, σ_P and σ_Q, at the line of passage is in direct proportion to the relative displacement. The latter can be measured in terms of wave lengths of the light by counting the order, n, of interference, hence:

$$\sigma_P - \sigma_Q = n\,C \ldots\ldots\ldots\ldots\ldots\ldots\ldots\ldots (74)$$

[10] "Photo-Elasticity", by Coker and Filon.

[11] "On the Equilibrium of Elastic Solids", by Clerk Maxwell. *Transactions*, Royal Soc. Edinburgh, Vol. XX, Pt. I; also, "Photo-Elasticity", by Coker and Filon, p. 198.

in which C is a constant which depends on the type of material, the thickness of the plate, and the wave length of the light. It will be shown later how C is determined. (It is to be noted in passing that the number of fringes is directly proportional to the thickness of the plate.)

The principal stress difference, $\sigma_P - \sigma_Q$, is equal to twice the maximum shear at the line of passage; hence, this quantity is known when the fringe order, n, is observed. Furthermore, $\sigma_P - \sigma_Q$ will change continuously from point to point in the plate; therefore, the optical displacements, δ, will do likewise, and equal integral values of n will occur along continuous interference bands called "isochromatics" which then may be defined as lines of equal maximum shear.

The plane polariscope is shown schematically in Fig. 8, with explanatory notes. The two Nicol's prisms, the polarizer and the analyzer, are "crossed"; that is, their polarizing planes are set at right angles so that no light will reach the screen, when the plate is not in the field or when it is unstressed.

As already explained alternate dark and light bands, "isochromatics", will appear on the screen when the stressed plate is placed in the path of the light. Along the edges of the model one of the stresses, σ_P or σ_Q, is known, and the fringe order, n, can be observed so that the other stress (σ_Q or σ_P) may be computed by Equation (74) when C is known.

Calibration

The simplest way to determine the value of C is to subject a beam of rectangular cross-section to uniform bending. The beam must be cut from the model material. The fringe pattern obtained in a bakelite test beam is shown in Fig. 9. The dark band at mid-height is the isochromatic of zero

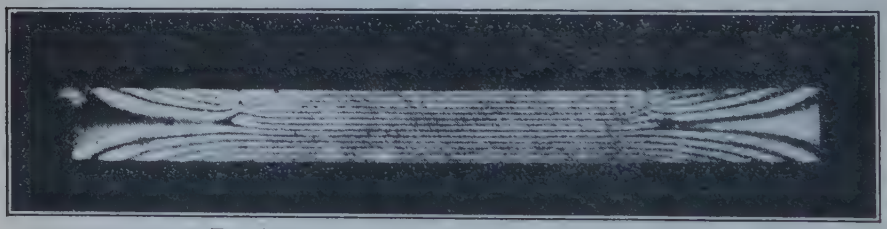

Fig. 9.—Isochromatics in Calibration Beam.

order ($n = 0$), or the neutral axis. The constant bending moment and the dimensions of the beam section can be measured so that the horizontal stress at the extreme fibers can be computed. In the present experiment, $\sigma_P = 1\,055$ lb per sq in. No load occurs at mid-span; that is, $\sigma_Q = 0$. The fringe order, n, is counted at the top or bottom (in this case, 6), the neutral axis being of zero order. Hence, by Equation (74),

$$C = \frac{\sigma_P - \sigma_Q}{n} \qquad (75)$$

or, $\frac{1\,055}{6} = 176$ lb per sq in. The even spacing of the parallel fringes shows

that the engineering assumption of linear stress distribution holds exactly for a beam of uniform thickness stressed with constant bending moment. The thickness of the beam was 0.346 in. and white light with a blue Wratten filter (about 4 100 Angstrom) was used. This filter and models, 0.346 in. thick, were used in both the experiments to be described. If the thickness, t, of the model were different from that of the test beam, T, merely multiply C in Equation (75) by $\frac{T}{t}$.

It may happen that Ray V_A (Fig. 8) is vibrating in the plane of the principal stress, σ_P, at the line of passage. In this case Ray V_A (= Ray V_P) will pass unmolested through the plate and the orthogonal component, V_Q, will be zero. Therefore, nothing will happen on the screen and darkness will prevail in the image of the point of passage, the Nicol's prisms being "crossed". When the polarizing plane of the polarizer is set at a known angle the rays automatically will seek the points in the model at which one of the principal stresses is parallel to the polarizing plane. The stress directions in a model will generally vary continuously (except at singular points) so that the dark points just described will also form a continuous band in the image known as an "isoclinic" or locus of points having their principal stresses parallel to the known plane of polarization. If the polarizer and analyzer are now rotated together through a certain angle, another isoclinic will appear, etc. In this manner the direction of the principal stresses can be found throughout the model.

Although the location of the isoclinic changes with each prism setting, the system of isochromatics will remain stationary and, therefore, are easily distinguished.

By using circularly polarized light, instead of plane polarized light the isoclinics can be eliminated. In this experiment the light vector, V_A, is made to rotate with a high, uniform, angular velocity while passing through the model and thus it can have no directional preferences; therefore, isoclinics cannot occur. Circularly polarized light is produced by inserting what is known as a "quarter wave plate" between each Nicol prism and the model. These crystalline plates are usually obtained by splitting mica to a thickness corresponding to a relative retardation of the two component rays, equal to one-fourth the wave length used in the experiment. The theory of this phenomenon may be found in treatises on passage of light through crystalline media.[12]

By using materials of low optical sensitivity (that is, a very large C in Equation (74)) such as plate glass, the isoclinic lines which are only a function of the stress direction can be made to appear sharply long before the model is stressed sufficiently for the isochromatics to show except as a slight illumination of the glass. The latter effect makes the isoclinic stand out clearly as a black line on a light background (see Fig. 8). Glass without initial stresses must be used, and is distinguished by holding the unstressed glass plate in the field of the polariscope before cutting it into the desired model.

[12] "Photo-Elasticity", by Coker and Filon, p. 73.

The bakelite plates used for the isochromatics generally had to be annealed before planing, polishing, and modeling, by heating them in a well controlled oven to about 80° C for a couple of hours and then cooling them gradually to room temperature over a period of about 10 hr. A newer type of bakelite usually does not need to be annealed.

Evaluation of Stresses

The lines of principal stress can be drawn when the system of isoclinic lines is known as explained subsequently under the heading, "Hydrostatic Loading: Isoclinic," (see, also, Fig. 10). The magnitude of stress along the

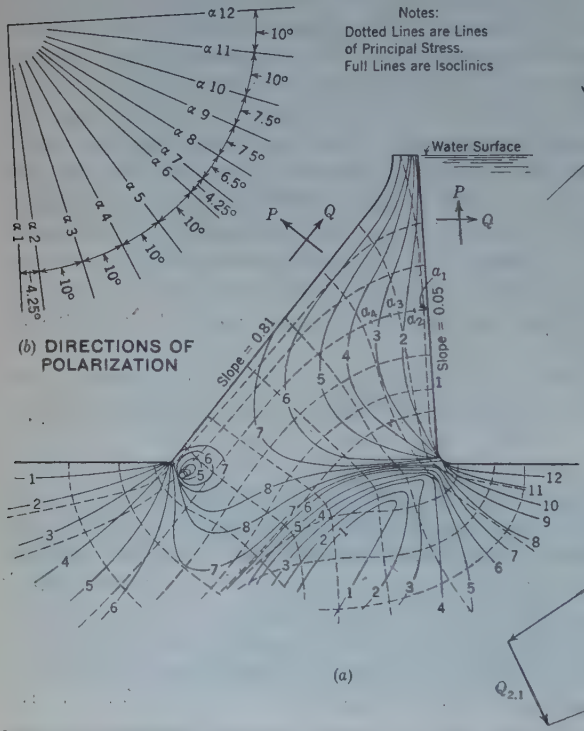

Fig. 10.—Isoclinics and Lines of Principal Stress; Hydrostatic Loading.

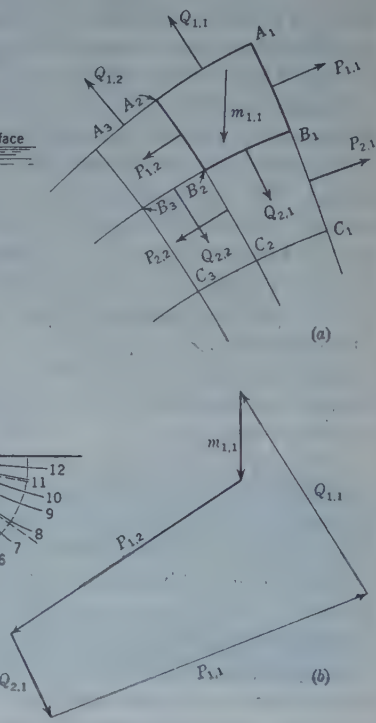

Fig. 11.—Graphical Integration of Principal Stresses.

lines of principal stress can then be integrated by use of the isochromatic lines, the known boundary forces, and Equation (74). Methods for this work are given in treatises on photo-elasticity.[13]

In many types of problems, even when body forces are to be dealt with, the following method is convenient for determining the magnitudes, σ_P and σ_Q, along given lines of principal stress. The method is essentially structural and was developed by considering that the structure is composed of two systems of orthogonal arches bounded by the lines of principal stress. These

[13] "Photo-Elasticity," by Coker and Filon, pp. 2, 47.

arch strips are interlaced in such a way that only normal forces (no shear) exist on any element or block bounded by the four principal stress lines; that is, two from each system. The integration problem is then reduced to the determination of the force polygon, being given the funicular curve and certain reactions.

Consider the element, A_1, B_1, A_2, B_2, bounded by the principal lines of stress shown in Fig. 11(*a*). The only forces acting on the element are $P_{1,1}$, $P_{1,2}$, $Q_{1,1}$, and $Q_{2,1}$, normal to Surfaces *A*, *B*, etc., and perhaps the mass force, $M_{1,1}$. If $P_{1,1}$, $Q_{1,1}$, and $M_{1,1}$ are assumed to be known in magnitude and direction, then $P_{1,2}$ and $Q_{2,1}$ can be found by constructing the force polygon.

Proceed to the element, A_2 B_2 A_3 B_3, etc., until all the forces, $P_{1,n}$ and $Q_{2,n}$, are found. It is necessary to start the construction at the boundary, A_1, A_2, A_3, etc., where the forces, $Q_{1,n}$ and $P_{1,}$ are known or can be found by the isochromatics and boundary forces. When all the forces, $Q_{2,n}$, are found, consider B_1, B_2, B_3, etc., as a new boundary, apply the now known forces, $Q_{2,n}$, reversed, and the known forces, $P_{2,1}$, and find the forces, $Q_{3,n}$ and $P_{2,n}$, by construction, etc. The average stresses over the elementary sides are found by dividing the forces by the corresponding sides. Finally, the principal stresses at B_2, say, will be:

$$\sigma_Q = \frac{1}{2}\left[\frac{Q_{2,1}}{B_1\ B_2} + \frac{Q_{2,2}}{B_2\ B_3}\right] \ldots\ldots\ldots\ldots\ldots\ldots (76a)$$

and,

$$\sigma_P = \frac{1}{2}\left[\frac{P_{1,2}}{A_2\ B_2} + \frac{P_{2,2}}{B_2\ C_2}\right] \ldots\ldots\ldots\ldots\ldots\ldots (76b)$$

It will be seen that Equations (74) furnish a check on $\sigma_P - \sigma_Q$ at all points, which should be made after the completion of the stresses along each line of principal stress.

The construction is easily arranged in a force diagram so that duplications of lines are avoided. Note that if the lines curve rapidly small elements must be used.

The integration of stresses along principal lines of stress is tedious and often not very accurate in complicated stress patterns. Consequently, efforts have been made to obtain other methods.

A two-dimensional state of stress is determined completely when the principal stresses, σ_P and σ_Q, and their directions are known at all points; $\sigma_P - \sigma_Q$ is known throughout by the isochromatics and by Equation (74). The directions are known by the isoclinics; hence, if $\sigma_P + \sigma_Q$ can be found, the state of stress is determinate; $\sigma_Q + \sigma_P$ can be obtained by measuring the lateral dilations of the model with an extensometer,[13] or by the membrane analogy.[14]

Body Forces

Body forces — weight and inertia — are difficult to apply correctly in photo-elastic experimentation. It is possible to examine isolated regions in the

[14] *Proceedings*, Am. Soc. C. E., May, 1935, p. 597.

model by substituting the surrounding mass forces by equivalent external loads as long as these forces are placed far enough away from the region in question to permit proper distribution. This method was used in the experiment shown in Fig. 2(*b*) and Fig. 12(*a*).

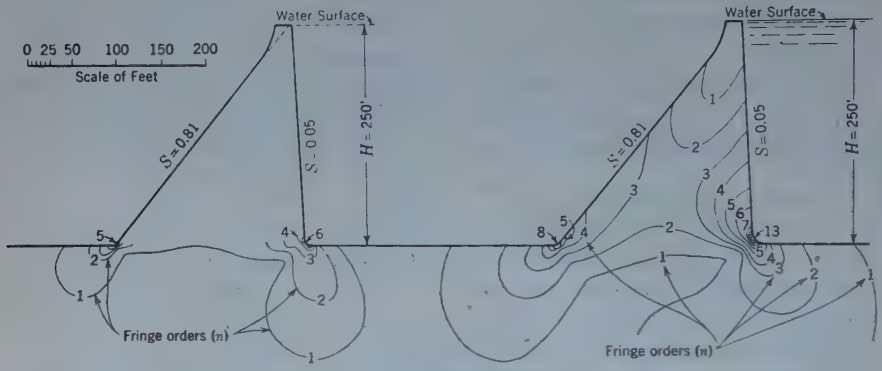

(*a*) DUE TO WEIGHT OF DAM CORRECT IN FOUNDATION ONLY

(*b*) FOR HYDROSTATIC PRESSURE ON UPSTREAM FACE AND FOUNDATION

FIG. 12.

The weight of the model itself is too slight to have any effect unless it is magnified many times. The easiest method would be to rotate the model and observe it whenever it passes through the optical field. This method has not yet been attempted, and it will require a steady rotor mechanism, free of vibration, to obtain a good photographic exposure of the photo-elastic lines. The polariscope used by the writer would be admirably suited for such an experiment. The model could be attached to one end of a rigid rotor and the photographic plate to the other end, each passing through the optical field simultaneously with the same relative angular velocity. A new method has been developed by the writer in connection with experimentation on the Grand Coulee Dam, by which only the corrections to the straight-line stress distribution are involved. An interesting equivalent boundary loading has recently been pointed out by M. A. Biot.[15]

Stresses have been determined experimentally for the section shown in Fig. 2, under all critical loading conditions, including earthquake accelerations and uniform shrinkage relative to the foundation.

Hydrostatic Load on the Up-Stream Face and Foundation: Isochromatics.—A bakelite model, with blue filter and quarter-wave plates, was used to produce isochromatics. The model scale was 1:600; the photographic scale, 1:900; and the loading factor, 4.6, which means that the hydrostatic pressure at any point in the model was 4.6 times as great as at the corresponding point of the actual dam. The up-stream face was loaded linearly by three levers, each applying the correct force through knife-edges to a steel shoe. The uniform distribution on the up-stream foundation was applied by a single lever

[15] *Transactions*, A. S. M. E., Vol. 2, No. 2, June, 1935.

acting on a heavy steel shoe. Soaped rubber paddings were used between the shoes and the edge of the model, in order to avoid shear forces and local concentrations.

The isochromatics are plotted in Fig. 12(*b*) and, from these, the maximum shear in the model, in pounds per square inch, is obtained directly by Equation (74); thus: $\tau_{max.} = \frac{\sigma_P - \sigma_Q}{2} = \frac{n\,C}{2} = 88\,n$, C being equal to 176 by Equation (75). The shear stresses at corresponding points of the actual dam will then be, in pounds per square inch,

$$\tau_{max.} = \frac{88\,n}{\text{Load factor}} = \frac{88\,n}{4.6} = 19\,n \qquad (77)$$

in which n is the fringe order given in Fig. 12(*b*). The actual boundary stresses are also determined by Equation (74):

$$\sigma_P - \sigma_Q = \frac{176\,n}{\text{Load factor}} = 38\,n \qquad (78)$$

On the rear face and foundation, $P = 0$; hence:

$$Q = -38\,n \qquad (79)$$

On the up-stream face and foundation of the dam, the hydrostatic pressure is, in pounds per square inch, $Q = \frac{-62.5}{144}\,h' = -0.434\,h'$, in which h' is the depth, in feet, to the point in the prototype, $= \frac{h \times 900}{12} = 75\,h$, and h is the depth, in inches, to the corresponding point in the photograph. Hence, by Equation (78),

$$P = 38\,n - 32.55\,h \qquad (80)$$

in which n is the fringe order at the point in question.

The experimental results obtained by substituting the fringe order, n, along the boundaries of Fig. 12(*b*) into Equations (79) and (80) are plotted in Fig. 2(*a*) with the theoretical values obtained in Part I of this paper.

It will be noticed that in the upper two-thirds of the dam the stresses obtained by Equations (18) agree with experimentation. In the base region the boundary stresses are in close agreement with the approximate methods discussed under the heading, "Application IV", in Part I. It can be shown that the isochromatics for the infinite wedge are concentric ellipses with their centers at the vertex, agreeing with the upper isochromatics in Fig. 12(*b*). A slight disagreement between the computed and experimental values may be expected due to the finite crown width, which is neglected in Equation (17).

Hydrostatic Loading: Isoclinics.—A plate-glass model and white light without the quarter-wave plates were used to produce isoclinics. The photo-

graphic scale again was 1:900. It is to be noted that the isoclinics are independent of the loading factor as defined previously, except that these lines become sharper with increased factor. In order to cover the entire region it is only necessary to obtain the isoclinics for various prism settings, α, through a range of 90°, as shown in Fig. 10(*b*). A separate photograph is necessary of course for each prism setting, a sample of which is shown in Fig. 13 cor-

FIG. 13.—ISOCLINIC LINES FOR PRISM SETTING, α_2, IN FIG. 10(*b*).

responding to the prism setting, α_3, in Fig. 10(*b*). The isoclinics are plotted in Fig. 10(*a*), and the lines of principal stress are obtained in the following manner: Through a_1 of Fig. 10(*a*) draw $a_1 a_2$ perpendicular to α_1 of Fig. 10(*b*); then draw $a_2 a_3$ perpendicular to α_2, etc. The points, $a_2 a_3$, etc., are taken approximately midway between the corresponding isoclinics, 1, 2, etc.

It can be shown that the isoclinics for the wedge are straight lines radiating from the vertex, agreeing approximately with the upper two-thirds of Fig. 10(*a*). The isoclinics perhaps show more clearly than any other argument the effect of the foundation on the stresses in the base region. The corners in the models were rounded; with sharp corners, all isoclinics would be represented at each corner.

Weight Forces (Correct in Base Region Only).—In this experiment the stresses were obtained near the base due to the weight. Owing to the loading difficulties only the stresses near the base and in the foundation were determined. The forces representing the weight of the dam above the base were applied through a single lever distributing the weight to four points in such a manner that the resultant was correct at the base. The isochromatics are plotted in Fig. 12(*a*) near the base and in the foundation. The photographic scale was 1:900, and the loading factor was 1.75, based on 156-lb concrete.

The stresses in the actual dam would be (see Fig. 12(*a*)):

$$\tau_{\max.} = \frac{P - Q}{2} = \frac{176\,n}{2 \times \text{load factor}} = 50\,n \ldots\ldots\ldots\ldots (81)$$

On the boundaries, $P = 0$; and hence,

$$Q = -100\,n \ldots\ldots\ldots\ldots\ldots\ldots\ldots\ldots (82)$$

The experimental results near the base obtained by substituting the fringe order, n, at the boundaries of Fig. 12(*a*) into Equation (82) are plotted in Fig. 2(*b*) together with the theoretical values. It will be seen that the stresses obtained in Part I agree fairly well with the experimental results. It is of interest to note that the compression at the down-stream corner is of considerable magnitude.

The results in Fig. 2 can be applied to a dam of similar proportions, but of height, H', merely by changing the stress scale in the ratio, $250 : H'$. If the concrete in the new dam weighs w lb per cu ft, the stress scale in Fig. 2(*b*) is changed further in the ratio, $156 : w$. The stress concentration in the base region at the down-stream face, due to weight, extends only a short distance into the dam.

The foundation was clamped between rubber gaskets to the steel frame along three edges. This arrangement allowed elastic deformation to take place so as to produce, as closely as possible, the effect of an infinite half-plane. The photo-elastic results in the foundation, of course, are only valid in the region near the base.

In the interpretation of experimental results from model to prototype it is important to note that in two-dimensional problems: (1) The stress distribution is independent of the elastic properties; and (2) the stresses in the prototype are directly proportional to the stresses at corresponding points in the model.

The discrepancy between the experimental and theoretical curves of Fig. 2(*a*) may be due partly to incorrectness in the pressure, Q, at the fillet of the model and partly to a slight shop error in the radius of the fillet. Other experiments with larger fillet radii showed much better agreement between experimental and theoretical values of fillet stresses. Very small radii were used in these experiments in order to produce as closely as possible the effect of sharp corners.

Based on the comparison between theory and photo-elastic experimentation the writer concludes that results obtained by the foregoing application of the mathematical theory for isotropic media which behave in accordance with Hooke's law are reasonably correct. It remains only to justify the application to materials, such as concrete masonry, which do not strictly follow Hooke's law. Of course, this can only be done by observations in the field and in testing laboratories. A great many such data are already available, but it is beyond the scope of this paper to treat on this subject. A well placed system of electrical strain-gauges was installed in a section of Morris Dam which, in time, will throw further light on this point, on the question of shrinkage effects, and on lateral stresses in long gravity dams.

AMERICAN SOCIETY OF CIVIL ENGINEERS

Founded November 5, 1852

PAPERS

FLOOD AND EROSION CONTROL PROBLEMS AND THEIR SOLUTION

By E. Courtland Eaton,[1] M. Am. Soc. C. E.

Synopsis

The flood and erosion control problem treated in this paper occur in highly developed areas where there is a relatively low seasonal run-off; these areas, however, are subject to brief, although violent, torrential storms, that result in floods of exceptionally high intensity. When fires denude the sparse vegetation from steep mountain slopes the flood intensities increase and added débris hazards occur, due to erosion.

Basic precipitation and run-off records are given in this paper, as are engineering methods of constructing hydrographs of expected floods, and the regulation needed for control. Similarly, measurements of erosion quantities are presented with suggested solutions of control and a method of avoiding unnecessary capital expenditures in advance of requirements. The incidental conservation of flood waters for domestic use and for irrigation is discussed.

Introduction

Los Angeles County in California, with a population of about 2 250 000 (of whom more than 85% are residents of cities), covers an area of 4 115 sq miles. Its population increase has been nearly 180% since the last major flood (1914), and assessed property values rose, in the same period (1914 to 1931), from $850 000 000 to more than $4 000 000 000. The County's petroleum, agricultural, motion picture, and manufacturing industries have an aggregate annual value of more than $1 000 000 000. It is estimated that only 8% of the present population have experienced, or have a realization of, the 1914 flood.

Property valued at more than $300 000 000 and containing 380 000 persons, is subject to possible inundation due to floods.[2] Hazards may be classi-

Note.—Discussion on this paper will be closed in December, 1935, *Proceedings*.

[1] Cons. Engr., Los Angeles, Calif.

[2] "Comprehensive Plan for Flood Control and Conservation," by E. C. Eaton, 1931.

fied under two main heads: The main valleys and coastal plains are subject to inundation by either the overflow of present channels or by the departure of the rivers from existing to new locations; and, in the foot-hill areas, the perils are from sudden flash floods, and débris flows, particularly following water-shed denudation by fires. Valley inundation may be anticipated, by at least hours from distant mountain rainfall records. Foot-hill débris flows may result if burned catchment areas, after becoming saturated with water, are subjected to high-intensity storms. Such flow occurs without warning and may follow storms of high intensity or cloudbursts, almost immediately.

The factors that combine to menace life and property in this region are: (*a*) Exceptionally precipitous gradients; (*b*) short mountain streams; (*c*) the unstable character of deep weathered mountain cover held from erosion by sparse vegetation; and (*d*) the characteristic violent torrential storms. Protection from floods may operate to conserve the average annual 120 000 acre-ft of flood water that is now wasted.

The paper describes physical conditions and methods of solving problems, especially those dealing with the relatively new engineering field of erosion control. Necessarily, full details cannot be included, but the foot-note references serve as a bibliography of public reports.

Physical Conditions

Of the 4 115 sq miles that constitute Los Angeles County, 70%, or 2 758 sq miles, is included in the south slopes which drain to the Pacific Ocean (see Fig. 1). The area comprises 1 589 sq miles of mountain water-shed (809 sq miles of which is in Federal forests); 285 sq miles of small water-sheds; and 884 sq miles of valley plains sloping toward the ocean. About 210 000 acres of valley land is under irrigation, and 235 000 acres is devoted to industrial and domestic purposes.

The high mountain areas form a northern boundary of approximately 45 miles, crest length, from which the two major collecting rivers—the San Gabriel and Los Angeles—originate and, after traversing the valleys, they converge and discharge into the ocean at points only six miles apart. Mountain peaks rise to Elevation 10 080 (United States Geological Survey datum). The main rivers are forced to converge by the foot-hills that project on to the plains—the Santa Monica hills from the west and the Puente and San José hills from the east.

The San Gabriel River has a tributary drainage of about 800 sq miles and the Los Angeles River one of about 900 sq miles. The largest catchment of the San Gabriel River is 213 sq miles of the San Gabriel water-shed; that of the Los Angeles River is the Big and Little Tujunga water-sheds with 137 sq miles. The remaining drainages of both rivers are made up of numerous small streams originating in more than 100 mountain and foot-hill water-sheds ranging in size from 0.5 sq mile to 30 sq miles.

A third drainage system is Ballona Creek fed from 134 sq miles, its principal supply being the run-off from the streets of Los Angeles, Hollywood, and Beverly Hills, transported to Ballona Creek through storm drains.

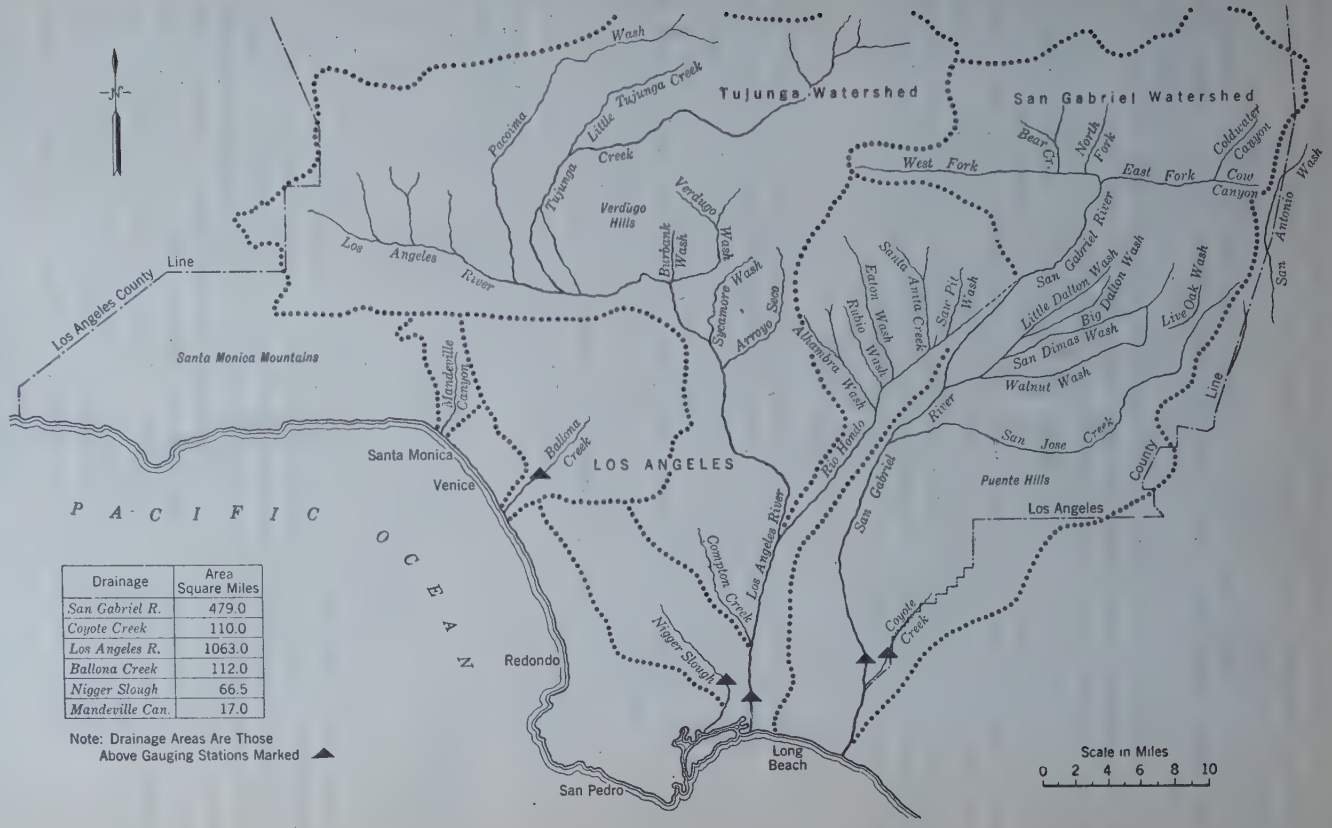

Drainage	Area Square Miles
San Gabriel R.	479.0
Coyote Creek	110.0
Los Angeles R.	1063.0
Ballona Creek	112.0
Nigger Slough	66.5
Mandeville Can.	17.0

Note: Drainage Areas Are Those Above Gauging Stations Marked ▲

FIG. 1.—MAP OF LOS ANGELES COUNTY: DRAINAGES TO PACIFIC OCEAN.

Its ocean outlet is near Venice, Calif. A fourth drainage is Nigger Slough, similarly deriving its main supply from impervious areas. Its discharge point is near San Pedro, Calif.

Along the coast from Venice westward to the Los Angeles County line about twenty individual streams flow directly into the Pacific Ocean. The largest are Malibu Creek, with a drainage area of 67 sq miles; Topanga Creek (20 sq miles), and Mandeville, Rustic, and Sullivan Canyons (12 sq miles), the latter group passing through Santa Monica, Calif.

Mountain and foot-hill drainages have well-defined canyon channels on precipitous grades of 20 to 30%, sharply flattening from 8 to 10% where they debouch on to unstable delta areas. In many instances cones show little evidence of active channels, and, during the dry cycle (1914 to 1931), home sites were sold readily in foot-hill territories by real estate agents who were themselves possibly ignorant of hazards. Normally, mountain and foot-hill watersheds are covered with a chaparral type of vegetation, efficiently functioning as retarders of flood flows and controlling erosion.

Historic Floods

The most recent major floods occurred in 1914 and 1916. In 1914 there were two storm periods: One on January 25, with a maximum intensity of 2.6 in. in 24 hr; and the other on February 18, with an intensity of 4.26 in. Exclusive of harbor damages the estimated loss from these two floods was $10 000 000. Conservatively estimated representative flood peaks were[3] as shown in Table 1. Many lives were lost, thousands of people were made

TABLE 1.—Representative Peak Flows

Stream	Drainage area, in square miles	Peak run-off, in cubic feet per second per square mile
San Gabriel River	229	117
Big Tujunga	118	115
Arroyo Seco	39	366
Sawpit	7	550

homeless, thirty-five bridges were destroyed, and, for six days, there was little communication with the outside world.

Engineers concede that this was by no means a record flood. During previous floods within a 70-yr period, main rivers have materially changed their courses, the Los Angeles River changing from westerly to southwesterly, and the San Gabriel River cutting its new channel from 3 to 6 miles southeasterly. A new river, the Rio Hondo, cut its way and connected the San Gabriel and the Los Angeles River.

Early settlers testify to the occurrence of severe floods in 1815, and again in 1825, and, successively, five major flood periods are recorded in 1861–62, 1884, 1886, 1889, and 1914.[3]

[3] Rept. of Board of Engrs. on Flood Control to the Los Angeles County Board of Supervisors, January 25, 1917, by H. Hawgood, Charles T. Leeds, J. B. Lippincott, and F. H. Olmsted, Members, Am. Soc. C. E.

During the unparalleled dry period, 1916 to 1931, rapid development altered conditions radically, crowding former channel and ponding areas. The increased development of paving and impervious areas alone, totaling more than 55 sq miles has increased the rates and quantities of run-off, and decreased the natural absorption and consequent replenishment of subterranean storages.

A curve prepared in 1931 (see Fig. 2) shows past trends of seasonal rainfall. After this curve was plotted a prediction was made of an uptrend into a wet cycle with increasing wet periods, comparable to the period, 1881–90, in which interval one or more major floods would occur.[2]

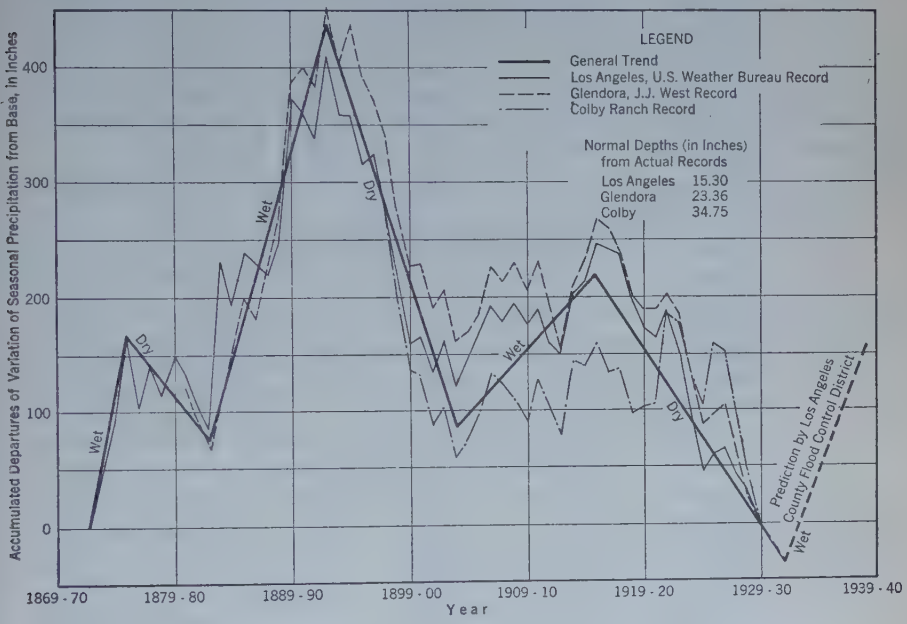

FIG. 2.—GENERAL TREND, SEASONAL RAINFALL.

RAINFALL—RUN-OFF

A co-ordinated system of 237 rainfall and 197 run-off stations was installed by the Los Angeles County Flood Control District commencing in 1927. The more important stations were equipped with recorders. The year, 1931–32, not a year of general flood, had valley rainfall totaling 114% of the normal, that in the mountains totaling 113% of its normal. The seasonal run-off from the San Gabriel River exceeded the combined run-off of the three previous years. Summarized records from three drainages follow: (*a*) San Gabriel-West Fork—area, 49 sq miles; (*b*) Little Tujunga Creek—area, 21 sq miles; and, (*c*) Ballona Creek—area, 112 sq miles.

The San Gabriel and Tujunga water-sheds are mountain catchments with cover in good condition. The San Gabriel water-shed was burned in 1924, but its brush growth is now (1935) restored. The Tujunga water-shed has

not been burned since 1919. Ballona Creek is of a different character, draining flat valley territory, including street drainage from Los Angeles, Hollywood, and Beverly Hills.

The season (1931–32) contained two storm periods, one in December, 1931, and the other in February, 1932. Table 2 gives the distribution of precipita-

TABLE 2.—DISTRIBUTION OF PRECIPITATION, 1931–32

Period		Days of precipitation	Total precipitation, in inches	Maximum precipitation in 24 hours, in inches	Total run-off, in inches	Ratio: Run-off to rainfall, percentage
From:	To:					
(a) SAN GABRIEL WATER-SHED						
October 1	December 24	18	14.10	3.50	0.35	2.5
December 25	January 2	7	8.20	5.04	1.12	13.7
Total for first storm period....		25	22.30	....	1.47	6.6
January 3	February 7	7	10.36	5.30	1.13	....
February 8	February 28	8	12.45	4.54	5.06	....
March 1	May 1	5	1.23	0.67	1.89	....
Total for second storm period.		20	24.04	....	8.08	33.7
(b) LITTLE TUJUNGA WATER-SHED						
October 1	December 24	11	5.15	1.55	Practically none	
December 25	January 2	4	7.00	2.75	0.12	1.7
Total for first storm period..		15	22.15	....	0.12	0.6
January 3	February 7	8	5.64	2.10	0.12	2.1
February 8	February 28	6	4.41	1.15	1.38	31.3
Total for second storm period.		14	10.05	....	1.50	15.0
(c) BALLONA CREEK WATER-SHED						
October 1	December 24	11	4.85	1.95	0.87	18.0
December 25	January 2	4	3.40	2.09	0.88	26.0
Total for first storm period...		15	8.25	....	1.75	21.0
January 3	February 7	10	3.43	1.94	0.54	15.7
February 8	February 28	8	4.55	1.95	1.23	27.0
Total for second storm period.		18	7.98	....	1.77	22.0

tion, maximum 24-hr intensities, and the resulting run-off. The distribution of the San Gabriel run-off was affected by snow. There was 6 to 8 in. of snow above Elevation 4 000 during December, 1931; and 4 to 8 in., during January, 1932; the snow disappeared by February 26, 1932.

Both mountain catchments (particularly the Little Tujunga, the flow of which was not affected by snowfall), show the relatively large proportion of annual precipitation required to produce sufficient saturation to permit run-off. Mountain and foot-hill catchments are deeply covered with weathered material, ranging from the porous disintegrated granites to the less porous soils with higher clay content; consequently, separate values for any water-shed under consideration must be determined. The flood flows will depend upon: (1) Slopes, character of soils and cover (organic growth, litter, etc); (2) the quantity and rate of rainfall required to produce saturation; (3) the

24-hr and 1-hr intensities; and (4) how closely the high-intensity storms follow upon the saturation period.

On the Little Tujunga water-shed from February 6 to 10, 1932, the rains totaled 5.13 in. with 24-hr intensities, on three consecutive days of 2.10, 1.10, and 1.15 in. The run-off in the succeeding five days totaled 1.05 in., or a ratio of run-off to rainfall, of —20 per cent.

On both mountain catchments a total of 10 in. of rainfall was required before appreciable run-off occurred. Contrasted with this is the relatively quick response of run-off to rainfall on Ballona Creek. A total rain of 0.17 in. was followed (November 15, 1931) by a 24-hr rain of 0.96 in., of which 17% appeared in a few hours as run-off. Table 3 shows the rainfall-run-off relation for maximum month, day, and hour, for the three catchments.

TABLE 3.—COMPARISON BETWEEN RAINFALL AND RUN-OFF, 1931–32

Water-shed	Maximum Month			Maximum Day			Maximum Hour		
	Rainfall, in inches	Run-off, in inches	Percentage of run-off	Rainfall, in inches	Run-off, in inches	Percentage of run-off	Rainfall, in inches	Run-off, in inches	Percentage of run-off
San Gabriel	19.74	5.8	29	3.80	1.58	41	0.69	0.08	16
Little Tujunga	7.71	1.47	19	2.10	0.48	23	....	....	....
Ballona Creek	5.95	1.36	23	2.09	0.60	28	0.27	0.07	26

A representative number of scattered records of 24-hr and corresponding 1-hr intensities is given in Table 4.

TABLE 4.—REPRESENTATIVE TWENTY FOUR-HOUR AND CORRESPONDING ONE-HOUR RAINFALL INTENSITIES

Station	Years of record	Elevation, in feet (U. S. Geological Survey)	Twenty-Four Hour Rainfall		One-hour rainfall, in inches
			Date	In inches	
Opids Camp	17	4 480	4– 5–26	12.30	2.00
Mt. Wilson	30	5 850	12–19–21	11.26	1.10
Alder Creek	..	.....	12–19–21	7.40	0.80
San Gabriel Intake	..	1 250	4– 5–26	6.76	1.16
Haines	17	2 500	4– 5–26	5.95	1.10
Valley Forge	..	3 400	2–15–27	5.58	0.87
Sister Elsie	..	.....	4– 5–26	4.77	0.62
Coldbrook Camp	..	3 300	4– 5–26	6.44	0.76

FLOOD HYDROGRAPH DETERMINATION

Studies of the Big Tujunga water-shed are given herein, showing a method of computing possible flood flows, the results, and the regulation required. This catchment, as yet only partly controlled, is the largest individual tributary of the Los Angeles River drainage. Its control is a necessity because of the flood hazard to the thousands living adjacent to the Tujunga Wash and to those living along the Lower Los Angeles River. That most of these people have not, personally, observed conditions causing or accompanying a major flood makes the hazard none the less real.

The Big Tujunga drainage area above the U. S. Geological Survey gauging station ($3\frac{1}{2}$ miles up stream from the mouth of the canyon) is 160 sq miles; to the mouth of the canyon it is 113.5 sq miles; and to a dam site farthest down stream (6 miles below the canyon mouth), 124.5 sq miles. Its average width is 7 miles. The range of elevation is from 1 250 ft at the canyon mouth to the highest peak, Pacifico Mountain, 7 078 ft (U. S. Geological Survey).

Rainfall records are available at thirteen stations in, or applicable to, the drainage. The longest dates back to 1872; the shortest to 1902. The U. S. Geological Survey has gauged the stream only since October 28, 1916, but, fortunately, long-time records are available on the contiguous San Gabriel water-shed. In computing the probable flood peak the procedure was as described in the following paragraphs.[4]

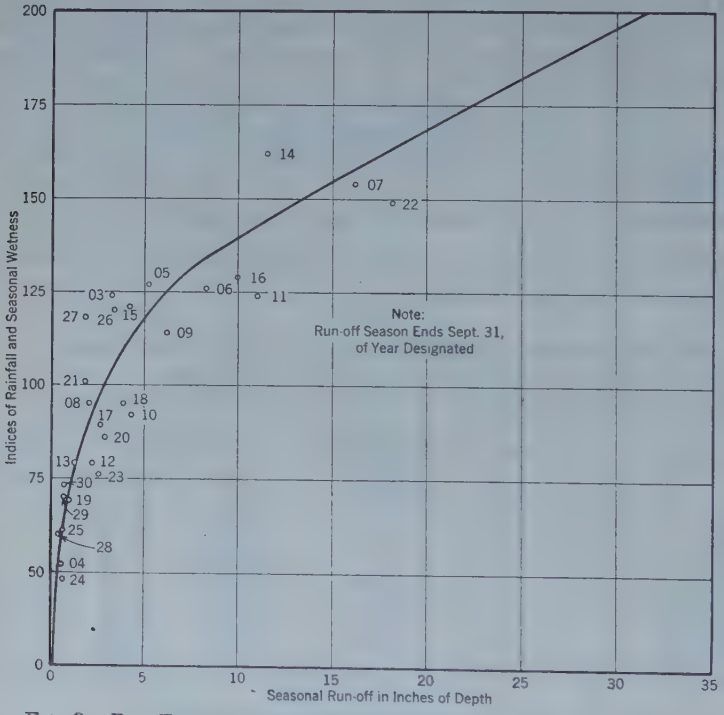

FIG. 3.—BIG TUJUNGA WATER-SHED—INDICATED SEASONAL RUN-OFF, IN INCHES OF DEPTH.

A correlation was prepared from the longer rainfall-run-off records on the San Gabriel water-shed. The results, together with actual Tujunga records, were plotted against the master indices of mean seasonal rainfall and are shown in Fig. 3 in which the seasonal run-off is expressed as depth, in inches, on the water-shed.

[4] Rept. on Big Tujunga Creek Flood Control and Conservation Possibilities, by Franklin Thomas, M. Am. Soc. C. E., September 22, 1931.

Table 5 is a summarization of the results. In its preparation, the curve, Fig. 3, was used to provide the values in Column (5) only when actual, or the correlated, records were not available. As summarized, Table 5 gave the following:

Seasonal Run-Off, in Inches of Depth:	
Fifty-eight year average	5.8
Maximum (1883–84)	47.7
Minimum (1876–77)	0.2
Seasonal Rainfall, in Inches of Depth (Composite for Tujunga Water-Shed):	
Fifty-eight year average	27.3
Maximum	65.8
Minimum	6.8
Ratio of Run-Off to Rainfall, in Percentage:	
Fifty-eight year average	21
Maximum	72
Minimum	2

Rainfall indices for years of largest flows are shown on Fig. 4. In arriving at the expectancy of a major flood it was decided to use the flood of 1883–84 as a criterion for protection, because all indications pointed to that year as the one of major flood in the 58-yr period.

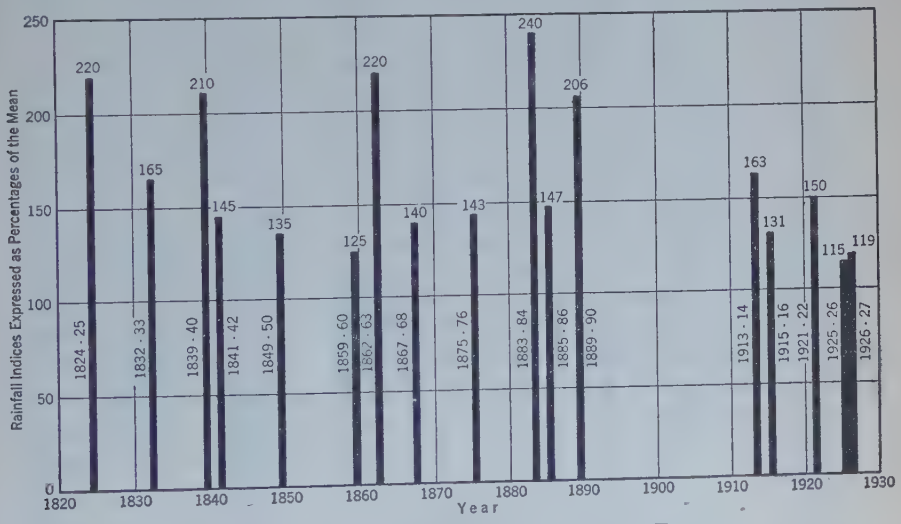

FIG. 4.—RAINFALL INDICES FOR YEARS OF LARGE FLOODS.

The mountain soil cover is disintegrated to great depth; practically no rain falls between May and October, both inclusive; and hydrographic experience has shown that on this area a total of about 10 in. of rainfall causes saturation. If this is closely followed by high-intensity storms, floods are inevitable, the magnitude rising rapidly with increasing intensities.

TABLE 5.—INDICATED PRECIPITATION AND RUN-OFF, BIG TUJUNGA WATER-SHED; PERIOD OF 1872–73 TO 1929–30, INCLUSIVE
(Flow at Dam Site No. 5; Drainage Area, 124.5 Square Miles)

Season	Index of seasonal wetness	Precipitation depth, in inches, October 1 to September 30	Ratio of run-off to rainfall, percentage	Run-off depth, in inches.	Index of seasonable run-off	Estimated seasonal run-off in acre-feet	Seasonal Discharge, United States Geological Survey Gauging Station	
							Correlated from the San Gabriel, United States Geological Survey	Measured
(1)	(2)	(3)	(4)	(5)	(6)	(7)	(8)	(9)
1872–1873	97	26.5	10	2.8	48	18 600	.....	.....
1874	155	42.3	36	15 2	263	100 930	.....	.....
1875	142	38 8	28	10 8	187	71 700	.....	.....
1876	175	47.8	47	22 3	386	148 000	.....	.....
1877	25	6 8	2	0.2	3	1 330	.....	.....
1878	111	30.3	14	4.2	73	27 890	.....	.....
1879	56	15.3	3	0.5	9	3 320	.....	.....
1880	117	32.0	15	4.9	85	32 540	.....	.....
1881	69	18.8	5	1.0	17	6 640	.....	.....
1882	69	18.8	5	1.0	17	6 640	.....	.....
1883	70	19.1	5	1.0	18	6 640	.....	.....
1884	241	65.8	72	47.7	827	316 700	.....	.....
1885	51	13.9	3	0.4	7	2 660	.....	.....
1886	143	39.1	3	11.2	194	74 370	.....	.....
1887	86	23.5	8	1.9	33	12 620	.....	.....
1888	109	29.8	13	3.9	67	25 900	.....	.....
1889	131	35.8	21	7.5	130	49 800	.....	.....
1890	216	59.0	64	37.9	657	251 660	.....	.....
1891	91	24.9	9	2.2	38	14 600	.....	.....
1892	74	20.2	6	1.2	21	7 970	.....	.....
1893	152	41.5	34	14.1	244	93 630	.....	.....
1894	47	12.9	2	0.3	5	2 000	.....	.....
1895	117	32.0	15	4.9	85	32 530	.....	.....
1896	54	14.8	3	0.4	7	2 660	.....	.....
1897	109	29.8	13	3.9	68	25 900	.....	.....
1898	43	11.8	3	0.3	5	2 000	.....	.....
1890	33	9.0	2	0.2	3	1 330	.....	.....
1900	54	14.8	3	0.4	7	2 660	.....	.....
1901	106	29.0	12	3.6	62	23 900	.....	.....
1902	63	17.2	4	0.7	12	4 650	.....	.....
1903	124	33.9	10	3.32	58	22 040	18 790	.....
1904	52	14.2	4	0.61	11	4 050	3 428	.....
1905	127	34.7	15	5.25	91	34 860	29 700	.....
1906	126	34.4	24	8.31	144	55 180	47 000	.....
1907	154	42.1	38	16.21	281	107 600	91 650	.....
1908	95	26.0	8	2.13	37	14 000	12 034	.....
1909	115	31.4	20	6.20	107	41 000	35 077	.....
1910	92	25.1	17	4.31	75	28 600	24 350	.....
1911	124	33.9	33	11.07	192	73 500	62 565	.....
1912	79	21.6	10	2.25	39	14 900	12 730	.....
1913	79	21.6	6	1.29	22	8 500	7 266	.....
1914	162	44.3	26	11.58	200	76 500	65 490	.....
1915	121	33.1	13	4.22	73	28 000	23 905	.....
1916	129	35.2	28	9.99	172	66 000	56 500	.....
1917	89	24.3	11	2.65	46	17 500	.....	15 000
1918	95	26.0	15	3.93	68	26 000	.....	22 200
1919	69	18.9	5	1.01	17	6 700	.....	5 730
1920	86	23.5	12	2.94	51	19 500	.....	16 600
1921	101	27.6	7	1.86	32	12 200	.....	10 500
1922	149	40.7	45	18 22	313	120 000	.....	103 000
1923	76	20.8	12	2.60	45	17 200	.....	14 700
1924	48	13.1	5	0.65	11	4 300	.....	3 670
1925	61	16.7	4	0.65	11	4 300	.....	3 700
1926	120	32.8	11	3.45	60	22 900	.....	19 500
1927	118	32.2	6	1.91	33	12 600	.....	10 794
1928	60	16.4	3	0.43	7	2 800	.....	2 441
1929	70	19.1	4	0.73	13	4 800	.....	4 130
1929–1930	73	20.0	4	0.77	13	5 000	.....	4 350
Summary:								
Total	.....	.....	.....	.....	.....	2 222 290	490 505	236 315
Mean	100	27.3	21	5.8	100	38 315	35 036	16 880
Maximum 1883–84	241	65.8	72	47.7	827	316 700	91 650	103 000
Minimum 1876–77	25	6 8	2	0.2	3	1 330	3 428	2 441

Although it would be possible, under conditions of concentrated rainfall of high intensity, for a flood to occur in a season of index of less than 100, ordinarily the distribution is such that years having indices less than 120 would seldom produce large floods; those with indices as high as 130 to 170 would almost invariably produce large floods; and indices above 200 represent so much rainfall that major floods would be inevitable.

In computing probable flood flow quantities it is necessary, therefore, to examine not only daily precipitation records but hourly intensities. Results of studies of probable maximum 24-hr precipitation of a frequency of once in 50 yr are shown as shaded zones in Fig. 5. Like studies of maximum sustained intensities, in inches per hour, are designated by lines and quantities also in Fig. 5.

A value for the possible 24-hr rainfall averaging 10.4 in. over the catchment, was adopted as well as hourly intensities ranging from 1.8 to 2.7 in. in various parts of the same water-shed. Isolated instances exist in small zones of 24-hr precipitation in excess of 12 in., but it was not expected that this quantity would be general over the entire water-shed.

Further experience showed that a critical 4-day storm may be expected, and that the run-off during that storm will not exceed 50% of the total seasonal run-off. Percentage ratios of maximum 4-day flows to seasonal run-off for the same years, are:

Year	Percentage of ratio	Year	Percentage of ratio
1906.....	23	1921.....	5
1914.....	12	1926.....	35
1916.....	25	1927.....	51

The flows from 1906 to 1916, inclusive, are derived by correlation with San Gabriel records, and the remainder are from actual records.

In a determination of desirable flood-regulating capacity it is necessary to know the effect of the lesser peak flows that will immediately precede the major flood peak. Daily discharges were plotted for critical periods during seven successive days on a number of water-sheds where rainfall-run-off records were available, which indicated that a 4-day hydrograph would involve as extensive a period as would materially affect flood storage; from such records the relation of successive peak flows was derived. The estimated distribution of run-off during a 4-day period on the Big Tujunga water-shed is given in Table 6. The successive peaks are shown on Fig. 6. The quantities refer to estimated flows at a point six miles down stream from the mouth of the canyon at Dam Site No. 5.

TABLE 6.—ESTIMATED DISTRIBUTION OF TOTAL RUN-OFF DURING FOUR-DAY PERIOD

Flood day	Run-off, in acre-feet	Rainfall, in inches	Run-off, in inches	Ratio: Run-off to rainfall
Maximum day.....	30 026	10.4	4.5	0.43
One day preceding.....	23 236	8.7	3.5	0.40
Two days preceding.....	13 316	6.7	2.0	0.30
Three days preceding.....	5 884	4.5	0.9	0.20
Total.....	72 462	30.3	10.9	0.36

The 30 000 acre-ft in one day is equivalent to 241 acre-ft per sq mile of water-shed; the corresponding peak is 48 300 cu ft per sec, or 388 cu ft per sec per sq mile; and the ratio of 4-day to seasonal run-off is $\frac{72\,462}{316\,700}$, or 23 per cent. All the values appear reasonable and quite readily obtainable during a year of excess precipitation.

Five reservoir sites are available in the canyon and below its mouth. Operation studies were made of all combinations resulting in a decision that regulating storage totaling 27 360 acre-ft would reduce the flood peak of 48 300 cu ft per sec to 14 500 cu ft per sec, at a capital cost of about $152 per acre-ft, equivalent to $125 per cu ft per sec, of regulation affected. This regulating storage can be created by dams at three locations, developing capacities of 6 240, 7 170, and 13 950 acre-ft, respectively.

Erosion and Erosion Control

Erosion, in this instance, is defined as the washing of loose material from weathered mountain and foot-hill areas, and its deposition upon the lower

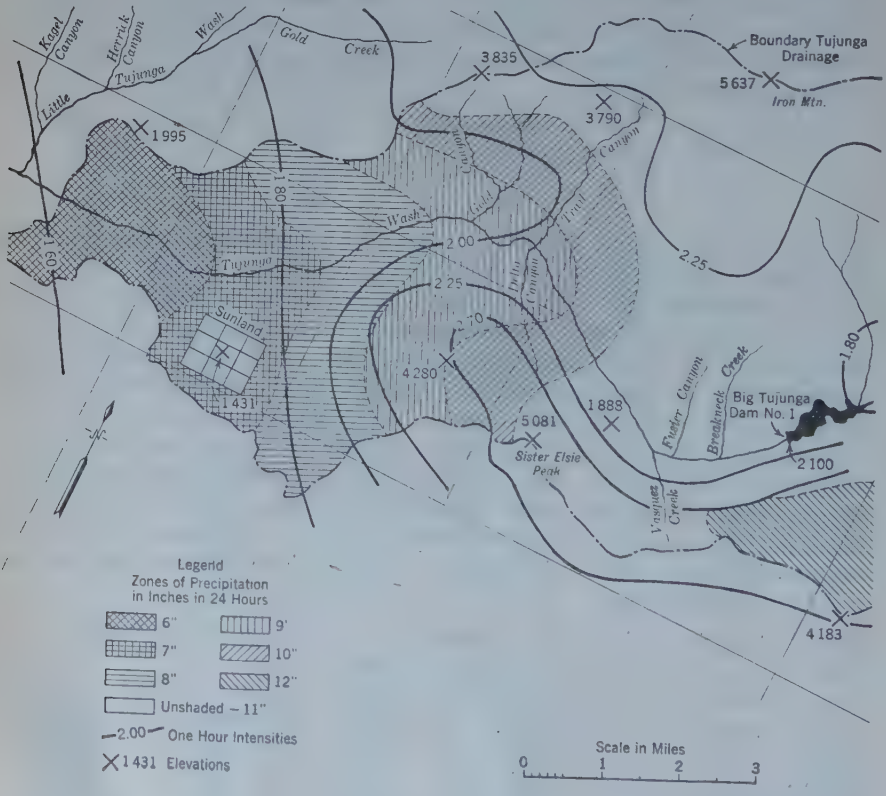

Fig. 5.—Big Tujunga Water-Shed: Zones

valley floors. It results from the same, still active, natural forces that have been building up, gradually, the valleys to many thousands of feet in depth. The removed material when being transported from its original source and after deposition is commonly called "débris."

Rates of débris movements (where mountain slopes are steep) depend primarily on the condition of natural mountain vegetative cover. Destruction of this protective cover by fires, or otherwise, will permit enormous débris flows to result from rainfall intensities which would create, normally, but small débris movement. This abnormal condition diminishes with re-growth of Nature's protective covering, which is often a slow process, since erosion has partly removed the top-soil capable of supporting vegetation.

Hazards from Débris Movements

Excessive débris waves first affect the lives and property of foot-hill residents. Run-off from smaller tributaries responds more quickly to rainfall than run-off in main rivers and, consequently, a débris-laden stream, upon entering a larger main channel, deposits temporary débris cones, forming

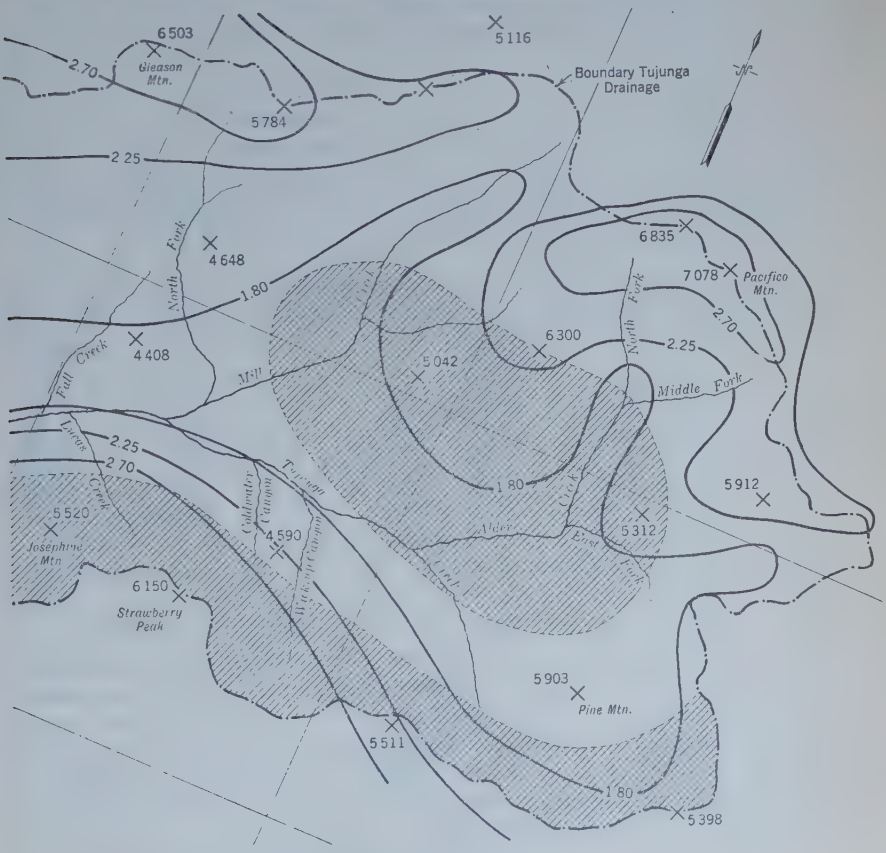

OF PRECIPITATION AND LINES OF INTENSITIES.

barriers of such proportions that the delayed peak of the main river cannot immediately remove them, and river overflow may result. To design an efficient channel under conditions of annual stream flow varying from 3 to 850% of means, is most difficult; when the problem is complicated by heavy débris flows construction costs increase enormously and erosion control at or near the origin of the débris becomes essential.

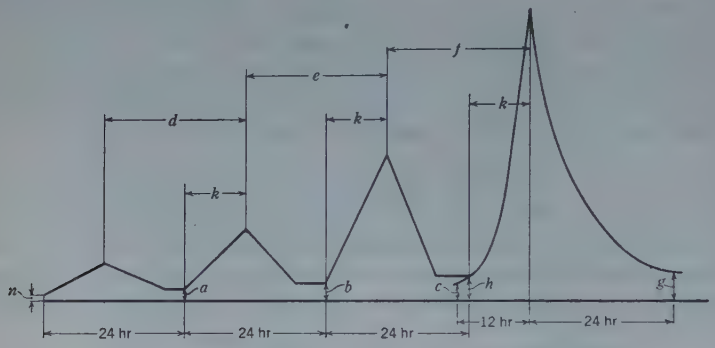

FIG. 6.—CONSTRUCTION OF FOUR-DAY HYDROGRAPH.

RECORDS OF WATER-SHED FIRES

Financial considerations govern in the matter of fire prevention and although Federal, State, and County agencies are entirely efficient, at present (1935), with the funds allocated, far from 100% effectiveness in fire prevention has been attained, as shown by forest fire records during the fourteen years since 1919. Major fire records are summarized[5] in Table 7.

TABLE 7.—BURNED WATER-SHED AREAS—1 000 ACRES OR MORE—1919 TO 1933

No.	Year	Area burned, in acres	No.	Year	Area burned, in acres
1	1919	60 000	10	1925	5 650
2	1919	60 000	11	1925	4 000
3	1921	4 000	12	1927	4 630
4	1921	3 500	13	1927	9 000
5	1921	3 300	14	1927	2 960
6	1921	1 500	15	1928	40 000
7	1922	20 000	16	1930	23 000
8	1924	52 000	17	1933	4 860
9	1924	22 000			
Total	....	.....	.....	....	320 400
Average per fire	....	.....	.....	....	18 900

What expenditures are warranted for fire prevention varies widely in different areas, depending upon population concentrations and values menaced. The foot-hill water-sheds of Los Angeles County are made up of many hundred individually small catchments, aggregating 285 sq miles. Of this, areas totaling nearly 60 sq miles, as yet not denuded, are located above incorporated territory having a combined population of more than 100 000 persons and assessed values of more than $200 000 000.

[5] Rept. on New Year's Foothill Débris Flood, by E. C. Eaton, March 19, 1934.

Erosion with Normal Water-shed Cover

Where water-sheds have not been disturbed by fires, roads, earth-slides, etc., erosion is relatively slight. Quantitative records of erosion from Los Angeles County water-sheds that have a normal cover are not as plentiful nor as accurate as those from water-sheds from which the débris flows are more readily measured; therefore, only estimates are available.

One estimate (cited as ample) of the extent to which the storage on the San Gabriel water-shed would be depleted, was 3 200 cu yd per sq mile annually.[6] This value probably includes assumptions of occasional burnings since the estimate was made in 1927, within the 3-yr critical period after more than 30% of the area was burned in 1924.

The measured débris deposited in Sweetwater Reservoir, San Diego County, is reported as averaging 1 400 cu yd annually per sq mile in 39 yr,[6] and Gibraltar Reservoir, in Santa Barbara County, averaged 1 380 cu yd per sq mile in its 11-yr period.[7] A major fire in 1923, burning over most of the water-shed, makes this value high. Twelve scattered records collected by the writer average 190 yd per storm per sq mile, ranging from 30 to 500 yd.

No single rate is applicable to all the catchments of Los Angeles County and, although admittedly based upon insufficient data, it is the writer's opinion that, with a water-shed undisturbed by fires for 10 yr or more, 1 500 yd per sq mile is a maximum quantity.

Débris Quantities from Burned Areas

One quantitative example of débris movement is that given by the case of Sunset and Brand Canyons[8] which debouch directly on the streets of Burbank, a city of 16 600 population and more than $28 000 000 assessed valuation in 1931. Brand Canyon discharges on a part of Glendale which has a total population of 60 000 persons and a total assessed property valuation of more than $80 000 000. The catchment area of Sunset Canyon is 1.10 sq miles; its length is about 1.5 miles, and its width ⅔ mile; and in elevation, it ranges from 886 to 3 126 (U. S. Geological Survey). Brand Canyon has a similar catchment of 1.03 sq miles. A fire that burned a total of 4 600 acres occurred from December 3 to 5, 1927, and included all of Sunset and Brand Canyons as well as adjacent canyons. One year later (October, 1928), the first rains occurred, recording a total depth of 0.40 in. During November, 2.10 in. of rain fell, of which more than 65% occurred in one day; a 0.59-in. rain of November 13 was followed on November 14 by a downpour with a sustained 1-hr intensity of 0.43 in., between 8:30 and 9:30 A.M., making a total for that day of 1.41 in. Intensities of 10-min duration were recorded as high as 0.35 in.

Canyon observers reported the resulting débris flows to have followed closely after the high-intensity period, with two distinct flash flows. The

[6] Rept. on Flood Control and Conservation, San Gabriel River, by F. H. Fowler, M. Am. Soc. C. E., C. D. Marx, Past-President and Hon. M. Am. Soc. C. E., and C. H. Paul, M. Am. Soc. C. E., March, 1927.

[7] "The Silt Problem", by J. C. Stevens, *Proceedings*, Am. Soc. C. E., October, 1934, p. 1179.

[8] Rept. on Sunset and Brand Park Canyons Flood of November 14, 1928, by E. C Eaton.

first was composed mostly of water, which rose 3.5 ft in a channel 55 ft wide; and this was succeeded by a second flow estimated, by observers, to flow at a rate of 20 to 30 ft per sec. The débris flow lasted 30 min.

From all available information, including cross-sections, it was estimated that 29 acre-ft of combined débris and water flowed from Brand Canyon in a 30-min period, of which 17 acre-ft (or nearly 60%) was débris, and 12 acre-ft was water, an equivalent run-off depth of 0.22 in. The average velocity was computed at about 6 ft per sec. The débris flow was equivalent to 26 000 cu yd per sq mile of water-shed, a quantity that checked closely with records of truck removals from streets and lawns. Débris removal costs by public agencies averaged $1 per cu yd, exclusive of the cost to residents for removals from cellars and lawns.

Another example was afforded by the Arroyo Sequis, on the western County boundary, which has a water-shed of 11.4 sq miles, discharging directly into the ocean. It is roughly triangular in shape and ranges in elevation from sea level to 3 060 (U. S. Geological Survey). An intense fire from October 29 to November 6, 1930, burned 90% of this area, leaving its decomposed granite slopes, of 300 to 500 ft per thousand, exposed to rain.

The nearest recording rain-gauge was 12 miles inland, at Elevation 600. Since storms approach from the west they strike the coast water-shed an hour earlier than the gauge and it is probable that the actual rainfall on the burned area was greater in quantity and intensity than that recorded. Rainfall records are listed in Table 8. Beginning at 1:00 P. M., on January 7, 1931,

TABLE 8.—Rainfall Records, Arroyo Sequis Water-Shed

Day	Month and year	Rainfall, in inches	Cumulative rainfall, in inches
.....	October, 1930	0.16	0.16
.....	November, 1930	2.09	2.25
.....	December, 1930	0.00	2.25
1.....	January, 1931	1.11	3.36
5.....	January, 1931	0.47	3.83
7.....	January, 1931	1.30	4.13

and continuing to 4:00 P. M., the intensity for 10-min periods, expressed in equivalent inches per hour, are listed in Table 9. The total rain falling in the 170 min. was 1.24 in., or an average rate for the period of 0.44 in. per hr.

TABLE 9.—Arroyo Sequis Water-Shed: Ten-Minute Rainfall Intensities

Time, January 7, 1931	Rate of rainfall for 10-min periods, in inches per hour	Time, January 7, 1931	Rate of rainfall for 10-min periods, in inches per hour	Time, January 7, 1931	Rate of rainfall for 10-min periods, in inches per hour
1:00 P. M..	0.00	2:00 P. M..	0.30	3:00 P. M..	0.54
1:10 P. M..	0.12	2:10 P. M..	0.33	3:10 P. M..	0.60
1:20 P. M..	0.06	2:20 P. M..	0.24	3:20 P. M..	0.24
1:30 P. M..	0.09	2:30 P. M..	0.36	3:30 P. M..	0.42
1:40 P. M..	0.15	2:40 P. M..	0.30	3:40 P. M..	0.63
1:50 P. M..	0.18	2:50 P. M..	0.45	3:50 P. M..	1.38
				4:00 P. M..	1.15

Quantitative measurements could not be made since much débris passed to the Pacific Ocean, but estimates based on mud marks on highway bridge piers (which were as much as 15 in. higher than adjacent bank marks), gave velocities of between 5 and 9 ft per sec. At least 50% by volume was solid matter and the combined débris and water flow was estimated as 700 cu ft per sec per sq mile of water-shed.

A third example—Delta Canyon, a 0.63-sq mile tributary, of Big Tujunga Wash—has a particularly large cone of débris at its mouth (see Fig. 7). In

FIG. 7.—DÉBRIS CONE AT MOUTH OF DELTA CANYON.

elevation it ranges from 1 650 to 4 500 ft (U. S. Geological Survey); its length is 1.9 miles from crest to mouth; its average width, 0.3 mile; and the grade increases from the minimum slope of 625 ft per mile at the lower end. The canyon forks $\frac{3}{4}$ mile from the mouth, and at the end of the small fork, running west, is a steep mountain peak which is considered as having contributed the major portion of the débris. A large slip along the entire side of this mountain was first noted in 1913, but some sliding probably occurred previous to that date. The area is badly faulted and the slopes are in an unstable condition.

Fire destroyed 80% of the canyon cover on September 13, 1913, and, during the 1914 flood, débris was deposited at its mouth, shifting the former stream bed to the west. Although slips had been noted prior to 1914 there is no record of débris at its mouth prior to the rains. The heavy rains of 1926 brought down additional deposits. No differentiation can be made between the relative quantities transported by the two débris flows, and a

part of the delta has been removed by channel cutting in the main arm of the Tujunga River. However, the volume transported in the two storms is estimated, conservatively, at 123 000 cu yd per sq mile, or more than 60 000 cu yd per sq mile per storm.

The La Crescenta-Montrose débris flow, on January 1, 1934, furnishes the best and most accurate, as well as the largest unit débris flow of authentic record.[5] In this case seventeen contiguous water-sheds have a combined crest length of 6 miles and a total area of 7.5 sq miles. The catchment areas in this region are steep and rugged, rising 2 500 ft in 1.75 miles. The catchments range, in size, from Pickens, the largest, with an area of 1.6 sq miles, to several as small as 0.2 sq mile. They debouch, through sixteen separate channels, on to developed foot-hill, city, and urban areas below the canyon mouths, aggregating about 7 sq miles. The area, which is mainly residential, extends from Tujunga City, the largest and at the western boundary, easterly through the unincorporated cities and towns of Highway Highland, La Crescenta, and Verdugo City to La Canada, the easterly boundary.

The aforementioned water-sheds were completely denuded by fire from November 21 to 24, 1933. They had not been burned previously since 1878. The early storms that began December 14, at 5:00 P. M., and ended on December 15, yielded 4 in. of rain which packed the ash residue into the surface pores of the heavy soil cover, built up during decades of undisturbed brush. Recording rainfall records are given in Fig. 8(*a*) and Fig. 8(*b*) from Flintridge Fire Station at Elevation 1 325 (U. S. Geological Survey). Following this preliminary saturation, came succeeding storms culminating with December 31, on which date successive 1-hr intensities increased from 0.5 in. per hr at noon to 0.78 in. at 1:00 P. M.; 1.8 in. at 2:00 P. M.; and 1.14 in. at 3:00 P. M. After 3:00 P. M. the rainfall subsided to 0.3 in. per hr until midnight when it increased suddenly to 1.28 in. per hr. A flash, 5-min intensity at a rate of 2.16 in. per hr began at 11:47 P. M. Three separate recording gauges, distributed over the area, registered sustained 1-hr intensities at midnight of 1.28, 0.85, and 0.87 in. per hr, respectively; and it is probable that a 1-in. intensity was representative of the entire area. No particular 1-hr intensity was a maximum, all-time record, but the successive cycles of sustained high intensity were without known parallel.

Beginning almost exactly at midnight on December 31, 1933, and lasting for an hour, the resulting succession of débris flows caused 30 deaths; 483 homes were either completely swept away or rendered uninhabitable; and the total property damage aggregated $5 000 000. All the loss of life and 80% of the damage occurred in the eastern part below Pickens and Hall-Beckley Canyons. The largest city, Tujunga, was completely protected by a débris basin at the mouth of Haines Canyon (see Figs. 9 and 10). Another basin was under construction at the head of Verdugo Wash, the main collector at which the smaller tributaries eventually terminate.

Falling on a completely saturated soil, the rain had caused sheet erosion over practically the entire mountain area concurrently with a slippage of numerous masses from steep canyon sides of weathered rock, into the narrow

canyon channels. Mass movements originated from canyon sides as high as 200 ft above stream bed, some of the masses being as much as 50 to 150 ft wide. Trees 2 ft, or more, in diameter slipped with the masses and were swept into the streams. When sufficient run-off was impounded behind the

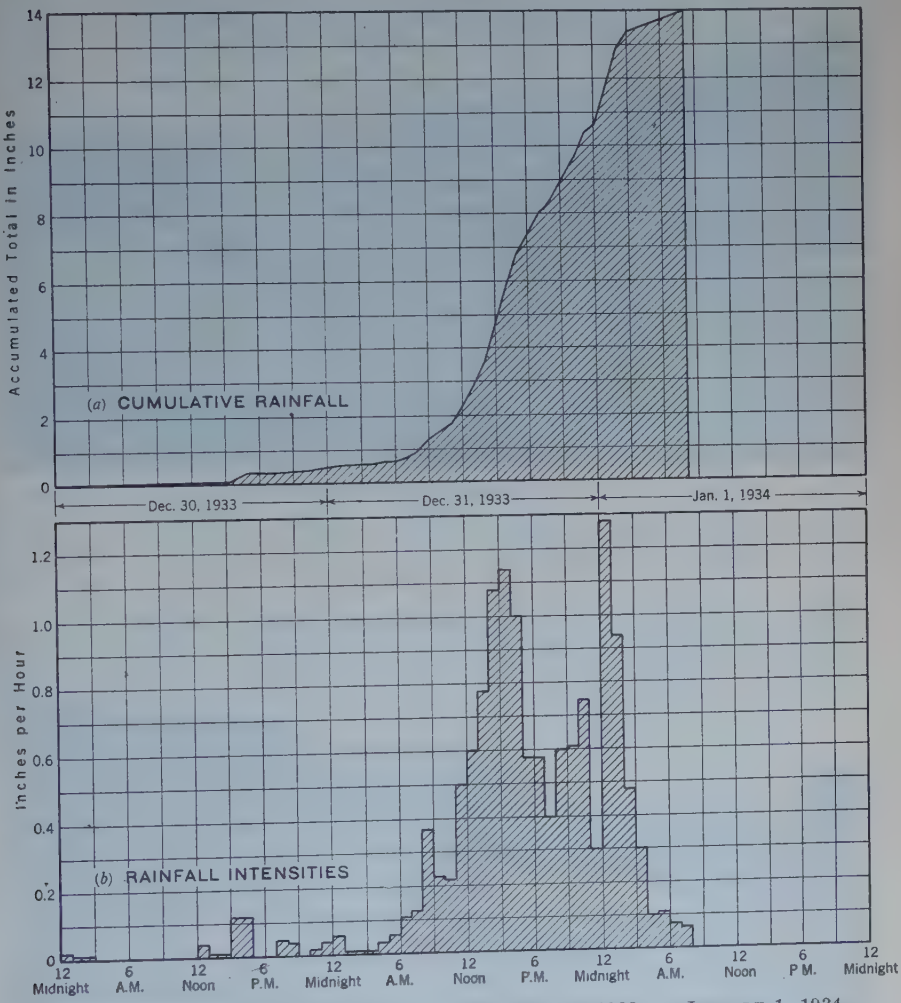

FIG. 8.—RAINFALL RECORDS, STORM OF DECEMBER 30, 1933, TO JANUARY 1, 1934.

earth barriers thus created, to saturate them, they moved down stream until they either drained sufficiently to retard progress, or were stopped by other slides farther down stream. As these movements were repeated, débris was collected in increasing volumes and the masses moved with increasing momentum. Simultaneously, the side tributaries attained peak flows and the combined effect was to release débris and water from canyons in waves 15 ft or more in height. Reaching open territory these waves flattened to

5 or 6 ft in height and spread to widths of 100 to 200 ft scouring new channels and thus picking up new débris loads. In canyons velocities were suffi-

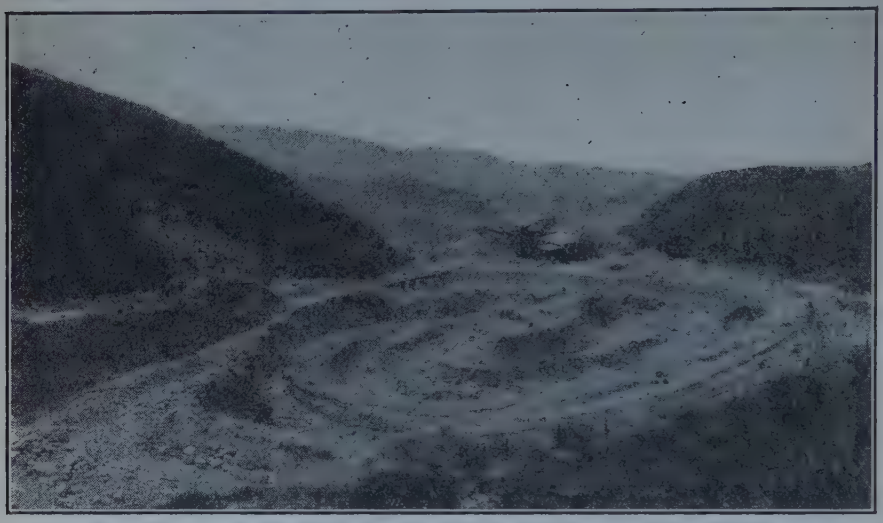

FIG. 9.—VIEW OF HAINES CANYON DÉBRIS BASIN, BEFORE STORM OF JANUARY 1, 1934.

cient to carry along many 10-ton boulders. One 59½-ton boulder was rolled on to a paved street at the mouth of Dunsmuir Canyon.

FIG. 10.—VIEW OF HAINES CANYON DÉBRIS CONE, AFTER STORM OF JANUARY 1, 1934.

Based on carefully computed quantities of deposits in the two débris basins, and on field and airplane surveys, débris deposits on property (in cubic yards) were:

In Haines Débris Basin	32 000
In Verdugo Débris Basin	92 000
On property and streets	535 000
Total	659 000

The foot-hill and urban area below the canyon mouths covers about 7 sq miles; of this area 1 040 acres, or 23%, were affected by débris (see Fig.11).

Practically all the débris was deposited within the 1-hr period after midnight, occurring in a succession of about fifteen sharp débris flows, moving at velocities estimated at from 5 to 10 ft per sec. Canyon velocities were considerably greater. Each sharp peak of major débris flow would be succeeded by a rapidly moving stream which contained less débris, cutting a channel to one side or through the deposited débris masses. In some instances these masses would drain out and, successively, become saturated by stream flow to a point at which they would again begin to move; and, encountering a rapidly moving stream, they would be carried along in a succession of surges. It is estimated that the flows containing maximum percentages of débris occupied about 30 min.

The east half of Haines Canyon (the westerly limit of the burned area) had been denuded. Practically the entire débris movement from this source originated from 0.47 sq miles, indicating a débris rate of 67 000 cu yd per sq mile scoured out by a single storm. Débris on property and streets and in the Verdugo Débris Basin came from 7.08 sq miles, equivalent to nearly 90 000 cu yd per sq mile.

An analysis of smaller sizes of débris collected from streets, is presented in Table 10.

TABLE 10.—ANALYSES OF DÉBRIS IN MONTROSE SECTION
(Average weight per cubic foot dry = 103 lb.)

Screen size	Sample No.								
	1	2	3	4	5	6	7	8	9
1½-in	.....	4.9	15.0	4.2	6.8	.....	3.2	13.5	.....
¾-in	5.5	7.7	5.7	10.9	10.3	3.8	4.8	11.9	2.1
⅜-in	4.1	9.9	5.7	6.6	8.9	7.6	4.0	6.4	2.9
No 4	5.8	6.8	7.1	5.4	4.1	6.8	5.6	4.8	5.7
No. 8	7.7	10.2	10.0	7.9	6.1	9.9	10.5	7.1	8.6
No 14	15.2	16.7	15.0	14.5	11.0	14.4	17.8	11.9	16.4
No. 28	19.4	19.1	16.5	19.4	15.1	16.7	19.4	13.5	21.5
No. 48	17.3	14.7	12.2	18.8	16.4	15.1	14.5	11.9	18.6
No. 100	12.1	6.6	7.1	9.1	11.0	12.1	9.7	7.9	12.1
Pan	12.9	3.4	5.7	4.2	10.3	13.6	10.5	11.1	12.1
Total (percentages)	100	100	100	100	100	100	100	100	100
Weight, in Pounds per Cubic Foot:									
Dry	109.6	110.7	98.0	96.3	101.3	107.0	105.0	95.3	104.0
Wet	127.5	127.5	118.1	116.5	126.6	123.7	128.7	126.0	126.0
Percentage of voids	33	32.5	39.1	39.2	35.0	32.0	34.3	36.9	35.1

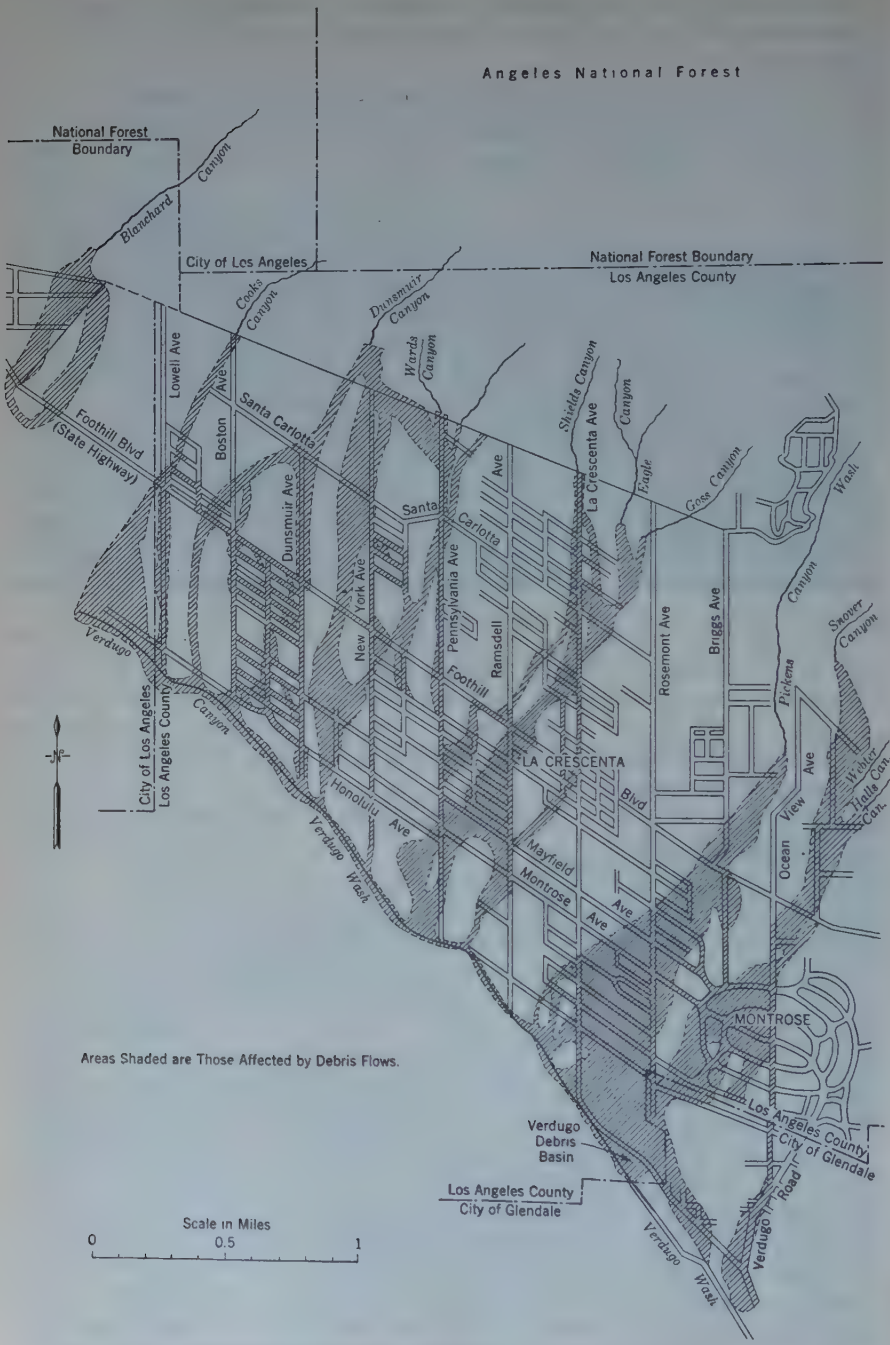

FIG. 11.--LA CRESCENTA-MONTROSE DISTRICT; AREAS AFFECTED BY DÉBRIS FLOOD OF JANUARY 1, 1934.

Cross-sections were taken, following the flood, of the principal canyon channels. A typical section showing Pickens Canyon is given in Fig. 12. The highest water or mud marks were left at moments when the débris flows were either practically stationary or were moving only slowly; but the final lowest channel sections as left resulted from cutting by the later and receding stream flows of higher velocities, which ground the stream bed far below its original grade and below that at the time of the making of the highest mud marks. Computations of peak flows based upon these highest marks and the final channel cross-sections must be modified by judgment, of course, as gained from those witnessing the flows at the time of their activity.

The writer's conclusions were that a sustained 1-hr run-off occurred, which was equivalent to an average depth of 0.9 in., or 580 cu ft per sec per sq mile, and that the maximum débris flow contained 70% of saturated débris to 30% of water by volume, flowing at an average velocity of 5 ft per sec. The relative quantities of débris and water discharged in the 1-hr period were estimated as 48 acre-ft of water and 55 acre-ft of débris.

Débris Control

For major débris movements, positive protection requires direct storage. The best protection thus far advised is the débris basin, which is admittedly expensive and not sightly. It is positive, however, and its first cost is often less than that of one débris removal from streets.

A case in point is the Haines Canyon Débris Basin (see Figs. 9 and 10). Its low capital cost of about $0.25 per cu yd was due mainly: (1) To its location in a Federal Forest area, consequently involving no cost for right of way; and (2) to the basin excavation created by an operating rock plant. Immediately after it was filled, the débris was removed with an average 500-ft haul, for a cost of $0.30 per cu yd. Débris basins at more than one hundred locations will be needed ultimately. Their capital costs per cubic yard of débris capacity will range from $0.30 to $1.00 per yd, depending mainly on excavation costs. Their physical locations are closely fixed, between the canyon mouths and the deltas, at points sufficiently toward the canyon mouths to prevent channel-cutting around them and as far down on the deltas as feasible toward the flatter slopes where excavation costs will be least.

Their storage capacity is obtained, in part, by cut-and-fill excavation in which considerable waste is necessary due to the safety requirement that the deepest part toward the outlet or spillway should be in solid cut. The sides of the basin may be leveed from part of the excavated material. Where feasible, side-channel spillways are advisable, thus forcing the débris flows to enter from the upper end and follow circular paths, facilitating maximum deposition of débris. Sufficient adjacent areas should be provided for future deposition of material.

Where water-sheds are unburned, the operating costs of débris basins are negligible, because little or no débris removal is necessary. After a fire and succeeding high-intensity storms, the basins must be emptied promptly.

The necessity of locating the basin largely in cut, results in excavation costs ranging from 50 to 75% of the total, the other costs being for spillways

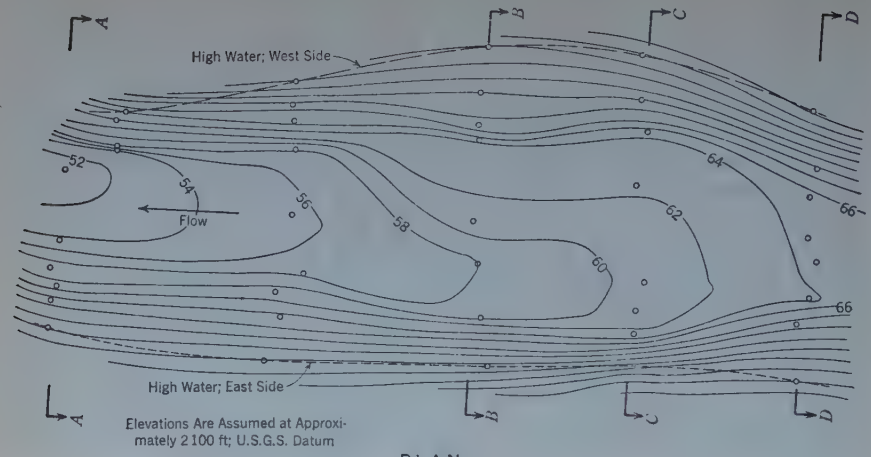

PLAN

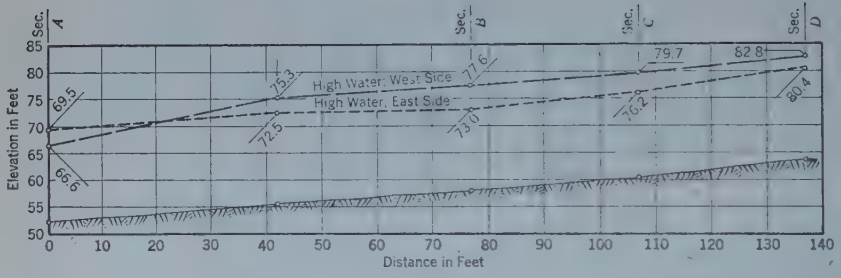

PROFILE

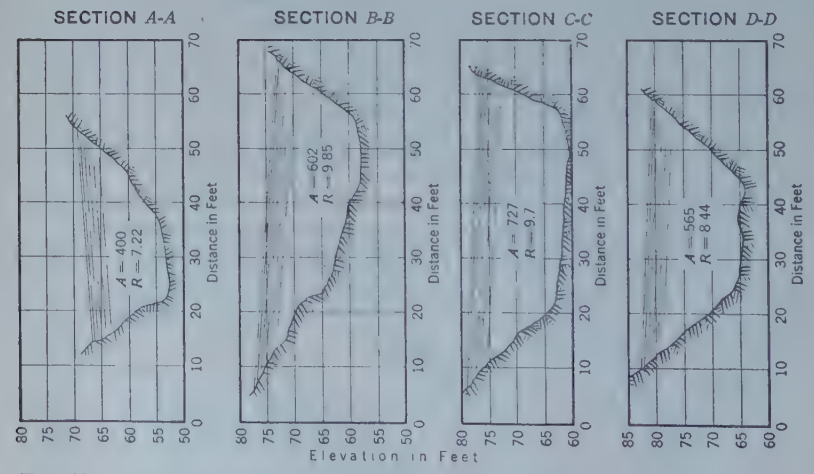

FIG. 12.—PICKENS CANYON: PLAN AND PROFILE OF CANYON, JANUARY 1, 1934.

and auxiliary structures connecting the basin to the head-works of channels. The spillway generally occupies limited space and requires considerable time to construct. On the other hand, the basin excavation covers a large area (1 acre to 2 acres, or more), and thus permits the use of large equipment and rapid construction. Two large power shovels, supplemented by large trucks, can excavate, on a conservative estimate, 20 000 cu yd per three-shift day. Under emergency conditions, a basin for protection from an area of 2 sq miles may be excavated in from 15 to 30 days. Although it is urgently needed during the 3 to 5-yr period following a fire, a débris basin will be inactive over the period of years when no fires have occurred. At best, it cannot be made attractive in appearance and must be located not far from residence property.

These factors suggest the possibility of saving in capital investment by setting aside definite areas, preparing detailed plans, and constructing spillways, channels, and auxiliary structures, but deferring the excavation of pits until fires have occurred. The large excavation equipment can be used later for prompt removal of débris deposits. After mountain cover has regrown, basins may be permitted to fill until fires again indicate that they should be re-excavated.

Water Conservation Incidental to Flood Regulation

Conservation of flood wastes will result from flood regulation for protective purposes.

Increased drafts on local water supplies have been accentuated by decreases in original replenishment due to paving and building activities which have changed former pervious surfaces to impervious surfaces. River channels have been improved reducing thus the original wetted areas. The over-draft from wells tapping the basins between 1914 (the last major flood year) and 1931, has created a present underground storage space of more than 2 250 000 acre-ft. The effects of pumping in excess of replenishment is especially marked in the basins of the coastal plain where serious intrusions of salt water have resulted. Here, water from wells on an area of more than 57 sq miles shows a salt content of more than 15 grains per gal, which is considered to be the limit for human consumption.

Surface Hold-Over Conservation Expensive

To provide conservation by surface hold-over storage under Los Angeles County water-shed conditions would run into enormous costs, particularly since hold-over of floods for five years or more would have to be provided. High surface storage costs are here due to the steep slopes and large number of individually small drainages that are characteristic of the mountain territory.

As indicating the costs involved, the twelve reservoirs constructed or under construction by the Los Angeles County Flood Control District will regulate the floods from 400 sq miles, having a combined capacity of 109 000 acre-ft, at an average capital cost of $200 per acre-ft. Under such condi-

tions capacities must be limited to those needed for regulation alone, and, following storm periods, the reservoirs must be emptied progressively at rates permitting percolation into underground basins.

Fortunately, there are available unparalleled natural reservoirs of high capacity. Created by the deposition of sand, gravel, and boulders through the ages, these basins are twenty-six in number. Dikes and geologic faults have created underground barriers, thus forming a series of reservoirs which retard underflow, the water passing over and through these dikes into succeeding basins down stream. Void spaces in the gravels range from 20 to 10%, the larger values applying to the main valley basins, the smaller to the coastal areas.

The logical solution is to conserve the present wastes by regulation and passage into the underground basins. Measured 1931-32 flood-water waste to the Pacific Ocean from 1 841 sq miles of major drainages, was 101 578 acre-ft, indicating conservation possibilities when flood regulation has been provided sufficient for percolation into existing underground basins. The distribution of this flood-water waste is shown in Table 11.

TABLE 11.—MEASURED FLOOD-WATER WASTES TO THE OCEAN, 1931–32

Stream	Drainage area, in square miles	Waste, in acre-feet	Waste, in acre-feet per square mile	Waste, depth in inches of run-off
Los Angeles River	1 063	50 958*	47.9	0.94
San Gabriel River	479	6 555	13.7	0.26
Ballona Creek	112	21 785	194.5	3.80
Malibu Creek	103	14 665	142.2	2.78
Nigger Slough	66	4 029	60.7	1.18
Topanga Creek	18	3 586	199.0	3.88
Total	1 841	101 578	54.9	1.07

* Includes part of San Gabriel run-off transported to Los Angeles River *via* Rio Hondo.

SPREADING TO INCREASE PERCOLATION

Regulated flood flows may be encouraged to percolate in increasing quantities by extending the wetted areas on overlying gravel cones by "spreading." A representative set of percolation measurements made in 1930–31 and 1932 at fifty-three different locations is given in Table 12.

Rates of percolation through surface gravels are mainly proportional to areas wetted and only to a minor degree upon depth of water. Flood flows, even when the main débris has been removed, contain sufficient fine suspended matter, with collodial content, so that a depth of deposit of from $\frac{1}{16}$ to $\frac{1}{8}$ in. is sufficient to reduce the percolation rates 50%, or more, or practically to seal the surface. In stream-bed areas the "scarification" of a few inches is sufficient to increase percolation rates markedly.

Scarification by plowing and harrowing of test sections on the San Gabriel River and Rio Hondo gave results indicated in Table 13.

Increased percolation may be effected by the construction of "spreading works." In their design, ponding alone, or the creation of large shallow

basins, does not furnish the complete solution for the percolation of waters containing sediment. It has been proved, however, that by keeping the streams of water moving and by flushing certain areas, the top gravel layers

TABLE 12.—Representative Percolating Rates

Stream	Date made	Flow, in cubic feet per second per wetted acre	Stream	Date made	Flow, in cubic feet per second per wetted acre
Rio Hondo	March 25, 1930	2.71	Big Tujunga Creek	February 18, 1932	3.17
	May 6, 1930	1.73		March 31, 1930	1.29
	May 7, 1930	1.81		May 12, 1930	5.05
	February 5, 1931	2.25	San Dimas Creek	February 26, 1931	1.72
	December 31, 1931	4.24		January 6, 1932	1.93
	March 16, 1932	1.89		January 7, 1932	1.25
	March 17, 1932	2.64		March 9, 1932	1.45
	April 6, 1932	1.72	San Antonio Wash	March 14, 1931	1.38
	April 15, 1932	0.91	Big Santa Anita Wash	February 18, 1931	1.42
	August 4, 1931	2.41	Arroyo Seco Wash	January 12, 1932	1.80
	August 4, 1931	1.70		January 14, 1932	1.39
San Gabriel River	March 25, 1930	3.18	Walnut Creek	May, 1930	0.50
	April 2, 1930	2.45	San Fernando Creek	September 29, 1930	2.02
	May 8, 1930	1.85	Pacoima Creek	September 30, 1930	1.86
	February 6, 1931	2.28	Sawpit Creek	March 7, 1932	4.00
	April 30, 1931	1.66	Average		2 02
	December 30, 1931	2.66			
	February 3, 1932	1.75	Spreading Grounds:		
	March 16, 1932	1.69	San Gabriel River	January 22, 1931	6.96
	March 17, 1932	1.88	San Gabriel River	May 5, 1932	3.38
	April 6, 1932	1.40	Big Dalton Wash	February 26, 1931	7.00
Little Dalton Wash	March 22, 1930	1.36		March 11, 1931	8.15
	May 14, 1930	0.95	San Antonio Wash	April 27, 1931	2.43
Big Dalton Wash	March 22, 1930	1.44		April 27, 1931	7.45
	May 15, 1930	1.57		March 22, 1932	3.07
Eaton Wash	February 26, 1931	1.65		April 18, 1932	3.27
	May 5, 1929	1.19	Average		5.23
Little Tujunga Creek	December 29, 1931	0.81			
	February 2, 1932	1.89			
	March 25, 1932	5.00			

receive a scrubbing action, and high percolation rates can be maintained. The velocities necessary range between 2 and 4 ft per sec and must be supplemented by flushing immediately before, and immediately after, a run. The quantity necessary to waste by flushing should not exceed 5% of the total quantity spread. Spreading works include head-gates from which main and lateral ditches take off through gates in effect similar to an irrigation system. The object of spreading is to provide a wetted area of water in motion covering as large a total area as possible.

TABLE 13.—Percolation Rates in the San Gabriel River and Rio Hondo

Length of section, in feet	Percolation Rates, in Cubic Feet per Second per Wetted Acre		
	Before	After	Percentage increase
2 700	1.75	1.90	10
2 610	0.52	0.88	69
4 270	4.21	4.77	13
2 020	2.15, 1.91	1.99	28
2 400	2.72	5.50	102
6 030			

Under a carefully planned spreading system it is possible to provide a net wetted area of from 25 to 35% of the gross area at construction costs ranging from $200 to $300 per gross acre of spreading grounds. Operating costs will range from $0.15 to $0.50 per acre-ft of water percolated, the quantity varying according to the area, its shape, and the layout of the ditch systems.

As a practical average value, from 0.5 to 1 cu ft per sec per gross spreading area may be spread, depending upon the location of the area, and the character and layout of the spreading works.

Conclusions

Under physical and weather conditions as described the conclusions are, as follows:

Flood Flows.—On the larger mountains with vegetation undisturbed, a total of 10 in. of rainfall will produce sufficient saturation to permit marked run-off. Storms of intensities of 1 in. per hr and more, if closely following the saturation period, will produce floods, their magnitude rising rapidly with increasing intensities. Twenty-four hour intensities may be expected, varying from 3 in. on the coastal plains to 13 in. on the mountains, with sustained 1-hr intensities of 1 in. to 3 in. Under the higher intensities, following saturation, flood flows of 400 acre-ft per day per sq mile are possible. With the characteristic sharp peaks of these areas this quantity will represent a 1-hr peak of 400 cu ft per sec per sq mile. The regulatory storage needed will depend upon the economic balance between channel costs and regulation costs. In Los Angeles County its range is from 150 to 300 acre-ft per sq mile.

On the lower foot-hills and valley areas with high percentages of impervious surfaces, little or no saturation is needed to produce an immediate response of run-off to rainfall. It is necessary to anticipate future development both domestic and industrial in designing drainage channels in such areas and to set aside adequate areas for the ultimately required drainages.

Débris Flows.—After a normal water-shed cover has been destroyed, erosion rates will increase from 50 to 100 times that with undisturbed vegetation. The best protection from débris is the normal vegetative cover. After denudation, any protective program is a secondary, far less efficient, and much more costly, defense. Erosion of a water-shed removes portions of the soil capable of supporting vegetation. Sufficient regrowth to afford protection will take from 5 to 10 yr, depending upon weather conditions and the extent to which the soil has been removed. With vegetation destroyed protection requires direct débris storage; this can be afforded by débris basins at or near the mouths of the canyons. Following denudation, erosion may produce from 50 000 to 100 000 cu yd of débris per sq mile, the quantity depending upon slopes and intensities. The larger quantity may result from intensities as low as 1 in per hr. Little preliminary saturation is necessary and may be as low as 5 in. if occurring in a short period.

In designing débris basins, flows of 75 000 to 150 000 cu yd per sq mile of drainage should be provided for, arrangement should be made for prompt removal, and adjoining areas should be provided for deposition.

Burning of water-sheds is not always of human origin. Lightning is one cause. Even with the best possible fire-prevention measures occasional fires will occur. Even a foot-hill water-shed 1 sq mile in extent may produce sufficient débris to cause heavy loss of life and immense property damage, when it is located above developed territory. In such areas, basins should be at least set aside; complete detailed plans prepared for their construction; and the auxiliaries of spillways, etc., should be built, so that in emergencies they may be constructed promptly.

Conservation.—Provision for flood regulation for protective purposes will give capacities in excess of that required for conservation of the flood waters that will result from increased percolation, which is principally in proportion to the stream-bed areas wetted. Where increased percolation above that of the natural channel is needed, spreading systems may be built at costs of $200 to $300 per gross acre, with percolation capacities of from 1 to 2 acre-ft per day per acre.

Acknowledgments

The writer desires to express his appreciation to Franklin Thomas, M. Am. Soc. C. E., who made, for the Los Angeles County Flood Control District, the report on the Big Tujunga water-shed, quoted in this paper. Appreciation is expressed to the many members of the District staff who collected the basic data from which this paper has been prepared; and, in particular, to F. H. Hay, Assoc. M. Am. Soc. C. E., Chief Hydrographer, and to R. S. Goodridge and F. J. Cornick, Assoc. Members Am. Soc. C. E., of the Hydrographic Department; also, to Mr. E. C. Kenyon, Jr., in charge of Erosion Control.

AMERICAN SOCIETY OF CIVIL ENGINEERS

Founded November 5, 1852

DISCUSSIONS

AN ASYMMETRIC PROBABILITY FUNCTION

Discussion

BY J. J. SLADE, JR., ESQ.

J. J. SLADE, JR.,[57] ESQ., (by letter).[57a]—In developing the function presented in his paper the writer has necessarily had to give considerable weight to the partly bounded function because it was by means of his analysis of it that he was able to construct the elements of the totally bounded curve. In his work, however, he has not had occasion to make use of it. This former function is merely a limiting case of the latter, in which one of the bounds becomes infinite, and in the problems that he has considered the bounds, obviously, have been finite. Perhaps one of the reasons that much of the work of statisticians has been unavailable to the engineer for hydrological investigations is that statisticians are interested usually in graduating the middle range of a frequency distribution, the extreme outer 1%, say, of the distribution being of relatively slight importance to them. The hydrologist, on the other hand, is frequently interested mostly in this outer 1% of the range. It is for this reason that one must insist on the determination of the limits of the range. It is absurd for a probability function to give a finite probability to a Noah's flood. In modern times, there simply is not enough energy resident in the atmosphere to produce anything like it.

Equations (45), as given in the writer's paper, are based on an easy generalization of Equations (44). It is apparent, at once, that the factor, p, belongs therein and that it is not merely "a kind of artificial *tour de force*," as Mr. Fisher expresses it. In the paragraph following these equations, the writer states that their form will probably need modification. A more extended analysis has shown that this is indeed the case. Their correct form, when $b < g$, is:

$$z = p\, c \log d \left(\frac{b + x}{g - x}\right) \ldots\ldots\ldots\ldots\ldots\ldots (88a)$$

NOTE.—The paper by J. J. Slade, Jr., Esq., was published in October, 1934, *Proceedings*. Discussion on this paper has appeared in *Proceedings* as follows: January, 1935, by Messrs. Gordon R. Williams and H. Alden Foster; February, 1935, by Messrs. R. D. Goodrich, and F. T. Mavis; March, 1935, by L. Standish Hall, Assoc. M. Am. Soc. C. E.: April, 1935, by Arne Fisher, Esq.; and May, 1935, by Arthur W. Kempert.

[57] Asst. Prof. of Eng. Mechanics, Rutgers Univ., New Brunswick, N. J.

[57a] Received by the Secretary July 22, 1935.

$$d = \frac{g}{b}\sqrt{\frac{g^2(\sigma^2 + b^2) - 4\sigma^2 b g}{b^2(\sigma^2 + g^2) - 4\sigma^2 b g}} \quad \ldots\ldots\ldots\ldots\ldots (88b)$$

$$\frac{1}{e} = \sqrt{\log \frac{g^2(\sigma^2 + b^2) - 4\sigma^2 b g}{b^2(\sigma^2 + g^2) - 4\sigma^2 b g}} \quad \ldots\ldots\ldots\ldots\ldots (88c)$$

and,

$$p = \sqrt{\frac{g - b}{g + b}} \quad \ldots\ldots\ldots\ldots\ldots\ldots\ldots (88d)$$

When $b = g$, then,

$$z = \frac{\sqrt{b^2 - 3\sigma^2}}{2\sigma} \log\left(\frac{b + x}{b - x}\right) \quad \ldots\ldots\ldots\ldots\ldots (88e)$$

In his discussion Mr. Williams states that "any purely mathematical treatment of stream-flow data presumes at the outset that all the data are equally reliable," and, from this, he infers that there are limitations in the analytical method which are partly absent in the graphical treatment. The analysis of a physical problem begins when all the data relevant to the problem are known, and these data necessarily include a knowledge of the reliability of the observations. The purely mathematical treatment begins, first of all, with the proper weighting of these observations, for which various methods are well known and widely used. The writer can not agree, therefore, with the idea that the analytical method is inferior to the graphical because the free-hand curve "can be shifted to give more or less weight to certain points."

Mr. Williams' objection to listing the complete set of peaks in a stream-flow record is well taken. In the first place, it is difficult to define a peak, particularly in the range of small flows, as he observes; second, it is difficult to estimate above what datum the peak should be taken (that is, statistically, a peak is an accidental irregularity above a smoothed hydrograph, and it is difficult to smooth the hydrograph properly); and, third, peaks are not uncorrelated quantities and, consequently, a simple analysis of their distribution is not possible. In presenting this paper the writer limited himself to the analysis of the generalized probability function, and he did not attempt to offer a method for the analysis of stream-flow characteristics. The illustration of the peaks of the Tennessee River record was given merely to show that an extremely skewed and platykurtic distribution could be closely fitted by means of this curve. Using the corrected Equations (88) and an estimate of the extreme flood (415 000 cu ft per sec) based on the following method, a much closer fit is obtained.

The use of the partial series of peaks above the "one-year flood" is open, at least statistically, to a fourth objection, namely, that an error, which may be serious, is introduced in assigning a probability to the "one-year flood." Because of the indeterminacy of this error the writer has not been able to make an estimate of the reliability of the probabilities obtained from a curve fitted to such series.

The writer concurs with Mr. Foster's opinion that Pearson's curves satisfy all the desiderata presented in his paper for a generalized frequency curve,

provided all the types in Pearson's development are included. Except in the border cases one type cannot be substituted for another, and in order to select the proper type for a given distribution it is necessary to use Pearson's criterion or something equivalent (implying the computation of moments through the fourth). The statistical characteristics beyond the standard deviation computed from small samples (say, samples with less than 100 items) are so unreliable that they are useless. This statement needs no mathematical proof (although such could be readily given); the experiment may be tried of drawing small samples from a fairly large population, and, from these samples, the mean, standard deviation, and the skewness may be computed. It will then be found that, although the first two characteristics will vary, they will show a remarkable uniformity, nevertheless, compared with the wide fluctuations in the latter.

Table 22 meets the objections to the labor involved in graduating distributions by means of this function. If greater detail is needed than is given in this table, then, by perfectly straightforward computation and the use of tables of the probability integral, Equations (88) may be utilized to fill in this detail. Tables of the probability integral have been published frequently and distributed widely; Mr. Foster's statement that these tables are "not always available to the practicing engineer" and that "even if available, might easily lead the average engineer into difficulties" is, therefore, quite disturbing. The answer to this objection is probably that the "average engineer" should not attempt, with his small equipment, to analyze a highly specialized and difficult problem. Undoubtedly, it is true that some kind of an answer may always be found easily to any statistical problem, but it is in the interest of "practical purposes" that this answer should be questioned and its reliability tested. It is unfortunate that statistical analysis does not offer many short cuts, particularly since a wide variety of important problems yield to no other kind of analysis.

Both Professors Goodrich and Mavis disagree with the writer's statements regarding the undesirability of graphical methods of analysis. These statements the writer intends, of course, to apply to the graphical analysis of statistical problems specifically, because he is well aware of the value of graphical analysis in general. Without entering into elaborate arguments, his objections to the graphical method may be stated briefly, as follows: If an n-parameter curve is to be fitted to a set of data, then exactly n independent statements must be used to determine these parameters. If a statistical series is capable of furnishing four independent, significant characteristics (for instance, the mean, standard deviation, skewness, and kurtosis, or, as the writer prefers for small samples, the mean, standard deviation, and the two end points of the range of variation), then these statements are sufficient to determine reliably a four-parameter curve; more parameters may be determined by making use of moments higher than the fourth, or by the method of least squares; but if the significant characteristics of the distribution are only four, the added work is meaningless; that is, there is a definite point beyond which the flexibility of a curve is undesirable. Now, a free-hand curve is a many-parameter curve (theoretically the number of

TABLE 22.—VALUES OF t FOR VARIOUS VALUES OF θ AND λ.

% - of - time	PROBABILITY FOR THE INDEX VALUE, λ =													
	1	1.5	2	2.5	3	3.5	4	4.5	5	6	7	8	9	10
						(*a*) $\theta = 1$								
0.0000001	.....	.....	2 00	2.50	2.96	3.37	3.73	4.01	4.28	4.68	4.96	5.18	5.32	5.45
0.000001	.....	.....	2.00	2.49	2.94	3.33	3.66	3.94	4.16	4.51	4.76	4.94	5.06	5.155
0.00001	.....	.....	2.00	2.485	2.92	3.28	3.58	3.82	4.02	4.31	4.525	4.66	4.76	4.845
0.0001	.....	.....	2.00	2.48	2.88	3.205	3.47	3.67	3.84	4.07	4.24	4.35	4.42	4.49
0.001	.....	.....	2.00	2.46	2.82	3.10	3.32	3.48	3.61	3.78	3.90	3.98	4.04	4.08
0.01	.....	.....	2.00	2.42	2.72	2.94	3.10	3.22	3.30	3.42	3.50	3.55	3.58	3.615
0.1	.....	.....	1.99	2.34	2.55	2.69	2.78	2.84	2.89	2.95	2.98	3.01	3.03	3.05
1.0	.....	.....	1.96	2.15	2.22	2.26	2.28	2.29	2.30	2.31	2.31	2.31	2.32	2.32
10	.....	.....	1.71	1.53	1.44	1.39	1.36	1.35	1.33	1.32	1.31	1.30	1.29	1.29
20	.....	.....	1.37	1.09	0.99	0.94	0.92	0.90	0.885	0.87	0.86	0.86	0.85	0.85
30	.....	.....	0.955	0.70	0.63	0.59	0.57	0.56	0.55	0.54	0.54	0.53	0.53	0.53
40	.....	.....	0.49	0.345	0.30	0.29	0.28	0.27	0.27	0.26	0.26	0.26	0.25	0.25
50	.....	.....	0	0	0	0	0	0	0	0	0	0	0	0
60	.....	.....	—0.49	—0.345	—0.30	—0.29	—0 28	—0.27	—0.27	—0.26	—0.26	—0.26	—0.25	—0.25
70	.....	.....	—0.955	—0.70	—0.63	—0.59	—0.57	—0.56	—0.55	—0.54	—0.54	—0.53	—0.53	—0.53
80	.....	.....	—1.37	—1.09	—0.99	—0.94	—0.92	—0.90	—0.885	—0.87	—0.86	—0.86	—0.85	—0.85
85	.....	.....	—1.56	—1.30	—1.20	—1.15	—1.12	—1.11	—1.09	—1.08	—1.07	—1.06	—1.06	—1.05
90	.....	.....	—1.71	—1.53	—1.44	—1.39	—1.36	—1.35	—1.33	—1.32	—1.31	—1.30	—1.29	—1.29
95	.....	.....	—1.86	—1.80	—1.75	—1.73	—1.71	—1.69	—1.68	—1.67	—1.66	—1.66	—1.65	—1.65
						(*b*) $\theta = 2$								
0.0000001	.....	3.00	3.95	4.73	5.32	5.76	6.05	6.25	6.38	6.52	6.59	6.60	6.595	6.57
0.000001	.....	3.00	3.93	4.67	5.18	5.55	5.78	5.93	6.05	6.14	6.17	6.15	6.15	6.12
0.00001	.....	3.00	3.89	4.555	5.005	5.30	5.48	5.595	5.65	5.72	5.72	5.72	5.68	5.675
0.0001	.....	2.995	3.84	4.41	4.77	4.98	5.10	5.18	5.21	5.24	5.245	5.20	5.18	5.15
0.001	.....	2.99	3.75	4.20	4.455	4.595	4.66	4.70	4.71	4.70	4.695	4.66	4.62	4.61
0.01	.....	2.97	3.59	3.895	4.05	4.11	4.13	4.125	4.125	4.10	4.075	4.04	4.00	3.99
0.1	.....	2.92	3.31	3.43	3.47	3.475	3.45	3.435	3.41	3.38	3.34	3.32	3.30	3.28
1.0	.....	2.72	2.75	2.70	2.66	2.62	2.58	2.56	2.54	2.51	2.48	2.46	2.46	2.45
10	.....	1.765	1.53	1.44	1.39	1.37	1.36	1.34	1.33	1.32	1.32	1.31	1.30	1.31
20	.....	1.02	0.92	0.88	0.86	0.85	0.85	0.84	0.84	0.84	0.85	0.85	0.83	0.83
30	.....	0.43	0.48	0.48	0.48	0.48	0.49	0.49	0.49	0.50	0.50	0.50	0.50	0.51
40	.....	0.04	0.12	0.16	0.17	0.19	0.20	0.20	0.20	0.21	0.22	0.22	0.22	0.22
50	.....	—0.42	—0.185	—0.13	—0.10	—0.08	—0.07	—0.06	—0.05	—0.04	—0.03	—0.03	—0.03	—0.03
60	.....	—0.72	—0.465	—0.36	—0.36	—0.34	—0.32	—0.32	—0.31	—0.30	—0.29	—0.285	—0.29	—0.28
70	.....	—0.97	—0.73	—0.66	—0.62	—0.60	—0.585	—0.58	—0.57	—0.56	—0.55	—0.545	—0.55	—0.55
80	.....	—1.17	—1.01	—0.945	—0.91	—0.90	—0.89	—0.88	—0.87	—0.87	—0.86	—0.86	—0.86	—0.855
85	.....	—1.26	—1.15	—1.11	—1.08	—1.07	—1.07	—1.06	—1.06	—1.055	—1.04	—1.04	—1.05	—1.05
90	.....	—1.34	—1.30	—1.28	—1.27	—1.27	—1.27	—1.27	—1.27	—1.27	—1.26	—1.26	—1.27	—1.28
95	.....	—1.41	—1.485	—1.51	—1.53	—1.55	—1.56	—1.57	—1.58	—1.58	—1.59	—1.59	—1.61	—1.60

TABLE 22.—(*Continued*).

% - of - time	Probability for the Index Value, $\lambda =$:													
	1	1.5	2	2.5	3	3.5	4	4.5	5	6	7	8	9	10
						(*c*) $\theta = 3$								
0.0000001	.....	4.47	5.70	6.525	7.055	7.325	7.45	7.50	7.50	7.425	7.31	7.20	7.13	7.025
0.000001	.....	4.45	5.60	6.325	6.75	6.925	7.00	7.025	7.00	6.90	6.78	6.70	6.605	6.55
0.00001	.....	4.43	5.46	6.07	6.35	6.475	6.525	6.50	6.45	6.35	6.25	6.15	6.075	6.00
0.0001	.....	4.38	5.27	5.725	5.90	5.95	5.95	5.925	5.86	5.75	5.65	5.545	5.48	5.405
0.001	.....	4.30	4.995	5.275	5.355	5.35	5.30	5.25	5.20	5.08	5.00	4.92	4.86	4.80
0.01	.....	4.14	4.585	4.70	4.68	4.625	4.58	4.52	4.47	4.36	4.30	4.225	4.19	4.125
0.1	.....	3.81	3.95	3.92	3.86	3.78	3.71	3.67	3.63	3.54	3.48	3.45	3.42	3.38
1.0	.....	3.10	2.98	2.88	2.79	2.735	2.69	2.66	2.62	2.58	2.54	2.51	2.51	2.48
10	.....	1.53	1.435	1.40	1.37	1.35	1.34	1.34	1.335	1.32	1.31	1.32	1.31	1.30
20	.....	0.81	0.815	0.815	0.82	0.825	0.825	0.825	0.825	0.825	0.83	0.83	0.84	0.825
30	.....	0.32	0.40	0.42	0.44	0.45	0.47	0.47	0.48	0.48	0.48	0.51	0.51	0.51
40	.....	—0.04	0.07	0.12	0.14	0.16	0.17	0.18	0.19	0.19	0.20	0.22	0.22	0.22
50	.....	—0.32	—0.20	—0.15	—0.12	—0.10	—0.08	—0.08	—0.06	—0.06	—0.05	—0.04	—0.03	—0.03
60	.....	—0.57	—0.45	—0.395	—0.365	—0.35	—0.33	—0.33	—0.31	—0.30	—0.30	—0.29	—0.29	—0.27
70	.....	—0.78	—0.685	—0.64	—0.615	—0.60	—0.585	—0.58	—0.57	—0.57	—0.56	—0.54	—0.54	—0.55
80	.....	—0.98	—0.93	—0.90	—0.89	—0.88	—0.87	—0.87	—0.86	—0.86	—0.855	—0.855	—0.85	—0.85
85	.....	—1.075	—1.06	—1.05	—1.04	—1.04	—1.04	—1.05	—1.04	—1.04	—1.04	—1.04	—1.03	—1.04
90	.....	—1.17	—1.19	—1.21	—1.22	—1.23	—1.23	—1.24	—1.24	—1.25	—1.25	—1.255	—1.25	—1.26
95	.....	—1.28	—1.37	—1.42	—1.46	—1.49	—1.50	—1.53	—1.53	—1.55	—1.565	—1.57	—1.57	—1.58
						(*d*) $\theta = 4$								
0.0000001	4.00	5.875	7.225	7.995	8.35	8.405	8.375	8.28	8.20	7.945	7.75	7.54	7.395	7.29
0.000001	4.00	5.80	7.02	7.63	7.85	7.88	7.80	7.68	7.60	7.35	7.135	6.975	6.85	6.75
0.00001	4.00	5.73	6.75	7.20	7.30	7.275	7.165	7.045	6.92	6.68	6.525	6.36	6.26	6.155
0.0001	4.00	5.585	6.39	6.65	6.675	6.57	6.45	6.32	6.225	6.005	5.87	5.73	5.625	5.55
0.001	3.99	5.37	5.90	5.995	5.935	5.80	5.685	5.55	5.46	5.295	5.15	5.03	4.97	4.91
0.01	3.97	4.995	5.23	5.19	5.07	4.93	4.815	4.71	4.64	4.50	4.39	4.30	4.25	4.20
0.1	3.90	4.35	4.32	4.18	4.055	3.94	3.86	3.78	3.72	3.61	3.56	3.48	3.44	3.42
1.0	3.51	3.26	3.08	2.95	2.865	2.79	2.74	2.69	2.66	2.60	2.56	2.535	2.52	2.48
10	1.47	1.43	1.39	1.375	1.365	1.35	1.34	1.33	1.34	1.32	1.32	1.31	1.31	1.31
20	0.38	0.73	0.77	0.79	0.80	0.81	0.805	0.81	0.83	0.815	0.83	0.82	0.82	0.84
30	—0.20	0.29	0.36	0.40	0.42	0.44	0.44	0.45	0.47	0.47	0.49	0.48	0.48	0.48
40	—0.52	—0.04	0.06	0.10	0.13	0.15	0.16	0.16	0.19	0.19	0.20	0.20	0.21	0.22
50	—0.705	—0.30	—0.21	—0.16	—0.13	—0.11	—0.10	—0.09	—0.07	—0.06	—0.04	—0.04	—0.04	—0.03
60	—0.82	—0.52	—0.44	—0.40	—0.37	—0.35	—0.34	—0.33	—0.32	—0.31	—0.29	—0.29	—0.28	—0.28
70	—0.90	—0.72	—0.66	—0.63	—0.61	—0.60	—0.59	—0.59	—0.57	—0.57	—0.55	—0.55	—0.55	—0.55
80	—0.95	—0.90	—0.89	—0.88	—0.87	—0.87	—0.87	—0.87	—0.86	—0.865	—0.85	—0.86	—0.86	—0.85
85	—0.97	—1.00	—1.02	—1.02	—1.02	—1.03	—1.035	—1.03	—1.03	—1.04	—1.04	—1.035	—1.03	—1.03
90	—0.98	—1.095	—1.15	—1.18	—1.19	—1.21	—1.22	—1.23	—1.23	—1.25	—1.25	—1.25	—1.26	—1.25
95	—0.99	—1.21	—1.32	—1.38	—1.42	—1.45	—1.48	—1.50	—1.51	—1.54	—1.55	—1.56	—1.565	—1.58

TABLE 22.—(*Continued*).

% - of - time	Probability for the Index Value, λ =: 1	1.5	2	2.5	3	3.5	4	4.5	5	6	7	8	9	10
						(*e*) $\theta = 5$								
0.0000001	5.00	7.195	8.575	9.22	9.33	9.21	9.09	8.86	8.66	8.28	8.00	7.78	7.575	7.44
0.000001	4.995	7.06	8.25	8.70	8.70	8.55	8.36	8.15	7.98	7.63	7.37	7.16	6.99	6.86
0.00001	4.99	6.89	7.82	8.07	7.995	7.79	7.62	7.41	7.25	6.92	6.69	6.54	6.38	6.26
0.0001	4.95	6.64	7.275	7.375	7.20	6.975	6.80	6.60	6.45	6.19	6.01	5.86	5.71	5.625
0.001	4.91	6.25	6.60	6.52	6.31	6.09	5.92	5.76	5.645	5.41	5.25	5.145	5.03	4.95
0.01	4.80	5.67	5.70	5.52	5.31	5.12	4.99	4.85	4.75	4.60	4.46	4.40	4.30	4.25
0.1	4.495	4.74	4.57	4.37	4.19	4.03	3.94	3.86	3.77	3.65	3.58	4.53	3.48	3.46
1.0	3.62	3.35	3.15	3.02	2.90	2.825	2.77	2.725	2.68	2.62	2.58	2.56	2.52	2.51
10	1.36	1.38	1.375	1.36	1.36	1.34	1.34	1.33	1.33	1.32	1.32	1.32	1.29	1.30
20	0.49	0.69	0.75	0.77	0.79	0.79	0.80	0.81	0.81	0.82	0.815	0.83	0.83	0.82
30	0	0.27	0.35	0.39	0.415	0.42	0.44	0.45	0.46	0.47	0.48	0.49	0.495	0.495
40	−0.30	−0.04	0.05	0.10	0.12	0.13	0.15	0.17	0.17	0.19	0.19	0.20	0.20	0.22
50	−0.51	−0.29	−0.20	−0.16	−0.13	−0.12	−0.10	−0.08	−0.075	−0.07	−0.05	−0.05	−0.04	−0.04
60	−0.66	−0.50	−0.43	−0.40	−0.37	−0.36	−0.34	−0.33	−0.32	−0.31	−0.30	−0.29	−0.29	−0.29
70	−0.77	−0.69	−0.65	−0.63	−0.61	−0.60	−0.59	−0.58	−0.57	−0.57	−0.56	−0.56	−0.55	−0.55
80	−0.86	−0.87	−0.87	−0.87	−0.86	−0.87	−0.86	−0.86	−0.86	−0.86	−0.85	−0.85	−0.85	−0.85
85	−0.90	−0.96	−0.99	−1.01	−1.01	−1.025	−1.03	−1.03	−1.025	−1.035	−1.03	−1.03	−1.03	−1.04
90	−0.93	−1.06	−1.12	−1.16	−1.18	−1.20	−1.21	−1.22	−1.22	−1.24	−1.25	−1.25	−1.25	−1.25
95	−0.96	−1.17	−1.29	−1.36	−1.41	−1.445	−1.47	−1.49	−1.50	−1.53	−1.55	−1.55	−1.56	−1.58
						(*f*) $\theta = 6$								
0.0000001	5.97	8.435	9.75	10.20	10.10	9.85	9.57	9.245	8.95	8.545	8.185	7.90	7.70	7.525
0.000001	5.96	8.235	9.28	9.54	9.35	9.05	8.745	8.46	8.21	7.81	7.52	7.275	7.08	6.955
0.00001	5.935	7.95	8.72	8.75	8.50	8.20	7.92	7.655	7.425	7.07	6.82	6.60	6.46	6.34
0.0001	5.875	7.55	7.98	7.88	7.585	7.30	7.02	6.80	6.60	6.31	6.08	5.91	5.795	5.695
0.001	5.75	6.98	7.10	6.90	6.595	6.32	6.08	5.90	5.73	5.50	5.31	5.18	5.075	5.00
0.01	5.505	6.18	6.025	5.78	5.48	5.265	5.075	4.935	4.815	4.66	4.50	4.405	4.345	4.27
0.1	4.95	4.995	4.72	4.50	4.27	4.105	3.99	3.89	3.825	3.69	3.615	3.54	3.50	3.445
1.0	3.68	3.395	3.18	3.05	2.93	2.85	2.78	2.74	2.70	2.65	2.59	2.56	2.54	2.52
10	1.30	1.35	1.35	1.36	1.34	1.34	1.33	1.325	1.33	1.32	1.31	1.31	1.31	1.31
20	0.49	0.67	0.73	0.77	0.78	0.785	0.79	0.80	0.81	0.81	0.815	0.81	0.82	0.84
30	0.04	0.26	0.33	0.385	0.405	0.42	0.44	0.45	0.455	0.47	0.475	0.475	0.485	0.50
40	−0.24	−0.04	0.04	0.09	0.12	0.13	0.15	0.16	0.17	0.18	0.19	0.20	0.205	0.21
50	−0.44	−0.28	−0.21	−0.16	−0.135	−0.12	−0.105	−0.09	−0.08	−0.07	−0.06	−0.05	−0.05	−0.04
60	−0.59	−0.48	−0.43	−0.39	−0.37	−0.36	−0.35	−0.34	−0.325	−0.31	−0.31	−0.30	−0.30	−0.29
70	−0.71	−0.665	−0.64	−0.615	−0.60	−0.60	−0.59	−0.585	−0.57	−0.57	−0.56	−0.555	−0.56	−0.54
80	−0.81	−0.84	−0.86	−0.855	−0.86	−0.86	−0.86	−0.86	−0.855	−0.86	−0.86	−0.855	−0.86	−0.85
85	−0.85	−0.94	−0.98	−0.99	−1.00	−1.01	−1.02	−1.02	−1.03	−1.03	−1.03	−1.03	−1.04	−1.02
90	−0.89	−1.03	−1.10	−1.14	−1.16	−1.19	−1.20	−1.215	−1.22	−1.24	−1.235	−1.24	−1.25	−1.25
95	−0.94	−1.15	−1.265	−1.34	−1.39	−1.43	−1.46	−1.48	−1.49	−1.52	−1.53	−1.545	−1.56	−1.57

TABLE 22.—(*Continued*).

% - of - time	Probability for the Index Value, $\lambda =$:													
	1	1.5	2	2.5	3	3.5	4	4.5	5	6	7	8	9	10
						(*g*) $\theta = 7$								
0.0000001	6.94	9.60	10.8	11.03	10.75	10.34	9.94	9.56	9.23	8.70	8.325	8.05	7.80	7.625
0.000001	6.915	9.30	10.20	10.22	9.875	9.45	9.08	8.75	8.42	7.975	7.645	7.38	7.19	7.02
0.00001	6.85	8.91	9.48	9.35	8.93	8.51	8.175	7.86	7.60	7.20	6.915	6.72	6.52	6.42
0.0001	6.75	8.35	8.60	8.31	7.895	7.525	7.21	6.97	6.72	6.40	6.155	6.00	5.83	5.75
0.001	6.525	7.60	7.54	7.18	6.80	6.47	6.235	6.00	5.82	5.555	5.36	5.23	5.13	5.03
0.01	6.125	6.59	6.30	5.95	5.62	5.36	5.17	5.02	4.89	4.675	4.54	4.43	4.35	4.30
0.1	5.32	5.20	4.85	4.57	4.345	4.17	4.05	3.94	3.85	3.72	3.62	3.57	3.52	3.47
1.0	3.73	3.44	3.22	3.06	2.94	2.87	2.80	2.75	2.71	2.66	2.61	2.58	2.53	2.53
10	1.26	1.33	1.34	1.345	1.35	1.33	1.33	1.34	1.32	1.315	1.32	1.32	1.29	1.30
20	0.48	0.66	0.72	0.755	0.775	0.78	0.80	0.805	0.81	0.815	0.82	0.82	0.825	0.83
30	0.06	0.25	0.33	0.38	0.405	0.415	0.435	0.45	0.45	0.47	0.47	0.48	0.48	0.495
40	−0.21	−0.04	0.035	0.09	0.11	0.13	0.14	0.16	0.16	0.17	0.19	0.21	0.21	0.21
50	−0.41	−0.27	−0.21	−0.16	−0.14	−0.12	−0.11	−0.09	−0.09	−0.08	−0.065	−0.04	−0.04	−0.035
60	−0.56	−0.47	−0.42	−0.39	−0.37	−0.355	−0.35	−0.33	−0.33	−0.31	−0.31	−0.30	−0.30	−0.28
70	−0.68	−0.65	−0.63	−0.615	−0.605	−0.595	−0.59	−0 575	−0.58	−0.57	−0.57	−0.55	−0.55	−0.54
80	−0.78	−0.83	−0.85	−0.855	−0.86	−0.86	−0.86	−0.85	−0.85	−0.85	−0.85	−0.84	−0.85	−0.84
85	−0.83	−0.92	−0.97	−0.99	−1.00	−1.01	−1.02	−1.02	−1.03	−1.03	−1.03	−1.03	−1.03	−1.025
90	−0.87	−1.015	−1.09	−1.13	−1.16	−1.18	−1.19	−1.20	−1.21	−1.225	−1.24	−1.235	−1.25	−1.25
95	−0.915	−1.13	−1.255	−1.33	−1.38	−1.42	−1.45	−1.47	−1.49	−1.51	−1.535	−1.54	−1.56	−1.57
						(*h*) $\theta = 8$								
0.0000001	7.895	10.70	11.78	11.73	11.30	10.76	10.26	9.82	9.44	8.87	8.45	8.15	7.85	7.70
0.000001	7.83	10.30	11.00	10.775	10.31	9.78	9.30	8.93	8.59	8.10	7.74	7.455	7.25	7.05
0.00001	7.74	9.775	10.15	9.775	9.29	8.78	8.355	8.03	7.73	7.31	6.99	6.75	6.57	6.45
0.0001	7.55	9.06	9.10	8.64	8.15	7.71	7.35	7.075	6.83	6.47	6.21	6.03	5.87	5.765
0.001	7.245	8.15	7.90	7.42	6.975	6.60	6.32	6.10	5.90	5.64	5.40	5.27	5.14	5.055
0.01	6.675	6.95	6.545	6.07	5.75	5.45	5.225	5.06	4.92	4.725	4.56	4.47	4.40	4.32
0.1	5.61	5.38	4.97	4.63	4.41	4.22	4.08	3.97	3.88	3.75	3.64	3.58	3.52	3.50
1.0	3.78	3.47	3.24	3.08	2.975	2.88	2.81	2.78	3.72	2.66	2.60	2.575	2.56	2.54
10	1.225	1.32	1.335	1.34	1.34	1.33	1.33	1.33	1.33	1.33	1.30	1.31	1.31	1.31
20	0.48	0.65	0.71	0.75	0.77	0.78	0.79	0.80	0.80	0.825	0.81	0.825	0.83	0.82
30	0.07	0.25	0.32	0.37	0.40	0.41	0.43	0.44	0.45	0.47	0.46	0.485	0.485	0.495
40	−0.195	−0.04	0.03	0.08	0.11	0.13	0.14	0.155	0.17	0.18	0.19	0.20	0.21	0.195
50	−0.385	−0.27	−0.21	−0.17	−0.14	−0.125	−0.11	−0.09	−0.09	−0.07	−0.07	−0.045	−0.045	−0.04
60	−0.53	−0.46	−0.42	−0.40	−0.37	−0.36	−0.34	−0.34	−0.32	−0.32	−0.31	−0.30	−0.30	−0.28
70	−0.66	−0.64	−0.63	−0.61	−0.60	−0.60	−0.59	−0.58	−0.58	−0.57	−0.575	−0.56	−0.55	−0.54
80	−0.76	−0.82	−0.84	−0.85	−0.85	−0.86	−0.86	−0.86	−0.86	−0.86	−0.86	−0.85	−0.85	−0.84
85	−0.81	−0.91	−0.955	−0.98	−0.99	−1.01	−1.01	−1.02	−1.02	−1.02	−1.04	−1.03	−1.03	−1.03
90	−0.855	−1.00	−1.08	−1.13	−1.15	−1.18	−1.19	−1.210	−1.22	−1.23	−1.25	−1.24	−1.25	−1 24
95	−0.91	−1.12	−1.24	−1.32	−1.37	−1.42	−1.44	−1.47	−1.48	−1.51	−1.53	−1.55	−1.56	−1.56

TABLE 22.—(*Continued*).

% - of - time	Probability for the Index Value, λ =:													
	1	1.5	2	2.5	3	3.5	4	4.5	5	6	7	8	9	10
						(*i*) $\theta = 9$								
0.0000001	8.92	11.70	12.60	12.34	11.72	11.02	10.49	10.01	9.60	8.98	8.525	8.19	7.91	7.72
0.000001	8.74	11.20	11.71	11.30	10.67	10.02	9.50	9.10	8.745	8.22	7.775	7.50	7.27	7.14
0.00001	8.59	10.55	10.69	10.11	9.54	8.95	8.495	8.15	7.835	7.38	7.04	6.82	6.60	6.50
0.0001	8.34	9.695	9.52	8.90	8.35	7.83	7.45	7.17	6.90	6.55	6.25	6.07	5.92	5.80
0.001	7.90	8.57	8.17	7.595	7.11	6.695	6.375	6.17	5.95	5.65	5.44	5.30	5.185	5.09
0.01	7.13	7.20	6.70	6.18	5.78	5.49	5.28	5.115	4.97	4.76	4.595	4.47	4.405	4.345
0.1	5.845	5.46	5.02	4.70	4.43	4.23	4.09	4.00	3.895	3.77	3.66	3.59	3.53	3.49
1.0	3.79	3.47	3.25	3.10	2.98	2.89	2.82	2.78	2.72	2.68	2.61	2.59	2.55	2.54
10	1.20	1.30	1.32	1.32	1.33	1.32	1.32	1.34	1.31	1.32	1.31	1.32	1.32	1.32
20	0.47	0.635	0.71	0.75	0.76	0.77	0.79	0.80	0.80	0.82	0.81	0.83	0.82	0.82
30	0.07	0.24	0.32	0.36	0.39	0.40	0.43	0.445	0.45	0.47	0.47	0.49	0.49	0.49
40	−0.18	−0.04	−0.03	0.07	0.10	0.12	0.13	0.16	0.16	0.18	0.18	0.20	0.22	0.22
50	−0.37	−0.27	−0.21	−0.17	−0.145	−0.13	−0.11	−0.095	−0.09	−0.07	−0.07	−0.045	−0.045	−0.04
60	−0.52	−0.46	−0.42	−0.40	−0.37	−0.36	−0.36	−0.33	−0.33	−0.32	−0.31	−0.29	−0.30	−0.28
70	−0.64	−0.64	−0.62	−0.61	−0.60	−0.60	−0.585	−0.58	−0.57	−0.56	−0.56	−0.54	−0.54	−0.55
80	−0.745	−0.81	−0.83	−0.85	−0.85	−0.86	−0.85	−0.85	−0.85	−0.845	−0.86	−0.86	−0.85	−0.84
85	−0.795	−0.90	−0.95	−0.98	−0.99	−1.01	−1.01	−1.01	−1.02	−1.02	−1.03	−1.03	−1.03	−1.02
90	−0.84	−0.995	−1.07	−1.12	−1.15	−1.175	−1.19	−1.20	−1.21	−1.22	−1.24	−1.235	−1.24	−1.235
95	−0.89	−1.11	−1.24	−1.32	−1.37	−1.415	−1.44	−1.46	−1.48	−1.50	−1.53	−1.54	−1.56	−1.555
						(*j*) $\theta = 10$								
0.0000001	9.72	12.70	13.36	12.9	12.07	11.36	10.70	10.17	9.71	9.06	8.60	8.26	7.96	7.74
0.000001	9.60	12.09	12.36	11.78	10.94	10.29	9.68	9.21	8.81	8.25	7.85	7.58	7.31	7.125
0.00001	9.40	11.30	11.20	10.51	9.76	9.155	8.65	8.25	7.90	7.43	7.10	6.86	6.64	6.47
0.0001	9.05	10.30	9.89	9.18	8.50	7.99	7.55	7.24	6.97	6.57	6.305	6.075	5.93	5.795
0.001	8.48	9.01	8.425	7.75	7.175	6.80	6.45	6.20	5.99	5.69	5.47	5.325	5.20	5.09
0.01	7.54	7.45	6.825	6.29	5.86	5.575	5.325	5.12	4.985	4.755	4.61	4.50	4.40	4.335
0.1	6.01	5.575	5.09	4.74	4.46	4.275	4.10	4.00	3.91	3.76	3.67	3.60	3.52	3.48
1.0	3.78	3.49	3.26	3.11	2.98	2.91	2.83	2.77	2.72	2.67	2.62	2.59	2.55	2.54
10	1.18	1.29	1.32	1.33	1.325	1.33	1.32	1.32	1.32	1.325	1.33	1.33	1.31	1.30
20	0.46	0.63	0.70	0.74	0.76	0.78	0.78	0.80	0.80	0.81	0.815	0.83	0.81	0.82
30	0.08	0.24	0.31	0.36	0.39	0.41	0.43	0.43	0.45	0.46	0.47	0.49	0.49	0.48
40	−0.175	−0.04	0.03	0.07	0.10	0.13	0.14	0.15	0.16	0.18	0.19	0.20	0.20	0.20
50	−0.36	−0.27	−0.21	−0.17	−0.145	−0.125	−0.11	−0.10	−0.09	−0.07	−0.06	−0.05	−0.05	−0.045
60	−0.51	−0.46	−0.42	−0.39	−0.37	−0.36	−0.35	−0.34	−0.32	−0.32	−0.31	−0.30	−0.30	−0.29
70	−0.63	−0.63	−0.625	−0.61	−0.60	−0.59	−0.59	−0.58	−0.575	−0.57	−0.56	−0.55	−0.55	−0.55
80	−0.73	−0.80	−0.83	−0.84	−0.85	−0.855	−0.86	−0.86	−0.85	−0.85	−0.85	−0.85	−0.85	−0.85
85	−0.785	−0.895	−0.95	−0.98	−0.99	−1.00	−1.01	−1.02	−1.02	−1.02	−1.02	−1.02	−1.02	−1.035
90	−0.83	−0.985	−1.07	−1.12	−1.14	−1.17	−1.19	−1.20	−1.21	−1.21	−1.23	−1.24	−1.24	−1.25
95	−0.89	−1.10	−1.23	−1.31	−1.26	−1.41	−1.435	−1.46	−1.48	−1.50	−1.53	−1.53	−1.55	−1.56

parameters is infinite), and there seems to be no way of making the order of its flexibility agree with the flexibility that the statistics can significantly stand.

Professor Goodrich's method undoubtedly gives closer fits in a great many cases than are obtained by the function the writer proposes (the partly bounded function is obviously not flexible enough to represent the variations in the samples given as illustrations), but this added flexibility is scarcely a desirable feature when dealing with inadequate samples.

In functional analysis (as distinct from statistical analysis) the probable errors of the constants of a curve fitted to a set of data may be computed by the methods developed from the theory of least squares because of the reasonable assumption (in most cases, at any rate) that the variations in the observations from the true functional relation follow a symmetrical law closely represented by the Gaussian normal. In fitting a curve to a statistical series, however, the errors arise in an entirely different manner; they are errors in the characteristics of the distribution function itself. These errors are seldom small quantities of the first order, and so one is scarcely justified in computing the probable errors of the constants of the curve from them, even though by means of them the difficulties of correlation emphasized by Messrs. Fisher and Kemper are obviated (since statistical characteristics are mutually independent). In 1902, Pearson gave[68] the probable errors of statistical characteristics. The writer uses these values, reducing the order of the moments to any desired degree by a suitable recursion formula (Equations (22), for instance), and computes two curves, one with the errors added to the characteristics as computed from the sample and the other with the errors subtracted. This gives a range within which the curve characteristic of the population has something better than an even chance of lying. The important and difficult subject of errors of sampling has not yet received adequate attention from engineers.

Professor Mavis raises an important question with regard to the representation of finite and discrete variates by means of a smooth frequency curve. Few phenomena in applied mathematics have been so misunderstood as the nature of a frequency function. A smooth curve does not imply that the variate is continuous or that the variations are infinite in number, although in so-called derivations, still abundant in treatises, such motions appear implicitly and explicitly. The fact is that the ordinates of a frequency curve do not give frequencies. The frequencies are always given by the area included between the curve, the class interval, and the two class limits. These frequencies, therefore, are always discrete. It is true that the mid-ordinate of a class (when the class interval is taken as 1) is usually numerically close to the frequency of the class, so that this ordinate is often taken as the frequency; but the frequency is always given by an area. When the variate is continuous and the number of variations infinite, one may only estimate the frequency of the values of the variate within the class limits; in the continuous case, the frequency of a single value is always zero.

[68] "On the Mathematical Theory of the Errors of Judgment." *Philosophical Transactions*, Royal Soc. (London), A, 198, 1902, pp. 235–299.

In calling the totally bounded function the most general homograde function, the writer is stating a definition and, consequently, cannot be falling into a logical error. He is, in effect, formulating a physical law. This formulation is empirical, and it will take experience and not mathematics to prove it right or wrong. It is well known that the small errors of precise measurements are distributed, to a high order of approximation, according to the normal law. The mean and the standard deviation are the two characteristics necessary to determine such distributions and, for them, there are no other independent characteristics. When the causes producing variations are not infinite in number and are not mutually independent, then these two characteristics do not suffice and two others must be introduced. The writer then considers the four-parameter generalization of the Gaussian normal the most general homograde distribution, more complicated distributions being merely superpositions of this type.

Thiele's observations, as mentioned by Mr. Fisher, regarding the "pseudo-normal" variate, $t = h(x)$, are not discoveries in the theory of statistics, but merely special cases of theorems from the general theory of curves. Any two curves, provided they satisfy certain conditions of uniformity, may always be transformed into one another by suitable transformations. A theory of "pseudo-normal" variates, therefore, is quite as general as the integral equation or the Gram-Charlier formulations. The great use of such an observation (and the writer has availed himself of it) is that tables of the probability integral may be used with the more general function.

The writer was in error in attributing Equation (10) to Mr. Fisher, and he did not notice, until it was too late to acknowledge it, that the partly bounded function is exactly equivalent to his generic function; he was confused, on reading Mr. Fisher's treatise, by the discussion of the "mathematical zero." The writer objects to the use of it as a generic function, at least when dealing with small samples, for reasons already stated.

The work of the Danish statisticians is known to the writer only through Mr. Fisher's work and he was not aware of Thiele's generalization, Equation (68). Thiele, however, does not show how to compute the constants of this curve in terms of the statistical characteristics; in this respect, at any rate, the writer has shown some originality. The awkwardness in the writer's presentation, referred to by Mr. Fisher, was to a large extent, unavoidable. In the first place, the writer has definite limitations of expression and knowledge; in the second place, the "obvious" detail in the analysis and the choice of mathematical procedure was deemed desirable in presenting a paper of this sort to engineers instead of mathematicians. In defense of the analysis of Article 6, Section II, which Mr. Fisher considers superfluous, the writer should like to state that the approach of the logarithmic function to the limit, $\frac{x}{\sigma}$, as the skewness vanishes is by no means self-evident (although it may be well known to mathematicians). If the transformation chosen had been the simple "pseudo-normal" variate, $t = h(x) = ax^s$, then for no value of the parameter, a, would the resulting curve have reduced to the normal,

Thiele's theory notwithstanding. Thiele's theory leads to the Gaussian for the vanishing of the higher parameters simply because of the form he chose for his semi-variants. Another form would have led to a different fundamental function. The theory of integral equations teaches one that the normal functions of a problem depend on the kernel of the equation and not on whether the equation arises in the theory of statistics, or in mechanics, or in some other manner. Thus, it happens that Equations (75) and (78) are mathematically equivalent. Both represent any function, whether frequency or not, which is continuous and vanishes, together with its first derivative, at infinity in both directions.

Mr. Fisher is inaccurate in inferring that the writer's statements regarding the generality of these two equations implies that a Fourier series is inferior to a Taylor series. What they do imply is that both the Fourier and the Taylor series are mathematical devices which sometimes offer a comparatively easy means of solving a difficult problem — more often than not the solution thus obtained will be purely formal and of little practical value.

Elsewhere,[59] the writer has proposed a method for determining the maximum and minimum floods from a record of yearly floods. In this method the constants have been determined only for use with yearly floods and as it stands, it is not applicable to the example furnished by Mr. Hall. The form of the equations has been suggested by theory—physical and statistical—but their use in their present state can be justified only by the consistency of the results obtained by means of them in the problems attempted by the writer. The following quantities are used: g = maximum upper deviation from the mean, where the mean is taken = 1; b = maximum lower deviation from mean; g_o = maximum observed upper deviation; b_o = maximum observed lower deviation; A = drainage area, in square miles; M = mean flood, in feet per second; and, N = number of years in record. From these the following two quantities are computed: $\frac{0.4\, g_o}{b_o}$ = storm index; and, $\sqrt[3]{\frac{A}{M}}$ = flood index.

Using logarithms to the base 10, compute:

$$x = 6.7 - \left(0.5 \log N + 1.5 \log A + \frac{0.4\, g_o}{b_o}\right) + \sqrt[3]{\frac{A}{M}} \quad \ldots\ldots (89)$$

from which the maximum upper deviation is computed by the formula:

$$g = g_o\,(1 + 10^x)\left(0.7\sqrt[3]{\frac{A}{M}} + 0.8\right) \quad \ldots\ldots\ldots\ldots (90)$$

In cubic feet per second, the maximum flood will be given by $M(1 + g)$.

For the maximum lower deviation the same two equations are used, except that where g_o appears, $\frac{2\, b_o}{(1 - b_o)}$ is substituted, and where b_o appears $\frac{g_o}{(2 + g_o)}$

[59] Report to the Mississippi Valley Committee, July, 1935.

is substituted. Equation (90), then, gives a quantity, b', say, from which,

$$b = \frac{b'}{(2 + b')} \quad \ldots\ldots\ldots\ldots\ldots\ldots\ldots\ldots\ldots\ldots (91)$$

and the minimum flood is given in cubic feet per second by $M(1 - b)$.

The late Allen Hazen, M. Am. Soc. C. E., presented[60] an example that shows the effect of the large flood of 1913 on the yearly flood record of the Hudson River, at Mechanicsville, N. Y. If the 23-yr record[61] ending in 1912 is taken, then $N = 23$; $A = 4\,500$; $M = 41\,700$; $g = 0.43$; and, $b = 0.37$. Substituting these values in Equations (89) and (90), it is found that $g = 2.225$, from which $3.225 \times 41\,700 = 134\,600$ cu ft per sec for the maximum flood. If the 34-yr record[62] ending in 1923 is taken, then the quantities are: $N = 34$; $A = 4\,500$; $M = 44\,000$; $g = 1.56$; and $b = 0.41$; and thus $g = 2.285$ and the maximum flood is 144 600 cu ft per sec. Although the two graphs show quite different characteristics, the values computed from them for the maximum flood are seen to be fairly close. Likewise, from two records of the Arkansas River,[63] the maximum flood is computed to be close to 50 000 cu ft per sec. These two rivers have equal drainage areas, but quite different flood and storm indices. (The storm index as herein given is a very variable quantity and characteristic of the particular record only.)

To use Table 22: (*a*) Find the mean, M, and the standard deviation, σ; (*b*) estimate b and g; and, (*c*) compute $\lambda = \frac{b}{\sigma}$ and $\theta = \frac{g}{b}$. Table 22 gives values of t corresponding to percentages of time for various values of λ and θ. First-difference interpolations will usually be necessary. Then, compute (*d*) $X = (\sigma t + M)$, which is plotted against the corresponding %-of-time.

Table 2 of the paper simply gives the particular case in which g is infinite. It may be stated explicitly that the tables are computed for $\sigma = 1$, but that, because of the homogeneity of the function, any standard deviation is taken into account in Step (*d*) of the foregoing instructions. When b is greater than g, the function is left skewed. Because of the symmetry in b and g of the logarithmic linear fractional transformation, the same tables may be used in that case by merely interchanging b and g.

For instance, taking the 34-yr record for the Hudson River, $g = 2.285$; and, $b = 0.525$. Hazen gave the value, 0.37, for the standard deviation, CV, in this case, and if an attempt is made to fit the curve with this value, it is found to be too far off the main body of the statistics—the 1913 flood pulls it up considerably. Even this poor fit gives to this flood a probability of being equalled or exceeded but once in about 1 000 yr, so that since this flood contributes vastly more than its share to the standard deviation, one may conclude that a better estimate of this value may be made by taking only the forty-two values that exclude it. In this way the standard deviation is found

[60] "Flood Flows," by Allen Hazen, Wiley & Sons, New York, 1930.
[61] *Loc. cit.*, Fig. 38, p. 89.
[62] *Loc. cit.*, Fig. 15, p. 78.
[63] *Loc. cit.*, Fig. 29, p. 89, and Fig. 34, p. 84.

to be 0.26. (For all these computations the flood magnitudes have been scaled from the diagrams previously cited,[60] and a 10-in slide-rule has been used.)

To compute the standard error in the standard deviation, first calculate,

$$\beta = \left(\frac{\sigma^3}{b^3} + \frac{3\,\sigma}{b}\right)\left(\frac{g-b}{g+b}\right) \quad \ldots\ldots\ldots\ldots\ldots\ldots\ldots\ldots (92)$$

from which the required error is given by,

$$\epsilon\,(\sigma) = \tfrac{1}{2}\,\sigma\sqrt{\frac{3\,\beta^2+4}{2\,N}} \quad \ldots\ldots\ldots\ldots\ldots\ldots\ldots\ldots (93)$$

Equation (93) is obtained from Pearson's relations for the error in the moments in connection with the recursion formulas, Equations (22), and

TABLE 23.—Computation of Probability Curve.

(1)	(2)	(3)	(4)	(5)
6.41	7.66	6.86	3.06	0.000001
6.22	7.36	6.63	2.95	0.00001
5.99	6.96	6.34	2.90	0.0001
5.63	6.42	5.55	2.77	0.001
5.11	5.66	5.31	2.60	0.01
4.34	4.66	4.46	2.34	0.1
3.17	3.25	3.20	1.96	1
1.41	1.38	1.40	1.42	10
0.75	0.72	0.74	1.22	20
0.32	0.31	0.32	1.10	30
0.01	0.00	0.01	1.00	40
—0.25	—0.24	—0.25	0.92	50
—0.48	—0.47	—0.48	0.86	60
—0.69	—0.67	—0.69	0.79	70
—0.90	—0.87	—0.89	0.73	80
—1.10	—0.97	—1.05	0.69	85
—1.12	—1.09	—1.11	0.67	90
—1.26	—1.23	—1.25	0.63	95

modified so as to be applicable to the general function. These expressions are not exact, but they give values for the error comparable to those obtained by the cumbersome exact formulas. Using the foregoing values for the Hudson River, the error is found to be 0.04. The curve for $\sigma = 0.26 + 0.04 = 0.3$ will be computed. With this value, $\lambda = 1.75$ and $\theta = 4.36$. From Table 22(d) by interpolating between the columns for $\lambda = 1.5$ and $\lambda = 2.0$,

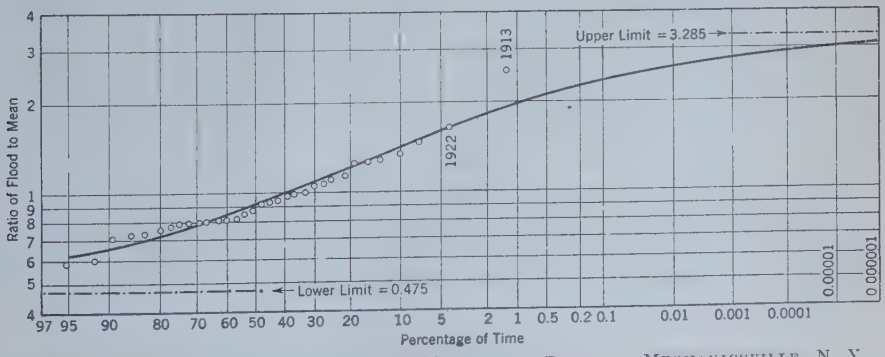

Fig. 9.—Yearly Flood Record, 1881–1923, Hudson River at Mechanicsville, N. Y.

Column (1) of Table 23 is obtained. Column (2) is obtained from Table 22(*e*) by the same interpolation. Then, adding to Column (1) Table 23, 0.36 times the differences between the entries in Columns (1) and (2), Column (3) is obtained. Column (4) = 0.3 × Column (3) + 1, and is plotted against the %-of-time values given in Column (5), Table 23. The curve is shown in Fig. 9. For $\sigma = 0.26$ the curve is slightly flatter and crosses the plotted curve at about the mean.

Equations (89) and (90) should not be used for areas of less than 1 000 sq mile nor for records of less than about 20 yr.

Acknowledgment.—Equations (89) and (90) were developed while the writer was employed by the United States Geological Survey on the work of the Mississippi River Commission. The writer wishes to express his great indebtedness to Messrs. D. Abramowitz and A. Mandel for constructing Table 22 and for much other assistance, and to Thorndike Saville, M. Am. Soc. C. E., for making their labor available and for valuable criticism and encouragement.

AMERICAN SOCIETY OF CIVIL ENGINEERS

Founded November 5, 1852

DISCUSSIONS

ANALYSIS OF CONTINUOUS STRUCTURES BY TRAVERSING THE ELASTIC CURVES

Discussion

BY RALPH W. STEWART, M. AM. SOC. C. E.

RALPH W. STEWART,[24] M. AM. SOC. C. E. (by letter).[24a]—The discussion has brought up criticisms and questions relating to specific items not satisfactorily covered in the paper. It has also raised the broader question as to whether the traverse method is a special method of limited scope, or whether it is a general method which may be used for the analysis of structures for which slope deflection and end-moment distribution are not suitable. To answer the latter query it will be necessary first to show its application to some cases of single-span beams.

Figs. 12(*a*), 12(*b*), and 12(*c*) show the simple moment areas and the positions of their centers of gravity for all conditions of normal loading; Figs. 12(*d*), 12(*e*), 12(*f*), 12(*g*), and 12(*h*) show traverse diagrams for beams of constant cross-section having various conditions of end restraint. The double hatching indicates a fixed end; the single hatching a restrained (but not fixed) end; and, absence of hatching, a hinged end. In the following equations, A is the area of the simple $\frac{M}{EI}$-diagram and Δ, the area of a triangular $\frac{M}{EI}$-diagram (not shown), with a base extending the full length of the beam and an altitude which is the end moment due to restraint, divided by E and I. If the beam has a constant cross-section and is of the same material throughout, and movements of supports are not involved, both E and I may be omitted, and the moment areas used instead of the $\frac{M}{EI}$-areas.

NOTE.—The paper by Ralph W. Stewart, M. Am. Soc. C. E., was published in October, 1934, *Proceedings*. Discussion on the paper has appeared in *Proceedings*, as follows: December, 1934, by Messrs. Garrett B. Drummond, Austin H. Reeves, E. G. Paulet, Adolphus Mitchell, and David M. Wilson; March, 1935, by Messrs. W. H. Kirkbride, R. B. Ketchum, A. Floris, and Ivan M. Nelidov; and May, 1935, by Fang-Yin Tsai, Assoc. M. Am. Soc. C. E.

[24] Engr. of Bridge and Structural Design, City of Los Angeles, Los Angeles, Calif.

[24a] Received by the Secretary June 25, 1935.

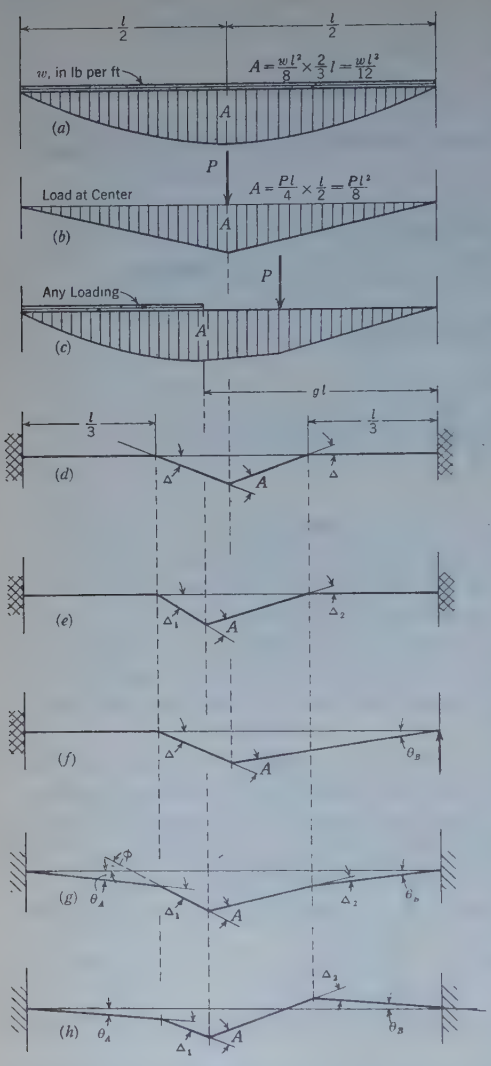

FIG. 12.

For these beams of constant section all Δ-angles in the traverse are at the one-third length points and $\Delta = \frac{Ml}{2}$, in which M is the appurtenant end moment.

For cases in which a traverse forms a single triangle, it is often more convenient to use the angle relationships of the triangle for obtaining values of the unknowns than to write a traverse equation. In Fig. 12(*d*), the isosceles triangle formed by the traverse gives $\Delta = \frac{1}{2} A$, and from this, $\frac{Ml}{2} = \frac{wl^2}{24}$ for uniform loading, or M (the end moment) $= \frac{1}{12} wl^2$. In Fig. 12(*e*), $\Delta_1 \left(\frac{l}{3}\right) = A \left(g\ l - \frac{l}{3}\right)$; and $\Delta_1 = \frac{M_1 l}{2}$. Therefore, $M_1 = \frac{2A}{l} (3g - 1)$. In Fig. 12(*f*), $\Delta \left(\frac{2}{3} l\right) = A\ g\ l$; and, $\Delta = \frac{M_1 l}{2}$. Therefore, $M_1 = \frac{3Ag}{l}$. If the load is as in Fig. 12(*b*), then $g = \frac{1}{2}$ and $A = \frac{Pl^2}{8}$, giving $M_1 = \frac{3}{16} Pl$.

In Fig. 12(*g*) (assuming counterclockwise rotations to be negative, as in slope deflection), for symmetrical loading from left to right:

$$\theta_A + \tfrac{2}{3} \Delta_1 - \tfrac{1}{2} A + \tfrac{1}{3} \Delta_2 = 0 \ldots\ldots\ldots\ldots\ldots\ldots (66)$$

and right to left,

$$-\theta_B - \tfrac{2}{3} \Delta_2 + \tfrac{1}{2} A - \tfrac{1}{3} \Delta_1 = 0 \ldots\ldots\ldots\ldots\ldots\ldots (67)$$

If the loading is unsymmetrical, use $A\ g$ instead of $\frac{1}{2} A$ in Equation (66) and $A(1 - g)$ in Equation (67). Solving these equations for Δ_1 and Δ_2, and substituting the M-values of the Δ-angles, standard slope deflection equations

are obtained. When the beam and loading are symmetrical, $\phi = \frac{A}{2}$ and may often be used to advantage in solutions. In formulas such as Equations (66) and (67) only the coefficients of l are used as l, if written in each term, will be eliminated.

In Fig. 12(h) a dominating moment in an adjoining span has reversed the direction of the end slope, θ_B. This will be discussed subsequently.

Fig. 13 illustrates the traverse of a beam of variable section and complete dissymmetry having fixed ends. All dimensions and properties of this

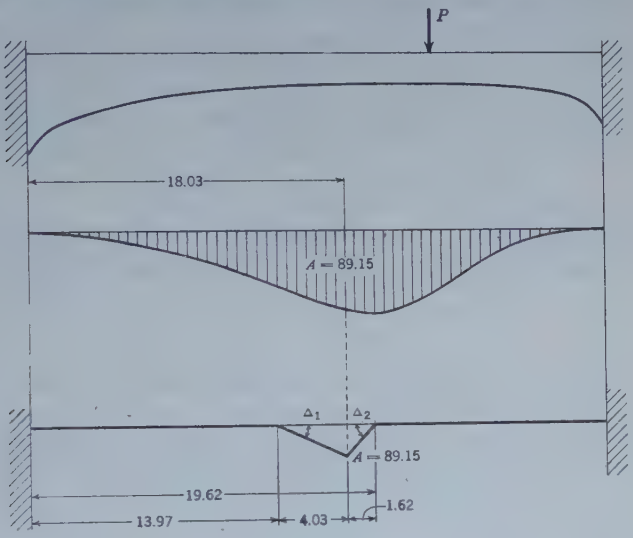

FIG. 13.

beam have been presented[25] by George E. Large, Assoc. M. Am. Soc. C. E., including the computations for the A and Δ locations and magnitudes.

From the triangle in the traverse: $\Delta_1 = \frac{1.62}{5.65} \times 89.15 = 25.56$; $M_1 = \frac{25.56}{9.12} \times 10 = 28.00$; $\Delta_2 = \frac{4.03}{5.65} \times 89.15 = 63.59$; and $M_2 = \frac{63.59}{12.27} \times 10 = 51.83$. This solution gives the fixed-end moments by a simpler procedure, involving less computation, than the previously published solution.[26] Problems of the fixed-end moments in restrained beams cannot be solved by slope deflection or by end moment distribution. Their solution as herein demonstrated shows that the traverse method is applicable to fundamentals.

Frequently, in a continuous beam, the direction of rotation at a support cannot be forecast by inspection, and the question arises as to how to apply the traverse. This condition is illustrated by Fig. 14, in which the slopes

[25] "The Analysis of Continuous Frames by Distributing Fixed-End Moments," by Hardy Cross, M. Am. Soc. C. E., *Transactions*, Am. Soc. C. E., Vol. 96 (1932), p. 102; also, *Bulletin No. 66*, Ohio State Univ.

[26] *Transactions*, Am. Soc. C. E., Vol. 96 (1932), p. 105, Equations (86) and (87).

over the intermediate supports are purposely drawn in the wrong direction. The procedure for drawing the traverse lines is described in connection with Fig. 7. Before the sketch is completed, it announces the error in assumption by the disproportionate sizes of the A-angles. Disregarding this, now obvious, error in the diagram, write the traverse equation from left to right and from right to left for the full length of the beam; combine the numerical terms and the coefficients of the respective Δ-angles; and obtain: $28\,\Delta_1 + 30\,\Delta_2 = 2\,160$; and, $-12\Delta_1 - 26\,\Delta_2 = -1\,620$. (The signs in these equations follow the rules for slope deflection.) Solving, $M_B = 6.85$ and $M_C = 17.61$. Continuing the solution it is found that $\theta_B = -8.80\,E\,I$ and

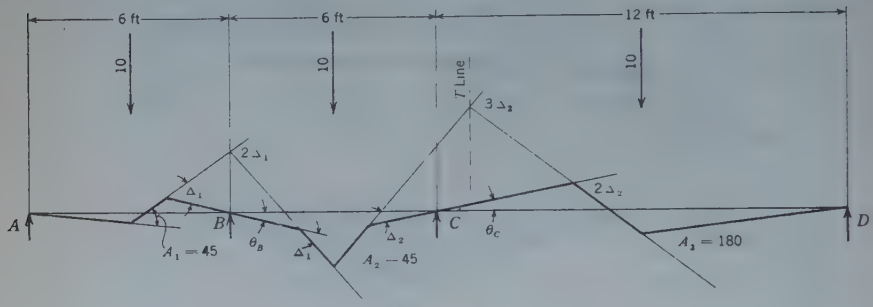

Fig. 14.

$\theta_C = +\,19.57\,E\,I$. The solution was not affected by the error in the diagram. Attention is invited to the fact that a mechanical solution of this problem could be obtained by drawing the A-angles to a suitable scale on separate slips of tracing paper and manipulating them with their legs intersecting on the T-lines until proper closure is obtained. The result would be rather rough, but probably more accurate than that obtained by using the arbitrary coefficients of various building ordinances.

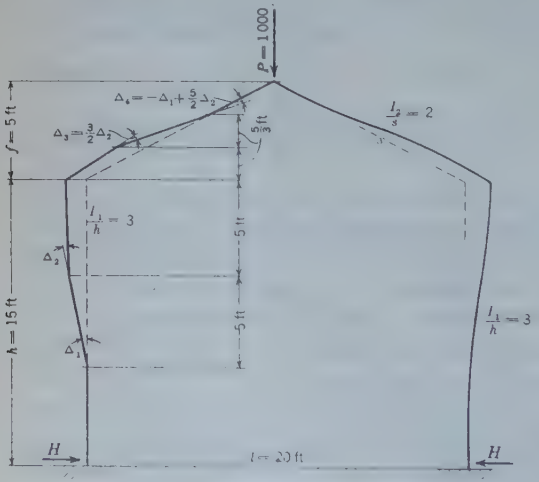

Fig. 15.

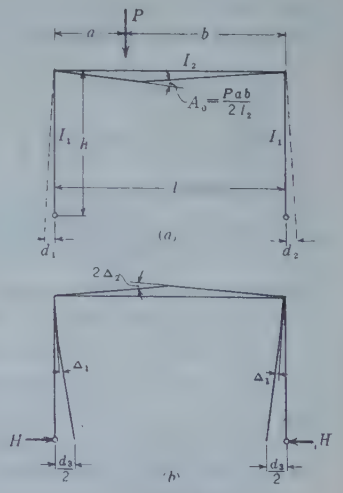

Fig. 16.

The fact that a computed traverse can be checked quickly by plotting, and that errors in assumed direction of joint rotations are disclosed while the traverse is being drawn, is an advantage of no small importance, which is not available with other methods.

The discussion of Mr. Nelidov shows comprehensive understanding of the traverse method and also shows that it can be applied to frames with sloping roof members. In order to do the method justice, however, it will be necessory to show a shorter and simpler solution of the problem that he presented. Fig. 15 shows (in its deflected position) the same frame and loading as Fig. 9, the right half indicating the elastic curvature and the left half, the traverse diagram. The value of Δ_3 results from the relative stiffness factors of the column and the rafter. The value of Δ_4 is obtained by summation of angles from Δ_1 upward.

Beginning at Δ_1 the following traverse equation for the horizontal movements of Δ_4 may now be written:

$$-13\tfrac{1}{3}\,\Delta_1 + 8\tfrac{1}{3}\,\Delta_2 + 2\tfrac{1}{2}\,\Delta_3 = 0 \qquad (68)$$

For the left half of the frame two moment-shear equilibrium equations—one for the column and one for the rafter—may be written as follows:

$$M_1 + M_2 = 15\,H \qquad (69)$$

and,

$$M_3 + M_4 = 500 \times 10 - 5\,H \qquad (70)$$

in which H equals the horizontal thrust caused by the load. After transforming M-values to Δ-values, Equations (68), (69), and (70) are easily solved, giving $H = 220.1$, and moments which agree with those found by Mr. Nelidov (Moment-shear equilibrium formulas of the type of Equations (69) and (70) are used in the analysis of wind stresses in buildings. The principle is that the shear in a column is equal to the sum of its top and bottom moments divided by its height.)

No trigonometric functions are necessary in this solution, the number and size of equations are less impressive, and the labor is reduced.

Several discussers thought that the original paper was confined too much to symmetrical structures and loading. The following illustrations will show that the traverse method readily solves unsymmetrical cases. Fig. 16 is introduced because its solution may be checked conveniently by other methods or by handbooks. It will serve to illustrate the method of approach to the general case which succeeds it.

If the columns in Fig. 16(a) were on rollers the beam would deflect as if it were simply supported. The joint rotations would be equal to the end slopes of the simple beam, and the spread, $d_0 = d_1 + d_2$, at the bottoms of the columns would be equal to the sum of the end slopes times the height of the frame, which is equal to the area of the $\frac{M}{EI}$-diagram for the beam (considered as simply supported) times the height of the frame. For equilibrium, since the column bases do not spread, a force, H, must be exerted with

a magnitude sufficient to produce inward deflections of the columns equal to the spread, d_0, as indicated in Fig. 16(b). Thus, in Fig. 16(a),

$$d_1 + d_2 = d_0 = Ah = \frac{P\,a\,b\,h}{2\,I_2}$$

and, in Fig. 16(b),

$$d_3 = 2\,(\Delta_1 \times \tfrac{2}{3}\,h) + 2\,\Delta_2\,h = \frac{2\,H\,h^3}{3\,I_1} + \frac{H\,h^2\,l}{I_2}$$

Equating d_0 to d_3; letting k = the ratio of the stiffness of the beam to the stiffness of the column $= \dfrac{I_2\,h}{I_1\,l}$; and solving for H,

$$H = \frac{3\,P\,a\,b}{2\,h\,l\,(2\,k+3)} \qquad \text{.....(71)}$$

which is a handbook formula.[27] With H known, the moments are statically determinate. This solution takes into account the effect of side-sway.

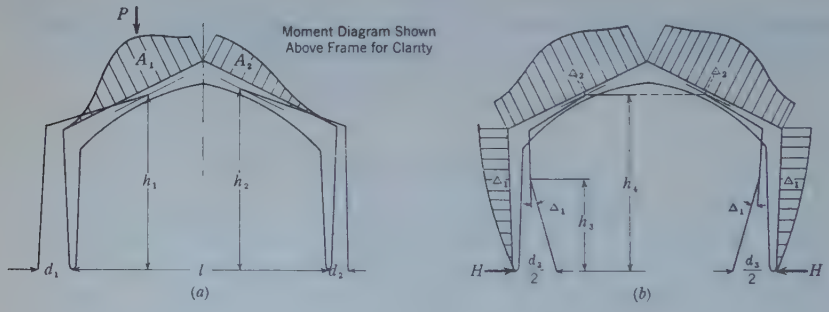

FIG. 17.

Fig. 17 shows unsymmetrical loading for a hinged-base, gable roof frame of variable moment of inertia. Following the method of approach indicated for Fig. 16, the equations by which this frame may be solved are, as follows:

In Fig. 17(a),

$$d_1 + d_2 = d_0 = A_1 h_1 + A_2 h_2 \qquad \text{.....(72)}$$

For a trial H in Fig. 17(b), compute,

$$d_3 = 2\,(\Delta_1 h_3 + \Delta_2 h_4) \qquad \text{.....(73)}$$

and,

$$\text{True } H = \frac{d_0}{d_3} \times \text{trial } H \qquad \text{.....(74)}$$

With H computed, the problem becomes statically determinate. This solution also includes the effect of side-sway.

These applications of the traverse method show that it is not restricted in its scope as are slope deflection and end-moment distribution. The latter methods require the assistance of some other type of analysis to obtain the

[27] "Rahmenformeln," von A. Kleinlogel, Wilhelm Ernst & Son, Berlin.

fixed-end moments needed. They are also unsuitable for frames with sloping roof members. The traverse method is applicable to the entire field of flexure, in which moments only and straight members only are involved. Even where axial shortening of members is involved the traverse can be passed through the altered positions of the joints as shown by Fig. 10, and solved. The method, therefore, appears to be entitled to the adjective, "general," rather than "special."

Mr. Paulet feels that the bending-moment diagram should be available as a guide, so that the traverse can be sketched. Proper observance of laws governing the angles will make it as easy or easier, to draw the traverse independently.

Note that in all diagrams each obtuse angle which is the supplement of each A-angle presents its opening toward the load, and if there is restraint to resist free rotation of an adjoining joint, there will be a Δ-angle of opposite direction between the A-angle and the joint. Using this rule the writer finds it easier to draw the traverse first, the moment diagram being either omitted or drawn as a by-product of the traverse. It was noted with pleasure that Mr. Nelidov omitted the moment diagram from his Fig. 9.

Mr. Paulet gives Equations (15) and (16) to express the series for relative moments and slopes, respectively, in Fig. 6 (c), with the letters exchanged for the series in Fig. 6(d). The fact that a single simple equation—namely, $M_{n+1} = 4\,M_n - M_{n-1}$, in which M = either moment or slope—expresses the law of progression for all four series is of more interest.

With reference to Mr. Paulet's feeling that for single spans the moment-area method is preferable to the traverse method, it is suggested that Fig. 13, and the supporting text, be examined. The traverse method is simply an amplification of the moment-area method by expressing moment-area relationships as a geometrical traverse, which clarifies the computations, discloses "short cuts" which would not be evident except for the traverse diagram, provides a graphical check, and also an easily understood method of treating settled supports.

The statement by several discussers that the traverse method compares unfavorably in speed with other methods merits a brief investigation. The solution for Fig. 3 was presented in complete detail to illustrate the principle of the traverse. A computer familiar with the method would not write Equation (6), but would analyze the traverse as follows: In Fig 3 where two lines intersects to form a Δ or A-angle, note that the intersection displays both an acute angle (the Δ-angle or the A-angle) and an obtuse angle which is the supplement of the Δ-angle or the A-angle. Designate angles with obtuse openings that face the interior of the frame as negative and the angles with obtuse openings that face outward, as positive. The sum of the negative angles must equal the sum of the positive angles. Noting that each column traverse forms an isosceles triangle, the computer can add the angles mentally and write, $3\,\Delta_2 = \dfrac{P\,l^2}{8\,E\,I}$. The subsequent steps can also be performed by mental arithmetic.

A good illustration of the speed of the traverse method is given by Fig. 18 which is the demonstration problem used by T. Y. Lin, Jun. Am. Soc. C. E., in his paper "A Direct Method of Moment Distribution."[28] Let Δ equal the curvature in the bottom member due to one of its end moments. Then Δ

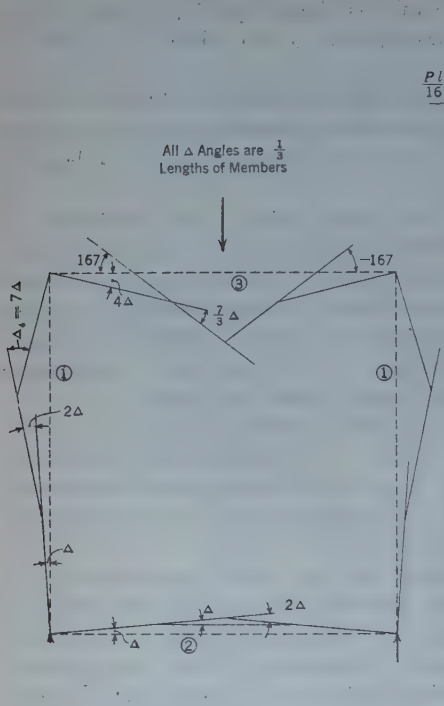

FIG. 18.

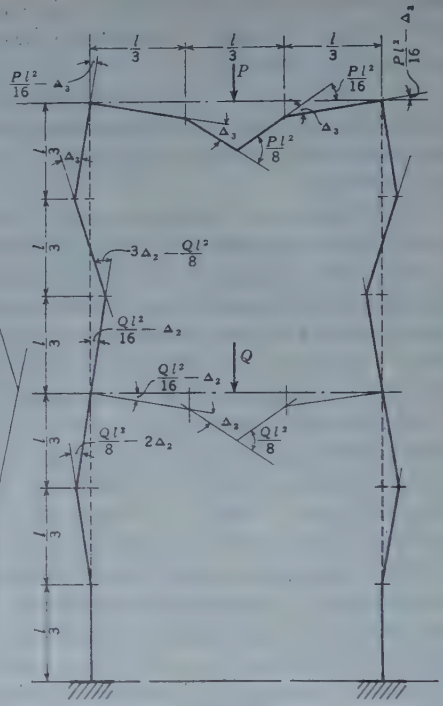

FIG. 19.

will also equal the rotation at each bottom corner. From the stiffness ratios the curvature due to the moment in the bottom of the column will be $2\,\Delta$, as shown. The fixed-end moment of 1 000 at the end of the top member gives a ϕ-angle of 167, as shown. The solution is now given by the following equations: Traversing from the bottom to the top of the column, $-3\,\Delta - 4\,\Delta + \Delta_4 = 0$; and, therefore, $\Delta_4 = 7\,\Delta$. The upper joint rotation, by adding angles from the bottom to the top of the column, is equal to $4\,\Delta$; the curvature due to the end moment in the beam, by stiffness ratios, will be $\frac{7}{3}\Delta$; and the closure of the triangle under the end of the upper beam gives, $\frac{19}{3}\Delta = 167$, from which $\Delta = 26.32$, and the bottom and top moments in the column are, respectively, 105.2 and 368.2. This is a direct solution which appears to the writer to be more expeditious than the previous solution cited and will compare well with solutions by slope deflection or by progressive end-moment distribution.

[28] *Proceedings*, Am. Soc. C. E., December, 1934, p. 1460.

Fig. 19 illustrates a two-story frame with members all of which have equal stiffness factors and joint rotations with unknown directions. Assume the direction of joint rotations as shown, and write, by inspection, all the angle values shown on the diagram, the Δ-value at the lower third point of the upper column being obtained by balancing moments about the adjoining joint.

Upward and downward traverses of the upper column now give:

$$\left(\frac{Q\,l^2}{16} - \Delta_2\right) - \frac{2}{3}\left(3\,\Delta_2 - \frac{Q\,l^2}{8}\right) + \frac{1}{3}\,\Delta_3 = 0$$

and,

$$\left(\frac{P\,l^2}{16} - \Delta_3\right) - \frac{2}{3}\,\Delta_3 + \frac{1}{3}\left(3\,\Delta_2 - \frac{Q\,l^2}{8}\right) = 0$$

Solving,

$$\Delta_2 = \frac{P\,l^2}{224} + \frac{11\,Q\,l^2}{224}$$

The rotation at the left end of the lower beam is $-\dfrac{P\,l^2}{224\,EI} + \dfrac{3\,Q\,l^2}{224\,EI}$. Therefore, if $P < 3Q$, the rotation is positive, as shown, and if $P > 3Q$, the rotation is counter-clockwise.

Continuing the solution it is found that if $Q > 5P$, the left top corner of the frame will rotate contra-clockwise. It is observed that slope-deflection sign rules may be applied to the traverse method of solving problems involving unknown directions of joint rotations.

Mr. Mitchell showed an application of the traverse method to Fig. 3, assuming that the column bases are 50% fixed. The traverse method, however, offers a shorter solution than that given by him, as follows: For the columns fully fixed at the base, $\Delta_1 = \frac{1}{2}\,\Delta_2$. For 50% fixation, Δ_1 will become equal to $\frac{1}{4}\,\Delta_2$ and a rotation will occur at the bottom of the column which will be two-thirds of the change in the value of $\Delta_1 = \frac{1}{6}\,\Delta_2$.[29] This angle of rotation will present its obtuse opening outward the same as Δ_1. Equating the sum of the negative angles around the frame to the sum of the positive angles, one may write at once $3\frac{1}{6}\,\Delta_2 = \dfrac{P\,l^2}{8}$, from which $M = \dfrac{3}{38}\,P\,l$, agreeing with Mr. Mitchell's result, but doing away with his Equations (17), (18), and (19), and his traverse equation.

The writer cannot agree with Mr. Mitchell that the traverse method "holds no advantage over slope deflection", nor with his findings as to the number of equations required.

Professor Tsai indicated in his discussion that he had fully grasped the traverse method. His equations showing how simple moment areas and the positions of their centers of gravity may be derived from (although not "given in") the Ruppel tables[6] constitute a useful contribution to the

[29] See properties of 1:2:3 diagrams in "Improved Method of Finding Beam Deflections," by Ralph W. Stewart, M. Am. Soc. C. E., *Civil Engineering*, February, 1934.

[6] *Transactions*, Am. Soc. C. E., Vol. 90 (1927), pp. 167–187.

practical application of the method. His comment that he could use the equations of three moments involving settled supports or the slope-deflection method with greater facility than the traverse method to solve Fig. 10, indicates that for this problem it is easier to apply ready made formulas than to work from basic principles, provided the formulas are memorized.

Professor Wilson has also grasped the traverse method, but leans to the end-moment distribution method as "the most workable of the special methods". In this connection it is worth noting that Hardy Cross, M. Am. Soc. C. E., has stated[30] that for single bents he preferred the column analogy method[31] to the end moment-distribution method. The traverse solutions for single-span frames, including arched frames as given herein, should certainly compete with the column analogy, especially for frames of variable moment of inertia to which the Ruppel tables are applicable.

The writer thanks Professor Drummond, Mr. Reeves, Mr. Kirkbride, Professor R. B. Ketchum, and Mr. Floris for their interest and the last three particularly for their encouraging comments. He feels that considering the versatility and general applicability of the traverse method, it should gain recognition.

It is superior to slope deflection in the following respects: (1) It provides an easy graphical verification of the computed analysis; (2) it uses basic principles rather than memorized formulas ("the anæsthetics of thought"); (3) it does not require the assistance of some other method; and (4) the entire elastic deformation of a structure may be pictured from the solution by the traverse method.

It is superior to end-moment distribution in Items (3) and (4), and also in its utility in deriving specific formula which may be recorded for future use.

[30] *Transactions*, Am. Soc. C. E., Vol. 96 (1932), p 145.

[31] *Bulletin No. 215*, Eng. Experiment Station, Univ. of Illinois, Urbana, Ill.

AMERICAN SOCIETY OF CIVIL ENGINEERS

Founded November 5, 1852

DISCUSSIONS

THE SILT PROBLEM

Discussion

BY HERMAN STABLER, M. AM. SOC. C. E.

HERMAN STABLER,[38] M. AM. SOC. C. E. (by letter).[38a]—The author has performed a real service to water-supply engineers by making available for ready reference such a mass of quantitative information on the silting of reservoirs and the suspended matter carried by streams. His statement of the silt problem and his discussion of the origin, transportation, and control of silt and of sedimentation processes include a summarization of facts and principles, largely devoid of expressions of opinion, that serves to round out a general picture of the silt problem in a manner both interesting and illuminating. In his discussion of the origin of silt the author touches on geology but, in the writer's opinion, gives it too little emphasis. As defined by the author, silt is stream-borne material derived from the disintegration of rocks. Two processes, weathering (disintegration in place) and corrasion (the tearing away or placing in motion of disintegrated material) are involved in the origin of silt, and the speed of the first of these processes is materially affected by the nature of the country rock. Igneous rocks, in general, are hard, dense, and crystalline; and they weather slowly. The older sedimentary rocks are likewise relatively dense and offer resistance to weathering. The younger sedimentary deposits, particularly recently laid alluvium, are especially susceptible to rapid weathering. Consequently, other things being equal, regions of igneous and precarboniferous rocks are regions of clear-water streams, and regions of recent sedimentaries and valleys filled with alluvial deposits are most likely to give rise to streams heavily laden with silt.

Among the younger sedimentary rocks, differences of texture and cementation are reflected by differences in speed of weathering. Loosely cemented sandstones and friable sandy shales are readily susceptible to weathering and corrasion and are prolific producers of silt.

The chemical composition of rock material is likewise a factor in the silt problem. Rocks that contain high percentages of aluminum silicate weather

NOTE.—The paper by J. C. Stevens, M. Am. Soc. C. E., was published in October, 1934, *Proceedings*. Discussion on this paper has apeared in *Proceedings* as follows: February, 1935, by Harry G. Nickle, Jun. Am. Soc. C. E.; March, 1935, by Messrs. E. W. Lane, and Frank E. Bonner; and May, 1935, by Messrs. Morrough P. O'Brien, Harry F. Blaney, W. W. Waggoner, and Philip R. R. Bisschop.

[38] Chf., Conservation Branch, U. S. Geological Survey, Washington, D. C.

[38a] Received by the Secretary July 29, 1935.

into clays with fine flaky particles readily susceptible to corrasion and water transportation. Regions of such rocks are likely to be regions of cloudy although not necessarily heavily silt-laden streams.

The geologic mission of rain and other forms of precipitation, from the moment they strike the earth, is to wear the land surface down to the level of the sea. This is accomplished mainly by weathering and corrasion, by solution, and by water transportation. In some regions of the United States more material is carried by streams in solution than as silt. In other sections the opposite is true. By and large the silt load of the streams of the United States is several times as great as the load carried in solution, but the latter is by no means an unimportant factor.

The relative speed of weathering and of removal and transportation of the weathered material, depending primarily on geology, topography, and climate, is a factor in the silt problem. In some regions streams run clear because little transportable material is available for water to move and only extraordinary storms and floods can muddy the waters. In other regions relatively gentle rains are sufficient to place in motion a wealth of weathered material awaiting only the means of transportation.

Vegetation, an incident of climate, is an important factor in the weathering of rocks and in the availability of weathered material for water transportation. By disruptive action of roots and chemical action of organic solvents vegetation aids weathering and adds to the volume of material suitable for transportation as silt and to the dissolved load of streams. By protection of the land surface from action of wind and water it retards or prevents silty material from corrasion and thus tends to avoid the overloading of streams with suspended matter. Cultivation of field crops artificially aids weathering and accelerates the speed of the natural process. Road building, the herding of stock, lumbering, and a multitude of other activities of Man that scar the earth's surface also speed up the natural process of weathering. Most of these activities are essential to human occupation of the land but some of them may be modified so as to minimize their effect on weathering and still retain their beneficial character. On the other hand, works of Man, such as buildings, streets, and paved roads, substantially prevent weathering whereas his river-regulating works and consumptive uses of water tend to decrease the power and quantity of water that may serve to transport silt and other rock débris. After all, Man's activities, although by no means a negligible factor in the silt problem, must be considered as incidental. Wisely guided, Man will undertake, when practicable, to diminish the removal of material valuable *in situ* to places where it will be deleterious, and to direct the deposition of transported silt at places where it may serve a useful purpose. In attempting to abolish the silt problem Man can be but a Don Quixote tilting at the windmills of Nature.

In attacking the silt problem, should the energies of Man be directed toward prevention or cure? Rather obviously good productive soil in a farming region should be maintained in place for agricultural use so far as practicable. In this case prevention pays, regardless of the silt problem; but

it is not so clear that great effort should be made to retain in place the surface material of non-agricultural regions. Regulation of grazing to maintain a maximum permanent useful vegetable cover for forage purposes is itself a profitable conservation measure, and, incidentally, will tend toward silt prevention. This is a practicable measure of silt prevention that may

FIG. 10.—SUBDIVISIONS OF THE COLORADO RIVER BASIN ABOVE THE PRINCIPAL GAUGING STATIONS

reasonably be undertaken in a relatively arid or non-agricultural region. To be practicable, however, it should be undertaken primarily in the interests of the stock industry rather than for the purpose of limiting the silt load of streams. Otherwise, costs are likely to exceed the values conserved.

The Colorado River occupies one of the major stream basins in the United States and has silt problems perhaps in greater degree than any other major stream of the country. Its problems of water supply, water utilization, land use, and silt have interested the writer for many years. Most of the extensive surveys of its stream channels, reservoir sites, and dam sites made by the U. S. Geological Survey in the two decades, 1915–1935, were under his general direction. The quality-of-water surveys (determination of daily silt load and dissolved mineral load of the Colorado and of its more important tributaries for a period continuous from 1929, which were made largely by C. S. Howard and S. K. Love under the direction of W. D. Collins, of the Geological Survey) were instigated by him and he has studied their results with interest. These researches, basic to land and water planning, although still inadequate to supply full information, afford probably the best available basis for the study of the silt problems of a large river in the United States. A brief consideration of some of their results will serve by example to throw light on some of the problems discussed by Mr. Stevens. Fig. 10 is a map showing the subdivisions above the principal gauging stations of the Colorado River Basin and Table 13 shows some of the characteristics of these

TABLE 13.—Data Related to the Silt Problem on Colorado River Above Grand Canyon, Arizona.

Description	Water-Shed Subdivisions (See Fig. 10)						
	A	*B*	*C*	*D*	*E*	*F*	*G*
Area, in square miles	40 600	24 100	24 000	31 000	19 300	50 300	139 000
Area, in percentage of total	29.2	17.3	17.3	22.3	13.9	36.2	100.0
Surface Geology, Percentage of Area:							
Pre-Triassic	14.3	38.5	10.8	30.8	16.0	24.5	21.6
Triassic-Jurassic	3.0	7.3	21.5	37.5	55.3	45.0	22.2
Post-Jurassic	82.7	54.2	67.7	31.7	28.7	30.5	56.2
Total	100.0	100.0	100.0	100.0	100.0	100.0	100.0
Vegetable Cover in Percentage of Area:							
Timber (pine, spruce, lodgepole)	23.5	70.2	30.0	26.1	11.0	19.8	30.9
Woodland (juniper, piñon)	16.9	17.0	28.6	36.0	26.3	31.8	24.4
Brush and grass	59.6	12.8	41.4	37.9	62.7	48.4	44.7
Total	100.0	100.0	100.0	100.0	100.0	100.0	100.0
Palatable cover, animal-unit, years per square mile	4.8	6.25	4.4	4.25	3.4	3.9	4.5
Stock population, animal units per square mile	12.9	16.6	12.0	8.3	7.8	8.0	11.6
Area irrigated, in acres per square mile	13.7	25.8	7.6	0.6	4.8	2.2	10.6
Human population per square mile	2.1	3.3	2.3	1.9	0.6	1.4	2.1
Rainfall, 1929–1934, in inches	10.30	14.05	12.55	11.20	7.75	9.72	11.12
Rainfall, 1929–1934, in Percentage of Area:							
More than 10 in.	46.2	59.4	58.8	51.6	13.2	35.3	46.6
6 to 10 in.	51.1	40.6	41.2	41.6	60.7	49.7	47.0
Less than 6 in.	2.7	0.0	0.0	6.8	26.1	15.0	6.4
Total	100.0	100.0	100.0	100.0	100.0	100.0	100.0
Run-off, 1929–1934, in inches	2.00	4.46	1.55	0.21	0.62	0.38	1.78
Run-off, 1929–1934, in percentage of total	33.2	43.9	15.1	2.8	5.0	7.8	100.0
Silt, 1929–1934, in tons per square mile	696	737	2 440	2 230	3 770	2 810	1 770
Silt, 1929–1934, in percentage of total	12.1	7.6	19.7	29.5	31.1	60.6	100.0

subdivisions above Grand Canyon, with special reference to the silt load. The lettered subdivisions are identified as follows:

A = the basin of Green River above Green River, Utah.
B = the basin of the Colorado River above Cisco, Utah.
C = the basin of San Juan River above Goodridge, Utah.
D = the basin of the Little Colorado, Paria, and other tributaries of the Colorado River between Lee's Ferry and Grand Canyon, Ariz.
E = the basin of the Colorado River and tributaries between Lee's Ferry, Ariz., and Green River, Cisco, and Goodridge, Utah, including San Rafael, Fremont, and Escalante Rivers.
F = the basin of the Colorado River from Grand Canyon, Ariz., to Green River, Cisco, and Goodridge, Utah.
G = the basin of the Colorado River above Grand Canyon, Ariz.

In Table 13, the information on area, surface geology, palatable cover, run-off, and silt are from records of the Geological Survey; that on rainfall, from the records of the Weather Bureau; that on population, stock population, and area irrigated from the Bureau of the Census, and that on vegetable cover from the vegetation map of the United States by H. L. Shantz, of the Bureau of Plant Industry. The 5-yr period considered is from October, 1929, to September, 1934, inclusive. Acknowledgment is made of assistance by J. C. Miller, C. E. Nordeen, Assoc. M. Am. Soc. C. E., and Depue Falck, all of the Conservation Branch of the Geological Survey, in the compilation of the information.

Inspection of Table 13 shows that, for the period considered (which includes a year of high rainfall and run-off, a year of low rainfall and run-off, and, as a whole, is not far from an average 5-yr period) about 77% of the water and 20% of the silt at Grand Canyon came from the basin above Green River and Cisco, Utah, which comprises 46.2% of the entire area of the basin above Grand Canyon (see Subdivisions *A* and *B*, Table 13); and that less than 8% of the water and more than 60% of the silt came from 36% of the basin's area, situated below Green River, Cisco, and Goodridge, Utah, and above Grand Canyon, Ariz. (see Subdivision *F*). Properly belonging to this region of low run-off and heavy silt load is about one-half the area related to Subdivision *C*, or approximately that part of the San Juan Basin above Goodridge that is situated in Arizona, New Mexico, and Utah. Including this part of the San Juan Basin it is probable that what is commonly known as the plateau region of the Colorado, comprising an area of 60 000 to 65 000 sq miles, contributes less than 10% of the water and more than 75% of the silt load recorded at the Grand Canyon gauging station. Clearly, if silt prevention on the Colorado is a worthy objective, intensive study should be made of the origin, and the possibilities of the prevention of silt derived from this plateau region of the basin. Referring to Table 13, it is evident that this is, relatively, a region of Triassic and Jurassic rocks—loosely cemented sandstones and sandy friable shales—and to these rocks must be attributed the origin of most of the silt.

The plateau region has a low rainfall. One-half the area has an annual rainfall of 6 to 10 in. per yr, 15% has a rainfall of less than 6 in.; and

the average for the 5-yr period considered is 9.72 in. The distribution of the rainfall is of importance, and the records show that, substantially, it all occurs in one to six storms during the year. These desert storms are torrential in character, well adapted to corrasion of the rather finely divided weathered material that abounds in the region.

To the arid climate may be attributed the excess of weathered material awaiting transportation and to the torrential character of the storms, the heavy though sporadic flows of silt.

The plateau region has a cover of brush, grass, junipers, and piñon, there being little timber and that is confined to the mountainous outer rim of the basin. The palatable cover is light, being confined to brush interspersed with grass and weeds, occurring as single plants, and the stock and human population is low. In small areas there is a grassy vegetational aspect but in the main the region has the appearance of a desert with vast expanses of bare rock and sand. Probably 90% of the surface of the region is devoid of vegetation. The irrigated area is small and confined almost entirely to the head-waters of streams. It is a land of stock ranges that will furnish year-round feed supply for less than 225 000 cattle, or the equivalent in other stock. The sparseness of vegetation permits the torrential rains to do their work with a minimum of hindrance.

What measures of silt prevention can be undertaken to advantage in such a region? Artifical stimulation of vegetable growth on 60 000 sq miles of surface now devoid of cover and more than one-half of which has rainfall of less than 10 in., is a stupendous, and a hopeless, task. Could it be accomplished to an appreciable degree there is no doubt that the results would be beneficial. There is no lack of fertility, no lack of seeds in the ground. After every soaking rain grass and weeds spring up in abundance, wither, and die. Moisture alone is needed, and moisture it is impracticable for Man to supply. Already 96% of the scant precipitation is devoted to evaporation and transpiration. Only by decreasing the former can much additional moisture be conserved for beneficial use. Stimulation or vegetable cover by regulation or grazing operations is worthy of consideration. Total exclusion of stock from the region for a time would encourage stronger root growth, heavier crowns, and a full opportunity for natural reseeding. This would be beneficial, but how much of the 190 000 000 tons of silt per yr contributed by the plateau region would it keep from the river and for how long and at what cost? The principal cost would be the annual loss of forage valued at about $1 500 000. To this would be added the administrative expense of excluding stock. An annual cost of $2 000 000 might be justified if 10% of the silt could be prevented from reaching Boulder Reservoir and it were worth $150 to $200 per yr to maintain an acre-foot of reservoir capacity. Total exclusion of stock would be impossible because of the human relations involved. Over considerable parts of the area, in the Navajo Indian reservations, for example, stock raising is practically the entire source of livelihood for the people. Nevertheless, the principle of reducing stock population is worthy of consideration, and it is reasonably assured that, where possible,

limitation of grazing to that compatible with maintenance of normal cover, would prove profitable to the local stock industry and to some slight degree lengthen the life of reservoirs on the streams below. Increased vegetable growth, of course, would deplete the water supply.

Since the transporting power of flowing water is required to convey it to perennial streams, a second method of preventing silt, would be to conserve the water supply of the plateau region so far as practicable for irrigation or other consumptive use within that region. If the value of the water of the plateau region is $2 per acre-ft for irrigation in the Lower Colorado Basin and 25 cents per acre-ft for the development of power in the canyons, a total value of the order of magnitude of $3 000 000 per yr is indicated. Exclusion of this water from the main river, even without beneficial use in the plateau region on the basis of such an assumed value, would cost at the rate of less than 2 cents per ton of silt excluded with it—far less than the cost of maintaining reservoir capacity by operations at the side under any known method. Reservoir capacity could thus be maintained at a cost of only $20 to $30 per acre-ft per yr. It seems rather clear that the development of beneficial consumptive uses of water in the plateau region should be encouraged to the utmost for whatever effects in silt prevention may result.

A third method of holding silt in the plateau region would be through the construction of detention reservoirs and spreading works. There are many good and some very large reservoir sites in the region. Eventually, many of them will be developed. They could serve to retard the flow of silt to the Colorado although its eventual movement could not be thus prevented. The effective life of such reservoirs would be rather short but the cost of many could doubtless be justified by their beneficial effects in conservation of water and retardation of silt movement. Theoretically, at least, spreading works have merit. If 1 in. of torrential rainfall on 1 000 acres could be spread to 0.01 in. on 100 000 acres, serious silt movement could be prevented. In the process, local vegetable growth would be encouraged and flow of water to the Colorado prevented. Doubtless there are favorable localities in the plateau region for works of such character.

Summarizing, regulation of grazing, development of beneficial consumptive use of water, and construction of reservoirs and spreading works in the plateau region all seem to the writer to merit consideration as means of withholding silt from the Colorado River. He would urge that before expending largs sums of money in any such undertaking economic benefits commensurate with the costs be reasonably well assured, full consideration being given to the limitations imposed by the value of storage capacity in reservoirs below and the capitalized cost of maintaining such capacity by operations at the reservoirs. He ventures the opinion, based on personal knowledge of the physiography of the plateaus herein considered, that no practicable means will be found for holding back permanently from the Colorado more than a minor percentage of the silt load derived from the sandstones and shales of the region. It is his firm belief that after all reasonable preventive measures have been exhausted, a now unknown cure for the

silt problem will have to be developed, or the inexorable geologic processes that give it rise will deplete seriously, within relatively few generations, and will finally destroy the effectiveness, of the water supply systems of the arid Southwest. It should be recognized, however, that the processes of silt accumulation and deposition have been generally beneficial to mankind. The best agricultural regions of the country are the result of Nature's solution of former silt problems. In the course of geologic time, in the arid Southwest, as elsewhere, the relatively useless sands and clays of the uplands may be expected to contribute their share to the building up of the fertile loams of rich agricultural valleys. Man must adjust his activities to Nature.

AMERICAN SOCIETY OF CIVIL ENGINEERS

Founded November 5, 1852

DISCUSSIONS

THE SPRINGWELLS FILTRATION PLANT, DETROIT, MICHIGAN

Discussion

BY EUGENE A. HARDIN, M. AM. SOC. C. E.

EUGENE A. HARDIN,[10] M. AM. SOC. C. E. (by letter).[10a]—The favorable attitude of the discussers leaves the writer with very little excuse for a closure, except to express his gratitude. To complete the description of this plant it appears that a summary of operating results should be included. Therefore,

FIG. 19.—INTERIOR VIEW OF OPERATING FLOOR, SPRINGWELLS FILTRATION PLANT, DETROIT, MICHIGAN.

the data in Table 5, taken from the March, April and May, 1935, reports of W. M. Wallace, Superintendent of Filtration, Department of Water Supply,

NOTE.—The paper by Eugene A. Hardin, M. Am. Soc. C. E., was published in November, 1934, *Proceedings*. Discussion on the paper has appeared in *Proceedings*, as follows: January, 1935, by Messrs. F. H. Stephenson, and Robert Spurr Weston.

[10] Asst. Engr.-Designer, Black & Veatch, Kansas City, Mo.

[10a] Received by the Secretary July 2, 1935.

Detroit, Mich., on the operation of both the Water-Works Park and the Springwells Filtration Plants are submitted.

Mr. Stephenson's reference to the architectural treatment may be appreciated from Fig. 19, a view of the plant interior. It should be explained, however, that the architectural features were placed secondary to the functional design features. The architect developed his design from a general layout and plant skeleton already planned and given to him for architectural treatment. With this handicap, architecturally, he succeeded commendably in obtaining a very pleasing appearance from the straight lines and mass of the structures with a minimum of embellishment and with the use of plain, and not unduly expensive, materials.

The writer agrees with Mr. Weston that the Wheeler bottom is a very desirable type of filter under-drain system. It was one of a number of types considered for the Springwells Plant, but was not adopted on account of its considerably greater cost than the perforated pipe under-drain system.

TABLE 5.—OPERATING DATA, DETROIT FILTRATION PLANTS: MONTHLY AVERAGES

	March, 1935		April, 1935		May, 1935	
	Water-Works Park Plant	Springwells Plant	Water-Works Park Plant	Springwells Plant	Water-Works Park Plant	Springwells Plant
	(*a*) PLANT OPERATION					
Plant Output:						
Water filtered, in million gallons daily	128.819	97.105	126.787	97.080	128.129	101.654
Water pumped to mains, in million gallons daily	125.389	95.687	125.068	95.933	125.953	99.290
Loss or use in plant, in million gallons daily	3.402	1.418	1.719	2.147	2.176	2.364
Percentage of loss or use in plant	2.66	1.46	1.36	2.15	1.7	2.32
Wash water, in million gallons daily	3.045	.....	2.046	.....	1.973	.....
Percentage of wash water	2.63	.....	1.62	.....	1.53	.....
Filters:						
Filters in service	66	29	60	29	61	29
Filters washed	28	25	19	24	18	32
Average filter run, in hours	38.5	28	60.8	29.1	72.3	22.2
Filtering rate, in million gallons daily	119	137	113	139	111	144
Rate of head loss, increase in feet per hour	0.14	0.20	0.10	0.21	0.09	0.28
Gallons per square foot per foot of head loss	826	643	1 082	666	1 173	511
Chemical Treatment:						
Alum used, in pounds per million gallons	83.5	61.8	107.1	69.0	78.8	81.8
Alum used, in grains per gallon	0.58	0.43	0.75	0.48	0.55	0.57
Ammonium Sulfate Used:						
Sulfate, in pounds per day	469	211.2	460	213.3	471	228.7
NH_3, in pounds per day	117	52.8	115	53.3	118	57.2
NH_3, in pounds per million gallons	0.91	0.54	0.91	0.55	0.92	0.56
NH_3, in parts per million	0.11	0.06	0.11	0.07	0.11	0.07
Chlorine Used:						
In raw water, in pounds per million gallons	1.96	1.78	1.87	1.50	1.86	1.50
In raw water, in parts per million	0.23	0.21	0.22	0.18	0.22	0.18
In filtered water, in pounds per million gallons	1.06	0.99	1.44	1.00	1.24	1.00
In filtered water, in parts per million	0.13	0.12	0.17	0.12	0.15	0.12

TABLE 5.—(*Continued*)

	March, 1935		April, 1935		May, 1935	
	Water-Works Park Plant	Springwells Plant	Water-Works Park Plant	Springwells Plant	Water-Works Park Plant	Springwells Plant
(b) Laboratory Results						
Agar Plate Counts:						
20°C, raw water	15 628	3 000	1 432	300	1 439	255
20°C, applied water	61	86	22	15	21	14
20°C, filtered water	40	38	10	57	6	23
20°C, tap water	10	4	2	7	1	1
37°C, raw water	33	38	19	21	8	8
37°C, applied water	24	18	11	5	4	2
37°C, filtered water	5	3	2	2	1	0
37°C, tap water	4	2	2	1	1	0
Confirmed *B coli* Out of 900 Tubes:						
10 cu cm raw water	291	340	201	172	314	205
10 cu cm applied water	0	0	1	5	5	0
10 cu cm filtered water	0	0	1	0	1	0
10 cu cm tap water	0	0	0	0	0	0
Turbidity, in Parts per Million:	Ave. Max.	Ave. Max.	Ave. Max.	Ave. Max.	Ave. Max.	Ave. Max.
Raw water	14 39	12 32	38 131	32 112	31 102	30 94
Applied water	9 31	8 17	16 25	9 15	15 22	10 13
Filtered water	0.16 0.77	0.04 0.3	0.26 1.65	0 0.1	0.21 0.73	0.03 0.5
Plankton Count:						
Raw water	261 422	159 228	333 418	272 364	312 343	419 493
Applied water	170 222	89 139	122 187	125 146	113 128	145 229
Chemical:						
Chlorine Residual, in Parts per Million:						
Applied water	0.07	0.10	0.07	0.09	0.10	0.10
Filtered water	0.04	0.08	0.03	0.06	0.02	0.04
Weir water	0.11	0.19	0.10	0.19	0.08	0.19
Tap water	0.13	0.15	0.16	0.12	0.13	0.13
pH-value, raw water	0.1	7.9	8.1	7.9	8.2	8.0
pH-value, tap water	7.5	7.4	7.5	7.4	7.7	7.4
Alkalinity, in Parts per Million:						
CO_3, raw water	2.4	2.4	2.4	3.6	2.8	4.0
CO_3, tap water	0	0	0	0	0	0
Total, raw water	81.9	82.3	84.4	85.0	84.4	85.9
Total, tap water	77.0	77.7	78.3	80.1	80.2	81.1

AMERICAN SOCIETY OF CIVIL ENGINEERS

Founded November 5, 1852

DISCUSSIONS

ANALYSIS OF MULTIPLE ARCHES

Discussion

BY A. A. EREMIN, ASSOC. M. AM. SOC. C. E.

A. A. EREMIN,[25] ASSOC. M. AM. SOC. C. E. (by letter).[25a]—A simplified method of computing stresses in a system of multiple-arch spans on elastic piers has been developed in this paper. The table of moments and thrusts in Fig. 11 is a useful guide in the practical application of the method.

In using the alternative method developed by the author in Fig. 11, time may be saved by releasing points starting from the end span of a system. This is true especially in reference to a series of variable lengths of arch spans. The advantage is twofold: First, the error in computing distribution factors for moments and thrusts may be traced easily because the effect of one additional span on distribution factors is more evident than in the case of a series of spans in which the structure is divided into two or more series of spans as suggested by the author; and, second, the step of balancing distribution factors in far spans may be omitted because they are negligible.

Mr. Hrennikoff assumed that joints in a system of multiple-arch spans do not move vertically. If the support is compressible, forces at the joint are balanced after it has rotated through an angle, α, moved horizontally for a distance, Δ, and vertically for a distance, δ. The angle of rotation, and the horizontal and vertical displacements of the joint may be determined from the equations of equilibrium of the joint: $\Sigma H_B = 0$; $\Sigma V_B = 0$; $\Sigma M_B = 0$. Thus,

$$h_\alpha \alpha + h_\Delta \Delta + h_\delta \delta + h_B \text{ (fixed)} = 0 \ldots\ldots\ldots\ldots\ldots (36)$$

$$v_\alpha \alpha + v_\Delta \Delta + v_\delta \delta + v_B \text{ (fixed)} = 0 \ldots\ldots\ldots\ldots\ldots (37)$$

and,

$$m_\alpha \alpha + m_\Delta \Delta + m_\delta \delta + m_B \text{ (fixed)} = 0 \ldots\ldots\ldots\ldots\ldots (38)$$

in which, h_δ, m_δ = the horizontal force and moment factors, respectively, corresponding to a vertical displacement of a joint; r_α = vertical force fac-

NOTE.—The paper by Alexander Hrennikoff, Esq., was published in December, 1934, *Proceedings*. Discussion on the paper has appeared in *Proceedings*, as follows: May, 1935, by Messrs. L. E. Grinter, N. M. Newmark, T. Y. Lin, A. H. Finlay, and A. W. Fischer.

[25] Assoc. Bridge Designing Engr., Bridge Dept., Div. of State Highways, Public Works, Sacramento, Calif.

[25a] Received by the Secretary July 18, 1935.

tor with reference to an angle of rotation; v_Δ = vertical force factor with reference to a horizontal displacement; v_δ = vertical force factor with reference to a vertical displacement; and v_B = the sum of the fixed-end vertical forces at a joint from the given loading.

Mr. Hrennikoff's method, may be extended so that stresses can be computed in a system of multiple-arch spans on elastic piers with flexible tie-rods

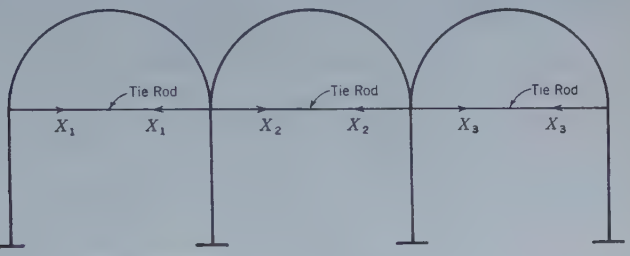

FIG. 19.—MULTIPLE-SPAN ARCH ON ELASTIC PIERS WITH TIE-RODS AT JOINTS.

in arches, such as that in Fig. 19. Equations for computing stresses in tie-rods may be written according to Maxwell's theorem:

$$X_1 (\Delta_{11} + \Delta_1) + X_2 \Delta_{21} + X_3 \Delta_{31} = \Delta_{01} \ldots\ldots\ldots\ldots (39)$$

$$X_1 \Delta_{12} + X_2 (\Delta_{22} + \Delta_2) + X_3 \Delta_{32} = \Delta_{02} \ldots\ldots\ldots\ldots (40)$$

and,

$$X_1 \Delta_{13} + X_2 \Delta_{23} + X_3 (\Delta_{33} + \Delta_3) = \Delta_{03} \ldots\ldots\ldots\ldots (41)$$

in which, X_1, X_2, X_3 = stresses in the tie-rods (subscripts indicate number of the span); Δ_{01}, Δ_{02}, Δ_{03} = changes in lengths of spans at the tie-rods of the system (Fig. 19 with tie-rods removed and loaded with the given loading); Δ_{11}, Δ_{12}, Δ_{13} = changes in span lengths at the tie-rods when the system of arch spans is sustaining a unit force, $X_1 = 1$, acting along the axis of the tie-rod in the first span; Δ_{21}, Δ_{22}, Δ_{23} = changes in span lengths at the tie-rods when the system of arch spans is sustaining a unit force, $X_2 = 1$, acting along the axis of the tie-rod in the second span; Δ_{31}, Δ_{32}, Δ_{33} = changes in span lengths at the tie-rods when the system of arch spans is sustaining a unit force, $X_3 = 1$, acting along the axis of the tie-rod in the third span; and Δ_1, Δ_2, Δ_3 = changes in the lengths of tie-rods corresponding to a unit load acting along the axis of the tie.

Then: $\Delta_1 = \dfrac{L_1}{A_1 E_s}$; $\Delta_2 = \dfrac{L_2}{A_2 E_s}$; and $\Delta_3 = \dfrac{L_3}{A_3 E_s}$, in which L_1, L_2, and L_3 = lengths of tie-rods; A_1, A_2, and A_3 = sectional area of tie-rods; and, E_s = modulus of elasticity in steel.

Stresses in a system of multiple-arch spans on elastic piers with removed ties (Fig. 19), sustaining external loading, or unit forces acting along the axes of the ties, may be determined by Mr. Hrennikoff's method. The hori-

zontal displacements at tie-rods (Fig. 19) may be determined either graphically, or analytically. By solving simultaneously, Equations (39) to (41), stresses in the tie-rods (Fig. 19), X_1, X_2, and X_3, are determined. Equations similar to Equations (39) to (41) may be written for a system with any number of spans.

Computation of the stresses in a multiple-span arch on elastic piers has been generally recognized as an involved problem, and in simplifying it the author deserves the highest credit.

AMERICAN SOCIETY OF CIVIL ENGINEERS

Founded November 5, 1852

DISCUSSIONS

ANALYSIS OF THICK ARCH DAMS, INCLUDING ABUTMENT YIELD

Discussion

BY MESSRS. I. M. NELIDOV, AND A. FLORIS

I. M. NELIDOV,[7] ASSOC. M. AM. SOC. C. E. (by letter).[7a]—The development of the method by which the effect of abutment deformations on stresses in a circular arch ring can be estimated, is offered in this paper. The author has plotted curves for $E_r = E_c$; $m_r = m_c = 8$; and $\frac{h}{t} = 2 - 12$, so that the stresses can be determined directly as a function of $\frac{t}{r}$ and the central angle, $2\phi_1$. The method considers the deformation of the neutral fiber of the arch ring decreased by the effect of Poisson's ratio and by the introduction of a finite thickness of the arch. Furthermore, it is based on the assumption that plane sections remain plane after deformation. It ignores any possible interference from adjacent arch rings. As is known, the method is conventional, being derived from the use of thin railroad arches, in which the ratios of cross-sections to the length of the axial line are small. Its advantage is in the workable form of the equations. On the other hand, any attempt to introduce the effect of the finite thickness and of Poisson's ratio in the form of an interaction between the radial and tangential stresses leads to unusually complicated formulas.[8]

When an important structure is under consideration, a method based on the general equations of the theory of elasticity should be used preferably. For instance, applying such a method as that developed by C. W. Comstock,[9] M. Am. Soc. C. E., to an arch ring with $\frac{t}{r} = 0.345$ and $2\phi_1 = 60°$ and

NOTE.—The paper by Philip Cravitz, Jun. Am. Soc. C. E., was published in January, 1935, *Proceedings*. This discussion is printed in *Proceedings* in order that the views expressed may be brought before all members for further discussion.

[7] Senior Engr. of Hydr. Structure Design, State Dept. of Public Works, Sacramento, Calif.

[7a] Received by the Secretary July 2, 1935.

[8] "Stresses in Thick Arches of Dams", by B. F. Jakobsen, *Transactions*, Am. Soc. C. E., Vol. 90 (1927), pp. 500–507.

[9] "On the Stresses in Arch Dams", by C. W. Comstock. N. Y., 1931, pub. by the author.

with $p_e = 1.0$, one finds the results indicated in Table 3(a). For an arch ring with $\frac{t}{r} = 0.02$ and $2\phi_1 = 47°$, Table 3(b) will give the comparative results.

TABLE 3.—COMPUTATIONS BY THE THEORY OF ELASTICITY
(Tension is Positive)

Theory	Unit Stresses, in Pounds per Square Inch				Percentage of Divergence			
	Crown		Abutment		Crown		Abutment	
	Extrados	Intrados	Extrados	Intrados	Extrados	Intrados	Extrados	Intrados
(a) $\frac{t}{r} = 0.345$; and, $2\phi_1 = 60$ Degrees								
Curved beam	—2.75	1.99	3.89	—5.46	0	0	0	0
Comstock	—1.10	1.80	5.88	—5.46	—60	—10	66	48
(b) $\frac{t}{r} = 0.02$; and, $2\phi_1 = 47$ Degrees								
Curved beam	—74.5	—18.1	—6.1	—89.2	0	0	0	0
Comstock	—68.4	—26.5	—14.1	—79.8	—8	46	23	—11

It is to be noted that when the elastic properties of the material of the arch are considered there is a notable increase of tensile stresses in arches with large ratios of $\frac{t}{r}$ and small central angles. In the development of the results in Table 3 it was assumed that the plane between the adjacent arches remains a plane and that no shearing stresses occur within this plane.

Referring to the derivations of the paper, the writer wished to arrive at the author's results by following a different line of reasoning. Consider a circular arch ring of uniform thickness, loaded with the uniform radial load. Its main, or statically determinate, system is shown in Fig. 7(a). For this system the moments, thrusts, and shear are known, as follows: $M' = p_e r_e e'$; $P' = p_e r_e$; and $V' = 0$. Furthermore, in accordance with Fig. 8:

$$e' = \frac{\int_{r_i}^{r_e} \left(1 + \frac{r_t^2}{r_y^2}\right) r_y \, dr_y}{\int_{r_i}^{r_e} \left(1 + \frac{r_t^2}{r_y^2}\right) dr_y} \qquad \text{.....(44)}$$

Equation (44)[10] indicates that the funicular frame of the loads and the neutral line of the arch are spaced at a distance, e'.

If the left abutment is fixed, as shown in Fig. 7(b), and the right end of the arch is supported with a rigid cantilever extending to the elastic center, E, three unknown redundant forces, X, Y, and Z, are thus introduced, which will be determined if the deformations which they should counteract are made known.

[10] "Strength of Materials", by S. Timoshenko, Pt. II, p. 532, 1931 Edition.

Using the general equation of elastic work and considering only the work, W, of the tangential and shearing stresses:

$$W = \int_{-\phi_1}^{+\phi_1} \int_{r_i}^{r_e} \tfrac{1}{2}\, s_{mt}\, dr\, \Delta_{mt}\, d\phi + \int_{-\phi_1}^{+\phi_1} \int_{r_i}^{r_e} \tfrac{1}{2}\, s_{pt}\, dr\, \Delta_{pt}\, d\phi + \int_{-\phi_1}^{+\phi_1} \int_{r_i}^{r_e} \tfrac{1}{2}\, s_v\, dr\, \Delta_v\, d\phi \quad \ldots\ldots\ldots\ldots\ldots\ldots\ldots\ldots (45)$$

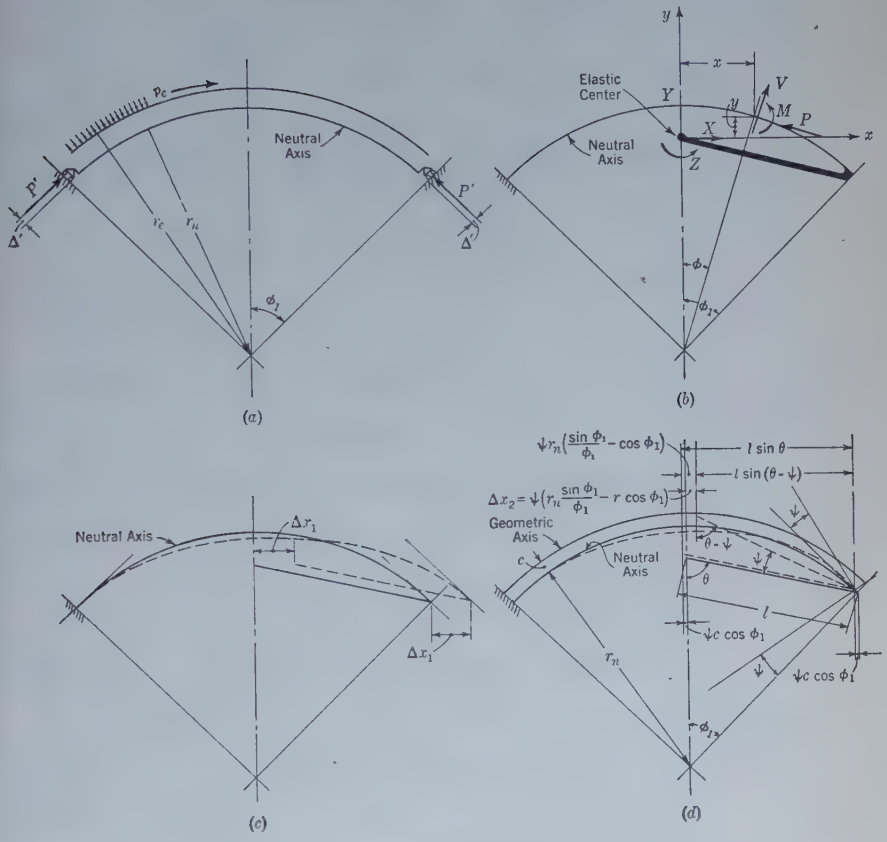

FIG. 7.

in which, s_{mt} is the unit tangential stress due to bending moment; s_{pt} is the unit tangential stress due to thrust; s_v is the unit tangential stress due to shear; and, e is the corresponding total deformation.

The unit stresses in a cross-section and the corresponding deformations are shown in Fig. 8. This stress and deformation distribution is modified near the supports by the influence of the deformation of abutments, but to an unknown extent.

The unit tangential stress due to water pressure and the force, X, will be:

$$s_{pt} = \frac{P\, r_n}{t\, r_y} = \frac{-p_e\, r_e + X \cos\phi\, r_n}{t r_y} \quad \ldots\ldots\ldots\ldots\ldots\ldots (46)$$

and the uniform deformation due to this stress is expressed by the equation:

$$\Delta_{pt} = \frac{-p_e r_e}{E_c t}\sigma + \frac{X \cos\phi\, r_n}{E_c t} \quad \ldots\ldots\ldots\ldots\ldots\ldots (47)$$

in which $\sigma = \frac{r_e}{2r}\left[1 + \frac{r_i^2}{r_n^2} - \frac{1}{m}\left(1 - \frac{r_i^2}{r_n^2}\right)\right]$.

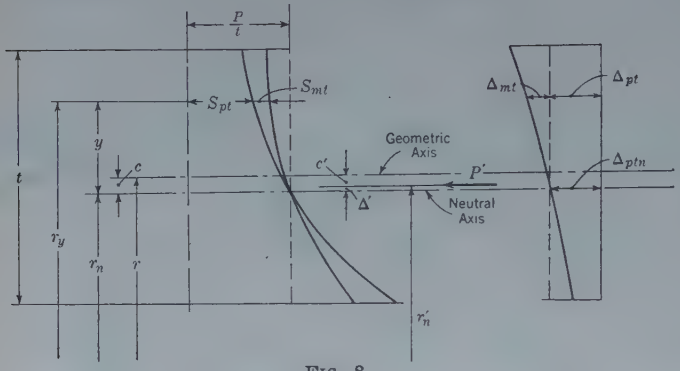

FIG. 8.

The unit tangential stress due to the bending moment produced by the water pressure and the force, X, will be:

$$s_{mt} = \frac{p_e r_e}{t}\left[\frac{r_n}{r_y} - \frac{r_e}{2r}\left(1 + \frac{r_i^2}{r_y^2}\right)\right] + X r_n\left(\cos\phi - \frac{\sin\phi_1}{\phi_1}\right)\frac{r_n}{I_n}\left(\frac{r_n}{r_y} - 1\right) \quad \ldots\ldots (48)$$

and the total deformation due to this stress is expressed by:

$$\Delta_{mt} = \frac{-p_e r_e^2 r_y}{2\,tr\,E_c}\left[1 + \frac{r_i^2}{r_y^2} - \frac{1}{m}\left(1 - \frac{r_i^2}{r_y^2}\right)\right] + \frac{p_e r_e r_n}{Et}\sigma$$
$$+ X r_n\left(\cos\phi - \frac{\sin\phi_1}{\phi_1}\right)\frac{r_n}{E_c I_n}\left(\frac{r_n}{r_y} - 1\right) r_y \quad \ldots\ldots (49)$$

In accordance with Fig. 7(b), the total stresses in a section are:

$$M = M' + X y + Z \quad \ldots\ldots (50a)$$

$$P = P' + X \cos\phi \quad \ldots\ldots (50b)$$

and,

$$V = 0 + X \sin\phi \quad \ldots\ldots (50c)$$

It is noted that as with $\phi = 0$, and $V = 0$, the force, $Y = 0$, and does not enter in Equations (50).

The relative displacement of the End E C of the rigid bracket directed along the X-axis will be in accordance with Fig. 7(c) and Fig. 7(d):

$$\Delta x = \Delta x_1 + \Delta x_2 = 2\,\Delta_N \cos\phi_1 - 2\,\Delta_V \sin\phi_1 - 2\psi\left(r_n\frac{\sin\phi_1}{\phi_1} - r\cos\phi_1\right)$$
$$= -\frac{\partial W}{\partial X} \quad \ldots\ldots (51)$$

Along the Y-axis, Δy is unimportant because $Y = 0$. The rotation of the rigid bracket will be:

$$\Delta\theta = 2\psi = -\frac{\partial W}{\partial Z} \quad \ldots\ldots\ldots\ldots\ldots\ldots\ldots\ldots (52)$$

The derivatives of the work are:

$$-\frac{\partial W}{\partial X} = -X\frac{r_n^3}{E_c I_n}\left(\frac{\phi_1}{2} + \frac{1}{4}\sin 2\phi_1 - \frac{\sin^2\phi_1}{\phi_1}\right)\sigma_m + \frac{p_e r_e r_n}{E_c t}\sin\phi_1\,\sigma_p$$
$$-X\frac{r_n}{E_c t}\left(\frac{\phi_1}{2} + \frac{1}{4}\sin 2\phi_1\right) - X\frac{r}{E_c t}\left(\frac{\phi_1}{2} - \frac{1}{4}\sin 2\phi_1\right)\sigma_v \ldots (53a)$$

and,

$$-\frac{\partial W}{\partial Z} = -Z\frac{\phi_1 r_n}{E_c I_n}\sigma'_m \quad \ldots\ldots\ldots\ldots\ldots\ldots\ldots (53b)$$

The coefficients, σ, in Equations (52) and (53) are: $\sigma_m = \sigma_{m'} = 1$; $\sigma_p = \dfrac{1+\sigma}{2}$; and $\sigma_v = 2.88$. In deriving these coefficients all the factors producing less than 1% of the divergence of the stress were omitted.

With the sign convention adopted the normal and tangential displacements and rotation of the abutment will be:

$$\Delta_N = \zeta\frac{P_1}{E_r} \quad \ldots\ldots\ldots\ldots\ldots\ldots\ldots\ldots (54a)$$

$$\Delta_v = -\zeta\frac{V_1}{E_r} + \eta\frac{M_{1g}}{E_r t} \quad \ldots\ldots\ldots\ldots\ldots\ldots\ldots (54b)$$

and,

$$\psi = -\eta\frac{V_1}{E_r t} + \mu\frac{M_{1g}}{E_r t^2} \quad \ldots\ldots\ldots\ldots\ldots\ldots\ldots (54c)$$

in which $M_{1g} = -p_e r_e c' + X r_n\left(\cos\phi_1 - \dfrac{\sin\phi_1}{\phi_1}\right) + Z$. Due to the small influence of Δ', $c' = c$ will be assumed in future operations.

After substitution of Equations (50) and (53) into Equations (51) and (52) and subsequent integration, the following expressions are obtained for evaluating the unknowns, X and Z:

$$-p_e r_e\left\{\frac{r_n}{t}\frac{E_r}{E_c}\sin\phi_1\,\sigma_p + \zeta\cos\phi_1 - \frac{c}{t}\left[\eta\sin\phi_1 - \mu\left(\frac{r_n}{t}\frac{\sin\phi_1}{\phi_1} - \frac{r}{t}\cos\phi_1\right)\right]\right\}$$
$$+X\left\{\frac{r_n^3}{I_n}\frac{E_r}{E_c}\left(\frac{\phi_1}{2} + \frac{1}{4}\sin 2\phi_1 - \frac{\sin^2\phi_1}{\phi_1}\right) + \frac{r_n}{t}\frac{E_r}{E_c}\left(\frac{\phi_1}{2} + \frac{1}{4}\sin 2\phi_1\right)\right.$$
$$+\sigma_v\frac{r}{t}\frac{E_r}{E_c}\left(\frac{\phi_1}{2} - \frac{1}{4}\sin 2\phi_1\right) + \zeta + \eta\sin\phi_1\left[2\frac{r_n}{t}\frac{\sin^2\phi_1}{\phi_1} - \left(\frac{r}{t} + \frac{r_n}{t}\cos\phi_1\right)\right.$$
$$\left.\left.+\mu\frac{r_n}{t}\left(\frac{\sin\phi_1}{\phi_1} - \cos\phi_1\right)\left(\frac{r_n}{t}\frac{\sin\phi_1}{\phi_1} - \frac{r}{t}\cos\phi_1\right)\right\}\right.$$
$$-\frac{Z}{t}\left[\eta\sin\phi_1 + \mu\frac{r_n}{t}\left(\frac{\sin\phi_1}{\phi_1} - \frac{r}{r_n}\cos\phi_1\right)\right] = 0 \quad \ldots\ldots (55a)$$

and,

$$-p_e r_e \mu \frac{c}{t} - X\left[\eta \sin \phi_1 + \mu \frac{r_n}{t}\left(\frac{\sin \phi_1}{\phi_1} - \cos \phi_1\right)\right] + \frac{Z}{t}\left[\mu + \phi_1 \frac{E_r}{E_c}\frac{r_n}{I_n} t^2\right] = 0 \quad \ldots\ldots(55b)$$

Equations (53) can be rewritten as follows:

$$A + BK + CK_1 = 0 \quad \ldots\ldots(56a)$$

and,

$$A' + B'K + C'K_1 = 0 \quad \ldots\ldots(56b)$$

in which $K = \frac{X}{p_e r_e}$ and $K_1 = \frac{Z}{p_e r_e t}$

The solution of these equations gives:

$$K = \frac{A - A'\frac{C}{C'}}{B'\frac{C}{C'} - B} \quad \ldots\ldots(57a)$$

and,

$$K_1 = -\frac{A' + KB'}{C''} \quad \ldots\ldots(57b)$$

The coefficients of Equations (57) are:

$$A = -\frac{r_n}{t} \sin \phi_1 \frac{E_r}{E_c} \sigma_p - \zeta \cos \phi_1 + \frac{c}{t}\left[\eta \sin \phi_1 + \mu \frac{r_n}{t}\left(\frac{\sin \phi_1}{\phi_1} - \frac{r}{r_n} \cos \phi_1\right)\right] \quad \ldots\ldots(58a)$$

$$B = \zeta + \eta\left[.2 \frac{r_n}{t} \frac{\sin^2 \phi_1}{\phi_1} - (r + r_n) \frac{\sin 2\phi_1}{2}\right] + \mu\left(\frac{r_n}{t}\right)^2\left(\frac{\sin \phi_1}{\phi_1} - \cos \phi_1\right)\left(\frac{\sin \phi_1}{\phi_1} - \frac{r}{r_n} \cos \phi_1\right) + \frac{r_n^3}{I_n}\frac{E_r}{E_c}\left(\frac{1}{2}\phi_1 + \frac{1}{4} \sin 2\phi_1 - \frac{\sin^2 \phi_1}{\phi_1}\right) + \frac{r_n}{t}\frac{E_r}{E_c}\left(\frac{1}{2}\phi_1 + \frac{1}{4}\sin 2\phi_1\right) + \sigma_v \frac{r}{t}\frac{E_r}{E_c}\left(\frac{1}{2}\phi_1 - \frac{1}{4}\sin 2\phi_1\right) \quad \ldots(58b)$$

$$C = -\left[\eta \sin \phi_1 + \mu \frac{r_n}{t}\left(\frac{\sin \phi_1}{\phi_1} - \frac{r}{r_n} \cos \phi_1\right)\right] \quad \ldots\ldots(58c)$$

$$A' = -\mu \frac{c}{t} \quad \ldots\ldots(58d)$$

$$B' = -\left[\eta \sin \phi_1 + \frac{r_n}{t}\left(\frac{\sin \phi_1}{\phi_1} - \cos \phi_1\right)\right] \quad \ldots\ldots(58e)$$

and,

$$C' = \mu + \phi_1 \frac{E_r\, r_n}{E_c\, I_n}\, t_1^2 \ldots\ldots\ldots\ldots\ldots\ldots (58f)$$

Equations (58) may be checked against Equations (18) to (25) of the paper by noting that Equation (52) is $\psi = \phi_1 \frac{r_n}{E_c\, I_n} Z$, and by comparing Equation (50*a*) with Equation (3) of the paper, from which it follows that $Z = X\left(r_n \frac{\sin \phi_1}{\phi_1} - r_c\right)$. After substituting these expressions into Equations (55), Equations (18) to (25) of the paper are obtained.

A question of the relative importance of Poisson's ratio and of the deformation of abutments arises. Table 4 shows a comparison of stresses, in

TABLE 4.—COMPARISON OF STRESSES

(Tension is Positive)

$\frac{t}{r}$	$2\phi_1$, (in degrees)	$m_c = m_r$	E_r	$\frac{h}{t}$	UNIT STRESSES					PERCENTAGE OF DIVERGENCE				
					At Crown		At Abutment			At Crown		At Abutment		
					s_x	s_z	s_x	s_z	s_y	s_z	s_x	s_x	s_z	s_y
0.01	150	∞	0	..	−44.2	−43.0	−41.9	−45.3	0.005	0	0	0	0	0
0.01	150	5	0	..	−44.2	−43.0	−41.9	−45.3	0.005	0	0	0	0	0
0.01	150	∞	E_c*	1	−44.2	−43.0	−41.9	−45.3	0.005	0	0	0	0	0
0.01	150	5	E_c*	1	−44.2	−43.0	−41.9	−45.3	0.005	0	0	0	0	0
0.01	150	∞	E_c*	30	−44.2	−43.0	−41.9	−45.3	0.005	0	0	0	0	0
0.01	150	5	E_c*	30	−44.2	−43.0	−41.9	−45.3	0.005	0	0	0	0	0
0.15	100	∞	0	..	−4.20	−1.07	+0.48	−6.78	0.28	0	0	0	0	0
0.15	100	5	0	..	−4.20	−1.07	+0.42	−6.76	0.27	0	0	−11	0	0
0.15	100	∞	E_c*	1	−4.23	−1.12	−0.11	−6.16	0.24	0	+5	†	−9	−12
0.15	100	5	E_c*	1	−4.22	−1.14	−0.14	−6.17	0.24	0	+7	†	−9	−12
0.15	100	∞	E_c*	30	−4.45	−0.78	+0.20	−6.46	0.27	+6	−27	−58	−4	0
0.15	100	5	E_c*	30	−4.43	−0.81	+0.16	−6.42	0.27	+6	−24	−66	−5	0
0.50	50	∞	0	..	−0.42	+0.17	+0.36	−1.13	0.38	0	0	0	0	0
0.50	50	5	0	..	−0.51	+0.19	+0.26	−1.08	0.37	+20	+12	−28	−4	−2
0.50	50	∞	E_c*	1	−0.78	+0.67	+0.00	−0.67	0.39	+85	+286	†	−41	+1
0.50	50	5	E_c*	1	−0.78	+0.62	0.00	−0.68	0.38	+85	+259	†	−40	0
5.50	50	∞	E_c*	30	−0.86	+0.84	−0.04	−0.54	0.40	+104	+386	†	−52	+3
0.50	50	5	E_c*	30	−0.85	+0.80	−0.05	−0.54	0.40	+101	+363	†	−52	+2

* Finite. † Reversal of sign.

pounds per square inch, for $p_e = 1$ lb and for arch rings varying from a very thin arch, with a very large central angle, to a very thick arch with a very small central angle. Table 4 also gives the percentage of divergence of stresses from those computed by a conventional method; that is, with small $\frac{t}{r}$; with $m_c = \infty$; and with rigid abutments.

The unit stresses in Table 4 were computed by the combined expressions, Equations (46) and (48). The bending stress due to water pressure expressed by the first part of Equation (48) is numerically equal to ±0.20 lb per sq in. for the arch, with $\frac{t}{r} = 0.15$, and to ±0.07 lb per sq in. for the arch,

with $\frac{t}{r} = 0.50$. This stress is of minor importance at the crown, but it is of significance at the abutment, if considered.

The data in Table 4 indicate that in an arch ring of an average thickness and with an average central angle the divergence of stresses is about 10%, and only the deformation of abutments causes a greater divergence. For a thick arch ring with small central angle, the divergence due to Poisson's ratio is about 20%, whereas that due to the deformation of abutments is increased many times this amount. The divergence of shearing stresses is negligible.

The limits of the ratio, $\frac{h}{t} = 1 - 30$, were assumed, in order to visualize the effect of the extremely large deformations, although actually this ratio will never be greater than 1. It was originally applied by Fredrik Vogt, Assoc. M. Am. Soc. C. E., for the case of an abutment of constant thickness, t, and with the forces, M, P, and V, uniformly distributed along the height, h. In the case of an arch dam this condition is not fulfilled; both the thickness, t, and the acting forces vary along the height, h, producing a warped surface of an original abutment plane (which is ordinarily a warped surface from the start, due to the requirements of the excavation).

The problem becomes complex and a practical issue for its solution must be found. If the arch rings of a unit height, as well as the areas near the abutment were separate one from another, then under the forces acting they would displace in relation to each other, as the keys of a piano, each one an independent element. The relative elasticity and continuity of the foundation makes the deformation spread to the neighboring units over a certain distance. From a list of seventy-four arch dams in California the writer found that the ratio, $\frac{h}{t} = \frac{1}{t}$, at the crest varied from 0.046 to 1.000 (average 0.200) and at the base from 0.009 to 1.000 (average 0.042). If the entire height of the dam was assumed as h, the same ratios would be: At the crest between 2 and 45 (average, 16); and, at the base, between 1.4 and 19 (average, 5). As the deformation coefficients, ζ, η, and μ, increase with $\frac{h}{t}$, the selection of larger values of $\frac{h}{t}$ will be on the side of safety; but even with an increase of five to ten times the ratios referred to, h will be only about equal to 1. The ratios in which the entire height of the dam is considered do not seem to be justified.

A. Floris, Esq.[11] (by letter).[11a]—The title of this practical paper and the introductory remarks made therein, are rather misleading, because the plotting of curves is not an analysis or graphical solution of a problem. The author utilizes a known theory by arranging its results in the form of diagrams for

[11] Dipl. Ing., Los Angeles, Calif.

[11a] Received by the Secretary July 22, 1935.

use in practice. From this point of view, of course, the paper is a valuable addition to the literature on the subject.

The usefulness of graphs would be greatly increased if they were made independent of the system of units. The author's diagrams, and those for arches with fixed abutments, referred to in the paper, have a common drawback. They cannot be utilized in countries in which the metric system of units is used. It is possible, however, to arrange the diagrams in such a way, as to make them independent of this restriction. N. Kelen, in his well-known book on arch and multiple-arch dams, for instance, gives graphs that can be used independently of the system of units.[12]

It would be appreciated if the author could include in his closing discussion, graphs that do not have the aforementioned restrictions. If this is not feasible, a brief outline demonstration of how such graphs are plotted would be a welcome addition.

The author is to be congratulated for his painstaking efforts to facilitate the work of engineers engaged in the design of arch dams.

[12] "Die Staumauern," von N. Kelen, Berlin, 1926.

AMERICAN SOCIETY OF CIVIL ENGINEERS

Founded November 5, 1852

DISCUSSIONS

THE HYDRAULIC JUMP IN TERMS OF DYNAMIC SIMILARITY

Discussion

BY MESSRS. NOLAN PAGE, ANDREI I. IVANCHENKO, AND F. T. MAVIS AND ANDREAS LUKSCH

NOLAN PAGE,[42] JUN. AM. SOC. C. E. (by letter).[42a]—A research problem with which the writer recently had contact, involved a study similar in general to that presented by the authors, but resulted in values for length of jump sufficiently different to be of interest. This problem is one of several which have been and are under study by the Corps of Engineers, War Department, at the Hydraulic Laboratory, University of Iowa, Iowa City, Iowa, in connection with construction activities in the Upper Mississippi River and Ohio River Divisions.

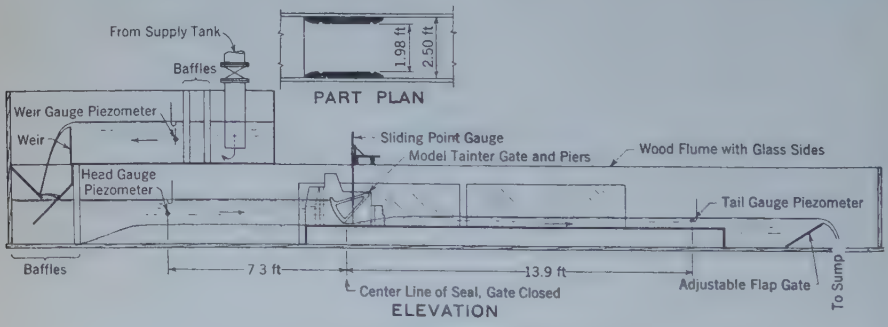

FIG. 11.—MODEL OF STILLING-BASIN DESIGN.

As a step in the development of criteria for design for stilling-basins to protect navigation dams being built in the Upper Mississippi River, the simplified model shown in Fig. 11 was constructed and tested through a range

NOTE.—The paper by Boris A. Bakhmeteff, M. Am. Soc. C. E., and Arthur E. Matzke, Jun. Am. Soc. C. E., was published in February, 1935, *Proceedings*. Discussion on this paper has appeared in *Proceedings*, as follows: March, 1935, by Hunter Rouse, Esq.; May, 1935, by Messrs. Sherman W. Woodward, Robert E. Kennedy, L. Standish Hall, and Morrough P. O'Brien; and August, 1935, by Messrs. F. V. A. E. Engels, Baldwin W. Woods, and J. C. Stevens.

[42] Asst. Engr., U. S. Engr. Sub-Office, Iowa City, Iowa.

[42a] Received by the Secretary July 31, 1935.

of conditions indicated in Table 3. The model consisted of one Tainter gate and one-half of each supporting pier, built one-twentieth the size of the gates for Mississippi River Dam No. 20, and set up in a glass-sided flume.

TABLE 3.—TEST DATA

Test No.	Measured flow, Q, in cubic feet per second	Energy head, $\epsilon_1 = d_0$, in feet	Measured Depths of Flow, in Feet		Measured length of jump, L, in feet	Ratio, $\frac{L}{d_2}$	Kinetic flow factor, $\lambda'_1 = \frac{\epsilon_1 - d_1}{d_1}$	Ratios:		
			d_1	d_2				$d'_1 = \frac{d_1}{\epsilon_1}$	$d'_2 = \frac{d_2}{\epsilon_1}$	$\frac{q_1}{\epsilon_1^{\frac{3}{2}}}$
(1)	(2)	(3)	(4)	(5)	(6)	(7)	(8)	(9)	(10)	(11)
11	0.404	1.004	0.031	0.295	1.6	5.42	62.8	0.031	0.294	0.203
13	0.800	1.004	0.058	0.396	2.1	5.30	32.6	0.058	0.394	0.398
14	0.800	1.004	0.072	0.406	2.1	5.18	25.9	0.072	0.404	0.398
16	0.800	0.764	0.066	0.364	2.05	5.63	21.2	0.087	0.476	0.606
17	0.800	0.763	0.072	0.376	2.1	5.58	19.2	0.094	0.493	0.607
19	1.205	1.002	0.084	0.472	2.95	6.25	21.9	0.084	0.471	0.606
20	1.207	1.001	0.090	0.484	2.5	5.17	20.2	0.090	0.483	0.606
22	1.980	1.000	0.140	0.584	3.1	5.31	12.3	0.140	0.584	1.000
23	1.988	1.002	0.153	0.599	3.0	5.01	11.1	0.153	0.597	1.000
25	2.000	0.765	0.180	0.529	2.1	3.97	6.50	0.235	0.691	1.510
26	1.992	0.768	0.213	0.565	2.5	4.42	5.21	0.278	0.736	1.498
28	2.990	1.004	0.227	0.682	2.65	3.89	6.85	0.226	0.680	1.502
29	2.996	1.006	0.256	0.719	3.0	4.17	5.86	0.254	0.715	1.498
31	2.010	0.763	0.187	0.549	1.8	3.28	6.17	0.245	0.720	1.523
32	2.985	0.827	0.273	0.625	1.7	2.72	4.06	0.330	0.755	2.005
33	2.985	0.826	0.274	0.632	1.8	2.85	4.03	0.331	0.765	2.006
34	2.990	0.827	0.274	0.642	1.85	2.88	4.03	0.331	0.776	2.008
36	4.00	1.002	0.341	0.778	2.5	3.21	3.88	0.340	0.775	2.010
38	5.00	1.162	0.446	0.931	2.4	2.58	3.21	0.384	0.800	2.015
40	5.01	1.001	0.463	0.836	1.75	2.09	2.32	0.462	0.835	2.520
41	5.00	0.999	0.453	0.800	.....	.....	2.41	0.454	0.801	2.525
46	4.98	1.163	0.389	0.906	3.1	3.42	3.98	0.334	0.778	2.010
49	6.00	1.312	0.422	1.000	3.2	3.20	4.21	0.322	0.761	2.020

Instead of the designed sill and stilling-basin, a smooth, level, wooden floor was installed, as shown in Fig. 11. Water was supplied to the model through a 10-in. line from a constant-head tank two floors above the flume, passed through the apparatus as indicated, and discharged into a sump where it was re-pumped to the constant-head tank. Model quantities were determined by means of a rectangular, suppressed weir. Depths up stream from the model gate and down stream from the hydraulic jump were measured by vernier hook-gauges in stilling cans connected to the piezometers indicated in Fig. 11. Depths below the Tainter gate, up stream from the hydraulic jump, were measured with a vernier point gauge.

Table 3 contains only those data taken in tests on this model which are pertinent to this discussion. The lengths of jump tabulated were measured directly in the model, taking the distance from the beginning of the jump, which was always sharply defined, to the point of highest rise down stream from the jump as observed through the glass sides of the flume. The accuracy of measurements has been indicated in the tabulation. It will be noted that the values, ϵ_1, in Table 3 are not computed from d_1, but were taken as equal to d_0, the height of pond-water surface above the temporary floor of the flume. This was considered more accurate than computing ϵ_1 because of the magnified effect of slight inaccuracies in measuring d_1. Theoretically, d_0 should have been corrected for velocity of approach and

the resulting ϵ_0 for friction loss at the Tainter gate, but neither correction was made, the one tending to offset the other and each being small.

In an apparatus such as this model, in which the hydraulic jump expanded laterally as well as vertically, measured values of d'_2 could not be expected to follow the curve for a straight-sided channel given in Fig. 3. However, with the widths at Section 1 and Section 2 known, the lateral expansion could be taken into account in theoretical equations for height of jump. This was done for the model and resulted in the curve marked "d'_2, computed for model" in Fig. 12. Except in the range near the maximum height of

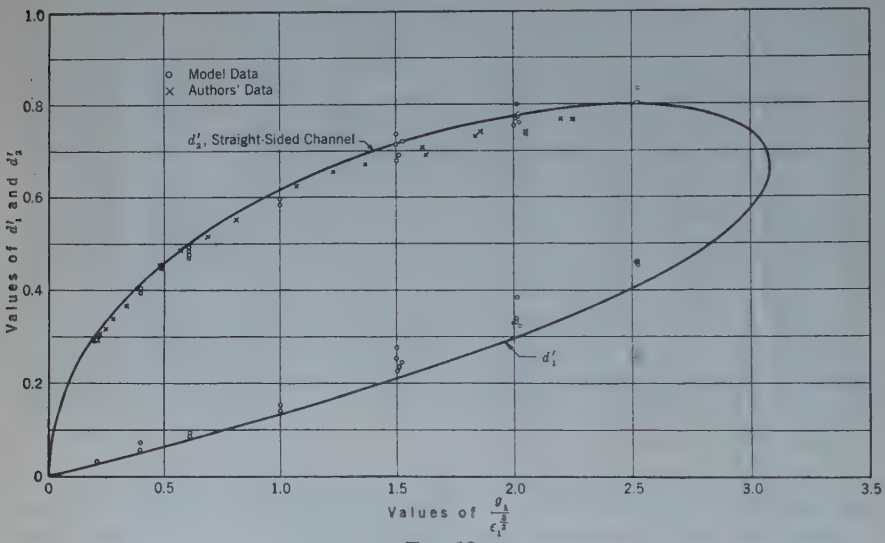

FIG. 12.

jump, measured values fall very close to the computed curve. As was the case in the authors' tests, the range in which the departure of measured from computed values occurs was one of unstable flow. In some tests a standing wave condition alternated with a hydraulic jump, the alternations following an approximately equal period for a given model setting.

Lengths of jump measured in the model have been expressed as ratios of the depths down stream from the jump, and are plotted in Fig. 12. The authors' curve expressing the relation of this ratio to λ_1 has been transferred from Fig. 6 to Fig. 12 in order to compare directly the results obtained in the model with those obtained by the authors. It will be noted that, although the two curves assume a uniform slope at about $\lambda_1 = 14$, the authors' curve is below the curve drawn through model test points and slopes downward as λ_1 increases, whereas the model curve in this range was drawn with zero slope at a value of $\frac{L}{d_2} = 5.60$. It is thought that the jump may have been shortened in the authors' apparatus by friction on the sides of the narrow channel.

From the viewpoint of practical design, the abscissa, λ_1, involving the value, d_1, makes the curves of Fig. 12 awkward to use. Ordinarily, the known values from which dimensions for toe protection must be derived, are the quantity passing a dam site, the upper pool water-surface elevation, and the tail-water elevation corresponding to the quantity. When using the curves of Fig. 12, it is necessary first, to assume a value for d_1; from that, compute an elevation for the stilling-basin floor; and, then, compute by means of d_2, an elevation of tail-water surface, repeating the process until the computed and the given tail-water elevations agree. In this procedure, successive values of d_1 are not directly indicated by computed values of tail-water elevations.

A curve that is more directly useful as a means of computing stilling-basin floor elevations is that shown in Fig. 13. This curve was first called

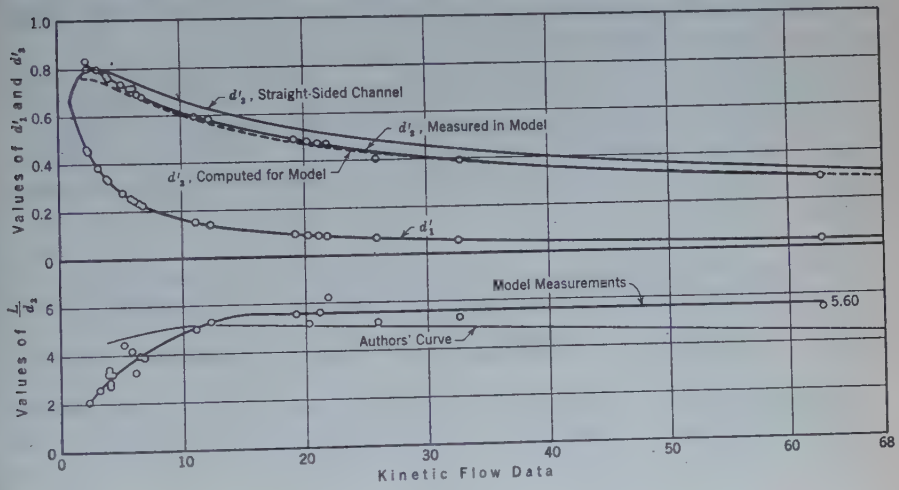

FIG. 13.

to the writer's attention by the late Floyd A. Nagler, M. Am. Soc. C. E., and was used in the design of Mississippi River Dam No. 2.[48] The abscissa in this case involves only the quantity per unit length of stilling-basin, which is readily determined from known river quantity and length of spillway, and the energy head up stream from the hydraulic jump, which may be taken as equal to the height of the pond-water surface above the stilling-basin floor. In using this curve, a stilling-basin elevation is assumed to provide data from which a basin elevation is computed, this process being continued until both elevations agree. Although trial and error methods must be used with this curve as with that of Fig. 12, computed and assumed values are directly related and converge rapidly. The basis for the abscissa of Fig. 13 is the equation for energy head at Section 1,

$$\epsilon_1 = d_1 + \frac{V^2_1}{2g} \quad \ldots\ldots\ldots\ldots\ldots\ldots\ldots\ldots (48)$$

[48] "Laboratory Tests on Hydraulic Models of the Hastings Dam," by Martin E. Nelson, *Bulletin* 2, Univ. of Iowa Studies in Eng.

transformed to:

$$\frac{q_1}{\epsilon_1^{\frac{3}{2}}} = \sqrt{2\,g}\,\frac{d_1}{\epsilon_1}\sqrt{1-\frac{d_1}{\epsilon_1}} \quad \ldots\ldots\ldots\ldots\ldots\ldots (49)$$

The curve presented in Fig. 13 is open to criticism in two respects; First, the test results are not entirely consistent with it; and, second, the value, $\frac{q_1}{\epsilon_1^{\frac{3}{2}}}$, is not dimensionless. Nevertheless, Fig. 13 should not be rejected as inadequate because of this. If theoretical curves are used, and they are usually sufficiently accurate for design purposes, either Fig. 12 or Fig. 13 will give identical results.

Acknowledgment is made to the District Engineer, U. S. Engineer Office, St. Paul, Minn., for permission to use the data given in this discussion. The tests were run by Frederick S. Witzigman, Jun. Am. Soc. C. E.

Andrei I. Ivanchenko,[44] M. Am. Soc. C. E. (by letter).[44a]—The results reported in this paper fully confirm the usefulness of the general methods of analysis applied. The authors have presented the first comprehensive explanation of the hydraulic jump, a phenomenon which was once considered quite puzzling.

Little can be added to the clear graphical representation of the relationships between various elements of the jump, and particularly the longitudinal characteristics illustrated in Figs. 6 and 9. The writer is particularly interested in the curve of $\frac{L}{d_j}$ plotted against λ in Fig. 9. This curve was considered by the authors as the basis of their solution of the longitudinal elements of the jump. The writer proposes the following expressions for the equation of this curve, obtained by the customary method:

$$\frac{L}{d_j} = 10.6\,\lambda^{-0.185} \quad \ldots\ldots\ldots\ldots\ldots\ldots (50)$$

or, solving for L,

$$L = 10.6\,d_j\,\lambda^{-0.185} \quad \ldots\ldots\ldots\ldots\ldots\ldots (51)$$

in which $d_j = d_2 - d_1$, or,

$$L = 10.6\,(d_2 - d_1)\,\lambda^{-0.185} \quad \ldots\ldots\ldots\ldots (52)$$

Equation (52) is quite simple, being derived from experiment; and, assuming that it is based on methods of approach that are physically correct, it is more justified than any other known formula for the length of the jump. In fact, the length of the jump is doubtless the function of the height of the jump, $(h_2 - h_1)$, and the state of flow, which is represented by λ, the kinetic flow factor.

---

[44] Civ. Engr.; Assoc. Prof., Hydraulics and Water Power Eng., Industrial Inst., Novocherkassk, Union of Socialistic Soviet Republics.

[44a] Received by the Secretary August 7, 1935.

The writer has checked the values of the ratio, $\frac{L}{d_j}$, by means of Equation (50) for all values of λ taken from Table 1. The results are given in Table 4.

TABLE 4.—CHECK COMPUTATIONS OF THE RATIO, $\frac{L}{d_j}$

Run No.	Kinetic flow factor, λ	Values $\frac{L}{d_j}$ By Experiment: From	To	By Equation (50)	From the curve, $\frac{L}{d_j} = f(\lambda)$, in Fig. 6	Run No.	Kinetic flow factor, λ	Values $\frac{L}{d_j}$ By Experiment: From	To	By Equation (50)	From the curve, $\frac{L}{d_j} = f(\lambda)$, in Fig. 6
(1)	(2)	(3)	(4)	(5)	(6)	(1)	(2)	(3)	(4)	(5)	(6)
27	3.76	7.47	8.77	8.297	8.23	36	16.79	6.21	6.63	6.290	6.30
30	3.94	7.55	8.79	8.225	8.12	18	20.80	5.83	6.32	6.046	6.05
40	4.51	7.06	8.32	8.022	7.87	6	24.80	5.40	5.90	5.852	5.85
43	4.52	7.67	8.91	8.019	7.80	17	29.66	5.43	5.99	5.662	5.70
25	5.35	6.51	7.65	7.773	7.65	39	30.53	5.32	5.67	5.630	5.63
45	5.47	6.62	7.55	7.740	7.55	35	44.81	5.11	5.53	5.246	5.25
41	6.63	7.13	7.79	7.470	7.35	37	53.89	4.98	5.42	5.188	5.10
24	6.72	7.06	7.83	7.452	7.30	32	62.25	4.67	5.14	4.940	4.95
28	8.55	6.63	7.10	7.127	7.13	34	68.70	4.81	5.06	4.847	4.85
26	9.90	6.63	7.03	6.936	6.94	33	74.56	4.65	5.17	4.774	4.80
29	11.87	6.73	7.13	6.710	6.70	38	78.69	4.24	5.10	4.727	4.72

The writer is fully aware that the data in Column (6), Table 4, indicate certain discrepancies. However, obviously, as the authors state, the tracing of the curves was carried out so "that they must pass within the plotted ranges, indicating the possible range of the *L*-values." For all the curves of Fig. 6 the range of *L*-values from Runs Nos. 25 and 45, as well as for Run No. 28, lies below the curves. This may indicate some degree of unreliability in the experimental data for these runs, because the proposed formula, Equation (50), agrees very well with experimental data in all other cases.

F. T. MAVIS,[45] ASSOC. M. AM. SOC. C. E., and ANDREAS LUKSCH,[46] ESQ. (by letter).[46a]—The authors' observations of the length of the hydraulic jump in a narrow channel are a welcome addition to the literature of hydraulic research. The transfer of data from the model tests to the prototype should be made with caution, however, in the light of the authors' statement (following Equation (15)) that "in analyzing open-flow cases * * * the principle [of similitude] in general may be applied to geometrically similar cases only."

Referring to Equations (16) and (17) presenting the theory of the hydraulic jump the authors state that these equations "apply equally to a jump at the foot of the Boulder Dam and a small-scale model in a laboratory flume." It should not be overlooked, however, that in the derivation of these equations the effects of channel friction are wholly neglected. It is not unreason-

[45] Assoc. Director in Charge of Laboratory, Iowa Inst. of Hydr. Research, and Acting Head of Dept. of Mechanics and Hydraulics, The State Univ. of Iowa, Iowa City, Iowa.

[46] Research Asst. Engr., Iowa Inst. of Hydr. Research, State Univ. of Iowa, Iowa City, Iowa.

[46a] Received by the Secretary August 26, 1935.

able that the height of the jump should be little affected by boundary friction, and that a well-defined relation should exist between depths of flow at alternate stages. The location at which the jump occurs in a level channel of rectangular cross-section can be changed, however, by seemingly insignificant changes in resistance to flow. For a given depth of flow and a given kinetic flow factor it seems reasonable that the length of jump in a narrow channel would be less than in a channel relatively much wider, even if the side walls of both channels were made of glass. Due to the effects of the side walls the length of the hydraulic jump in a narrow channel may be relatively less than in a wide channel. Further tests are needed to show what effect the relative width of a channel may have upon the length of the hydraulic jump under otherwise similar conditions.

On the basis of tests conducted for the Miami Conservancy District, Riegel and Beebe[47] stated that,

"The length of the jump is approximately five times its height. While the beginning of the jump is fairly definite, its lower end is indefinite, and this figure represents merely a general estimate. The lower end was taken as the place where the water surface became and remained sensibly level, a place which was variable in position and difficult to locate."

In 1927, Safranez[48] studied the hydraulic jump experimentally at the Technische Hochschule in Berlin, Germany. The tests were conducted in a glass channel 19.6 in. wide. Lengths of jump were reported[49] for eighteen tests in which the kinetic flow factor, $\lambda_1 = \frac{v_1^2}{g\,d_1}$ varied from 3 to 365, lengths of jump from 1.0 to 3.3 ft, and heights of jump from 0.18 to 0.76 ft. Safranez proposed a tentative formula for the length of the jump which, using the authors' symbols, reduces to:

$$L_j = 6\,d_1\sqrt{\lambda_1} \qquad (53)$$

An analysis of these data[49] for kinetic flow factors less than 80 (the range reported by the authors in Table 1), showed that the simple formula:

$$L_j = 5.2\,d_j \qquad (54)$$

was in better agreement with the observations than Equation (53). The observed ratios, $\frac{L_j}{d_j}$, for the nine tests ranged from 4.6 to 5.5 and the mean absolute error in calculated lengths of juhp, using Equation (54), was 6 per cent. For kinetic flow factors greater than 80 the length of the jump was 4.5 times its height, ranging from 4.0 to 5.1 for nine tests, with a mean absolute error of 5 per cent. The question naturally arises whether this general

[47] "The Hydraulic Jump as a Means of Dissipating Energy," by Ross M. Riegel and John C. Beebe, Technical Rept., Pt. III, Section XVI, p. 85, Miami Conservancy District (1917).

[48] "Untersuchungen ueber den Wechselsprung," von Kurt Safranez, *Der Bauingenieur*, v. 10, Heft 37, p. 38 (1929).

[49] *Loc. cit.*, Table 4.

reduction in the ratio, $\frac{L_j}{d_j}$, for higher values of λ_1 may not be due to the resistance offered by the side walls and whether the ratio might not be substantially constant for a wide channel?

As a part of a general study of stilling pools below spillways, tests were made at the Iowa Institute of Hydraulic Research to determine the geometrical properties of the hydraulic jump. The tests were conducted in a rectangular flume, 26 in. wide, lined with galvanized sheet metal. Water flowed under a sluice-gate with a rounded lower lip upon a level apron of steel plate and smooth cement mortar. The rates of flow varied from 0.48 to 1.44 cu ft per sec per ft width of channel, the depths of flow above the jump, from 0.05 to 0.15 ft, and the heights of jump, from 0.22 to 0.73 ft. In these tests the length of jump varied from 1.4 to 4.5 ft. Fig. 14(*a*) summarizing the data,

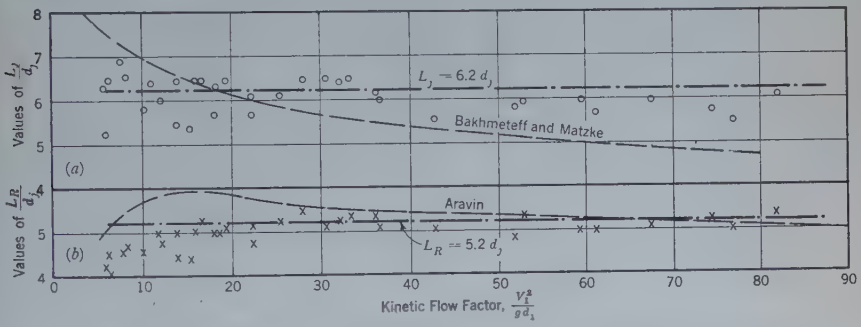

FIG. 14.—SUMMARY OF OBSERVATIONS, LENGTH OF HYDRAULIC JUMP.

shows as ordinates the ratio of length to height of jump and as abscissas, the kinetic flow factor. Fig. 14(*b*) shows as ordinates the ratio of length of roller to height of jump. An analysis of the tests conducted in a flume, 26 in. wide, indicated that the length of jump was approximately equal to 6.2 times its height and that the length of roller was approximately equal to 5.2 times its height.

V. J. Aravin[50] has presented a semi-rational analysis for determining the length of the hydraulic jump in which he followed the suggestion of Professor M. A. Velikanov "to divide the stream, when computing the losses, into two regions: dead zones, where only rotatory motion of the liquid is taking place, and zones where progressive motion is observed." Empirical coefficients were obtained from tests by Bakhmeteff, Pietrkowski, Safranez, Einwachter, and Aravin. The results obtained by the simplified formula suggested by Aravin, are:

$$\frac{L}{d_c} = 0.33\ A\ \frac{(\xi_2 - \xi_1)^3\ \xi^2_1}{\xi_2} \qquad (55)$$

[50] "The Determination of the Length of the Hydraulic Jump," by V. J. Aravin, *Transactions*, Scientific Research Inst. of Hydrotechnics, Vol. 15, pp. 48–57 (1935). (Translated from the Russian by Andreas Luksch.)

in which L = length of the hydraulic jump (roller); d_c = critical depth; $A = 0.54\,\xi_2^{4.35} + 75$; $\xi_2 = \frac{d_2}{d_c}$; $\xi_1 = \frac{d_1}{d_c}$; and d_1 and d_2 = depths of flow above and below the jump, respectively.

These data have been re-arranged for purposes of comparison and are show in Fig. 14(*b*). Within the range of kinetic flow factors included in the authors' tests the ratio, $\frac{L_j}{d_j}$, which follows from Aravin's analysis may be replaced by a constant value, 5.4, with a mean absolute error of approximately 5 per cent.

AMERICAN SOCIETY OF CIVIL ENGINEERS

Founded November 5, 1852

DISCUSSIONS

STABILIZING CONSTRUCTED MASONRY DAMS BY MEANS OF CEMENT INJECTIONS

Discussion

BY CHARLES W. COMSTOCK, M. AM. SOC. C. E.

CHARLES W. COMSTOCK,[6] M. AM. SOC. C. E. (by letter).[6a]—The unusual and almost unprecedented character of the work described, together with the author's clear, complete, and interesting account of methods, difficulties, and results, make this paper unique and, therefore, worthy of something more than casual and perfunctory discussion.

In order fully to appreciate the situation which the author's work was intended to, and undoubtedly did, improve, and how such a condition of affairs could come about, it is necessary to cast a glance backward over the development of hydraulic construction in India.

Masonry dams exceeding 100 ft in height, and about a mile long, were undertaken by the Public Works Department prior to 1870 and pushed to completion within a few years. These were the early years of the theory of dam design developed by Sazilly, Delocre, and Rankine, and not much had materialized from it except the rule of the middle third. During the ensuing third of a century many dams between 100 and 200 ft in height, each comprising more than 500 000 cu yd of masonry, were designed on this principle and constructed in various parts of the country. Because the dams were long the sections were made as small as possible, and it was considered good practice to bring the lines of pressure as near as possible to the limits of the middle third. This resulted in sections rather more slender than are to-day thought conservative.

As to materials, they were those which the country afforded. The earlier works would not have been possible otherwise. Portland cement, of course, was known, but it was manufactured in but few localities, was costly, and was little understood. Concrete was practically unheard of. The origin of surkhi

NOTE.—The paper by D. W. Cole, M. Am. Soc. C. E., was published in February, 1935, *Proceedings*. Discussion on the paper has apeared in *Proceedings*, as follows: August, 1935, by Messrs. Oren Reed, F. F. Fergusson, and Joseph Wright.

[6] Jackson Heights, N. Y.

[6a] Received by the Secretary July 17, 1935.

mortar is shrouded in the mysteries of the past, but its preparation and use are common knowledge among the Indian masons. It has unquestionable hydraulic properties, and tests have shown compressive strengths of 68 tons per sq ft at 12 months, and 79 tons at 18 months; respectively, 1 060 and 1 230 lb per sq in. Such material cannot be summarily dismissed from consideration.

The Indian people are essentially agriculturists. They are not mechanically minded. Elaborate and complicated machinery does not enter into their scheme of things, although their skill and patience in many handicrafts are revelations to the westerner. Time is not important to them. They do not think in terms of the individual's span of life.

In these circumstances it is not surprising that the administrators of the Indian public works designed and built as they did—with a rudimentary theory, native materials, a minimum of mechanical equipment, and a maximum use of manual labor of the kinds to which the people were accustomed. After half a century without a major failure, notwithstanding the construction of a great number of large and important works, they were justified in considering their practice sound, and it is not strange that they were slow to adopt the later developments in materials and methods.

With this background the engineer who designed the Walwhan and Shirawta Dams, and who had spent most of his long professional life in India, naturally preferred to follow a tried and proven road rather than to pursue what might be only a will-o-the-wisp.

The Shirawta Dam contains about 650 000 cu yd of masonry. To construct such a volume, almost entirely of one-man stone, by hand labor within a few working seasons required an army of men and women. These literally swarmed all over the work. In fact, seen from an elevation and from a little distance the activity resembles nothing so much as a gigantic swarm of bees. The labor turnover is enormous, for these people will work on outside employment only during such times as their personal agricultural operations do not require attention.

Herein lies the weakness of the system. Really good masonry can be and has been executed by this somewhat primitive procedure, but with hundreds of masons distributed over a large area and served by thousands of coolies who bring the stone and mortar, adequate supervision and inspection are impossible. Here and there a careless or indifferent mason, an occasional batch of improperly ground mortar, a few stones which are dirty or cracked—the result is a weak spot, a discontinuity, to and through which water under pressure may find its way. Time and the never-ending erosion by running water do the rest.

Thus the slowly but steadily increasing leakage through these dams was regarded as symptomatic of a condition which should not be allowed to persist. The loss of water was unimportant, at least in any quantity which might be reached for some years. It was not believed that the dams were unsafe, but it seemed certain that they would become so if the deterioration should be permitted to continue. If that time should come, every one would

be helpless. An edict of condemnation by Government would be a futile gesture, for no power on earth could prevent those reservoirs from filling. The waste-gates, designed only for use in the early stages of construction, are not large enough to empty the reservoirs in the period between monsoons.

To order the dams breached so that the reservoirs could not fill would deprive the City of Bombay and surrounding territory of tramway service, light, fans, and refrigeration. It would shut down about 80 cotton mills and deprive the railroads entering Bombay of power. In short, it would mean ruin and pestilence to a million and a half people. The Indian Government does not take a fiendish delight in destroying private capital, but even if it were indifferent to such destruction it could not face this possibility. On the other hand, failures of the dams would mean frightful havoc to agricultural regions below, and almost certainly much loss of life.

Clearly, the damage already suffered must be repaired and the structures must be rendered permanently immune to future deterioration, without interfering with the use of the reservoirs. The plan adopted after thorough investigation and careful study was endorsed by some of the most experienced engineers in India and received Government approval. The engineers for the contractor, François Cementation Company, Ltd., believed, in the light of their experience, that it promised success. They had not previously undertaken a precisely similar job, but no major engineering problem is an exact duplicate of any other. It was believed that cavities existing in the masonry, whether resulting from carelessness during construction or from subsequent washing out of mortar, could be filled with good cement grout, and that the old surkhi mortar in the neighborhood of these cavities might to some extent be impregnated with cement. It is the execution of this plan which has been so well described by the author.

It has been objected by some persons that the degree of betterment is uncertain since there is no visual evidence that all cavities are filled wholly or in part. No visual evidence, it is true, but the volume of cement retained in the structures (in the case of Shirawta 0.6% of the total volume of the masonry) is very convincing, especially as the pressures employed were sufficient to force the grout through minute openings. It is not claimed, of course, that the dams are of as high quality as though they had been originally laid up in cement mortar under close inspection, but they are certainly as good as (probably even better than) any of those built with surkhi mortar in the manner prevailing in India, and many of which have served for more than fifty years without manifesting any sign of distress.

It has been said that this work was almost unprecedented. The grouting of rock formations underlying dams prior to construction is a well-established practice, as is also subsequent grouting of parts of the structure through holes left for that purpose.

Grouting at the Camarasa Dam in Spain, completed in 1931, was not a parallel case to the Indian dams. At Camarasa the dam was absolutely tight and sound; leakage through the surrounding and underlying rocks was the fault to be remedied. This object was accomplished with marked success.

The Delta Barrage, in Egypt, consists of a series of piers, each 16 m long by 2 m thick and about 14 m high. These are spaced 7 m on centers, and rest on a continuous concrete mat 4 m thick. Construction was begun about the middle of the Nineteenth Century. As a result of political interference the foundation work was not properly done, cracks and settlements appeared almost immediately, it was impossible to maintain the pool level which had been intended—the dam was a failure. When Sir Colin Scott-Moncrieff became head of the Public Works Department in Egypt he took immediate steps to remedy the difficulties. The final stage of the repair job was to drill five vertical holes along the axis of each pier and to inject cement grout. No pressure was used except that due to static head; however, cement injected at one pier frequently appeared in the holes in adjoining piers. One pier took as much as 73 tons of cement; a total of 1 000 tons was used in 132 piers. This work was completed in 1898 or 1899; the dam has given no trouble since.

One work which in some respects parallels the Indian dams is the "barrage de l'Oued Fergoug" in Algeria. This dam, 34 m high, also was designed in the early days of the middle-third theory, construction completed about the beginning of 1872. Like the Indian dams, it was built of one-man rubble by native workmen using lime mortar, perhaps feebly hydraulic. From the beginning it leaked profusely at many places, and lime deposits on the down-stream face indicated serious destruction of the mortar. In December, 1881, a length of 125 m of the highest part of the structure was carried away, most of it clear down to the foundation. Between 1881 and 1885 the gap was filled by a new structure of slightly greater section than the old, but built in the same manner and with the same kinds of materials except that some hydraulic lime and some Portland cement were used in places regarded as especially critical. The dam continued to leak but in 1900 it withstood an unprecedented flood with no indication of weakness. In November, 1927, there was another major failure, carrying away a part of the old and a part of the later work, and resulting in heavy loss of life and property. For some time prior to the failure the authorities had been disturbed over the persistent leakage and the continual leaching of lime from the mortar, and had approved a project for drilling and the injection of cement. This work was in actual process near the left bank at the time of the failure, but had not progressed far enough to throw any light on the condition of the masonry. Whether this method of reinforcement and stabilization would have been effective if undertaken a few years earlier can only be conjectured.

The outstanding peculiarity of hydraulic construction in India is the general aversion to the use of Portland cement. This was understandable in the early days when cement would have had to be imported from Europe and would have been very costly. To-day, however, excellent Portland cement, meeting all standard specifications, is manufactured at several places in India and can be purchased at the factory at prices of about 35 rupees per ton—equivalent to about 9 shillings per bbl—so that this reason is no longer operative.

The late Robert Batson Joyner, who spent nearly a life time in India, and who designed Walwhan and Shirawta Dams and their appurtenant works, wrote[7] in 1919:

"Indian engineers never use Portland cement in the construction of masonry dams, whether of stone or of concrete, except perhaps in wet foundations; not merely on account of its high cost—though good cement is now being made in the country more cheaply—but also because it is considered inferior to good hydraulic-lime mortar for dams. Cement work is too rigid, whilst the hydraulic-lime mortar, being somewhat elastic, withstands the variations of temperature without cracking. There is therefore not the somewhat alarming necessity of providing expansion joints. The range of temperature is probably not greater in India than in England, but it may occur more suddenly."

These are arguments devised to justify an existing practice rather than reasons on which that practice is based. The reader may judge for himself of their validity.

With increasing education of Indian masons in the properties of Portland cement, and with the gradual change in personnel of the Public Works Department with the retirement of the seniors and the advent of younger men, it is probable that Indian practice in dam construction will eventually come to conform quite closely with that in other parts of the world. Tradition is strong in the East, and the inertia of 350 000 000 people is not easily overcome.

One of the most valuable features of this paper is that it emphasizes the dominant importance of execution, as compared with design, in the construction of masonry dams. Volumes of mathematical formulas and theoretical discussions in many languages have come and gone, each purporting to be the last word as to stresses in dams; yet sections have changed little in seventy-five years. On the other hand, with few exceptions, all important dam failures have been traced to defective materials or faulty execution. A dam is made safe, or otherwise, on the job—not in the office.

The author is entitled to great credit for his masterly handling of a difficult job. He is further to be commended for the exhaustive and incisive manner in which he has presented the subject in print. There is nothing superfluous; nothing has been omitted. Aspiring authors of engineering papers should be referred to this as a model.

[7] "The Tata Hydro-Electric Power-Supply Works, Bombay," by the late Robert Batson Joyner, *Minutes of Proceedings*, Inst. C. E., Vol. CCVII, p. 55.

AMERICAN SOCIETY OF CIVIL ENGINEERS

Founded November 5, 1852

DISCUSSIONS

LINE LOAD ACTION ON THIN CYLINDRICAL SHELLS

Discussion

BY I. K. SILVERMAN, JUN. AM. SOC. C. E.

I. K. SILVERMAN,[13] JUN. AM. SOC. C. E. (by letter).[13a]—That thin shells, properly supported, serve as very economical structures, has been known for some time. Mr. Schorer, for the first time, has introduced into American engineering literature the theory of such shells which has been developed largely by German and Swiss engineers.

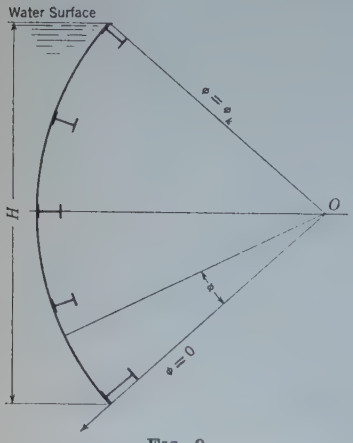

FIG. 9.

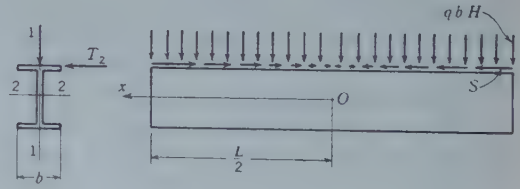

FIG. 10.

Even with the simplifications introduced in this paper, the application of the theory requires considerable computation as, for example, when the structure analyzed is not a complete surface of revolution and the loading is not symmetrical. Such a condition occurs in the analysis of the structure such as the sector gate shown in Fig. 9.

NOTE.—The paper by Herman Schorer, Assoc. M. Am. Soc. C. E., was published in March, 1935, *Proceedings*. This discussion is printed in *Proceedings* in order that the views expressed may be brought before all members for further discussion.

[13] With U. S. Reclamation Bureau, Denver, Colo.

[13a] Received by the Secretary July 15, 1935.

When applied to a structure of this type, the thin shell theory tends to show that large stresses may occur in the longitudinal supporting members, especially in the member at $\phi = 0$. These large stresses are due to the fact that the inevitable arch action developed in the curved skin-plate causes the member to bend about Axis 1–1, Fig. 10. Furthermore, stresses of the type, S, subject the longitudinal supporting members to loads which are axially eccentric. In combination with the direct water load, these stresses may reach large values, especially in gates of long spans.

In outline, the method of attacking such a structure as that presented in Fig. 9 is perfectly straightforward. The author has shown that the loads on a structure are carried by a primary system of stresses, the membrane system, and by a self-equilibrating system (secondary), the function of which is to preserve geometrical continuity. The stresses of the secondary system are applied along a line common to the shell part of the structure and its supporting members.

The stresses and deflections of the membrane system are obtained as if the shell were a complete surface of revolution by means of Equations (101) to (110). The stresses at $\phi = 0$ and $\phi = \phi_k$ (it is assumed now that intermediate longitudinal members have been removed) are applied to the supporting members as reactions, and the deflections and stresses in these members are obtained in the usual manner. In general, there will be differences in these stresses and deflections, and it is the purpose of the secondary system to annul such geometrical discrepancies. It is the object of the author to derive the stresses and deflections in the shell due to this secondary system. When these stresses and deflections have been obtained in the shell for the various conditions of loading (see Fig. 4), the corresponding stresses and deflections are obtained for the supporting members.

In general, there will be eight elastic equations for the indeterminate quantities in the secondary system. In a symmetrical structure under symmetrical loading, such as that treated by the author, these equations reduce to four.

Finsterwalder[14] has reduced the number of unknowns to six by assuming that $\theta = 0$ at the connection of shell to supporting member. This condition is quite possible because of the relative rigidities of shell and boundary member. Corresponding to Equations (91) to (94) for symmetrical loading there would result three sets of four simultaneous equations each for the determination of the constants, A, B, C, and D, namely: in Equation (92), $N_2 = \frac{4}{c}$; $N_2 = 0$; and $N_2 = 0$; in Equation (93), $T_2 = 0$; $T_2 = \frac{4}{c}$; and $T_2 = 0$; in Equation (94), $\frac{\partial S}{\partial x} = 0$; $\frac{\partial S}{dx} = 0$; and $\frac{\partial S}{\partial x} = \frac{4}{c}$; and in Equation (98), $\theta = 0$; $\theta = 0$; and $\theta = 0$.

In all cases, M_2 (Equation (91)), would be different from zero. With the constants known the method of procedure follows that of the author

[14] "Die Theorie der zylindrischen Schalengewölbe, System Zeiss-Dywidag," von Dr. Ing. Ulrich Finsterwalder, International Assoc. for Bridge and Structural Eng., Zurich, 1932.

except that for a case of symmetrical loading and symmetrical structure, the equations of continuity are, as follows: For $\phi = 0$:

$$\Delta w = (w)_s - (w)_b = 0 \quad \ldots\ldots\ldots\ldots\ldots\ldots (144)$$

$$\Delta v = (v)_s - (v)_b = 0 \quad \ldots\ldots\ldots\ldots\ldots\ldots (145)$$

and,

$$\Delta \sigma = \left(\frac{T_1}{t}\right)_s - \sigma_b = 0 \quad \ldots\ldots\ldots\ldots\ldots\ldots (146)$$

in which the subscripts, s and b, refer to shell and beam, respectively, and σ = the unit stress. When the loading is unsymmetrical or the edge members are not identical, six or eight elastic equations are necessary. The equation for w will be set up in general form using the following definitions: w_1 = deflection of shell due to membrane system at $\phi = 0$; w'_1 = deflection of shell due to membrane system at $\phi = \phi_k$; w_2 = deflection of beam due to membrane system at $\phi = 0$; w'_2 = deflection of beam due to membrane system at $\phi = \phi_k$; w_3 = deflection of shell due to secondary system at $\phi = 0$; w'_3 = deflection of shell due to secondary system at $\phi = \phi_k$; w_4 = deflection of beam due to secondary system at $\phi = 0$; and, w'_4 = deflection of beam due to secondary system at $\phi = \phi_k$. These deflections are broken up so that a symmetrical and contra-symmetrical system of secondary stresses may be applied.

For the symmetrical system:

$$\Delta w = \frac{(w_1 + w'_1)}{2} - \frac{(w_2 + w'_2)}{2} + \frac{(w_3 + w'_3)}{2} - \frac{(w_4 + w'_4)}{2} = 0 \quad \ldots (147)$$

and, for the contra-symmetrical system:

$$\Delta w = \frac{(w_1 - w'_1)}{2} - \frac{(w_2 - w'_2)}{2} + \frac{(w_3 - w'_3)}{2} - \frac{(w_4 - w'_4)}{2} = 0 \quad \ldots (148)$$

Corresponding equations are obtained for v and σ. Unsymmetrical loadings tend to cause large secondary stresses, and it is to be expected, in the case of the sector gate, that these high moments and stresses occur at $\phi = 0$.

AMERICAN SOCIETY OF CIVIL ENGINEERS

Founded November 5, 1852

DISCUSSIONS

PHOTO-ELASTIC DETERMINATION OF SHRINKAGE STRESSES

Discussion

BY MESSRS. THOMAS H. EVANS, AND I. K. SILVERMAN

THOMAS H. EVANS,[6] JUN. AM. SOC. C. E. (by letter).[6a]—The problem of determining, with some exactness, the stresses in a concrete dam due to shrinkage seems well adapted to the photo-elastic method. Although the writer disagrees with the author's contention that the stress problem is only two-dimensional, it will not greatly affect the "philosophical picture" to consider it as such. The principal inaccuracy in the determination is not in the method itself but, as Mr. Smits points out, in the physical inconsistency between the prototype and the necessarily idealized model. However, the method does provide a rational first approximation to an extremely complex stress distribution. It should be a distinct aid in supplementing the engineering experience and judgment of the designer.

As indicated by the author, the "membrane analogy" as a supplement to photo-elastic analysis appears to have decided advantages over the method of graphical integration for the determination of the principal stress sum. There was also another excellent paper by Supper and McGivern[7] that exhibited in great detail the use of the membrane analogy for the determination of the quantity, $p + q$. The accuracy of this method decreases, however, as the slope of the membrane increases. This occurs in regions of high stress concentration, such as the heel and toe of the dam illustrated in the paper. Since a designer might have more interest in such regions than in others, it would be desirable to avoid the effects of this limitation of the membrane analogy.

Another supplementary procedure which seems to be adaptable to all cases is that proposed[8] by Professor V. Tesar. This is a purely optical method requiring even less additional apparatus than the membrane analogy, and its accuracy is independent of the concentration of stress in the model. Its

NOTE.—The paper by Howard C. Smits, Esq., was published in May, 1935, *Proceedings*. This discussion is printed in *Proceedings* in order to bring the views expressed before all members for further discussion.

[6] Asst. Prof. of Civ. Eng., Dept. of Eng., Univ. of Virginia, Charlottesville, Va.

[6a] Received by the Secretary June 25, 1935.

[7] *Journal*, Franklin Inst., April, 1934.

[8] *Revue d'Optique*, March, 1932.

fundamental principle is the interference of light waves as they are reflected from the bounding surfaces of a thin wedge of air. The surfaces in this case are a face of the model and an optically flat glass. Changes in thickness in the model (which are a function of the quantity, $p + q$, cause corresponding variations in the interference fringe pattern across the image of the model on a screen. These variations can be calibrated, and, therefore, $(p + q)$ can be found for a given load.

I. K. SILVERMAN,[9] JUN. AM. SOC. C. E. (by letter).[9a]—What would be the stress pattern in the bakelite model of a triangular dam resting on a continuous elastic foundation and subjected to shrinkage? In this paper, Mr. Smits has described a conception of this phenomenon. His description of how the stresses might vary seems logical. Based on this preconceived picture, he proceeds to load his model so as to obtain this possible distribution of stress and, in Figs. 10 and 11, presents curves for the resulting stress distribution near the base. He has failed to show, however, that this is the only way this stress pattern could have been produced and, for this reason, and for others cited herein, no great value can be attached to the numerical results shown in Fig. 10.

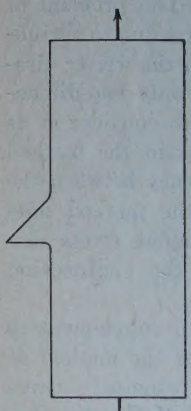

FIG. 12.

The author states that the form of the test specimen was chosen so that the stress pattern would be a gauge of the degree of axial loading. It is evident that in choosing this type of specimen, he has clouded the stress distribution in the very region that he is examining. The stress distribution in any model is dependent to a high degree on its geometry. From Fig. 8 the width of the strap is of the same order of dimension as that of the base of the dam. For this reason the stress distribution of Fig. 7 may be far different from that in a model which is of the form shown in Fig. 12.

By means of Fig. 9 Mr. Smits has shown the accuracy obtained in measuring the stresses shown in Fig. 7. It would be interesting if, in his closing discussion, he would present curves similar to those of Fig. 9 for the resultant stress distribution shown in Fig. 10. Evidently, the total areas under these curves should be zero.

[9] With U. S. Bureau of Reclamation, Denver, Colo.
[9a] Received by the Secretary August 3, 1935.